Synthesis, Spectroscopy, and Photochemistry of Reactive Organic Molecules

By

Stephanie N. Knezz

A dissertation in partial fulfillment of

the requirements for the degree of

Doctor of Philosophy

(Chemistry)

at the

UNIVERSITY OF WISCONSIN-MADISON

2016

Date of final oral examination: 08/11/2016

The dissertation is approved by the following members of the Final Oral Committee:

Robert J. McMahon, Professor, Chemistry

Tehshik P. Yoon, Professor, Chemistry

Samuel Gellman, Professor, Chemistry

Sandro Mecozzi, Professor, Chemistry

R. Claude Woods, Professor, Chemistry

For my father, whose passion and curiosity continues to inspire my drive for discovery.

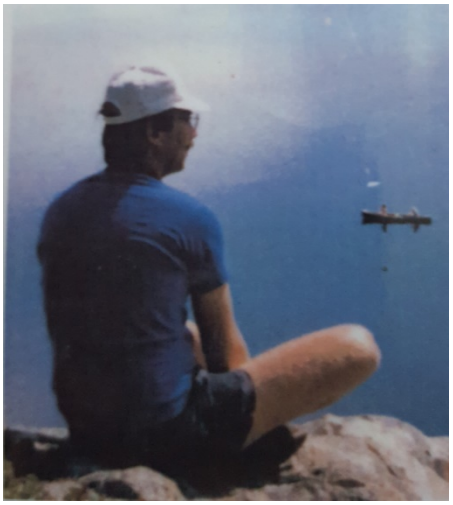

1957-2016

Acknowledgements

When I began graduate school five years ago, all I knew was that I liked chemistry and thought it would be neat to study it. At the time I had no sense of the challenges that I would face to develop from a college student to a Ph.D. scientist. There are so many people who facilitated this transition, and I hope I can at least recognize the major players.

In the most direct and tangible sense, I have my mentors to thank. Every faculty member I have engaged with has influenced my enthusiasm and motivation to continue in the field. UW-Madison hosts such a rich community of passionate scientists; it would have been hard to be here five years without it catching on. In addition to faculty, the facility staff are inspiring scientists in each of their fields. In particular, Martha Vestling not only taught me about mass spectrometry, but instilled a curiosity about all chemical systems that I have applied to my own research that has proven instrumental to my development as a chemist. More than anyone, I have Bob to thank for my development as a scientist. He took me on when I was unexperienced and excited about every possible project he could dream up and has continued to support me as I tried them all out. His interest in a diverse array of research fields allowed me to develop many different skills and learn about a great number of areas of physical organic chemistry. In addition to all my endeavors in chemistry, he has wholeheartedly supported my interest in developing my skills and knowledge in teaching.

With this support, I began my development in the Delta program. Delta has had such a profound influence on who I am as a teacher and as a scientist. It was through my experiences in Delta that I was able to discover how I perceived my professional identity in higher education and pursue the opportunities that followed. In particular, Devin Wixon, Jess Maher, and Don

Gillian-Daniel have been amazing mentors. They have not only exposed me to the current developments in STEM education but have allowed me the opportunity to experience it myself. These experiences have been crucial to my future.

Through everything, I couldn't have survived all the work without my friends and coworkers. All my friends in the 2011 entering class have been supportive starting with our first year of classes and continuing throughout, and I wish the best for every one of them. You guys are all brilliant. The McMahon lab has been a dynamic force from the time I started until now, and I have high hopes for Vanessa, Andrew, and all of our undergrad and masters students who have already accomplished so much. Those who came before me: Brian, Laura, Terese, and Brent helped show me the ropes and set me up to take on a lot of independent projects as well as those started by others. I have to thank Ben especially, for being the one constant through all the change in the group and for working closely with me on several projects. All the computational work in the MeC_3Me chapter was carried out by Ben, and we spent a lot of time talking about chemistry as well as a host of other things. I know you'll go on to be a great educator.

Behind the scenes there are those whose support has allowed me to get through all the toughest parts of the last five years, my core four: Leigh, Spenser, my sister Emily, and my mom. The selfless devotion to my success and well-being that each of them has displayed reminds me daily that I am capable of accomplishing whatever I set my mind to. In particular, my mother always set an example of dreaming up overly ambitious goals and working hard as heck until she accomplished them. It is this process of goal-setting and putting on the blinders that has gotten me to where I am. Leigh has been such a strong support in my entire journey through graduate school and has the ability to relate to my ups and downs in a way that no one else ever could. She never hesitated to lend a hand in any situation where it was necessary, and I can't thank her

enough for that. Spenser has been there to support me whenever I needed him, even when I didn't take him up on it, and that support is a comfort that allows me to push myself. Emily constantly instills a joy for life and a perspective that allowed me to take my failures in stride and always look forward. Having people who know me well entirely outside the realm of the scientific community allowed me to focus on the big picture. I truly couldn't have made it without each of your emotional and logistical support.

Above all, I have my father to thank for this accomplishment. He only had a high school education, but he was the single greatest influence on my decision to become a scientist. He viewed the natural world with an eye for detail and a curiosity that rivals that of most professionals in the field. Being a stay-at-home dad, I got a lot of his influence. He would often take us on hikes, and it was a rare day that I could escape without being asked, "Why do you think the trees grow that way? How do you think the clouds form those shapes? What caused this rock formation?" As long as I can remember, he was asking me to pose hypotheses about the origin physical phenomena, and these internalized skills have been the most valuable tools in my development as a scientist. He always taught me to pay no mind to the senselessness in the world and simply do my best to seek whatever truth I can find and revel in it. I hope that my small contribution to the world's stock of fundamental truths will help fuel the sense of joy and wonder embodied in his memory.

SYNTHESIS, SPECTROSCOPY, AND PHOTOCHEMISTRY OF REACTIVE ORGANIC MOLECULES

Stephanie N. Knezz

Under the supervision of Professor Robert J. McMahon

at the University of Wisconsin-Madison

The exploitation of fundamental chemical reactivity is a universal focus across the field of chemistry. No matter the specific research area, understanding the driving forces that make a reaction proceed allows for greater intentionality and control in experimentation and innovation. Research in the McMahon group focuses on understanding inherently reactive organic systems, many of which feature intermediates operative in common processes like combustion, soot formation, and processes operative in organic electronics. By studying systems of this type, the structure and behavior of high-energy intermediates can be revealed, and a richer understanding of reactivity and mechanism can be fully realized. This focus manifests in a variety of different projects based on the group member's interests, and the research described in this work encompasses a number of them.

Because the compounds we study are often a challenge to generate and characterize by traditional methods employed by organic chemists, the techniques we utilize span the divisional boundaries of chemistry. Throughout the course of my studies, I have employed organic synthesis, matrix isolation techniques, a wide variety of spectroscopic analyses, and integration of computational data in order to complete numerous projects. In each case, the result is the profile of a unique molecule that provides depth to the way we think about electronic structure and photochemistry.

In Chapter 1, I describe the investigation of the alkylated carbon chain Me-C_3-Me. The structure and photochemistry of this surprisingly complex substituted propargylene requires the combination of nontrivial synthesis, elaborate computational analysis, and IR, UV-vis, and EPR spectroscopies to fully understand. The very subtle differences between isomers on the potential energy surface made the results difficult to interpret at first glance but also contribute to the rich depth of understanding the study provides to systems of this type.

The second chapter details my contributions to a project originating from a matrix-isolation study in the lab of Rui Fausto and facilitated on site at Wisconsin by Dr. Cláudio Nunes. Our work together involved probing a hydrogen-migration reaction of an aldehyde hydrogen to a nitrene that is believed to occur through a tunneling process. Much like the matrix-isolation study in Chapter 1, this project involves synthesis of precursors to the nitrene species, matrix isolation, and IR, UV/vis, and EPR spectroscopies. By using this diverse array of techniques, we were able to collect a variety of convincing evidence that a tunneling mechanism is operative for the observed H-migration reaction. If tunneling is operative, the reaction would be notable from two perspectives: 1. It is the first observation of an sp^2 H-migration through tunneling. 2. It is the first documented tunneling reaction to a nitrene.

The third chapter shifts gears from low-temperature studies of reactive intermediates to the study of thermally activated Bergman cyclization reactions. The project originates from observed enetetrayne dimers formed from linear carbon chains like those described in Chapter 1. These enetetrayne species are known to undergo Bergman cyclization reactions *via p*-benzyne intermediates during combustion and soot formation. The connection between the linear carbon chain species and the formation of larger aromatic systems warranted further investigation, and a former student in our lab, Dr. Katherine Windsor, made great strides to characterize the kinetics

of Bergman cyclizations involving tetraethynylethene and various derivatives. The work described in Chapter 3 involves progress toward applying the kinetic studies done by Dr. Windsor to be done *in situ* using React-IR.

Chapter 4 describes a body of work in collaboration with the Zwier research group at Purdue University. In line with our focus on astrochemistry, the Zwier group is interested in sophisticated spectroscopic investigations of the photochemistry and discharge-driven chemistry of chemical systems relevant to the atmosphere of Saturn's largest moon, Titan. Their interest in expanding their spectroscopic search to nitrile functionality (particularly relevant to chemistry on Titan) necessitated the synthesis of a small family of unsaturated nitriles. The synthesis of these compounds, especially that of 1-cyano-1,3-butadiene, proved to be a fascinating story in itself.

My training in the lab has allowed me great flexibility and provided a rich skill set that can be applied in a number of different arenas. Engaging in a wide breadth of disciplines has allowed me to benefit from the diversity inherent in the field of chemistry. Furthermore, it has forced me to confront the challenging problem of communicating across divisional boundaries. The ability to articulate my work to an audience from a different disciplinary background has been crucial to my development both as a scientist and as an educator. The joy of effectively facing this challenge revealed my passion for education and ultimately led me toward research questions regarding the best way to facilitate this type of understanding in the classroom. In addition to my disciplinary research, I carried out a pedagogical research internship that allowed me to apply my research skills from the lab to questions about the best way to enable student learning. While the methods and goals were quite different, the focus in many ways remained the same. The focus on fundamental reactivity derived from structural and electronic features of molecules is at the core of my teaching philosophy. The project I worked on revealed methods

that I can use in the future to maintain this focus without sacrificing the inclusion of critical content.

Chapter 5 introduces my experiences in discipline based education research that I have pursued through my internship with the Delta program. In this project, I implemented a flipped classroom in a general chemistry class at Madison College and assessed the cognitive skills engaged by the students. The project not only showed me how valuable evidence based teaching techniques are as an instructor but also how drawn I am to innovations in chemical education. In researching the literature for the project, I became aware the mounting body of evidence describing the efficacy of active learning. Using data performed by education researchers to inform my teaching follows naturally from my training as a scientist, and I am thrilled to contribute to this body of work during my next step as a postdoctoral fellow in chemical education. By treating my teaching as a research endeavor, I will continue to develop my skills as a scientist and continue to emphasize the focus on fundamental chemistry in research and in the classroom.

While the projects described in this work cover a wide breadth of topics, the element that brings them together is the drive for a deeper fundamental understanding of chemical systems. Through the course of my time in graduate school, I have found consistency between my research and educational interests by remaining grounded in crosscutting concepts and emphasizing them in the presentation of my research and in the classroom. By maintaining this focus, a firm foundation can be built from which knowledge can be constructed and discovery can flourish.

Table of Contents

List of Schemes

List of Figures and Tables

Chapter 1

Chapter 1: Matrix Isolation Spectroscopy and Photochemistry of 1,3-Dimethylpropynylidene (Me-C_3-Me)

The content contained in this chapter has been submitted for publication.

Contributions have been made by Terese A.Waltz, Benjamin C. Haenni, and Nicola J. Burrmann

Introduction

The study of acetylenic carbenes and conjugated carbon chain molecules offers a deeper understanding of many chemical systems. The fundamental reactivity of these molecules can be exploited to reveal nuances in fields such as organometallic chemistry[1,2] with applications to organic synthesis,[3,4] conducting polymers, and other electronic and optical materials.[5-9]

The structure determination of carbon chains is a challenge that can be undertaken using a variety of tools and careful analysis. Specifically, it is important to determine whether each species more closely reflects a localized carbene or delocalized diradical, a computational challenge due to the effects of delocalization on the treatment of the system.[10-14] Traditionally in the McMahon group, this family of compounds has been investigated using EPR, IR, and UV/vis spectroscopies in conjunction with an appropriate computational method to determine structural signatures.

The subtleties in the structure of MeC_3Me make nomenclature challenging. The singlet and triplet states of MeC_3Me are each described by important resonance contributions from both carbene (propynylidene nomenclature: 1,3-dimethylpropynylidene or pent-3-yn-2-ylidene) and diradical (allene-diyl nomenclature: 1,3-dimethylallen-1,3-diyl or penta-2,3-dien-2,4-diyl) structures. For this reason, we often refer to the species by formula (MeC_3Me) rather than by name.

Background

Propynylidene (HCCCH; ^{3}**1**), the simplest acetylenic carbene, is an intermediate in reactions relevant to astrochemistry[15,16] and combustion of fuel-rich hydrocarbon flames.[17-19] The geometry and electronic structure of triplet propynylidene were once debated, but it is now generally accepted that ^{3}**1** exists as a quasilinear species with C_2 equilibrium geometry (Scheme

Scheme 1.1.

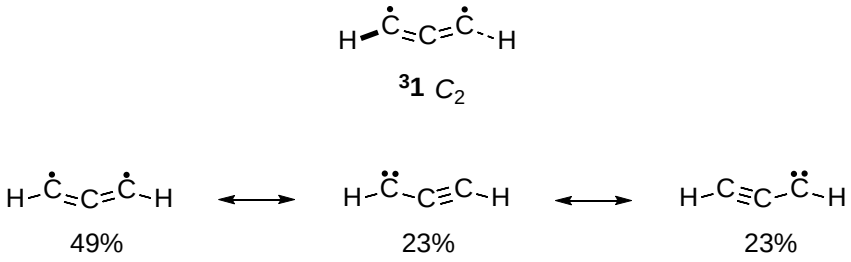

1.1).[20-23] The electronic structure of ^{3}**1** is best described as a nearly equal admixture of carbenic (1,1-diradical) and allenic (1,3-diradical) character (Scheme 1.1).

The case of triplet propynylidene notwithstanding, the study of acetylenic carbenes inevitably confronts the possibility of a localized carbene structure and the existence of bond-shift isomers (Scheme 1.2). 1,3-Diphenylpropynylidene (PhC_3Ph; ^{3}**2**), the most carefully studied substituted derivative of propynylidene, exhibits a symmetrical, allenic diradical structure with a triplet ground state.[24] In the current investigation, we describe experimental and computational studies of 1,3-dimethylpropynylidene (MeC_3Me) (^{3}**3**). Although spectroscopic characterization (IR, UV/vis, and EPR) of MeC_3Me (^{3}**3**) under matrix isolation conditions reveals many similarities to the parent HC_3H system, theory predicts that symmetrical substitution of HCCCH with two methyl substituents leads to an unsymmetrical, localized carbenic structure. The studies

described herein answer some questions, and raise others, concerning the structure of triplet MeC_3Me (^{3}**3**).

Scheme 1.2.

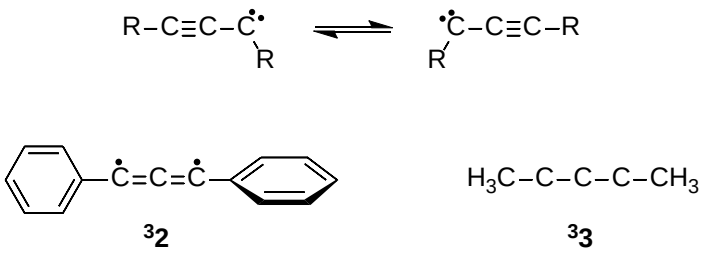

^{3}**2** ^{3}**3**

Matrix isolation (N_2 or Ar) of the diazo precursor 2-diazo-3-pentyne (**2**) and subsequent photolysis affords the molecule of interest, triplet MeC_3Me (^{3}**3**). Characterization by IR, UV/vis, and EPR spectroscopy reveals many similarities to the parent system. UV irradiation of matrix isolated ^{3}**3** results in photochemical isomerization to penten-3-yne (**4**), confirmed by computational results as well as matrix isolation of a genuine sample. Determination of EPR zero-field splitting parameters of ^{3}**3**, study of photoreactivity through IR spectroscopy, and signatures in the electronic absorption spectrum provide information about how alkyl substituents affect the reactivity and structure of species in the R^1-C_3-R^2 family.

Results and Discussion

Carbene Precursor

The preparation of 2-diazo-3-pentyne (**11**) was not as straightforward as our prior work would lead us to believe. Pent-3-yn-2-one (**8**) was prepared according to literature procedures (Scheme 1.3).[25,26] Tosylhydrazone formation is occasionally problematic with simple ynals or ynones because of either conjugate addition or intramolecular cyclization of the initially formed

Scheme 1.3.

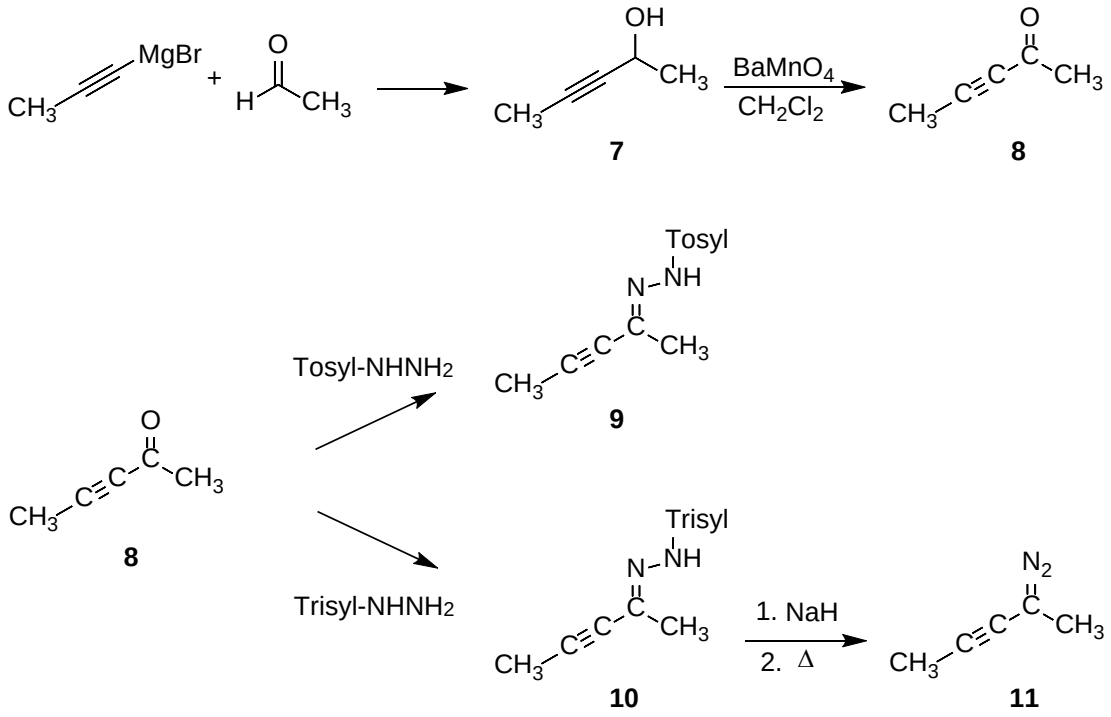

tosylhydrazone to yield a pyrazole derivative.[27,28] In the current case, tosylhydrazone formation seemed to proceed normally, but subsequent treatment of the adduct with NaH under usual reaction conditions did not afford the sodium salt. Although we were able to prepare the lithium salt of the tosylhydrazone with *n*-BuLi, thermolysis of the salt with matrix isolation trapping of the products afforded diazo compound **11** in low yield and impure form, as judged by the matrix IR spectrum. Thus, we turned to the preparation of the trisylhydrazone derivative – an approach that we employed in the related case of 1-diazo-1,3-diphenyl-2-propyne.[24] Trisyl hydrazone was prepared according to Scheme 1.3 and acquired in 58% yield. Gentle thermolysis of the sodium salt of trisylhydrazone **10** smoothly afforded 2-diazo-3-pentyne (**11**).

Spectroscopy and Photochemistry of Me–C–C–C–Me (^{3}3).

Scheme 1.4.

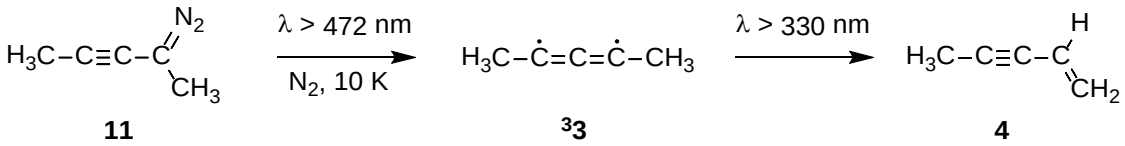

Photolysis (λ > 472 nm) of 2-diazo-3-pentyne (**11**) under matrix isolation conditions (Ar or N_2, 10 K) produces spectroscopic features attributable to triplet Me-C-C-C-Me (^{3}**3**) (Scheme 1.4), as observed by IR, UV/vis, and EPR spectroscopy. Triplet MeC_3Me (^{3}**3**) is photosensitive to near-UV irradiation (λ > 330 nm), undergoing an intramolecular 1,2-hydrogen shift to produce pent-1-en-3-yne (**4**). In the following sections, we will discuss the details of the spectroscopic characterization of ^{3}**3**.

IR Spectroscopy

Photolysis (λ > 472 nm, 6 h; N_2, 10 K) of 2-diazo-3-pentyne (**11**) results in disappearance of IR absorptions associated with the diazo compound and appearance of new bands that can be attributed to triplet MeC_3Me (^{3}**3**) (Figure 1.1). It should be noted that the computed IR spectra presented in Figure 1.1 reflect not merely different levels of computational theory, but also different predicted structures. The high symmetry structure (D_3) predicted by B3LYP/6-31G(d) does not exhibit an IR-active C=C=C symmetric stretching vibration, while the low symmetry structure (C_1) predicted by CCSD(T)/ANO1 does (1818 cm^{-1}). Neither computational method takes into account the effects of anharmonicity. The unusually sharp peak at 1598 cm^{-1} in the experimental spectrum occurs in a region of the spectrum that is often contaminated by water in the spectrum. We are not confident in assigning this feature to triplet MeC_3Me (^{3}**3**), and we note

that the agreement with the feature at 1818 cm^{-1} in the predicted spectrum is much poorer than would be expected for a computation at this high level of theory. Thus, our tentative conclusion is that the absence of a C–C–C symmetric vibration in the IR spectrum of triplet MeC_3Me (^{3}**3**) implies either a high-symmetry structure or a quasilinear molecular structure, in which degenerate unsymmetrical structures equilibrate because the barrier to linearity lies below the zero-point energy. (The parent HC_3H is quasilinear.[22,23])

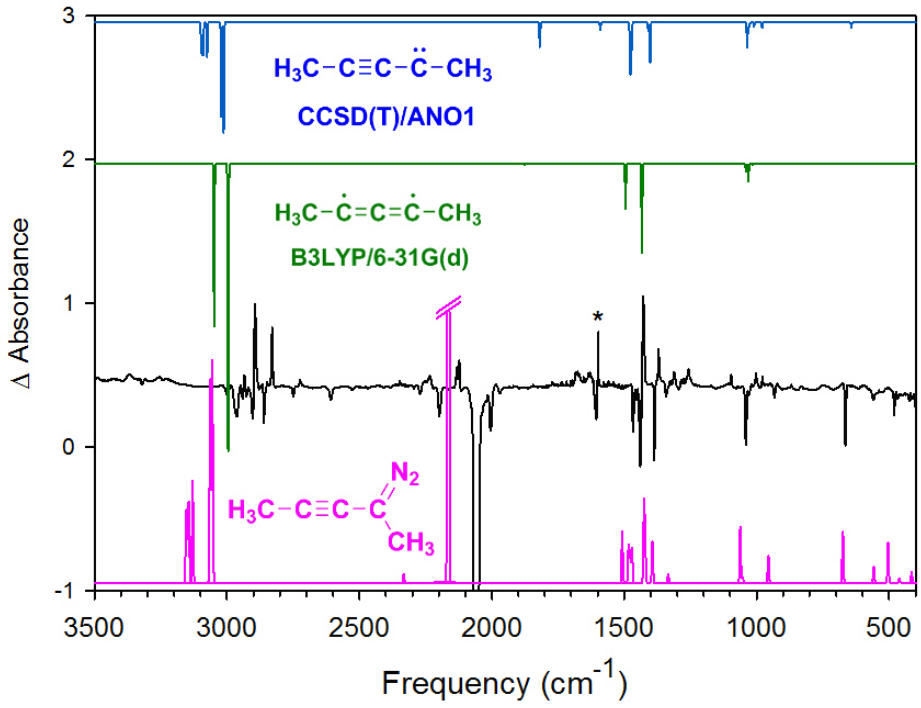

Figure 1.1. Above: Computed IR spectra for triplet MeC_3Me (^{3}**3**) at CCSD(T)/ANO1 (top) and B3LYP/6-31G(d) (below) Middle: IR subtraction spectrum showing the disappearance of 2-diazo-3-pentyne (**11**) and appearance of triplet MeC_3Me (^{3}**3**) upon irradiation ($\lambda > 472$ nm, 6 h, N_2, 10 K) Bottom: Computed spectrum for 2-diazo-3-pentyne (**11**) (CCSD/cc-pVDZ).

Subsequent irradiation ($\lambda > 330$ nm, 24 h, N_2, 10 K) of the matrix containing triplet MeC_3Me (^{3}**3**) causes the disappearance of the IR absorptions associated with the triplet species and the appearance of new absorptions (Figure 1.2). The identity of the photoproduct is assigned as pent-1-en-3-yne (**4**), the product of 1,2-hydrogen migration in Me–C–C–C–Me, by comparison with an IR spectrum of an authentic sample of enyne **4**. To determine whether the 1,2-hydrogen shift reaction might also proceed via a tunneling mechanism, we allowed a matrix containing triplet MeC_3Me (^{3}**3**) to stand in the dark at 10 K (see Supporting Information Figure

S1.3 for spectra). After 24 h, no changes were observed in the IR spectrum (UV/vis, also), thereby establishing that a hydrogen atom tunneling process is not operative.

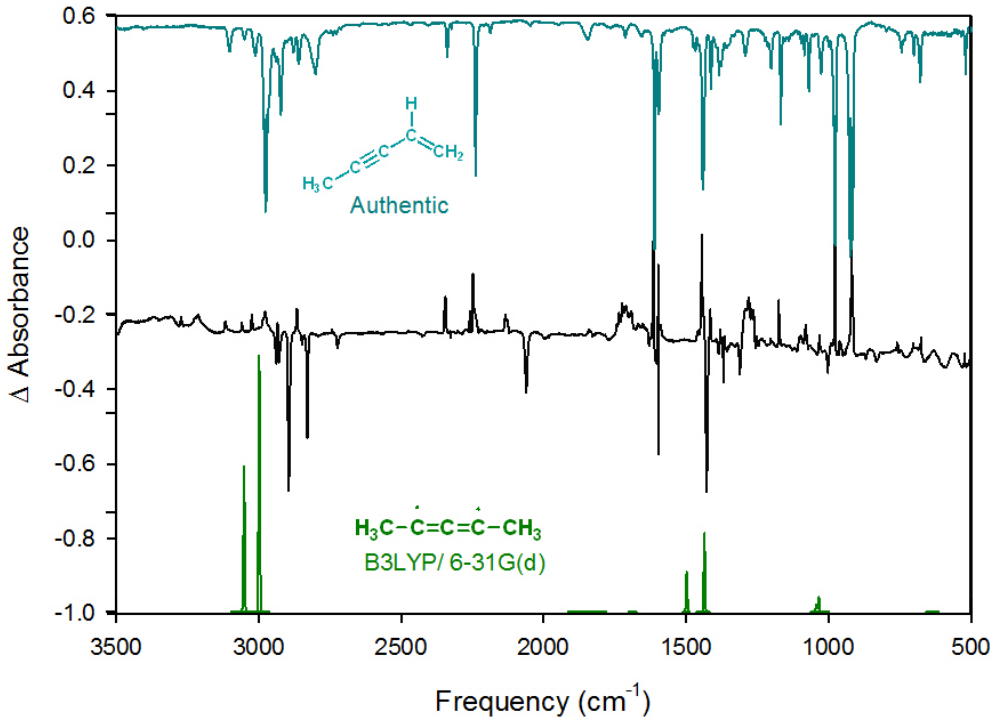

Figure 1.2. Top: Authentic IR spectrum of matrix isolated pent-1-en-3-yne (**4**) (N_2, 10 K). Middle: IR subtraction spectrum showing the disappearance of triplet MeC_3Me (^{3}**3**) and appearance of pent-1-en-3-yne (**4**) upon irradiation ($\lambda > 330$ nm, 24 h, N_2, 10 K) (D = residual diazo compound **11**). Bottom: Computed IR spectrum of triplet MeC_3Me (^{3}**3**) (B3LYP/6-31G(d)).

UV/vis Spectroscopy

Photolysis ($\lambda > 472$ nm, 11 h, N_2, 13 K) of 2-diazo-3-pentyne (**11**) results in bleaching of the strong UV absorption associated with the diazo compound (λ_{max} 250 nm) and appearance of a weak near-UV absorption (λ_{max} 350 nm) that can be attributed to triplet MeC_3Me (^{3}**3**) (Figure 1.3). The position and relative intensity of the electronic absorption of triplet MeC_3Me (^{3}**3**) is quite similar to that observed previously for triplet HC_3H (^{3}**1**), with the absorption of MeC_3Me (^{3}**3**) exhibiting a slight redshift (λ_{max} 350 nm vs. 310 nm).[21] In analogy to the behavior observed in the IR experiments, photoexcitation ($\lambda > 330$ nm, 3 h) into the near-UV electronic absorption (λ_{max} 350 nm) of triplet MeC_3Me (^{3}**3**) results in efficient bleaching of the absorption of ^{3}**3** and the appearance of a strong UV absorption (presumably) attributable to pent-1-en-3-yne (**4**), the product of 1,2-hydrogen migration (Figure 1.3). As noted above, when a matrix containing triplet MeC_3Me (^{3}**3**) was left in the dark for 24 h, no changes occurred in the electronic absorption spectrum.

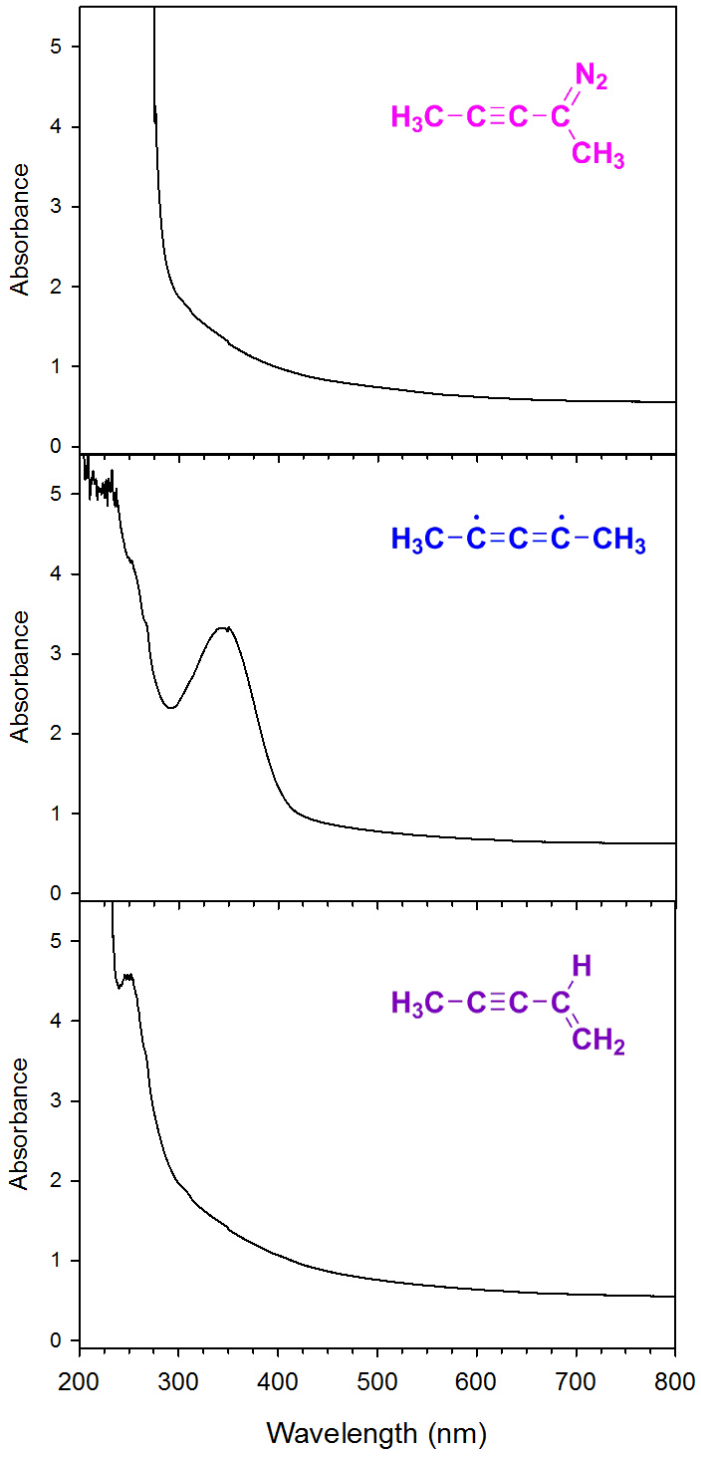

Figure 1.3. Top: Electronic absorption spectrum of 2-diazo-3-pentyne (**11**) after deposition (60 min, N_2, 13 K) Middle: triplet MeC_3Me (^{3}**3**) obtained upon irradiation of **11** ($\lambda > 472$ nm, 11 h). Bottom: pent-1-en-3-yne (**4**) obtained upon irradiation of ^{3}**3** ($\lambda > 330$ nm, 3 h).

EPR Spectroscopy

Photolysis (λ > 613 nm, 13.75 h; Ar, 10 K) of 2-diazo-3-pentyne (**11**) affords the triplet EPR spectrum of MeC_3Me (^{3}**3**) (Figure 1.4). The appearance of two sets of signals in the EPR spectrum (major and minor) could be a result of a matrix effect or the presence of distinct conformational isomers. An axially symmetric structure for MeC_3Me (^{3}**3**) should exhibit a single XY_2 transition rather than distinct X_2 and Y_2 transitions. That being said, the deviation from axial symmetry is not large. The issues of matrix effects and relaxed vs. non-relaxed structures have been dealt with, in considerable detail, for the closely related cases of HC_3H

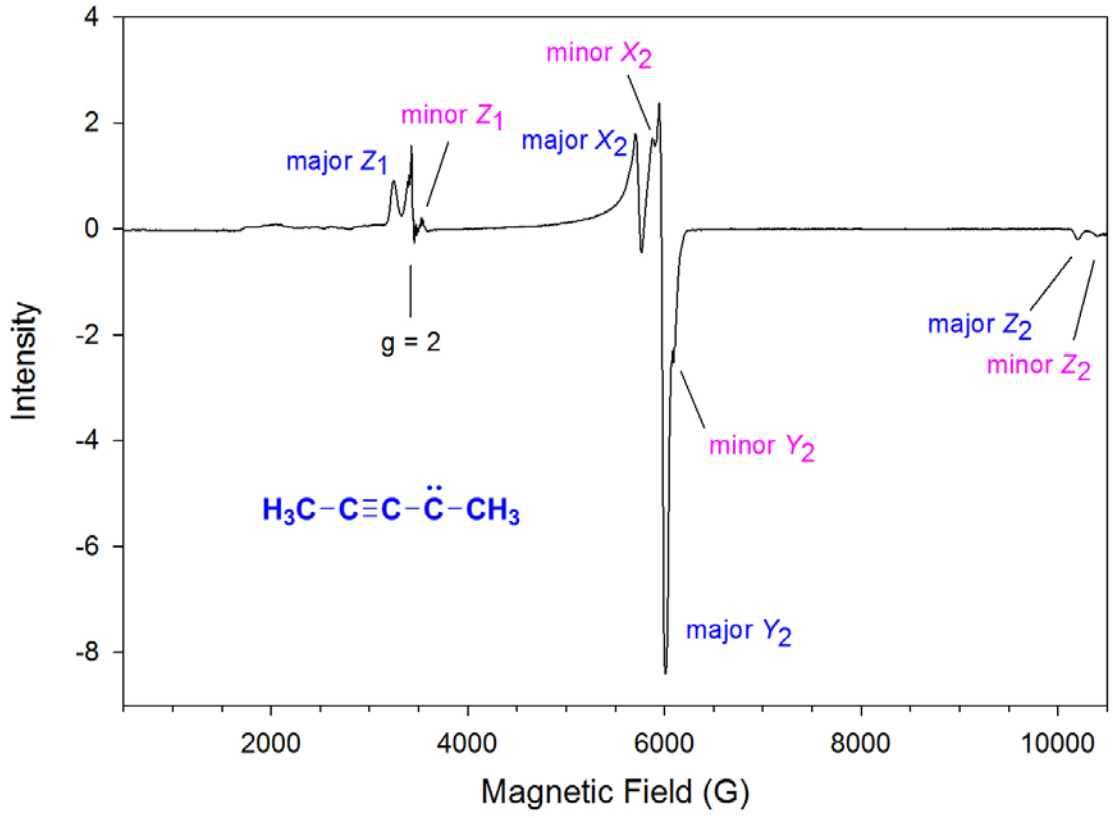

Figure 1.4. EPR spectrum of triplet MeC_3Me (^{3}**3**) after irradiation of 2-diazo-3-pentyne (**11**) (λ > 613 nm, 13.75 h, Ar, 10 K).

(^{3}**1**)[22] and PhC_3Ph (^{3}**2**).[24]

The values of the zero-field splitting parameter *D* (major: $|D/hc| = 0.627$ cm$^{-1;}$; minor: 0.651 cm^{-1}) are comparable to the parent HC_3H ($|D/hc| = 0.64$ cm^{-1}),[21,22] indicating that alkyl substituents do not greatly affect the spin density of the π system. A similar relationship was observed among the triplets HC_5H, MeC_5H, and MeC_5Me.[29] While the large *D* value might seem to favor a carbenic structure rather than a 1,3-allenic diradical structure, it is now understood that one-center dipolar couplings of the unpaired spins at the C-1 and C-3 positions of the carbon chain give rise to large *D* values in systems of this type.[22] The very small values of the zero-field splitting parameter *E* (major: $|E/hc| = 0.0073$ cm^{-1}; minor: 0.0048 cm^{-1}) are consistent with small deviations from axial symmetry – whether they be intrinsic to the structure or imposed by subtle perturbations of the host matrix.

Subsequent irradiation (λ > 299 nm) of the matrix containing triplet MeC_3Me (^{3}**3**) causes a substantial decrease of the triplet signal, consistent with the photoisomerization of MeC_3Me (^{3}**3**) to pent-1-en-3-yne (**4**). No new triplet EPR transitions were observed in subsequent irradiations at shorter wavelengths.

Photochemistry

The family of structures on the C_3H_2 potential energy surface exhibits a rich network of photoisomerization reactions,[21] many of which involve hydrogen migration. In the phenyl-substituted series (PhC_3Ph), the analogous migration reactions of phenyl substituents are not observed, but the photocyclization reaction of triplet PhC_3Ph to form singlet 2,3-diphenylcyclopropenylidene still occurs.[24] In analyzing our IR data involving the photochemistry of MeC_3Me (^{3}**3**), we checked for the formation of 2,3-dimethylcyclopropenylidene (**5**) but found none. Photoexcitation (λ > 330 nm, 3 h) into the near-UV electronic absorption (λ_{max} 350 nm) of

triplet MeC_3Me (^{3}**3**) affords 1,2-hydrogen migration, to form pent-1-en-3-yne (**4**), as the dominant photochemical process. This mode of photochemical reactivity has also been observed with MeC_5H,[30] MeC_5Me,[29] and MeC_7H.[31] We explored broad range of irradiation wavelengths in the study of triplet MeC_3Me (^{3}**3**), but no additional photoproducts were observed.

Summary of Computational Results (*Calculations performed by Ben Haenni*)

C_5H_6 Isomers

Computed relative energies of several pertinent C_5H_6 isomers (CCSD/cc-pVDZ + ZPVE) are provided in Figure 1.5. The relative energies of the isomers on the C_5H_6 potential energy surface help rationalize observed photochemistry. Enyne **4** is predicted to be 32.5 kcal/mol below any other isomer on the surface and is the only photoproduct observed. Although isomer **5** is predicted to be lower in energy than ^{3}**3** and HC_3H precedent would lead us to expect it as a photoproduct, the relative stability of enyne **4** explains the absence of any other photoproduct.

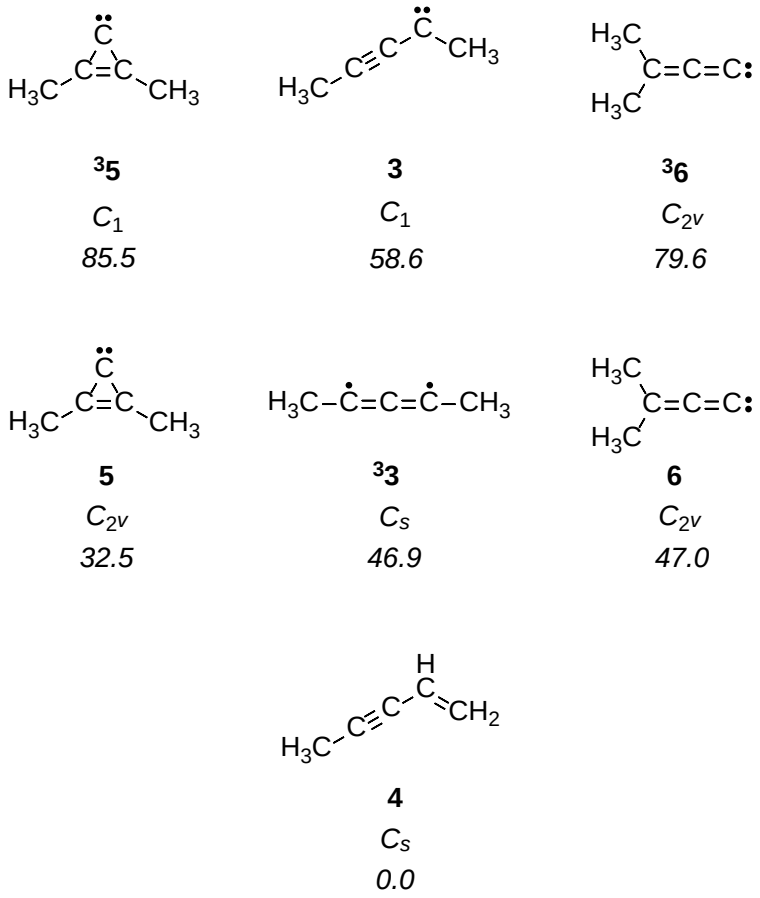

Figure 1.5. Computed relative energy (kcal/mol; CCSD/cc-pVDZ, including ZPVE) of selected C_5H_6

Structure of MeC_3Me.

The computed structures of triplet MeC_3Me (^{3}**3**) exhibit subtle differences that depend on the computational method and basis set employed (Figure 1.6). Because subtle differences in structure exhibit different IR spectra, analysis of various structures is necessary to properly assign spectroscopic signatures in the IR. Density functional methods (B3LYP) predict a symmetrical, delocalized structure (D_3 symmetry) in which the deviation from an idealized D_{3d} structure varies with basis set (Figure 1.6a) (Huang *et al.* reported D_{3d} for the optimized structure at B3LYP/6-311G(d,p).[32]) Our DFT studies find that D_{3d} and D_{3h} structures each exhibit one imaginary vibrational frequency. At the CCSD/cc-pVDZ level, the carbon chain is bent and adopts an unsymmetrical, carbene-like structure in which the methyl groups are nonequivalent (C_s geometry) (Figure 1.6b). At the highest level of theory employed in this study (CCSD(T)/ANO1), a further distortion involving the dihedral angle of one of the methyl groups relative to the CCC plane removes all symmetry (C_1 geometry) (Figure 1.6d). In contrast to these subtle complications associated with triplet MeC_3Me (^{3}**3**), the computed structure of singlet MeC_3Me (^{1}**3**) is less sensitive to the levels of theory. At the CCSD/cc-pVDZ level, the structure of singlet MeC_3Me (^{1}**3**) is similar to the C_1 structure obtained for triplet MeC_3Me (^{3}**3**), except for a more pronounced C-C-CH_3 angle at the 'carbene' carbon (155° in ^{3}**3** vs. 114° in ^{1}**3**) (Figure 1.6c). The computed singlet-triplet energy splitting for MeC_3Me is 11.8 kcal/mol (CCSD/cc-pVDZ), which is quite similar to the experimentally measured value of 11.5 kcal/mol for the parent HC_3H.[23]

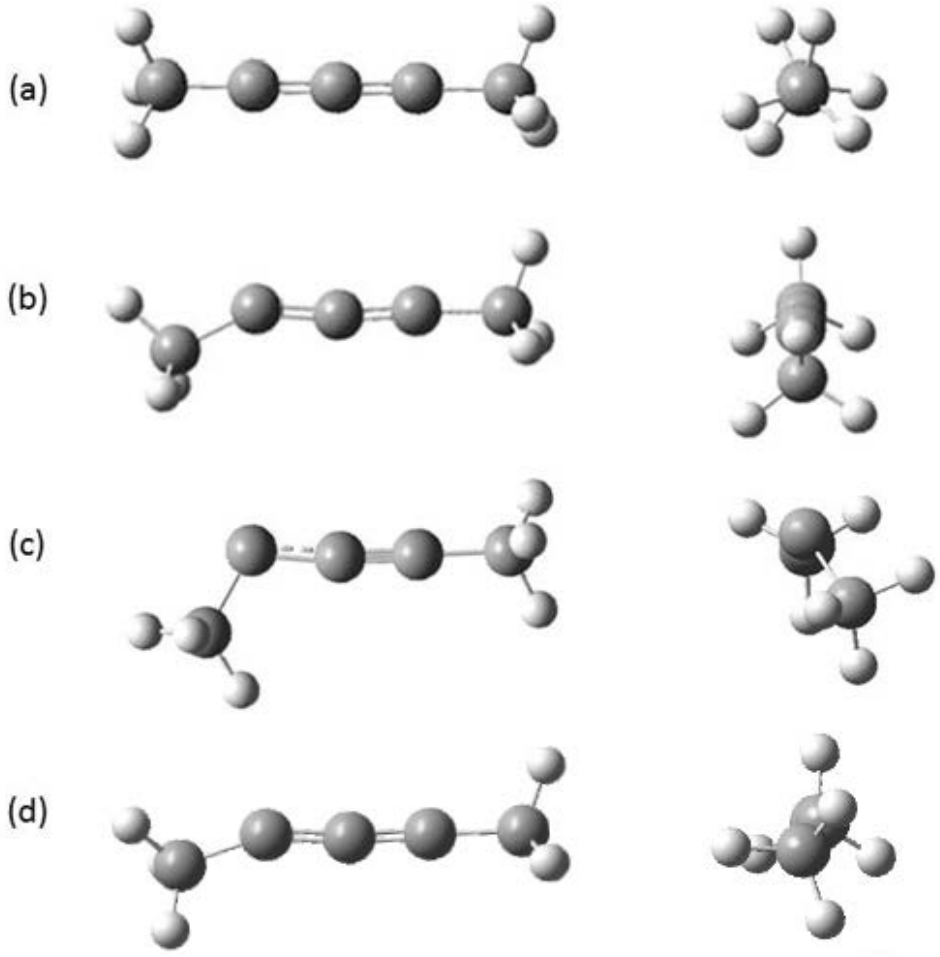

Figure 1.6 Computed structures for triplet and singlet MeC_3Me (**3**). (a) ^{3}**3** at B3LYP/6-31G(d) (D_3). (b) ^{3}**3** at CCSD/cc-pVDZ (C_s). (c) ^{1}**3** at CCSD/cc-pVDZ (C_1). (d) ^{3}**3** at CCSD(T)/ANO1 (C_1).

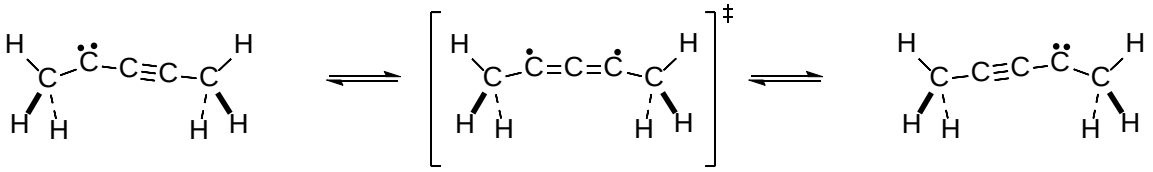

Figure 1.7. Qualitative depiction of putative automerization process in triplet MeC_3Me (^{3}**3**). CCSD/cc-pVDZ structure is C_s symmetry.

Prior experimental [21,22,31,33] and theoretical studies [10,12] establish symmetrical structures for HC_3H, HC_5H, and HC_7H. It was unexpected that symmetrical disubstitution of the symmetrical HC_3H (**1**) would result in an unsymmetrical structure for MeC_3Me (**3**). For the first time, we seem to have stumbled into an acetylenic carbene that favors an unsymmetrical structure. If the molecule is indeed unsymmetrical, then there must be two equivalent unsymmetrical structures (bent at one end, or the other) (Figure 1.7). The atomic motion required to transform one structure into the other is very small. Thus, the putative barrier cannot be very large. We searched the potential energy surface diligently, but without success, to find a transition state between these two equivalent structures.

Because of the subtlety of the structure, the computational investigation of this molecule extended beyond the scope of the spectroscopic work described here. We studied the singly methylated analog (MeC_3H) to get a clearer sense of the effect of methyl substitution on the carbon chain. We also undertook Natural Resonance Theory / Natural Bond Orbital analysis to provide insight concerning spin densities and electron delocalization along the carbon chain in these systems. Details of these investigations are included in our publication of this work.[34] Using these tools, we were able to probe the potential energy surface, gain insight about spin polarization in our EPR data, and accurately interpret the IR spectrum of triplet MeC_3Me, This

information ultimately led to the conclusion that the structure of MeC_3Me is likely quasilinear, as was established for HC_3H.[22,35]

Conclusions

Triplet carbene MeC_3Me (^{3}**3**) has been synthesized and matrix isolated by photolysis of precursor 2-diazo-3-penyne (**11**) in N_2. Its IR, UV/visible, and EPR spectra have been analyzed to determine its structure and photochemistry. The experimental IR spectrum exhibits strong features in the C=C stretching region (~1600 cm^{-1}) analogous to HC_3H[21] and PhC_3Ph.[24]

The photochemistry of the system deviates slightly from HC_3H. UV irradiation ($\lambda > 330$ nm) results in the photoisomerization to penten-3-yne (**4**). The absence of 1,3-dimethylcyclopropenylidene (**5**) and 3,3-dimethylpropadienylidene (**6**) can be rationalized by the energetic favorability of enyne formation. Dark experiments and annealing studies show no indication that the isomerization occurs by tunneling or thermally. Complementary UV/vis experiments confirm observations made in IR experiments. Upon formation of ^{3}**3**, a transition appears at 350 nm. Upon short-wavelength irradiation, the transition disappears. Although quantum chemical calculations predict an unsymmetrical equilibrium structure, they also reveal a shallow potential energy surface. The experimental IR spectrum of triplet MeC_3Me (^{3}**3**) is best interpreted in terms of a quasilinear, axially symmetric structure. Theoretical analysis of the electronic structure of this intriguing molecule suggests that the methyl substituents confer significant spin polarization to this small, open-shell, carbon-chain molecule.

Experimental Section

General Information Chemicals and solvents were purchased and used without purification, unless otherwise noted. ^{1}H NMR spectra (300 or 400 MHz) and ^{13}C NMR spectra (75.4 or 100.6 MHz) were obtained in $CDCl_3$ on a Bruker Avance III 400 spectrophotometer or a Bruker AC+ 300; chemical shifts (δ) are reported as ppm downfield from internal standard $SiMe_4$. Chemicals and solvents were purchased and used without purification, unless otherwise noted. Mass spectra were acquired using a Waters LCT^{TM} high performance liquid chromatography electrospray ionization quadrupole mass spectrometer.

Computational Methods. Equilibrium geometries, harmonic vibrational frequencies, and infrared intensities were computed using density functional or coupled-cluster methods. Density functional calculations were performed using the B3LYP functional and the 6-31G(d) basis set, as implemented in the Gaussian 09 program suite.[36] Coupled-cluster calculations were performed at CCSD or CCSD(T) levels with the cc-pVDZ or ANO1 basis sets, as implemented in the CFOUR program suite.[37] Natural Bond Orbital (NBO) and Natural Resonance Theory (NRT) calculations[38] were performed as implemented in the Gaussian program suite.

Experimental Methods. The matrix isolation apparatus and technique have been described previously.[39,40] Irradiation was carried out with an ILC Technology LX300UV 300 W high-pressure xenon arc lamp, and wavelength selection was achieved with cut-off filters (λ > 613 nm, Corning 2-58; λ > 534, Corning 3-66; λ > 497 nm, Corning 3-69; λ > 472 nm, Corning 3-71; λ > 444 nm, Corning 3-72; λ > 399 nm, Corning 3-74; λ > 363 nm, Corning 3-75; λ > 328 nm, Schott WG 345; λ > 300 nm, Schott WG 320; λ > 280 nm, Pyrex; λ > 261 nm; Corning 0-53; λ > 237 nm, Corning 0-56) or a Spectral Energy GM 252 monochromator (bandpass of 20 nm). All IR spectra were recorded on a Nicolet Nexus 870 FT-IR spectrometer with a DTGS

detector. Electronic spectra were recorded with a Varian Cary 5000 UV/vis/NIR spectrophotometer utilizing a spectral bandwidth of 2.0 nm. EPR spectra were obtained on a Bruker ESP 300 spectrometer with a Bruker ER 042 MRH E microwave bridge and an EIP Model 625A microwave frequency counter. EPR ZFS parameters were determined by a best fit of the observed spectrum to the spin Hamiltonian utilizing the assumption $g_x = g_y = g_e$.[41]

Synthetic Information

Pent-3-yn-2-ol (7).[25] 1-Propynyl magnesium bromide (100 mL, 50 mmol) was concentrated at reduced pressure to approximately 50 mL, purged with nitrogen, and cooled to 0 °C. A solution of freshly distilled and dried acetaldehyde (6 mL, 105 mmol) in 40 mL anhydrous diethyl ether was added dropwise via syringe under nitrogen at 0 °C. The flask was warmed to room temperature and allowed to stir under nitrogen. After 5 h, the reaction was quenched by addition of 60 mL saturated ammonium chloride solution. The white precipitate was removed by vacuum filtration. The aqueous layer of the resulting biphasic solution was extracted twice with diethyl ether. The combined organic layers were washed with water, followed by brine. The ether solution was dried over $MgSO_4$, filtered, and concentrated at reduced pressure to reveal a yellow oil. The crude product was distilled at reduced pressure to afford pent-3-yn-2-ol (**7**) (2.58 g, 30.7 mmol, 61%). ^{1}H NMR (300 MHz, $CDCl_3$): δ 4.50 (qq, *J* = 6.6, 2.1 Hz, 1H), 2.46 (s, br, 1H), 1.84 (d, *J* = 2.1 Hz, 3H), 1.42 (d, *J* = 6.6 Hz, 3H).

Pent-3-yn-2-one (8).[42] To a flame-dried 100 mL round-bottom flask were added 20 mL dry CH_2Cl_2, 6.55 g BaMnO4 (25.6 mmol), and 1.20 mL 3-pentyn-2-ol (12.8 mmol). The mixture was allowed to stir under nitrogen at room temperature overnight. The mixture was filtered through a medium fritted funnel to remove $BaMnO_4$, and the solution was concentrated under reduced pressure to reveal pent-3-yn-2-one (**8**) (0.76 gm 9.27 mmol, 72% yield) as a gold

oil. No purification was necessary. ^{1}H NMR ($CDCl_3$) δ 2.31 (s, 3H), 2.02 (s, 3H). ^{13}C NMR ($CDCl_3$) 184.9, 90.1, 80.6, 32.9, 4.1.

Pent-3-yn-2-one tosylhydrazone (9). To a flask containing 0.76 g (9.23 mmol) pent-2-yn-2-one (**8**) was added 7.0 mL glacial acetic acid and 2.80 g (15.1 mmol) tosylhydrazide. The mixture was allowed to stir under nitrogen at room temperature overnight. The mixture was poured into a beaker containing 100 mL of saturated sodium bicarbonate solution, stirred for 15 min, and poured into a separatory funnel containing dichloromethane and water. The organic layer was dried with anhydrous magnesium sulfate, filtered, concentrated under reduced pressure, and purified using flash column chromatography ($CHCl_3$). Concentration of the appropriate fractions revealed pent-3-yn-2-one tosylhydrazone (**9**) (1.24 g, 4.93 mmol, 53%) as a white powder. ^{1}H NMR (300 MHz, $CDCl_3$) δ 8.61 (s, 1H), 7.84 (d, *J* = 8.0 Hz, 2H), 7.30 (d, *J* = 8.0 Hz, 2H), 2.40 (s, 3H), 2.05 (s, 3H), 1.99 (s, 3H). ^{13}C NMR ($CDCl_3$) δ 144.0, 136.0, 135.7, 129.6, 127.7, 101.4, 71.2, 22.6, 21.3, 4.4. HRMS (ESI) *m/z* $[M+H]^+$ calcd for $C_{12}H_{15}N_2O_2S$ 251.0854, found 251.0856.

2,4,6-Triisopropylbenzenesulfonylhydrazide ("trisylhydrazide").[43] 2,4,6-Triisopropylbenzenesulfonyl chloride (2.05 g, 6.8 mmol) was dissolved in 10 mL THF in a 50 mL, oven-dried round-bottom flask. The solution was cooled to -5°C, and hydrazine monohydrate (1.3 mL, 26.7 mmol) was added dropwise over 15 min. The solution was stirred at 0 °C for 4 h. Water was added to the solution until the precipitate dissolved, ether was added to form a substantial organic layer, and the aqueous layer was removed. The organic layer was washed 3 times with brine, dried over $MgSO_4$, filtered over a pad of Celite, and concentrated under reduced pressure to afford trisylhydrazide (1.74 g, 5.9 mmol, 86%) as a white solid. ^{1}H

NMR (300 MHz, $CDCl_3$): δ 7.20 (s, 2H), 5.44 (s, br, 1H), 4.15 (sept, *J* = 6.6 Hz, 2H), 2.92 (sept, *J* = 6.8 Hz), 1.61 (s, br, 2H), 1.28 (d, *J* = 6.6 Hz, 12H), 1.26 (d, *J* = 6.8 Hz, 6H).

Pent-3-yn-2-one trisylhydrazone (10).[44] Trisyl hydrazide (1.56 g, 3.8 mmol) was added to a 100 mL flask containing pent-3-yn-2-one (**8**) (0.32 g, 3.8 mmol), and the flask was purged with nitrogen for 15 min. To this flask was added 23 mL glacial acetic acid, and the reaction was stirred under nitrogen at room temperature for 2 h. The reaction was quenched by pouring the mixture into a large Erlenmeyer flask containing a solution of saturated $NaHCO_3$ slowly and stirring for 30 min. The solution was extracted three times with dichloromethane. The combined organic layers were washed with saturated $NaHCO_3$ solution, dried over $MgSO_4$, and the pH checked to ensure a neutral solution. The solution was concentrated to reveal a pale yellow solid. The solid was purified by column chromatography (SiO_2, 1:5 EtOAc : hexanes) affording pent-3-yn-2-one trisylhydrazone (**10**) (0.80 g, 2.2 mmol, 58%) as a white solid. ^{1}H NMR (300 MHz, $CDCl_3$): δ 8.28 (s, 1H), 7.16 (s, 2H), 4.21 (sept, *J* = 6.8 Hz, 2H), 2.90 (sept, *J* = 6.9 Hz, 1H), 2.10 (s, 3H), 1.99 (s, 3H), 1.27 (d, *J* = 6.8 Hz, 12H), 1.26 (d, *J* = 6.8 Hz, 6H). HRMS (ESI-Q-IT) *m/z* $[M+H]^+$ calcd for $C_{20}H_{31}N_2O_2S$ 363.2101, found 363.2097.

Pent-3-yn-2-one trisylhydrazone sodium salt. To an oven-dried 25 mL flask, pent-3-yn-2-one trisylhydrazone (**10**) (0.20 g, 0.57 mmol) and NaH (60% in mineral oil) (0.025 g, 0.62 mmol) were added and purged with N_2 for 15 min. To this was added 9.0 mL distilled diethyl ether, and the suspension was stirred under N_2 at room temperature. After 90 min, the suspension was filtered, and the precipitate was thoroughly rinsed with hexane. The white solid was dried overnight *in vacuo*.

2-Diazo-3-pentyne (11). Pent-3-yn-2-one trisylhydrazone sodium salt (0.15 g, 0.40 mmol) was added to the bottom of an oven-dried sublimator and placed under vacuum. The cold-

finger of the sublimator was filled with dry ice/acetone and the bottom of the sublimator was heated to 120 °C. Small pink droplets of 2-diazo-3-pentyne (**11**) began to form on the cold finger within 5 min. The reaction was allowed to continue for 45 min at which time the cold finger was removed, and the diazo compound was rinsed into a deposition tube using freshly distilled diethyl ether that had been dried over CaH_2. Ether was removed *in vacuo* with the deposition tube cooled to -78 °C to yield 2-diazo-3-pentyne (**11**) a bright pink residue at the bottom of the tube. IR (N_2, 10 K) 2965 w, 2928 w, 2901 w, 2860 w, 2199 w, 2067 vs, 2004 w, 1466 w, 1439 m, 1386 m, 1039 w, 664 w cm^{-1} (Figure 1.1); UV/vis (N_2, 10 K) λ_{max} 250 nm (Figure S1.5); UV/vis (MeOH, 298 K) λ_{max} 512, 250 nm (Figure S1.4).

Triplet 1.3-Dimethylpropynylidene (^{3}3). IR (N_2, 10 K) 2931 m, 2897 s, 2830 m, 2725 m, 1443 w, 1429 m, 1369 w, 1311 w, 1002 w cm^{-1} (Figure 1.1); UV/vis (N_2, 10 K) λ_{max} 350 nm (Figure 1.3); EPR (Ar, 10 K) $|D/hc|$ = major: 0.627 minor: 0.651 cm^{-1}, $|E/hc|$ = major: 0.0073 minor: 0.0048 cm^{-1}; Z_1 major: 3240 minor: 3525, X_2 major: 5700 minor: 5885, Y_2 major: 6008 minor: 6092, Z_2 major: 10200 minor: 10400 G; microwave frequency 9.713 GHz (Figure 1.4).

Pent-1-en-3-yne (4).[45] Triethylamine (180 mL) was degassed (nitrogen, 30 min) in a thick-wall pressure tube, and to it was added vinyl bromide (6.0 mL, 85.3 mmol), copper iodide (0.59 g, 3.1 mmol), and bis(triphenylphosphine) palladium(II) dichloride (0.997g, 1.4 mmol). In a separate flask, propyne (8 mL, 106 mmol) was condensed at -78 °C and added via syringe at -78 °C. The pressure tube was sealed with a Teflon screw cap, the cold bath removed, and the mixture stirred at ambient temperature for 18 h. The mixture was first purified by simple distillation. The resulting distillate was then fractionally distilled twice to afford pent-1-en-3-yne (**4)** with traces of triethylamine. To isolate the pure enyne in deposition glassware, a deposition tube was cooled to -78 °C in liquid N_2 under vacuum, and the sample was opened to the system.

The resulting IR spectrum did not show the presence of triethylamine. ^{1}H NMR (400 MHz, $CDCl_3$): δ 5.76 (ddq, *J* = 17.5, 11.0, 2.3 Hz, 1H), 5.55 (dd, *J* = 17.5, 2.2 Hz, 1H), 5.38 (dd, *J* = 11.0, 2.2 Hz, 1H), 1.95 (d, *J* = 2.3 Hz, 3H). IR (N_2, 10 K) 2976 s, 2925 m, 2862 w, 2341 w, 2241 s, 1848 w, 1716 w, 1613 s, 1598 m, 1443 s, 1415 m, 1387 w, 1295 w, 1170 m, 1071 m, 1028 w, 982 s, 929 s, 680 w cm^{-1} (Figure 1.2).

Notes and References

1. Casey, C. P.; Kraft, S.; Powell, D. R. Dimerization of Rhenium Alkynyl Carbene Complexes by a Process Involving Two [1,1.5] Rhenium Shifts and Coupling of the Remote Alkynyl Carbons. *J. Am. Chem. Soc.* **2000**, *122*, 3771-3772.

2. Casey, C. P.; Kraft, S.; Powell, D. R. Formation of cis-Enediyne Complexes from Rhenium Alkynylcarbene Complexes. *J. Am. Chem. Soc.* **2002**, *124*, 2584-2594.

3. Padwa, A.; Austin, D. J.; Gareau, Y.; Kassir, J. M.; Xu, S. L. Rearrangement of alkynyl and vinyl carbenoids via the rhodium(II)-catalyzed cyclization reaction of .alpha.-diazo ketones. *J. Am. Chem. Soc.* **1993**, *115*, 2637-2647.

4. Hansen, E. C.; Lee, D. Search for Solutions to the Reactivity and Selectivity Problems in Enyne Metathesis. *Acc. Chem. Res.* **2006**, *39*, 509-519.

5. Sixl, H. *Advances in Polymer Science* New York, 1984; Vol. 63.

6. Bloor, D. C., R.R. *Polydiacetylenes: Synthesis, Structure, and Electronic Properties* Dordrecht, 1985; Vol. 102.

7. Edelman, M. J.; Odermatt, S.; Diederich, F. Poly(triacetylene)s: A New Class of Linearly π-Conjugated Oligomers and Polymers with an All-carbon Backbone *Chimia* **2001**, *55*, 132-138.

8. Ikoma, T.; Okada, S.; Nakanishi, H.; Akiyama, K.; Tero-Kubota, S.; Möbius, K.; Weber, S. Spin soliton in a π-conjugated ladder polydiacetylene. *Phys. Rev. B* **2002**, *66*, 014423.

9. Akai-Kasaya, M.; Shimizu, K.; Watanabe, Y.; Saito, A.; Aono, M.; Kuwahara, Y. Electronic Structure of a Polydiacetylene Nanowire Fabricated on Highly Ordered Pyrolytic Graphite. *Phys. Rev. Lett.* **2003**, *91*, 255501.

10. Fan, Q.; Pfeiffer, G. V. Theoretical study of linear Cn (n=6−10) and HCnH (n=2−10) molecules. *Chem. Phys. Lett.* **1989**, *162*, 472-478.

11. Seburg, R. A.; McMahon, R. J.; Stanton, J. F.; Gauss, J. Structures and Stabilities of C_5H_2 Isomers: Quantum Chemical Studies. *J. Am. Chem. Soc.* **1997**, *119*, 10838-10845.

12. Horný, L. u.; Petraco, N. D. K.; Schaefer, H. F. Odd Carbon Long Linear Chains HC2n+1H (n = 4−11): Properties of the Neutrals and Radical Anions. *J. Am. Chem. Soc.* **2002**, *124*, 14716-14720.

13. Mavrandonakis, A.; Muhlhauser, M.; Froudakis, G. E.; Peyerimhoff, S. D. The electronic spectrum of linear pentadiynylidene in comparison with isomeric ethynylcyclopropenylidene. *Phys. Chem. Chem. Phys.* **2002**, *4*, 3318-3321.

14. Zhang, C.; Cao, Z.; Wu, H.; Zhang, Q. Linear and nonlinear feature of electronic excitation energy in carbon chains HC_{2n}+1H and $HC_{2n}H$. *Int.J.Quantum Chem.* **2004**, *98*, 299-308.

15. I. Kaiser, R.; Ochsenfeld, C.; Stranges, D.; Head-Gordon, M.; Lee, Y. T. Combined crossed molecular beams and abinitio investigation of the formation of carbon-bearing molecules in the interstellar medium via neutral-neutral reactions. *Faraday Discuss.* **1998**, *109*, 183-204.

16. Smith, I. W. M.; Herbst, E.; Chang, Q. Rapid neutral–neutral reactions at low temperatures: a new network and first results for TMC-1. *Mon. Not. R. Astron. Soc.* **2004**, *350*, 323-330.

17. Miller, J. A.; Klippenstein, S. J. From the Multiple-Well Master Equation to Phenomenological Rate Coefficients: Reactions on a C_3H_4 Potential Energy Surface. *J. Phys. Chem. A* **2003**, *107*, 2680-2692.

18. Taatjes, C. A.; Klippenstein, S. J.; Hansen, N.; Miller, J. A.; Cool, T. A.; Wang, J.; Law, M. E.; Westmoreland, P. R. Synchotron photoionization measurements of combustion intermediates: Photoionization efficiency and identification of C_3H_2 isomers. *Phys. Chem. Chem. Phys.* **2005**, *7*, 806-813.

19. Cool, T. A.; McIlroy, A.; Qi, F.; Westmoreland, P. R.; Poisson, L.; Peterka, D. S.; Ahmed, M. Photoionization mass spectrometer for studies of flame chemistry with a synchrotron light source. *Rev. Sci. Instrum.* **2005**, *76*, -.

20. Seburg, R. A.; DePinto, J. T.; Patterson, E. V.; McMahon, R. J. Structure of Triplet Propynylidene. *J. Am. Chem. Soc.* **1995**, *117*, 835-836.

21. Seburg, R. A.; Patterson, E. V.; Stanton, J. F.; McMahon, R. J. Structures, Automerizations, and Isomerizations of C_3H_2 Isomers. *J. Am. Chem. Soc.* **1997**, *119*, 5847-5856.

22. Seburg, R. A.; Patterson, E. V.; McMahon, R. J. Structure of Triplet Propynylidene (HCCCH) as Probed by IR, UV/vis, and EPR Spectroscopy of Isotopomers. *J. Am. Chem. Soc.* **2009**, *131*, 9442-9455.

23. Ehrenfreund, P.; Charnley, S. B. Organic molecules in the interstellar medium, comets, and meteorites: a voyage from dark clouds to the early Earth. *Ann. Rev. Astron. Astrophys*, **2000**, *38*, 427-483.

24. DePinto, J. T.; deProphetis, W. A.; Menke, J. L.; McMahon, R. J. Triplet 1,3-Diphenylpropynylidene (Ph−C−C−C−Ph). *J. Am. Chem. Soc.* **2007**, *129*, 2308-2315.

25. Muri, D.; Carreira, E. M. Stereoselective Synthesis of Erythronolide A via Nitrile Oxide Cycloadditions and Related Studies. *J. Org. Chem.* **2009**, *74*, 8695-8712.

26. Hamed, O.; Henry, P. M.; Becker, D. P. Palladium(II)-catalyzed dicarboxymethylation of chiral allylic alcohols: chirality transfer affording optically active diesters containing three contiguous chiral centers. *Tetrahedron Lett.* **2010**, *51*, 3514-3517.

27. Seburg, R. A.; Hodges, J. A.; McMahon, R. J. Propynal Equivalents and Diazopropyne: Synthesis of All Mono-^{13}C Isotopomers. *Helv. Chim. Acta* **2009**, *92*, 1626-1643.

28. Bowling, N. P.; Burrmann, N. J.; Halter, R. J.; Hodges, J. A.; McMahon, R. J. Synthesis of Simple Diynals, Diynones, Their Hydrazones, and Diazo Compounds: Precursors to a Family of Dialkynyl Carbenes (R1—C≡C—C̈—C≡C—R2). *J. Org. Chem.* **2010**, *75*, 6382-6390.

29. Thomas, P. S.; Bowling, N. P.; Burrmann, N. J.; McMahon, R. J. Dialkynyl Carbene Derivatives: Generation and Characterization of Triplet tert-Butylpentadiynylidene (t-Bu−C≡C−C̈−C≡C−H) and Dimethylpentadiynylidene (Me−C≡C−C̈−C≡C−Me). *J. Org. Chem.* **2010**, *75*, 6372-6381.

30. Thomas, P. S.; Bowling, N. P.; McMahon, R. J. Spectroscopy and Photochemistry of Triplet Methylpentadiynylidene (Me−C≡C−C̈−C≡C−H). *J. Am. Chem. Soc.* **2009**, *131*, 8649-8659.

31. Shaffer, C. J. Ph.D. Dissertation, University of Wisconsin-Madison, 2010.

32. Hu, J.; Cheng, Y.; Yang, Y.; Rao, Y. A general and efficient approach to 2 H-indazoles and 1 H-pyrazoles through copper-catalyzed intramolecular N–N bond formation under mild conditions. *Chem. Commun.* **2011**, *47*, 10133-10135.

33. Bowling, N. P.; Halter, R. J.; Hodges, J. A.; Seburg, R. A.; Thomas, P. S.; Simmons, C. S.; Stanton, J. F.; McMahon, R. J. Reactive Carbon-Chain Molecules: Synthesis of 1-Diazo-2,4-pentadiyne and Spectroscopic Characterization of Triplet Pentadiynylidene (H−C⁝C−C̈−C⁝C−H). *J. Am. Chem. Soc.* **2006**, *128*, 3291-3302.

34. Knezz, S. N.; Waltz, T. A.; Haenni, B. C.; Burrmann, N. J.; McMahon, R. J. Spectroscopy and Photochemistry of Triplet 1,3-Dimethylpropynylidene (Me–C–C–C–Me). **2016**.

35. Osborn, D. L.; Vogelhuber, K. M.; Wren, S. W.; Miller, E. M.; Lu, Y.-J.; Case, A. S.; Sheps, L.; McMahon, R. J.; Stanton, J. F.; Harding, L. B.; Ruscic, B.; Lineberger, W. C. Electronic States of the Quasilinear Molecule Propargylene (HCCCH) from Negative Ion Photoelectron Spectroscopy. *J. Am. Chem. Soc.* **2014**, *136*, 10361-10372.

36. Frisch, M. J.; Trucks, G. W.; Schlegel, H. B.; Scuseria, G. E.; Robb, M. A.; Cheeseman, J. R.; Scalmani, G.; Barone, V.; Mennucci, B.; Petersson, G. A.; Nakatsuji, H.; Caricato, M.; Li, X.; Hratchian, H. P.; Izmaylov, A. F.; Bloino, J.; Zheng, G.; Sonnenberg, J. L.; Hada, M.; Ehara, M.; Toyota, K.; Fukuda, R.; Hasegawa, J.; Ishida, M.; Nakajima, T.; Honda, Y.; Kitao, O.; Nakai, H.; Vreven, T.; Montgomery, J., J. A.; Peralta, J. E.; Ogliaro, F.; Bearpark, M.; Heyd, J. J.; Brothers, E.; Kudin, K. N.; Staroverov, V. N.; Kobayashi, R.; Normand, J.; Raghavachari, K.; Rendell, A.; Burant, J. C.; Iyengar, S. S.; Tomasi, J.; Cossi, M.; Rega, N.; Millam, N. J.; Klene, M.; Knox, J. E.; Cross, J. B.; Bakken, V.; Adamo, C.; Jaramillo, J.; Gomperts, R.; Stratmann, R. E.; Yazyev, O.; Austin, A. J.; Cammi, R.; Pomelli, C.; Ochterski, J. W.; Martin, R. L.; Morokuma, K.; Zakrzewski, V. G.; Voth, G. A.; Salvador, P.; Dannenberg, J. J.; Dapprich, S.; Daniels, A. D.; Farkas, Ö.; Foresman, J. B.; Ortiz, J. V.; Cioslowski, J.; Fox, D. J. 2009.

37. Stanton, J. F.; Gauss, J.; Harding, M. E.; Szalay, P. G., p with contributions from A. A. Auer, R. J. Bartlett, U. Benedikt, C. Berger, D. E. Bernholdt, Y. J. Bomble, L. Cheng, O. Christiansen, M. Heckert, O. Heun, C. Huber, T.-C. Jagau, D. Jonsson, J. Jusélius, K. Klein, W. J. Lauderdale, D. A. Matthews, T. Metzroth, D. P. O'Neill, D. R. Price, E. Prochnow, K. Ruud, F. Schiffmann, W. Schwalbach, S. Stopkowicz, A. Tajti, J. Vázquez, F. Wang, J. D. Watts and the integral packages: MOLECULE (J. Almlöf and P. R. Taylor), PROPS (P. R. Taylor), ABACUS (T. Helgaker, H. J. Aa. Jensen, P. Jørgensen, and J. Olsen), and ECP routines by A. V. Mitin, C. van Wüllen.

38. Glendening, E. D.; Badenhoop, J. K.; Reed, A. E.; Carpenter, J. E.; Bohmann, J. A.; Morales, C. M.; Landis, C. R.; Weinhold, F.; Theoretical Chemistry Institute, University of Wisconsin-Madison: Madison, WI, 2013.

39. McMahon, R. J.; Chapman, O. L.; Hayes, R. A.; Hess, T. C.; Krimmer, H. P. Mechanistic studies on the Wolff rearrangement: the chemistry and spectroscopy of some .alpha.-keto carbenes. *J. Am. Chem. Soc.* **1985**, *107*, 7597-7606.

40. Seburg, R. A.; McMahon, R. J. Photochemistry of matrix-isolated diazoethane and methyldiazirine: ethylidene trapping? *J. Am. Chem. Soc.* **1992**, *114*, 7183-7189.

41. Wasserman, E.; Snyder, L. C.; Yager, W. A. ESR of the Triplet States of Randomly Oriented Molecules. *J. Chem. Phys.* **1964**, *41*, 1763-1772.

42. Coleman, R. S.; Lu, X.; Modolo, I. Total Synthesis of 2‘-O-Methylmyxalamide D and (6E)-2‘-O-Methylmyxalamide D. *J. Am. Chem. Soc.* **2007**, *129*, 3826-3827.

43. Pattabiraman, V. R.; Stymiest, J. L.; Derksen, D. J.; Martin, N. I.; Vederas, J. C. Multiple On-Resin Olefin Metathesis to Form Ring-Expanded Analogues of the Lantibiotic Peptide, Lacticin 3147 A2. *Org. Lett.* **2007**, *9*, 699-702.

44. Kirmse, W.; Heese, J. Methanolysis of diazoalkynes. *J. Chem. Soc. D, Chem. Commun.* **1971**, 258-259.

45. Brewitz, L.; Llaveria, J.; Yada, A.; Fürstner, A. Formal Total Synthesis of the Algal Toxin (−)-Polycavernoside A. *Chem. Eur. J.* **2013**, *19*, 4532-4537.

Supporting Information for Chapter 1: Matrix Isolation Spectroscopy and Photochemistry of 1,3-Dimethylpropynylidene (Me-C_3-Me)

Experimental Methods. The matrix isolation apparatus and technique have been described previously.[1,2] Irradiation was carried out with an ILC Technology LX300UV 300 W high-pressure xenon arc lamp, and wavelength selection was achieved with cut-off filters ($\lambda > 613$ nm, Corning 2-58; $\lambda > 534$, Corning 3-66; $\lambda > 497$ nm, Corning 3-69; $\lambda > 472$ nm, Corning 3-71; $\lambda > 444$ nm, Corning 3-72; $\lambda > 399$ nm, Corning 3-74; $\lambda > 363$ nm, Corning 3-75; $\lambda > 328$ nm, Schott WG 345; $\lambda > 300$ nm, Schott WG 320; $\lambda > 280$ nm, Pyrex; $\lambda > 261$ nm; Corning 0- 53; $\lambda > 237$ nm, Corning 0-56) or a Spectral Energy GM 252 monochromator (bandpass of 20 nm). All IR spectra were recorded on a Nicolet Nexus 870 FT-IR spectrometer with a DTGS detector. Electronic spectra were recorded with a Varian Cary 5000 UV/vis/NIR spectrophotometer utilizing a spectral bandwidth of 2.0 nm. EPR spectra were obtained on a Bruker EleXsys E-500-A EPR spectrometer consisting of: Bruker ER 049SX X-band microwave bridge (Gunn diode), ER 041-1161 microwave frequency meter, and high-sensitivity resonator with optical port. EPR zero-field splitting parameters were determined by a best fit of the observed spectrum to the spin Hamiltonian utilizing the assumption $g_x = g_y = g_e$.[3]

.

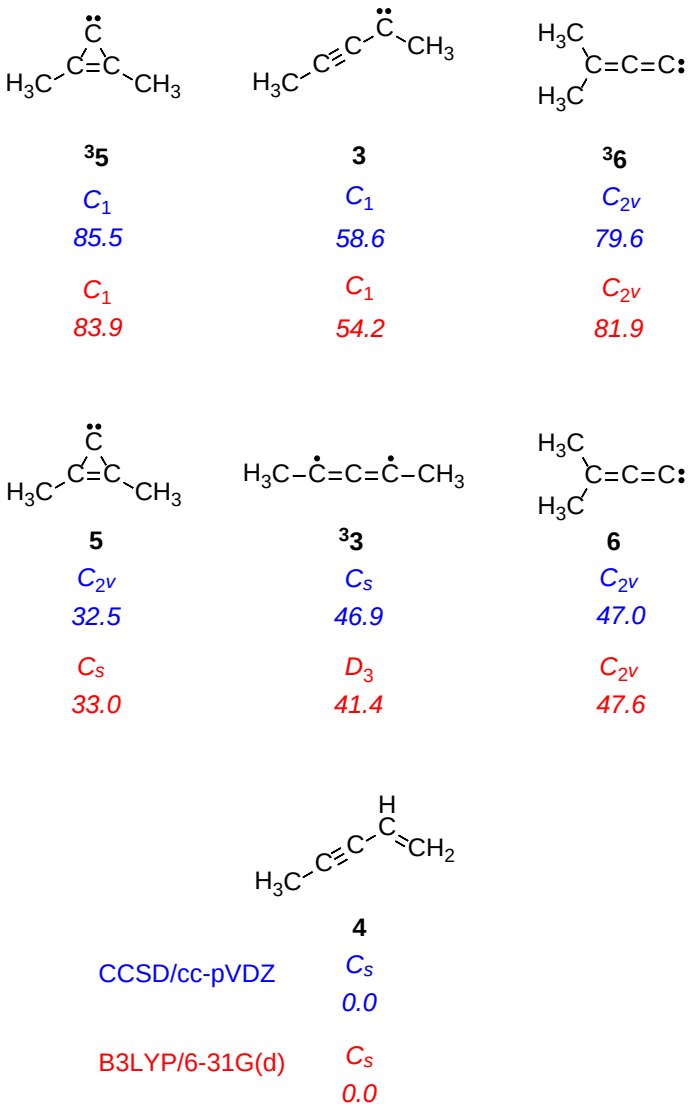

Figure S1.1. Computed relative energies of selected C_5H_6 isomers (kcal/mol; includes ZPVE). Above in blue: CCSD/cc-pVDZ. Below in red: B3LYP/6-31G(d).

Relative energies for isomers **4**, **5**, and **6**, computed using DFT methods (B3LYP/6-31G(d)) show qualitatively good agreement with the CCSD values, but the energies for the delocalized carbon chain isomer, MeC_3Me (^{1}**3**, ^{3}**3**), are too low, reflecting the well-established problem of the B3LYP functional in over-stabilizing delocalized systems of this type.[4-6]

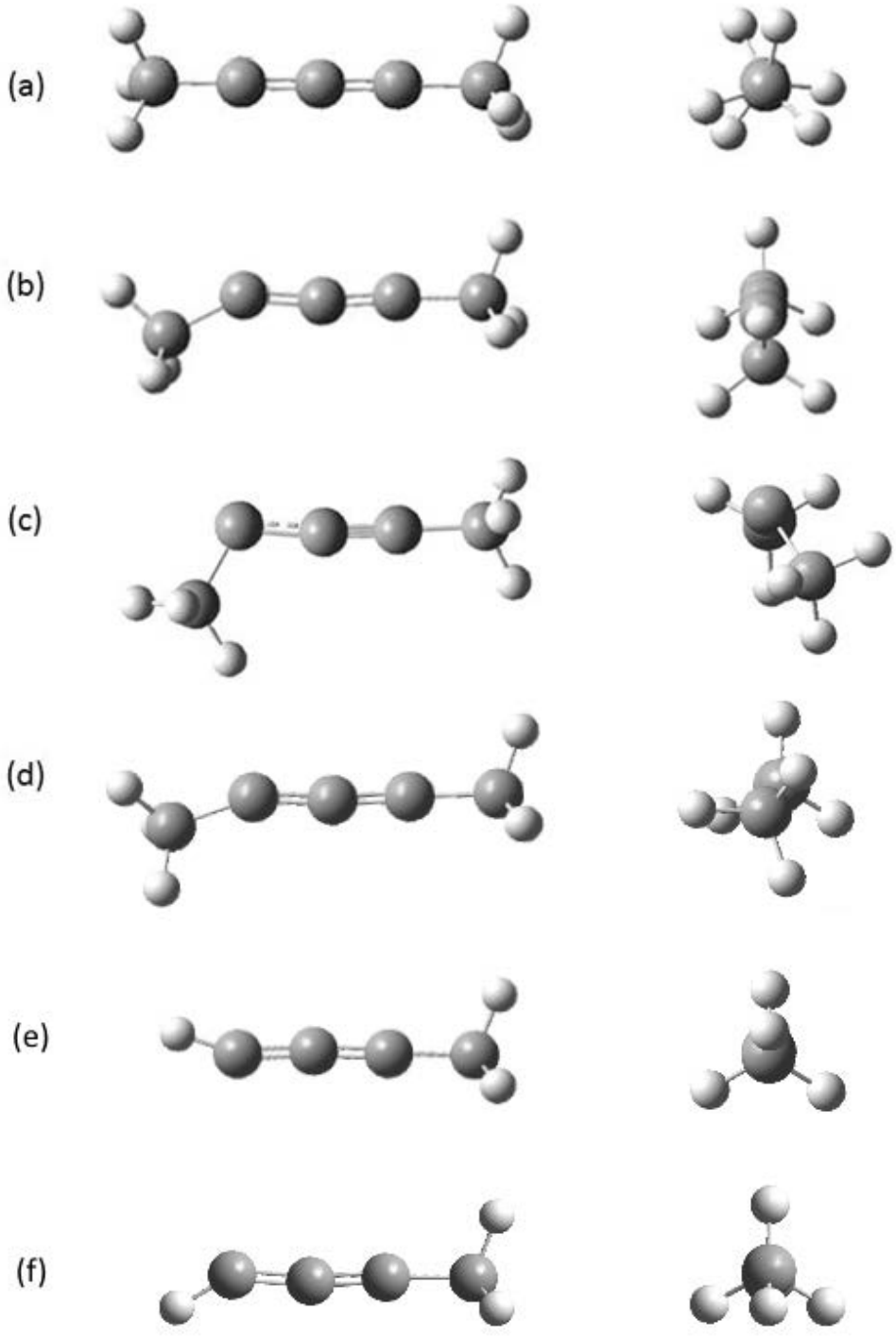

Figure S1.2. Computed structures for MeC_3Me (**3**) and MeC_3H (**12**). (a) ^{3}**3** at B3LYP/6-31G(d) (D_3). (b) ^{3}**3** at CCSD/cc-pVDZ (C_s). (c) ^{1}**3** at CCSD/cc-pVDZ (C_1). (d) ^{3}**3** at CCSD(T)/ANO1 (C_1). (e) ^{3}**12** at B3LYP/cc-pVTZ (C_s). (f) ^{3}**12** at CCSD/cc-pVDZ (C_s).

Isomerization of MeC_3Me (3) to Pent-1-en-3-yne (4). Experiments described in the body of the article establish the isomerization of triplet MeC_3Me (^{3}**3**) to pent-1-en-3-yne (**4**) under photochemical conditions. To gain a more thorough understanding of the reactivity scope, we sought to determine whether the H-shift isomerization might also occur on the ground state through a tunneling mechanism. After generating matrix isolated MeC_3Me (^{3}**3**), the sample was left in the dark at 12 K. No changes were observed in either IR or UV/vis spectra after 24 h, indicating that a tunneling process is occurring. In order to see if temperature affected the reactivity, an annealing experiment was carried out. The temperature of the matrix was increased by 5 K every hour, and an IR spectrum was obtained. This experiment was largely inconclusive due to the poor spectral quality at higher temperatures. It appears that triplet MeC_3Me (**3**) is disappearing; however, signature bands of enyne **4** were not observed. It is possible that these bands were obscured by the noise in the spectrum, but it is impossible to say with confidence that the reaction had occurred (Figure S1.3).

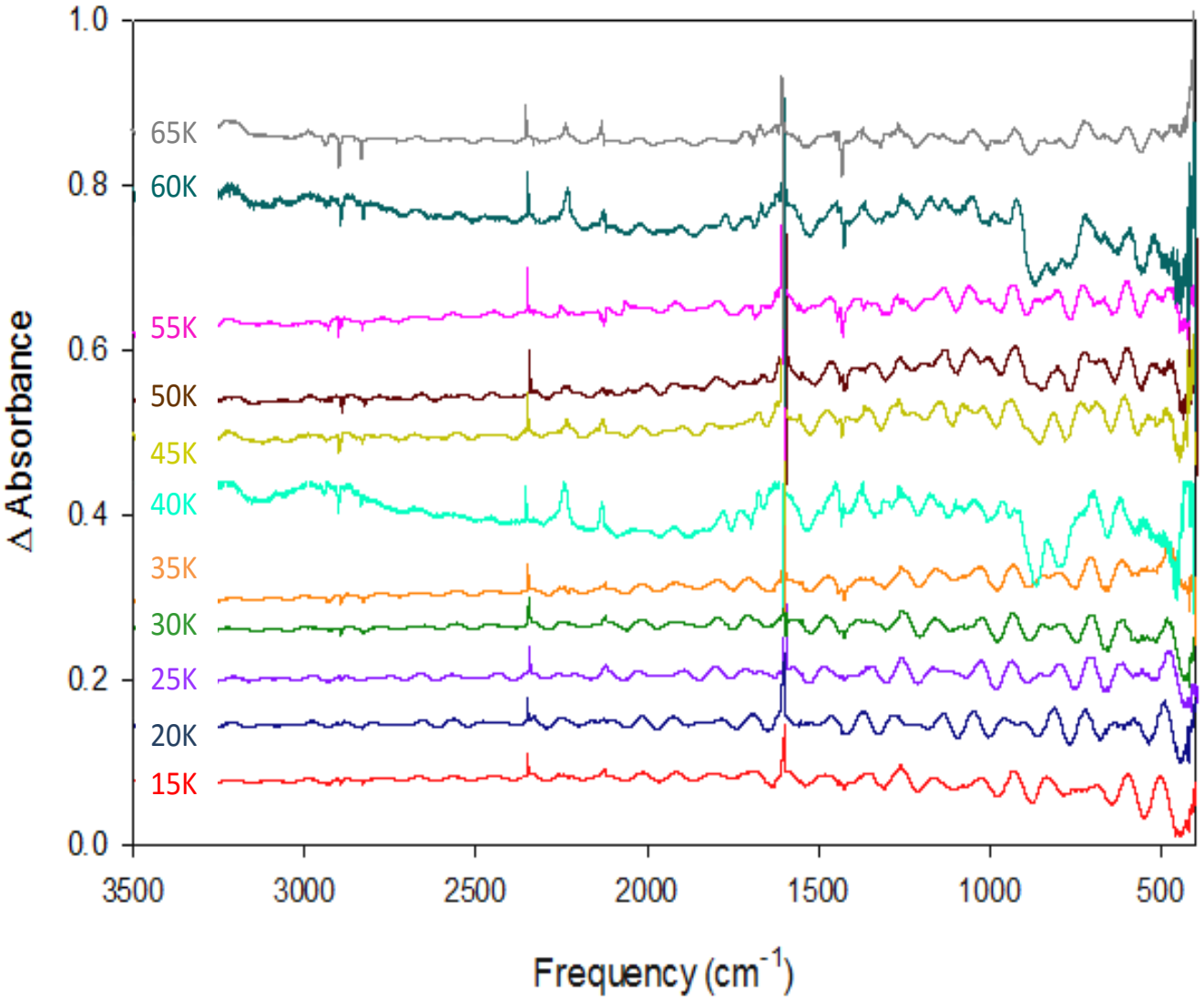

Figure S1.3. IR spectra for the annealing experiment with MeC_3Me (^{3}**3**). A matrix containing ^{3}**3** (N_2, 10 K) was exposed to increasing temperatures (15 K to 65 K when the matrix melted), and IR spectra were acquired at 5 K increments.

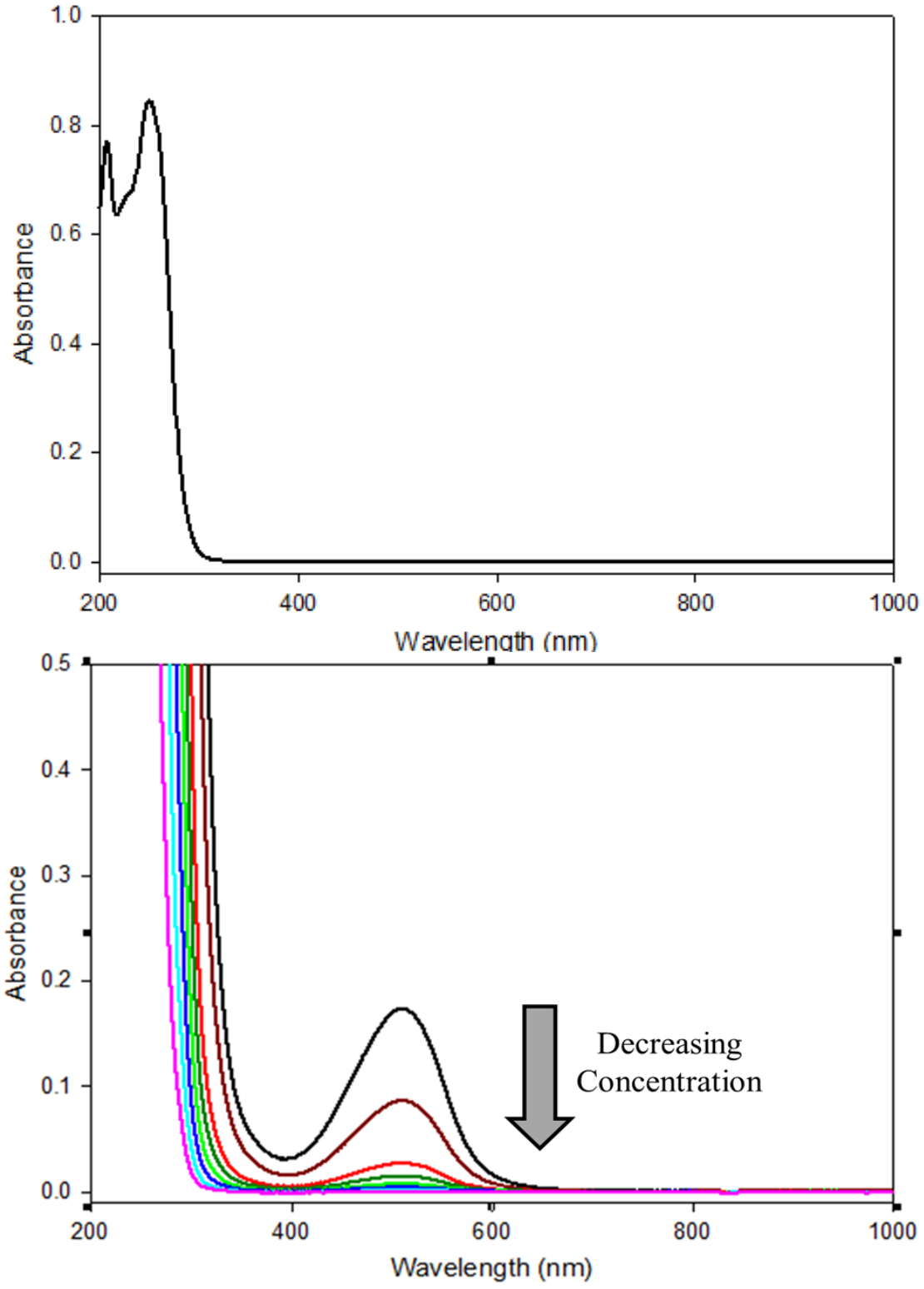

Figure S1.4. Solution phase electronic absorption spectrum of 2-diazo-3-pentyne (**11**) in MeOH at 298 K. Top: Full spectrum revealing λ_{max}= 250 nm. Bottom: Expansion revealing λ_{max} = 512 nm.
Spectra taken of samples obtained upon a series of dilutions. (Actual concentration unknown)

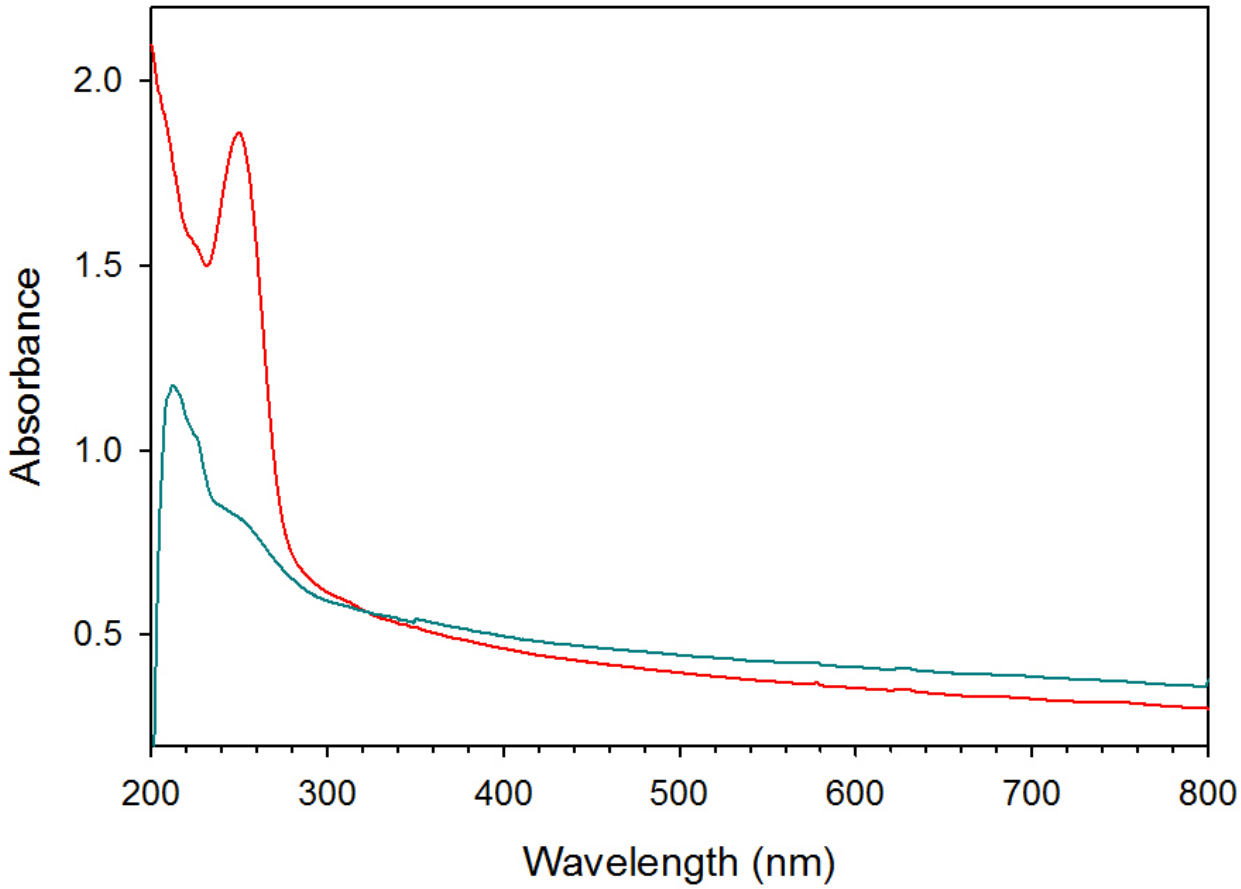

Figure S1.5. Electronic absorption spectrum of 2-diazo-3-pentyne (**11**) (red spectrum) after sample deposition (5 min, N_2, 10 K) and after irradiation ($\lambda > 472$ nm, 16 h; N_2, 10 K) (cyan spectrum).

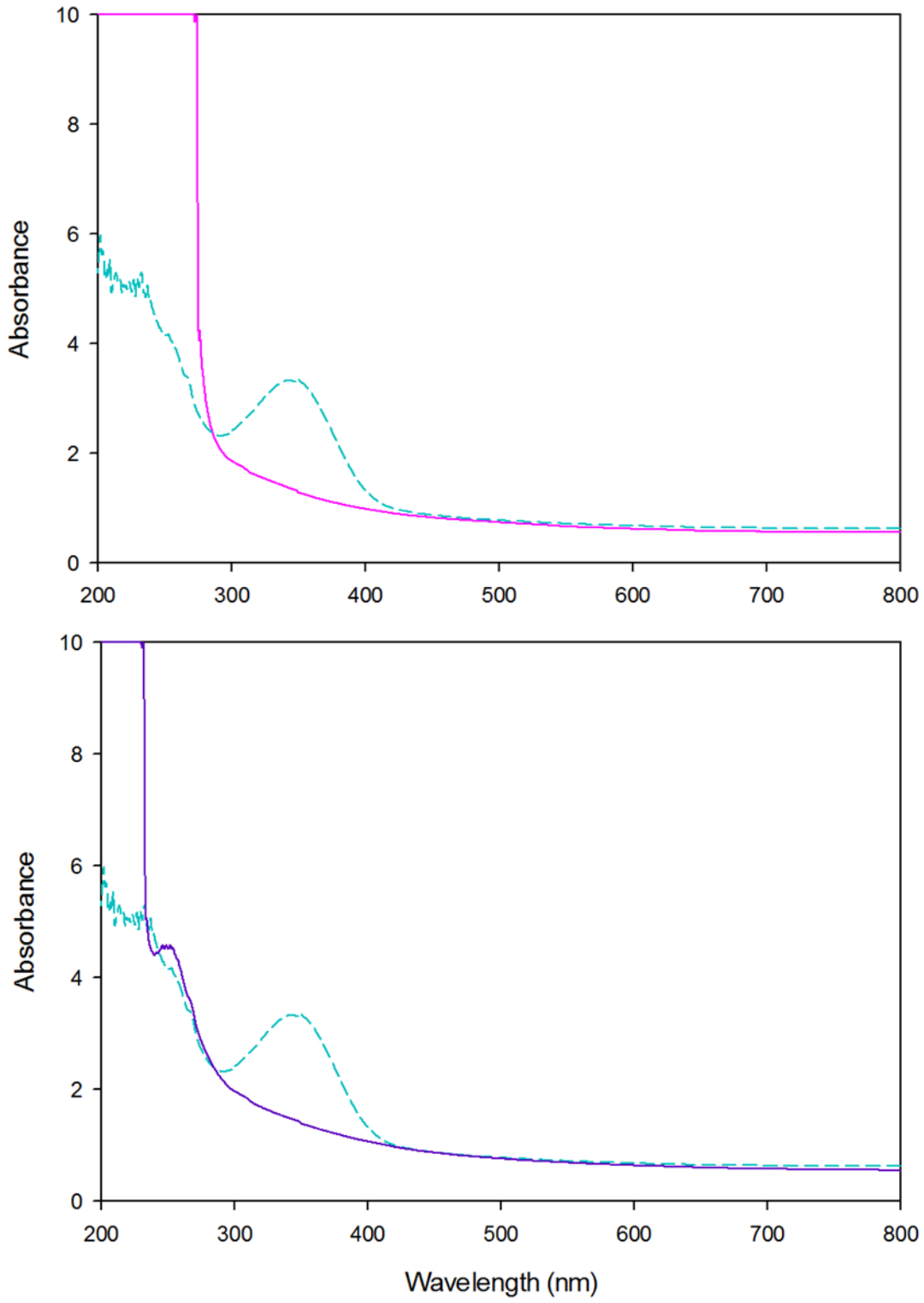

Figure S1.6. Above: Electronic absorption spectrum of 2-diazo-3-pentyne (**11**) (pink solid line) after deposition (60 min, N_2, 25 K) and after irradiation ($\lambda > 472$ nm, 11 h N_2, 13 K, blue dotted line).Below: Electronic absorption spectrum of ^{3}**3** (N_2, 13K, blue dotted line) and after irradiation ($\lambda > 330$ nm, 3 h N_2, 13 K, purple solid line

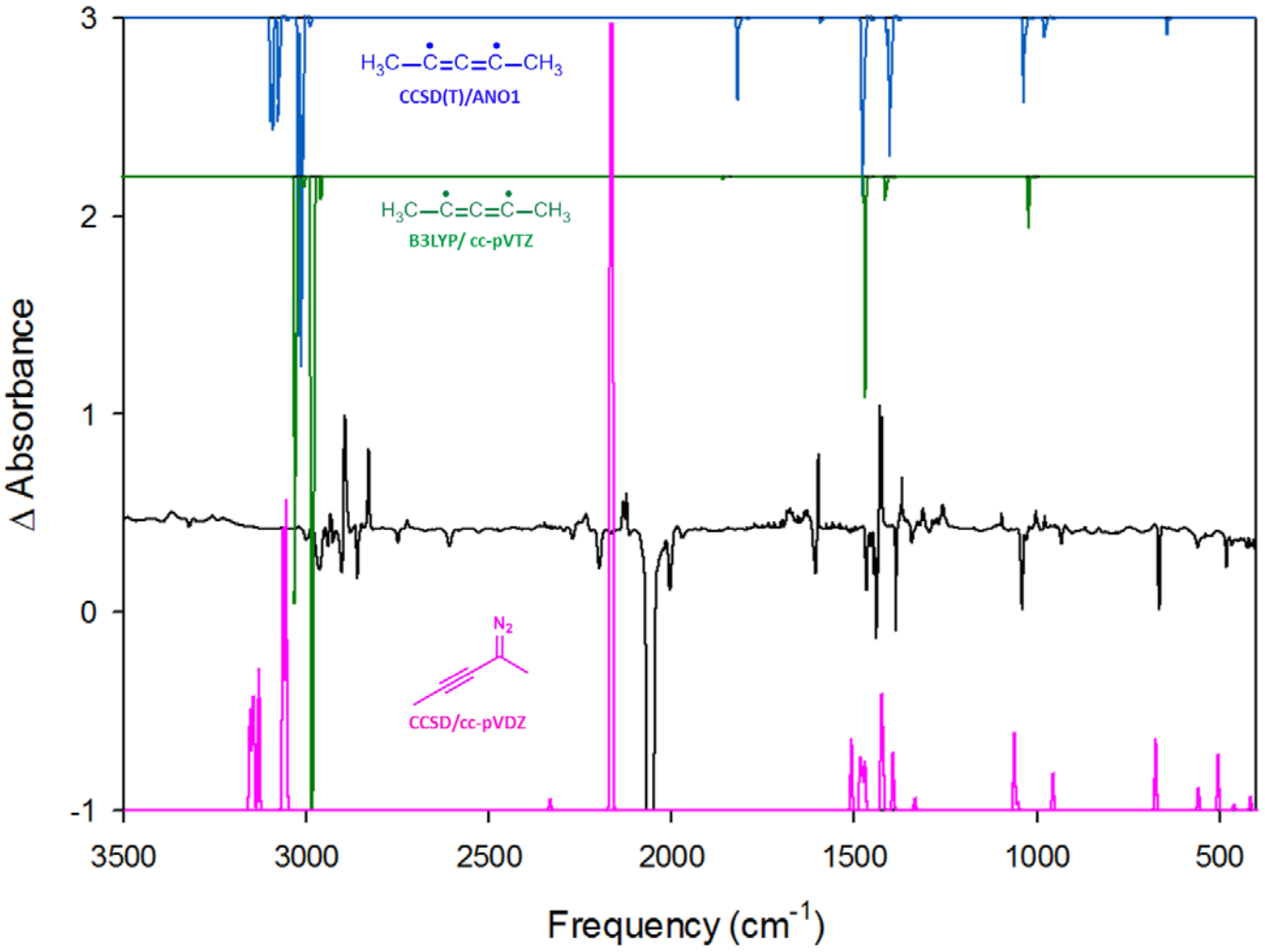

Figure S1.7. Above: Computed IR spectra for triplet MeC_3Me (^{3}**3**) at CCSD(T)/ANO1 (top) and B3LYP/cc-pVTZ (below) Middle: IR subtraction spectrum showing the disappearance of 2-diazo-3-pentyne (**11**) and appearance of triplet MeC_3Me (^{3}**3**) upon irradiation ($\lambda > 472$ nm, 6h, N_2, 10 K) Bottom: Computed spectrum for 2-diazo-3-pentyne (**11**) (CCSD/cc-pVDZ).

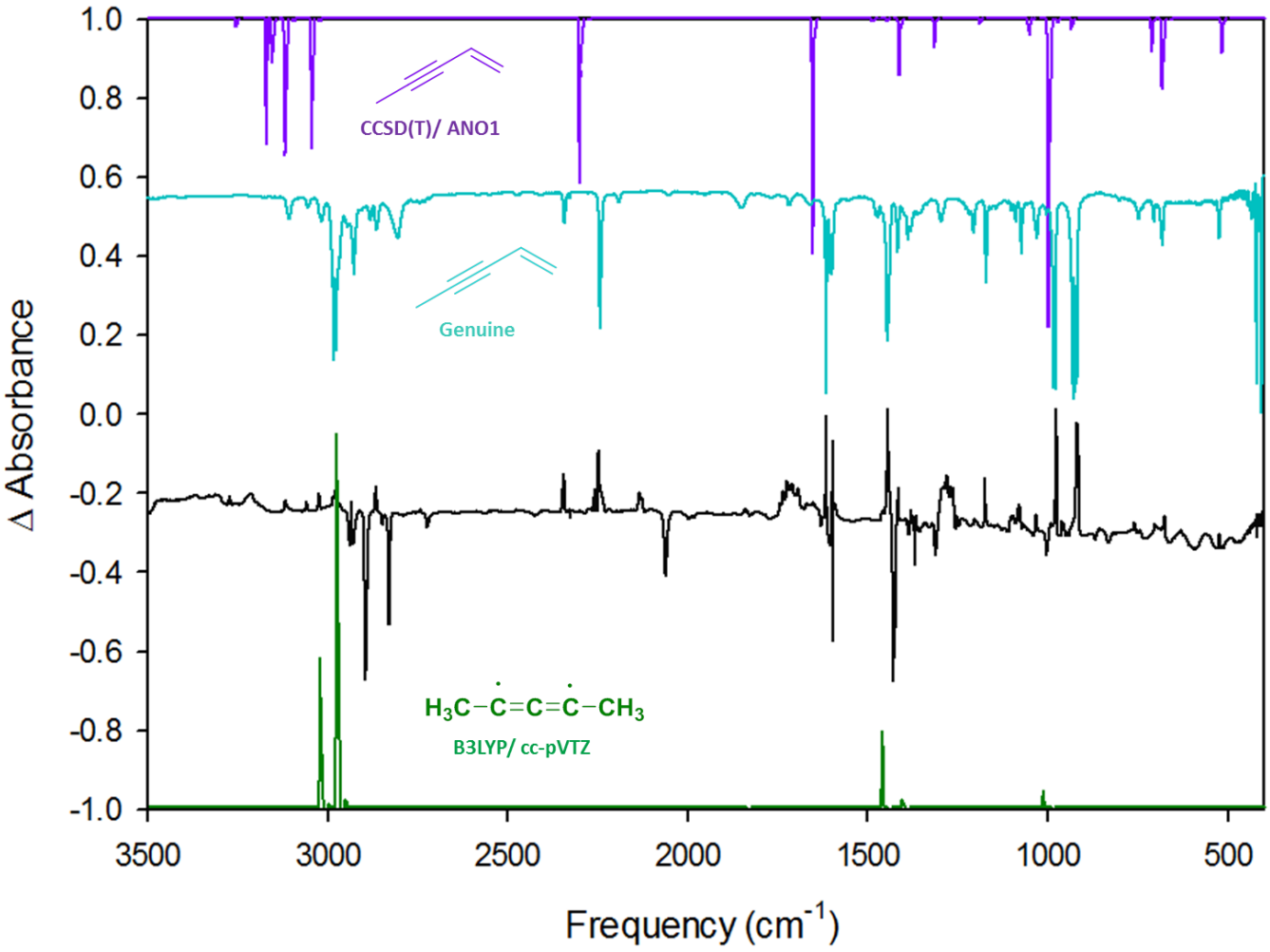

Figure S1.8. Above: Computed IR spectra for triplet at CCSD(T)/ANO1 (top) and B3LYP/6-31 g(d) (below) Middle: IR subtraction spectrum showing the disappearance of triplet MeC_3Me and appearance of pent-1-en-3-yne upon irradiation ($\lambda > 330$ nm, 24 h, N_2, 10 K) Bottom: Computed spectrum for 2-diazo-3-pentyne (**11**) (CCSD/cc-pVDZ).

Table S1.1. Experimentally observed IR frequencies and intensities. Intensities are normalized relative to the most intense band (=100).

MeC_3Me (^{3}3)		**2-diazo-3-pentyne (11)**	
Frequency (cm^{-1})	Relative intensity	Frequency (cm^{-1})	Relative intensity
2931	16	2965	7
2897	100	2928	10
2830	74	2901	7
2725	35	2860	8
2231	40		
2123	43	2199	5
		2067	100
		2004	6
		1466	6
1443	46	1439	13
1429	84	1386	10
1369	39		
1311	20		
1002	16	1039	6
		664	6

Table S1.2. Experimentally observed IR frequencies and intensities. Intensities are normalized relative to the most intense band (=100).

MeC_3Me isomerization product		**Pent-1-en-3-yne (4) Authentic sample**	
Frequency (cm^{-1})	Relative intensity	Frequency (cm^{-1})	Relative intensity
2984	21	2976	81
2933	17	2925	42
2866	31	2862	19
2349	28	2341	16
2249	62	2241	71
1842	10	1848	8
1724	34	1716	7
1615	93	1613	100
1597	59	1598	42
1444	100	1443	77
1415	62	1415	31
1365	3	1387	25
1270	31	1295	15
1174	38	1170	47
1096	3	1071	32
1033	7	1028	24
977	100	982	100
918	86	929	100
674	3	680	28

Notes and References:

1. McMahon, R. J.; Chapman, O. L.; Hayes, R. A.; Hess, T. C.; Krimmer, H. P. Mechanistic studies on the Wolff rearrangement: the chemistry and spectroscopy of some .alpha.-keto carbenes. *J. Am. Chem. Soc.* **1985**, *107*, 7597-7606.

2. Seburg, R. A.; McMahon, R. J. Photochemistry of matrix-isolated diazoethane and methyldiazirine: ethylidene trapping? *J. Am. Chem. Soc.* **1992**, *114*, 7183-7189.

3. Wasserman, E.; Snyder, L. C.; Yager, W. A. ESR of the Triplet States of Randomly Oriented Molecules. *J. Chem. Phys.* **1964**, *41*, 1763-1772.

4. Plattner, D. A.; Houk, K. N. C_{18} Is a Polyyne. *J. Am. Chem. Soc.* **1995**, *117*, 4405-4406.

5. Seburg, R. A.; McMahon, R. J.; Stanton, J. F.; Gauss, J. Structures and Stabilities of C_5H_2 Isomers: Quantum Chemical Studies. *J. Am. Chem. Soc.* **1997**, *119*, 10838-10845.

6. Woodcock, H. L.; Schaefer, H. F., III; Schreiner, P. R. Problematic Energy Differences between Cumulenes and Poly-ynes: Does This Point to a Systematic Improvement of Density Functional Theory? *J. Phys. Chem. A* **2002**, *106*, 11923-11931.

Chapter 2: Evidence of a Nitrene Tunneling Reaction: Spontaneous Rearrangement of 2-Formyl Phenylnitrene to an Imino Ketene in Low-temperature Matrices

The content contained in this chapter has been submitted for publication.

Contributions have been made by Cláudio M. Nunes, Igor Reva, and Rui Fausto at the University of Coimbra in Coimbra, Portugal

Introduction

Arylnitrenes are reactive intermediates containing a monovalent nitrogen atom commonly formed from the decomposition of aryl azides, a class of compounds that has found utility in organic synthesis,[1] lithographic applications,[2] and the formation of conducting polymer films.[3] By understanding the properties of the arylnitrene intermediate, these processes can be better understood and the utility of the precursor more appropriately exploited. Synthetic utility of aryl azides was initially thought quite limited. Upon photolysis in alcohol, alkene, aromatic, and alkene solvents, phenylazide only yields modest amounts of phenylnitrene and primarily forms a polymeric tar.[4] However, recent developments in synthetic organic chemistry have found great potential in aryl azides. The azide-alkyne Huisgen reaction,[5] used to synthesize 1,2,3-triazoles, has been described as the premier example of a "click reaction." Click chemistry has proven to be a remarkably facile class of reactions and has held a place at the forefront of synthetic organic chemistry for the last few decades.[6] This and similar cycloaddition reactions of azides have proven to be remarkably useful for a variety of transformations,[7] and a deeper look into the reactivity of azides and their associated intermediates stands to shed light on how to optimize the utility of these promising reactions. The history of the carbon analogue of the phenylnitrene, phenylcarbene, is longer and more established. Phenyldiazomethane has been found to react efficiently as a precursor in organic synthesis as well but in different ways. Phenylcarbene reacts with alcohols and alkanes as well as stereospecifically with alkenes, and adducts are formed in high yield.[8]

At low temperatures, additional differences in reactivity are observed. While phenylcarbenes undergo H-migration reactions by a quantum tunneling process,[9] the analogous reactivity expected in nitrenes is not observed.[10] Variations in reactivity such as these reveal

fundamental differences in the two reactive intermediates so frequently regarded as analogs. By understanding the fundamental differences and similarities in reactivity between arylcarbenes and arylnitrenes, the limitations and potential for each might be better understood and more efficiently utilized in the future.

Background

In the world of reactive intermediate chemistry, nitrenes can be most closely likened in characteristics and reactivity to their isoelectronic carbon analogue, carbenes.[11] While nitrenes are an obvious parallel to carbenes, there are a few significant differences that have resulted in

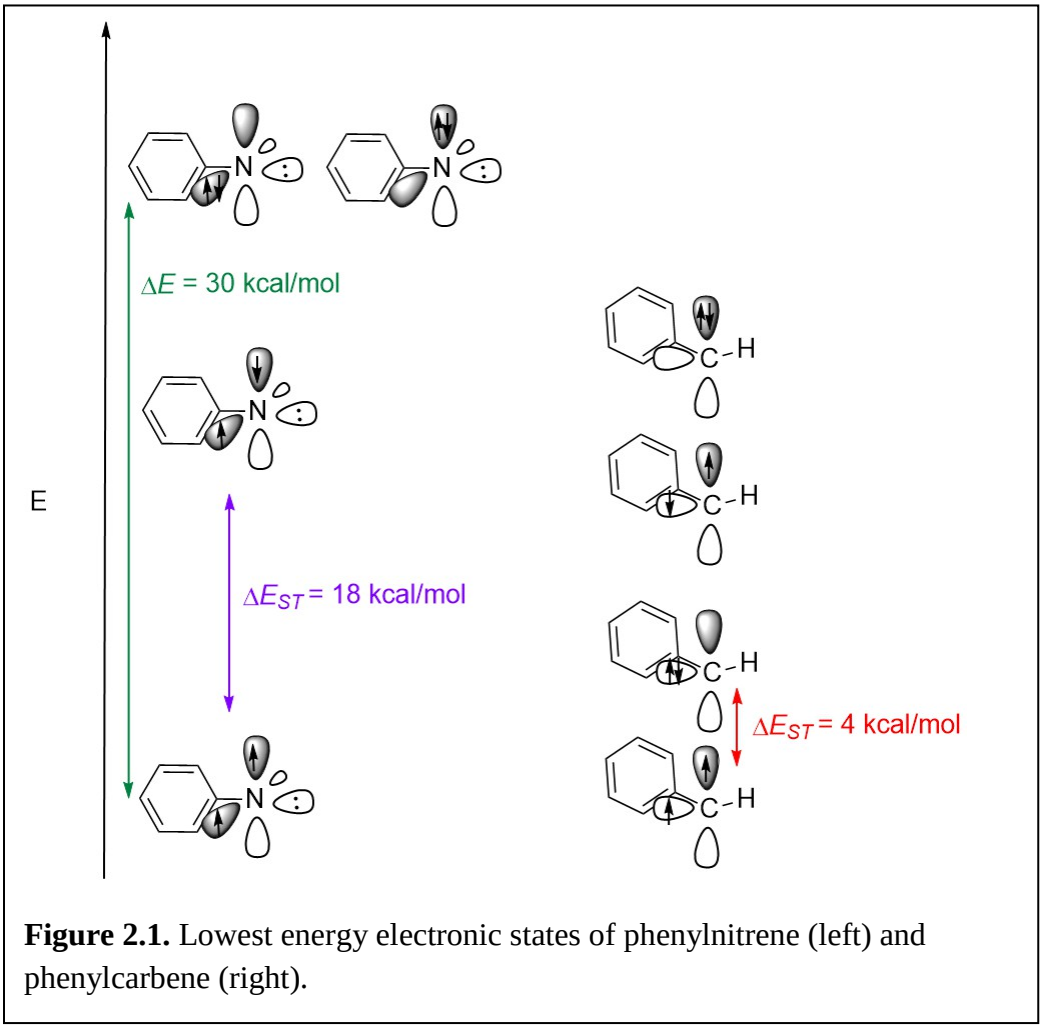

Figure 2.1. Lowest energy electronic states of phenylnitrene (left) and phenylcarbene (right).

divergence of their respective behavior. EPR temperature dependence studies show that ground state of phenylnitrene is the triplet state.[12] While this is also true for phenylcarbene, the electronic structure of phenylnitrene is distinctly different. The lone pair of the nitrogen occupies a hybrid orbital, while the unpaired electrons occupy two nearly degenerate p orbitals. Computations[13] as well as gas phase photoelectron spectroscopy[14,15] agree that the lowest spin states of phenylnitrene (in order of increasing energy): a triplet, an open-shell singlet, and two closed-shell singlets (Figure 2.1).[13] In contrast, singlet phenylcarbene has a rather flat potential energy surface and a floppy geometery.[16,17] It is approximately sp^2 hybridized, with one hybrid σ-type orbital predicted to be at a much lower energy than the other p-π orbital, based on analogy to singlet methylene.[18] The triplet remains the lowest spin state, but the stabilization provided by lower-energy closed-shell singlet configuration makes the gap between triplet and singlet much smaller (Figure 2.1). The differences between the two species electronic states can be invoked to rationalize many variances observed in their chemistry.

Scheme 2.1.

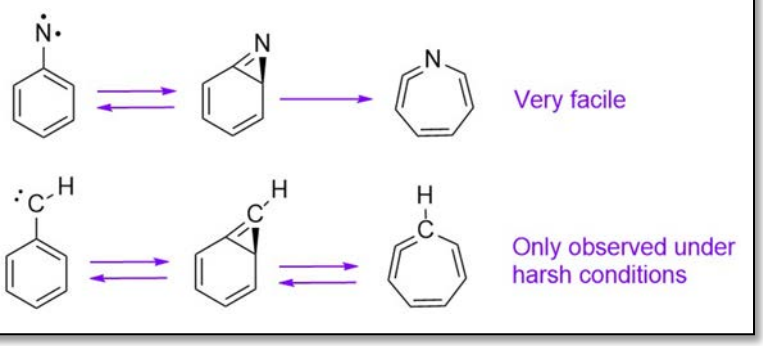

In effect, singlet carbenes are closed-shell species that display strong Lewis acidity and/or basicity; whereas singlet nitrenes are open shell species that behave like diradicals.[11] The characteristic reactions of the species, as a result, differ slightly. For example, in the case of phenylnitrene, the most prevalent mode of reaction is rearrangement to a benzazirine intermediate followed immediately by facile rearrangement to a ketenimine species.[13] In the case of phenylcarbene, the barrier to this type of cyclization is higher by about 9

kcal/mol and can only accomplished from a higher energy closed shell singlet state;[13] moreover, bimolecular reactions from phenylcarbene are quite facile, and these reactions dominate (Scheme 2.1).

The singlet-triplet gap is another major difference between phenylnitrene and phenylcarbene—the former has a computed ΔG_{ST} of about 18 kcal/mol[19,20] and the latter of 2-4 kcal/mol.[17,21] Because of this, singlet and triplet carbene interconvert rapidly, while the intersystem crossing of phenylnitrene is irreversible.[22,23] As such, reactions of arylnitrenes on the triplet surface are of particular interest, especially in comparison to those of triplet carbenes. Furthermore, singlet nitrenes undergo intersystem crossing much slower than carbenes.[21] This is due to the fact that spin orbit coupling, an effective mechanism of ISC, is spin forbidden in singlet open shell nitrenes and spin allowed in singlet carbenes. However, upon initial photolysis of the azide precursor, the fate of the singlet nitrene is highly temperature dependent. At ambient temperatures, singlet nitrenes primarily persist and undergo ring expansion; whereas at low temperatures, ISC to triplet nitrenes is favored.[24]

While these differences are well-established for the singlet species of phenylnitrene, comparisons between phenylnitrene and phenylcarbene on the triplet energy surface have not been quite as well studied. One particularly interesting mode of reactivity that triplet carbenes has displayed at low temperatures is the tunneling reaction.

The phenomenon of quantum tunneling was first recognized in the reactions of highly reactive compounds as a result of deviations from predicted transition state theory behavior. Transition state theory has long stood as the method of choice for predicting classical reaction kinetics in the organic community; however, in the realm of reactive intermediates, classical

predictions are occasionally not reflected in observed reactions. Unpredicted behavior such as reactions proceeding at rates much higher than predicted, not slowing as much as expected when the temperature is lowered, or disproportionate roles of geometry change and nuclei mass on the rate of reaction can be traced back to the quantum nature of the particles involved.[25,26] While classical mechanics require nuclei to pass over activation barriers, quantum uncertainties in the location of nuclei allow the penetration of sufficiently narrow barriers. This phenomenon is described as quantum mechanical tunneling, and the small activation barriers and minimal geometry changes between reactants and products characteristic of open-shelled organic reactive intermediates make them prime candidates for the process.[27] [28]

Simply put, the reason nuclei can tunnel through the barrier derives from the wave – particle duality of quantum mechanics, which describes particles as having an associated de Broglie wavelength (determined by its mass and velocity). If the wavelengths of the nuclei involved in reaction are similar to the barrier width, there may exist a nuclear wave function that extends to the other side of the barrier.[25,26] The signs that this type of process is at play include nonlinear Arrhenius plots, reaction rates faster than classically predicted, and anomalously large kinetic isotope effects.[27]

Scheme 2.2.

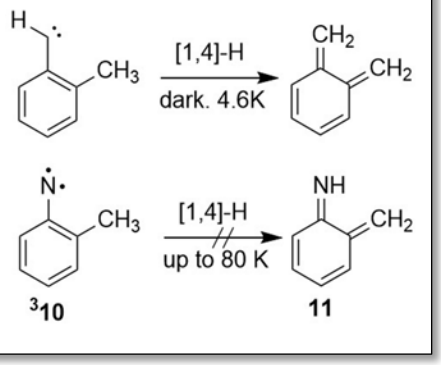

In several cases, triplet carbenes have been observed reacting in the dark at cryogenic temperatures. These reactions have taken the form of ring expansion[29-31] and hydrogen migration reactions.[9] While tunneling has been observed at cryogenic temperatures in the course of the azirine-ketenimine transformation associated with nitrene reactivity,[32] this observation occurs after the nitrene has already reacted to form the azirine. At present, the [1,4]-H migration observed in *o*-tolylcarbene has thus far been elusive in nitrene systems (Scheme 2.2).[10] The only report that indicates evidence of tunneling in the case of an arylnitrene was reported by Murata et al., where a H-shift reaction of an alkyl arylnitrene was observed at ambient temperatures[33]. The k_H/k_D ratio was slightly higher than would be predicted for the theoretical transition state maximum (14.7 vs ca. 12). While this is one indication of tunneling, the effect was not pronounced enough to be convincing. Additionally, the reaction was observed at ambient temperatures and the Arrhenius plot was only measured from -14 to 50 °C. The authors noted that more evidence would be necessary to determine the contribution of tunneling to the mechanism.

One hypothesis about the resistance of *o*-tolylnitrene to undergo [1,4]-H migration is that the distance between the H atom and the nitrogen of the nitrene is too large. Calculations of geometries using UMP2-FC/6-31G(d) indicate the heavy atom framework of both *o*-tolycarbene and nitrene are almost completely planar. The distance between the closest hydrogen atom and the carbene is 245.3 pm, while the distance between the closest hydrogen atom and the nitrogen

of the nitrene is 282.5 pm. It is possible that the increased distance creates an inhibitive barrier for tunneling, and a system with a shorter H—N distance will be more successful.

In the current system, 2-formyl phenylnitrene, the calculated H—N distance is 249.4 pm, a comparable distance to the carbene case. If the limiting factor for tunneling in the nitrene is the width of the barrier, this case could bypass that restriction. At matrix-isolation tempuratures (~10 K) the triplet state would definitely be favored. Initial studies, including temperature dependence studies, clearly indicate that the nitrene does undergo [1,4]-H migration *via* tunneling mechanism. This indicates both the first example of a nitrene and the first example of an sp^2-hybridized H undergoing a tunneling reaction.

Results and Discussion

Scheme 2.3.

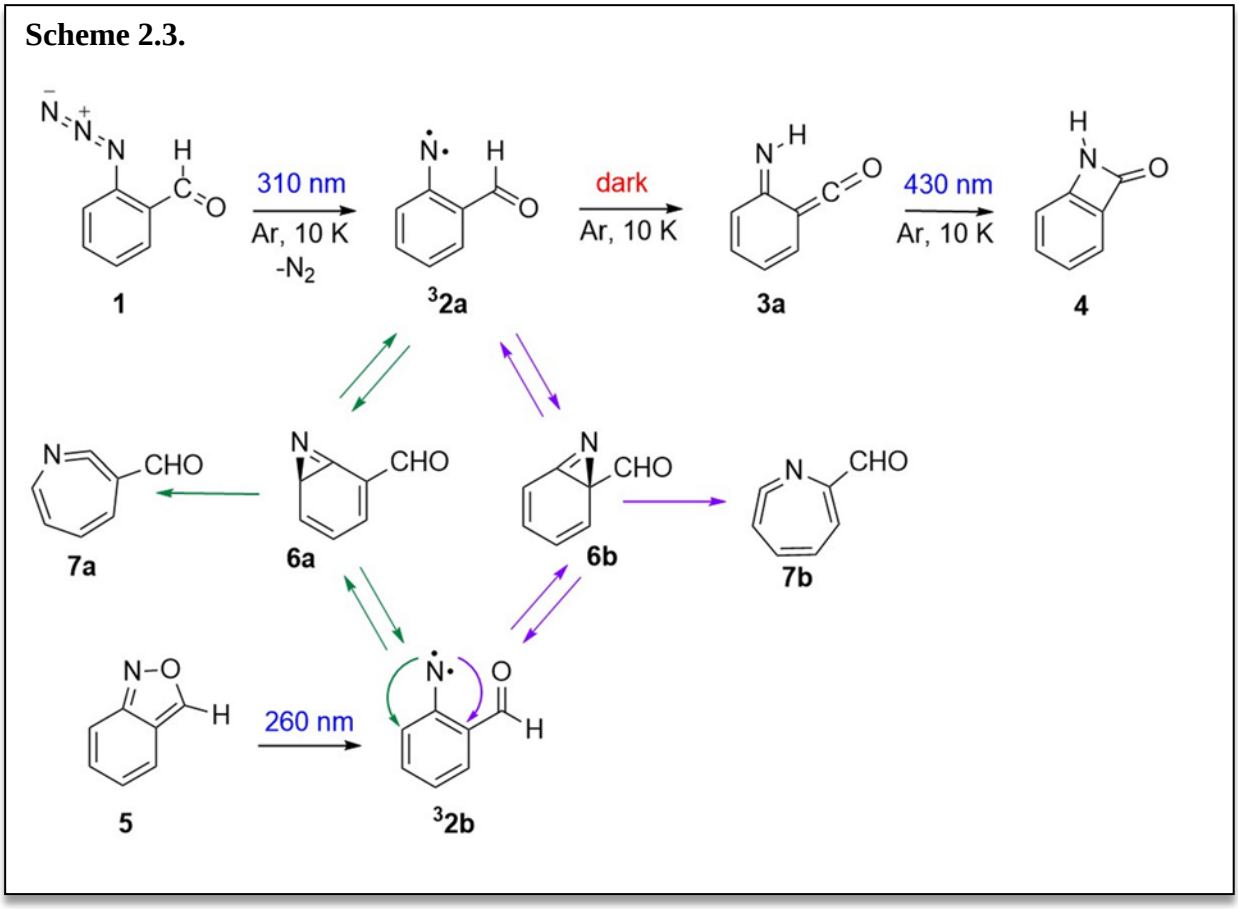

Initial Studies: 2,1-Benzisoxazole

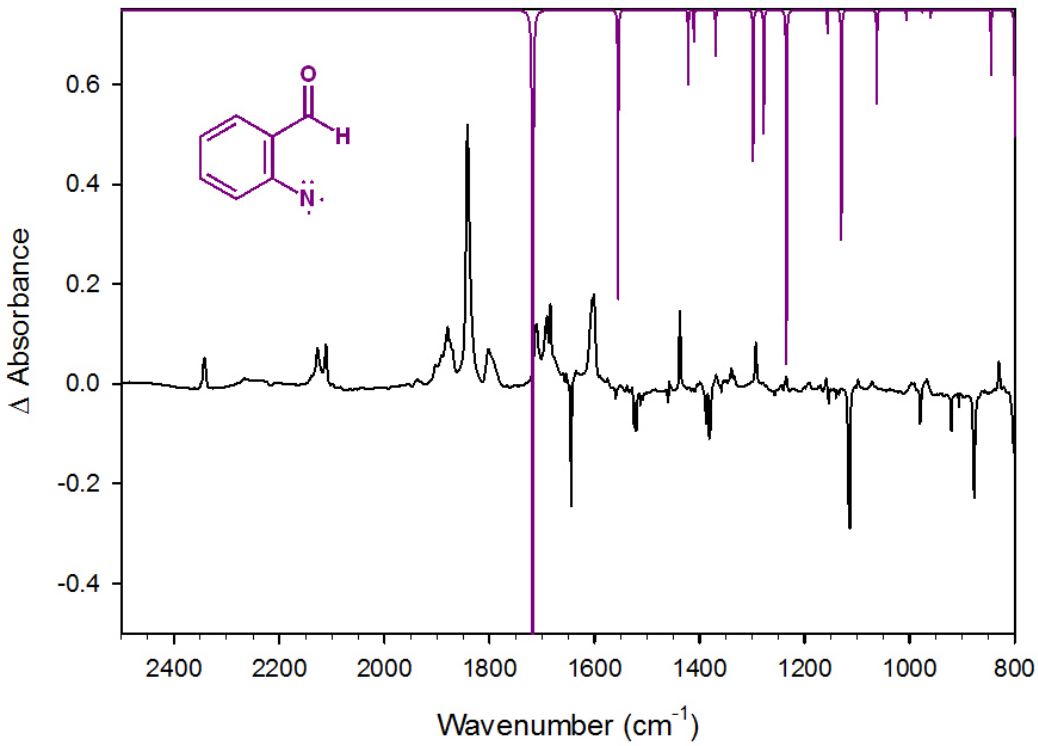

Figure 2.2. IR difference spectrum (center) of matrix isolated 2,1-benzisoxazole **5** (Ar, 10 K) irradiated (λ = full arc) for 65 minutes with calculated spectrum 2-formyl phenylnitrene ^{3}**2a** (above).

Initial investigations of this system involved the matrix isolation of 2,1-benzisoxazole (**5**). It was from this precursor that the tunneling [1,4]-H migration was initially observed; however, the system is complicated by the formation of many other side products along the way (Scheme 2.3). Because of the orientation of the benzisoxazole, the nitrene is initially formed in the *syn*- orientation (^{3}**2b**). From this orientation, the facile ring expansion pathway is favorable, and both kenetenimine (**7a** and **7b**) are observed in addition to *anti*- nitrene (^{3}**2a**). From ^{3}**2a**, the tunneling reaction can be observed and monitored; however it is obscured in the infrared by

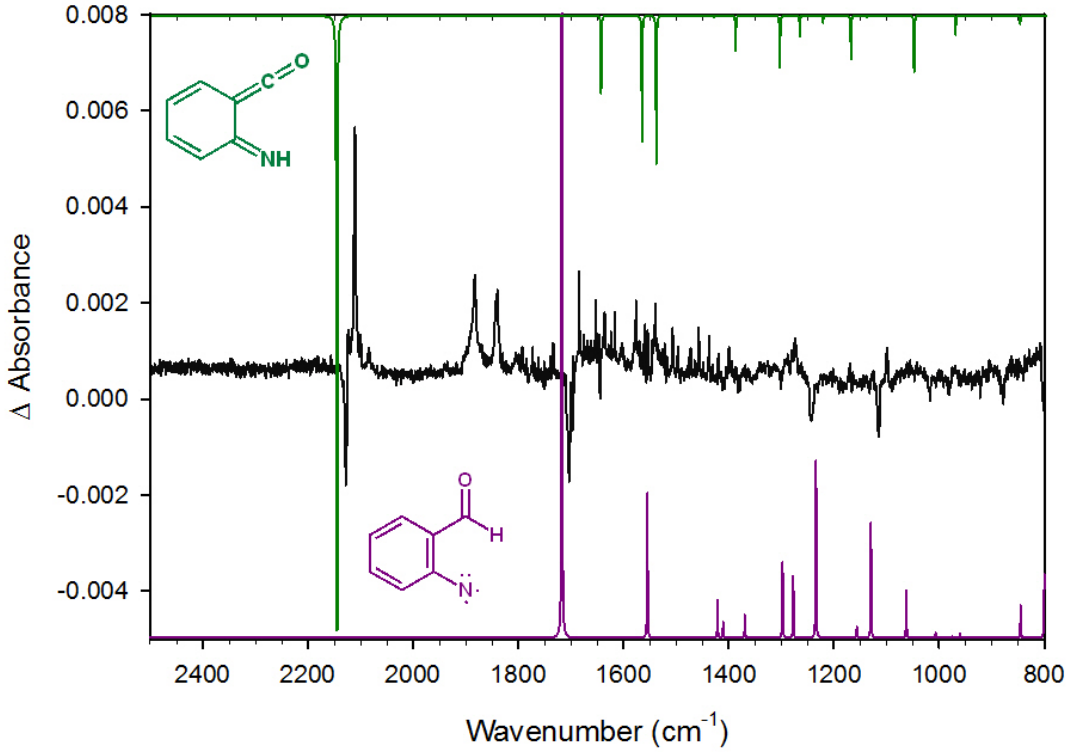

Figure 2.3. IR difference spectrum (center) of matrix isolated 2-formyl phenylnitrene generated from irradiation of 2,1-benzisoxazole **5** left in the dark (Ar, 10 K) for 2 h 45 min with calculated spectra of 2-formyl phenylnitrene ^{3}**2a** (below) and imino ketene **3a** (above).

transitions from many other products (Figures 2.2 and 2.3). As a result, UV/vis experiments were also difficult to interpret, as it was unclear what product was responsible for observed absorption features (Figure 2.4). Because of this, we pursued studies using the precursor 2-formyl phenylazide (**1**). Calculations indicate that conformation shown is the lowest energy conformer and the one that leads to the triplet phenylnitrene conformation ^{3}**2a**. Indeed, IR experiments from precursor **1** show much cleaner spectra with primarily nitrene ^{3}**2a** and imino ketene **3a** upon irradiation. Because of this, all subsequent studies were done from the 2-formyl phenylazide precursor (**1**).

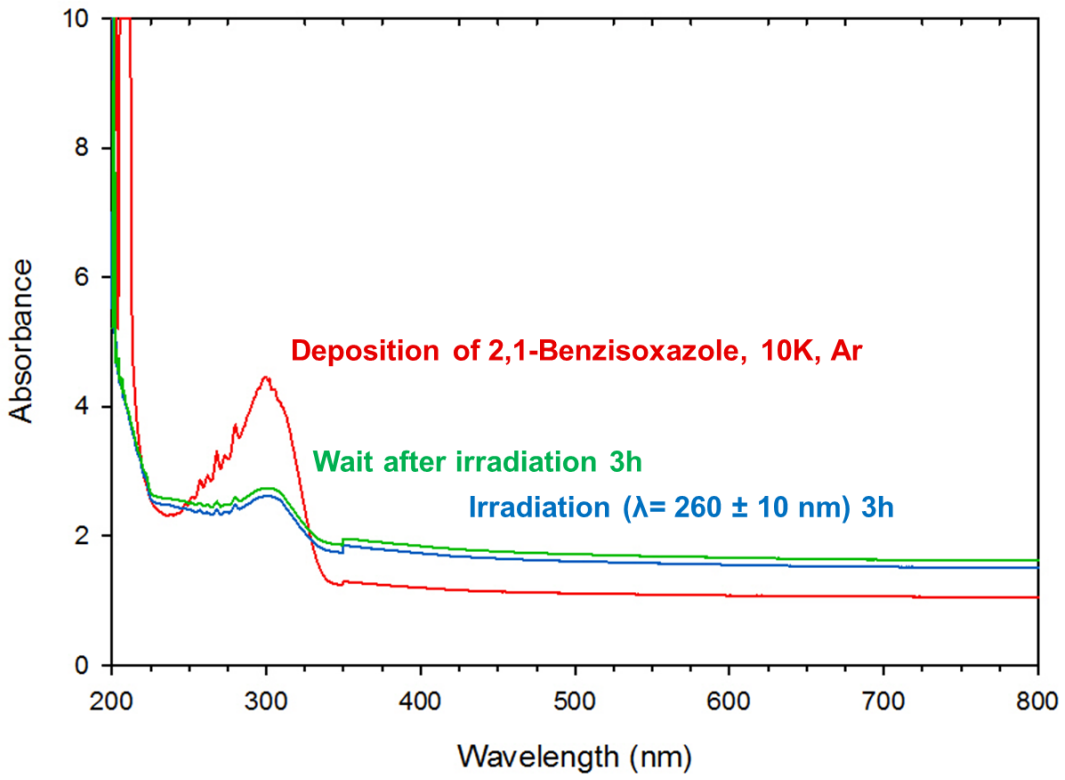

Figure 2.4. UV/vis absorption spectrum of of matrix isolated 2,1-benzisoxazole **5** after deposition (red trace) and irradiated (λ= 260 ± 10 nm, Ar, 10 K) for 3 h (blue trace) and waiting in the dark after irradiation for 3 h (green trace). No changes were observed upon waiting.

Synthesis of Precursors: 2-Formyl Phenylazide

2-Formyl phenylazide was synthesized from commercially available materials *via* S_NAr reaction according to the procedure by Capperucci *et al.*(Scheme 2.4)[34] NMR and mass spectrometric characterizations reflect those found in the literature.

Scheme 2.4.

Generation of Nitrene

In order to generate nitrene ^{3}**2a**, 2-formyl phenylazide (**1**) was transferred to a deposition tube and connected to the matrix isolation apparatus. The sample was kept at 0 °C in an ice water bath while it was placed under vacuum and co-deposited with Ar at 20 K. Both broadband ($\lambda \geq 330$ nm) and monochromatic ($\lambda = 320 \pm 10$ nm) irradiation were attempted for generation of the nitrene. In the case of broadband irradiation, the main product detected was most often lactam **4**, and it was difficult to detect a large enough concentration of nitrene to properly monitor the tunneling pathway. Best results came from monochromatic irradiation, and this is how nitrene ^{3}**2a** was generated in the subsequent studies described. Spectra from broadband irradiation experiments can be found in the Supporting Information following this chapter.

IR Spectroscopy

The photochemical characterization of 2-formyl phenylazide (**1**) to 2-formylphenylnitrene (^{3}**2a)** and subsequent tunneling reaction to imino ketene (**3a**) was monitored by matrix isolation IR spectroscopy in tandem with computed spectra (B3LYP/6-311++G(d,p)).

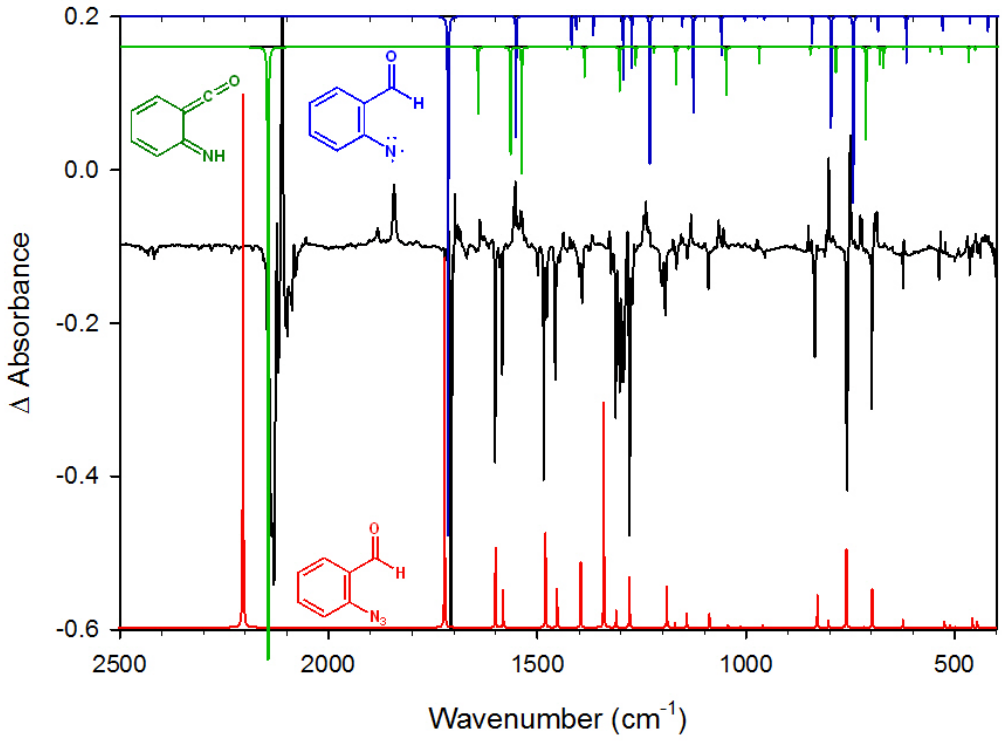

Figure 2.5. IR difference spectrum (center) of matrix isolated 2-formyl phenylazide **1** irradiated (λ = 320 ± 10 nm, Ar, 10 K) with calculated spectra of 2-formyl phenylazide **1** (below), 2-formyl phenylnitrene ^{3}**2a**, and imino ketene **3** (above).

2-Formyl phenylazide isolated in an argon matrix at 10 K was irradiated (λ = 320 ± 10 nm). After 60 minutes, IR bands corresponding to azide disappeared and were replaced by bands that correspond to predicted transitions for 2-formyl phenylnitrene **2** and imino ketene **3** (Figure 2.5). The first few seconds of irradiation generate almost exclusively photoproduct **2**, and with the increase of irradiation time the ratio of **3**:**2** increases. Therefore, **2** must be a primary

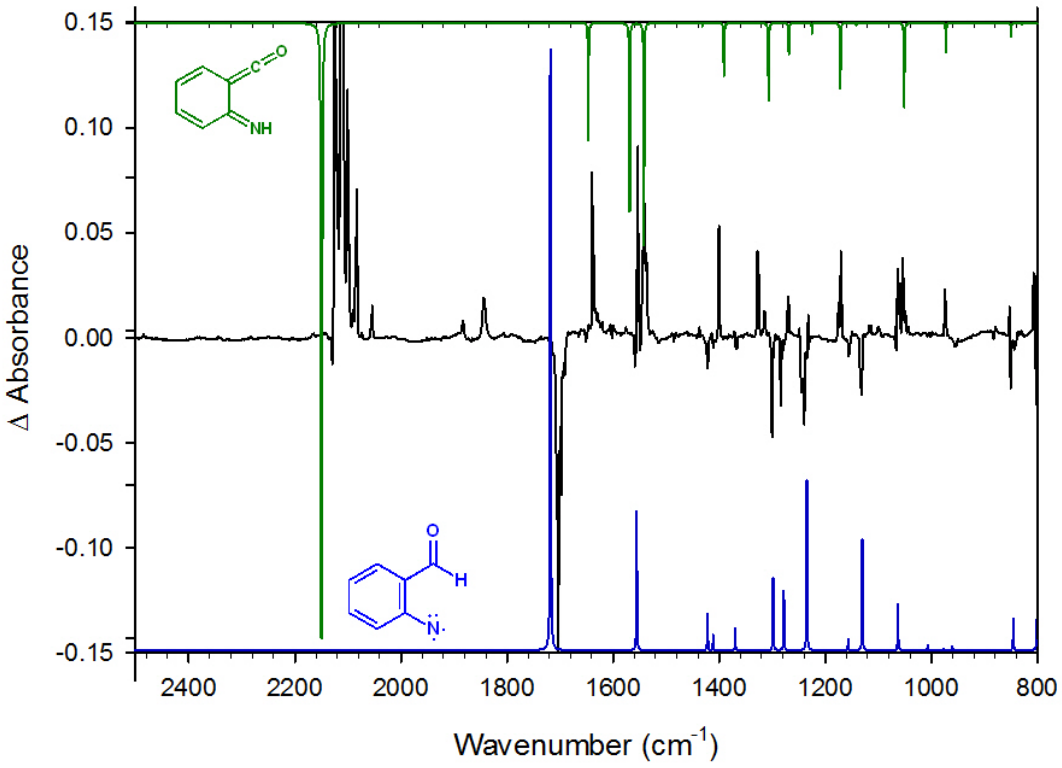

Figure 2.6. IR difference spectrum (center) of matrix isolated 2-formyl phenylnitrene ^{3}**2** formed from irradiation of 2-formyl phenylazide left in the dark at 10 K for 23 hours with calculated spectra of 2-formyl phenylnitrene ^{3}**2a** (below) and imino ketene **3a** (above).

photoproduct of **1**, whereas **3** is most likely a secondary photoproduct formed via **2**.

Irradiation optimization was delicate, as over-irradiation resulted in formation of the final lactam product **4** (Scheme 2.3). Generating a large enough concentration of nitrene to track the

tunneling transformation without reacting it away immediately requires careful attention to the changes occurring in the IR spectrum. The experimental IR spectrum of ^{3}**2a** agrees well with the theoretical IR spectrum of triplet nitrene ^{3}**2a** calculated at the B3LYP/6-311++G(d,p) level (Figure 2.5 and 2.6). Particularly characteristic are the bands observed at 2857, 1703, 1301, and 750 cm^{-1}, which correspond to the harmonic vibrational modes predicted at 2885 [ν(OC–H)], 1718 [ν(C=O)], 1298 [ν(C–N)], and 747 [γ(CH)] cm^{-1}.[35] A more complete assignment of the vibrations observed in the mid-IR spectrum of triplet nitrene ^{3}**2a** is given in Table S2.1.

After irradiation, the matrix containing 2-formyl phenylnitrene (^{3}**2**) was left in the dark. After ~5 minutes, changes in the IR spectrum can be observed. The changes can be traced directly to the transformation of 2-formyl phenylnitrene (^{3}**2a**) to 6-imino-2,4-cyclohexadien-1-ketene (**3a**). Figure 2.6 presents the changes in the spectrum that occur after 23 hours. The experimental IR spectrum compares well with the theoretical IR spectrum of imino ketene **3a** (Figure 2.6). The most distinctive bands are observed at 3266, 2110, 1553, and ~724 cm^{-1} and readily assigned to the vibrational modes predicted at 3283 [ν(N–H)], 2149 [ν(C=C=O)as], 1568 [ν(C=N)], and 716 [γ(CH)] cm^{-1}. The frequency and very high intensity of the band observed at 2110 cm^{-1} are especially characteristic of a ketene moiety, and compare well with the frequency of the ν(C=C=O)as band reported at 2125 cm^{-1} for the methylimino ketene analogue.[36] A comprehensive assignment of the observed IR bands for **3a** is given in Table S2.3.

UV/vis Spectroscopy

UV/visible absorption spectra of 2-formyl phenylazide (**1**), 2-formyl phenylnitrene (^{3}**2a**), and imino ketene (**3a**) were acquired and followed expectation based on reactivity observed in IR experiments. Deposition of 2-formyl phenylazide (**1**) at 20 K yields a spectrum with a characteristic transition at λ_{max} = 310-320 nm. Upon irradiation at λ = 320 ± 10 nm, the transition begins to deplete in favor of features attributed to nitrene ^{3}**2a** (Figure 2.7). The changes that occurr in the UV/vis spectrum through the course of the tunneling reaction were subtle, and as such, it is easier to depict them through a difference spectrum (shown compared to computational prediction in Figure 2.8).

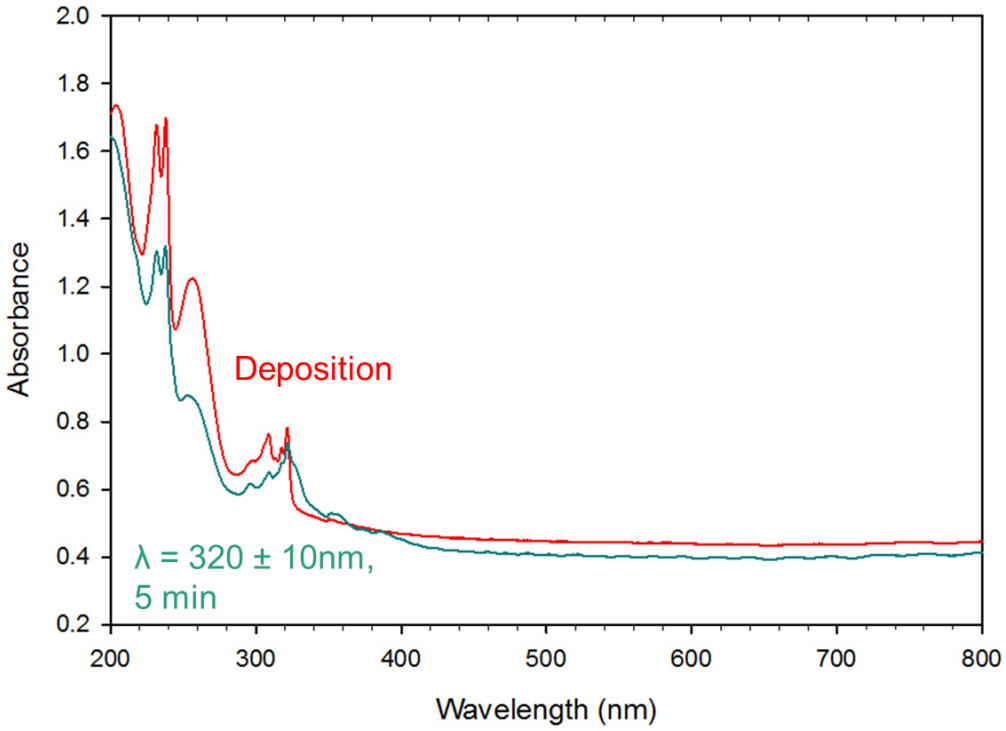

Figure 2.7. UV/vis absorption spectrum upon deposition of 2-formyl phenylazide **1** (red) and upon irradiation at λ = 320 ± 10 nm, Ar, 10 K, 5 min (teal).

In the experimental difference UV-spectrum three decreasing bands at 216, ~235 and 326 nm appear as result of the consumption of **A** (Figure 2.8).These bands are well reproduced in the TD-DFT simulated UV/vis difference spectrum, where the vertical transitions with higher oscillator strengths were estimated at 209, 223 and 338 nm for the triplet nitrene ^{3}**2a** (Figure 2.7b and Table S2.2). The band observed at 326 nm for **A** compares well with the strong absorption of the simplest triplet phenylnitrene at 308 nm or with the 336 nm absorption of the parent nitrene, which are assigned mainly to the $n_z \rightarrow n_y$ transitions localized on the nitrogen atom.[21,24] From the experimental difference UV-spectrum, the growing band of **B** at ~256 nm and a broad band with peak at ~375 nm, extending to ~460 nm, can be assigned to **3a** (Figure 2.8a). In a good correspondence with the experimental data, TD-DFT calculations for imino ketene **3a** estimate the three vertical transitions with higher oscillator strengths at 366, 242 and 234 nm (Figure 2.8b and Table S2.2). The experimental broad band of **B** that appears between 350-460 nm (assigned to the $\pi_{HOMO} \rightarrow \pi^*_{LUMO}$ transition) compares well with the broad band of the methylimino ketene analogue centered near 400 nm.[36]

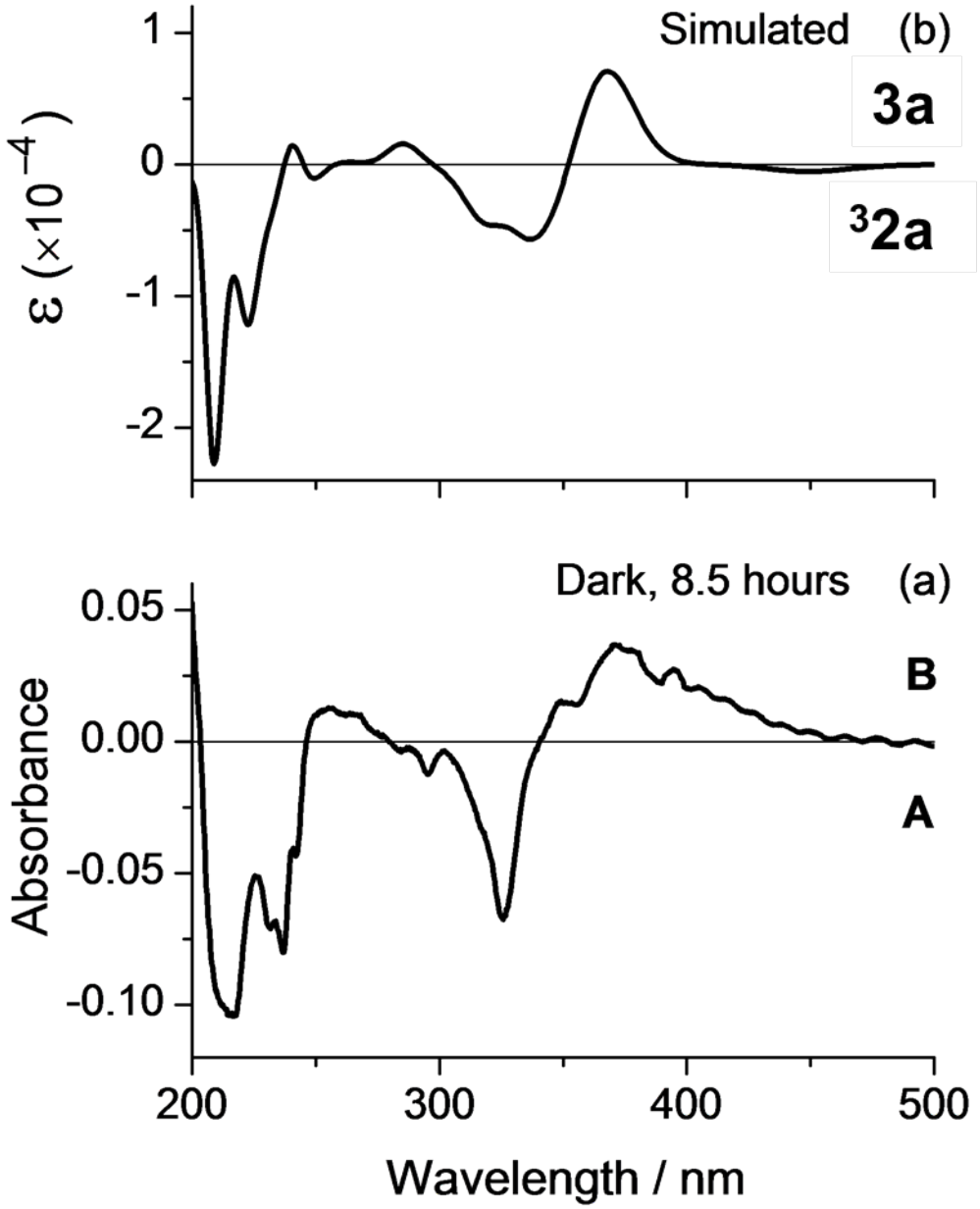

Figure 2.8. (a) Changes in the experimental UV-Vis spectrum resulting from keeping the sample for 8.5 hours in the dark, after irradiation of **1** isolated in Ar matrix at 10 K. (b) Simulated difference UV-Vis spectrum obtained from vertical transition energies determined by TD-DFT calculations at the B3LYP/6-311++G(d,p) level, considering production of imino ketene **3a** at the cost of triplet nitrene ^{3}**2a**.

EPR Spectroscopy

The EPR spectroscopic signature of arylnitrenes has been described previously by Wasserman[12,35] and Platz.[37] The dominating influence in a triplet nitrene EPR spectrum is the dipole –dipole interaction of the two unpaired electrons.[35] Because azide precursors do not allow for easy isolation of single crystals, most triplet nitrene EPR spectra are that of randomly oriented triplets. A procedure for extracting zero-field splitting parameters from spectra of this type has been determined, deriving from the phenomenological event that occurs when a principal axis of the nitrene is parallel to the applied field. In this instance, there is an abrupt change in the number of resonating molecules, causing a large change in the first derivative of the absorption spectrum. *D* and *E* can then be extracted from the first derivative of the randomly oriented triplet spectrum.[37]

EPR spectra of triplet species can be characterized by two zero-field splitting (ZFS) parameters, *D* and *E*, and derive from the principle magnetic axes of the molecule *X, Y* and *Z*. Since nitrenes are monovalent, the *X* and *Y* axes are often equivalent, changing their treatment from triplet carbenes. Most notably, *E* values, which correspond to a molecule's deviation from axial symmetry, are often zero or nearly zero. Deviations from axial symmetry in the rest of the molecule are often too subtle to affect the *E* value. The spectrum of nitrene **2** is characteristic of many randomly oriented triplet aryl nitrenes in exhibiting only a single transition (XY_2) in the X-band EPR spectrum (Figure 2.9).[35,37] This transition, located at 6818 G, corresponds to the R—N axis perpendicular to the applied field and falls well within the expected range of 5000 to 9000 G.[37] That the spectrum exhibits a single XY_2 transition, rather than features attributable to distinct X_2 and Y_2 transitions,[38] reveals that the local electronic environment at the nitrene center is

axially symmetric and establishes that the magnitude of the zero-field splitting parameter E is very small ($|E/hc| < 0.002$ cm^{-1}).

Qualitatively, a decrease in D corresponds to an increase of delocalization of the two unpaired electrons. The zero-field splitting parameter D was evaluated in the standard way using equation (1) to afford a value of $|D/hc| = 0.979$ cm^{-1}.[37,39] This value is in good agreement with those of other triplet arylnitrenes, which typically fall in the range 0.9-1.2 cm^{-1}. In principle, triplet nitrene **2** exists as mixture of conformational isomers (**2a** and **2b**) that differ in the relative orientation of the formyl substituent relative to the nitrene center. The fact that a single XY_2 transition is observed suggests either that only a single conformer is observed, or, more likely, that the conformational perturbation is too subtle to be manifest in the X-band EPR spectrum.

$$(H_{ext})^2 = H_0(H_0 + D) \qquad (1)$$

Equation 1. H_{ext} = resonance field of the XY_2 transition, H_0 = the resonance field of a free radical under the conditions, and the conversion factor between G and cm^{-1} is given by: 10,700 G = 1 cm^{-1}.

The timeframe available for EPR experiments did not allow for monitoring signal depletion over time. Further, the reaction profile would differ due to the temperature and matrix conditions being different (4 K in glass vs 10 K in argon matrix). The signal did decrease when the temperature was raised above 20 K, but it is unclear from the current experiment whether the depletion of signal is due to population of higher states or to reaction of the nitrene. Further experiments are necessary to probe the scope of the system with respect to EPR properties.

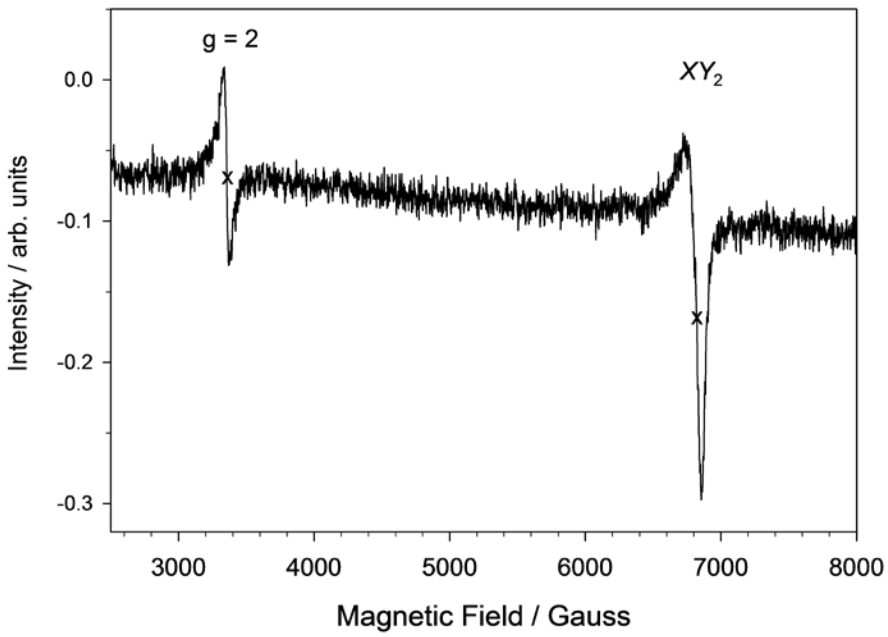

Figure 2.9. Experimental EPR spectrum of triplet 2-formyl phenylnitrene **2** generated by irradiation (λ = 310 ± 10 nm, 40 min) of 2-formyl phenylazide (**1**) in a methylcyclohexane (MCH) glass at 4 K. (microwave frequency = 9.405 GHz; H_0 = 3356 G; XY_2 = 6818 G)

This EPR spectrum serves as an initial characterization of the triplet nitrene, but subsequent EPR experiments have the potential to reveal a great deal about this system. Determining the temperature dependence of the EPR spectrum of ^{3}**2** will reveal experimental information concerning the ground electronic state of the nitrene. The intensity of the EPR signal of a molecule with a triplet ground state will vary inversely with temperature according to the Curie Law.[40,41] Additionally, if the triplet state is a thermally populated state (rather than the ground state), the EPR signal intensity is directly correlated with temperature. Experiments probing this property will involve warming the glass to various temperatures and cooling it back down to see the effect on the EPR signal. Additionally, using deuterated MCH as the glassing

solvent would give information about the interaction of the nitrene with the solvent, ensuring that any reaction that is observed is due to H-migration, rather than reaction with the solvent.[42,43]

Evidence of Tunneling

It is clear that the spontaneous rearrangement of triplet nitrene ^{3}**2a** to imino ketene **3a** cannot be explained by the classical rate theory considering an over-the-barrier process. A rate constant on the order of 3×10^{-5} s^{-1} at 10 K would correspond to an activation energy ~0.2 kcal mol^{-1}; such very low barrier is extremely improbable to exist. Actually, the analysis of the potential energy surface (PES) for the reaction of ^{3}**2a** to **3a** demonstrates this point and, furthermore, provides convincing evidence that tunneling effect is responsible for the spontaneous rearrangement observed.

Two different mechanisms can be invoked to rationalize the transformation of triplet ^{3}**2a** into singlet **3a**.[44] One hypothesis features the H-atom migration occurring concomitantly with the crossing from the triplet to the singlet surface. In such a case, the triplet ^{3}**2a** should be converted by ISC into a low lying excited singlet state, probably before reaching the barrier top on the triplet surface. This is unlikely because $\Delta E_{S\text{-}T}$ of phenylnitrenes is considerably high (~18 kcal mol^{-1}), and the barrier is lower than that (see below), making the ISC less plausible. Also, experiments in Xe matrices show a decrease in the reaction rate, contrary to the expected increase rate that would result from the external heavy atom effect.[45]

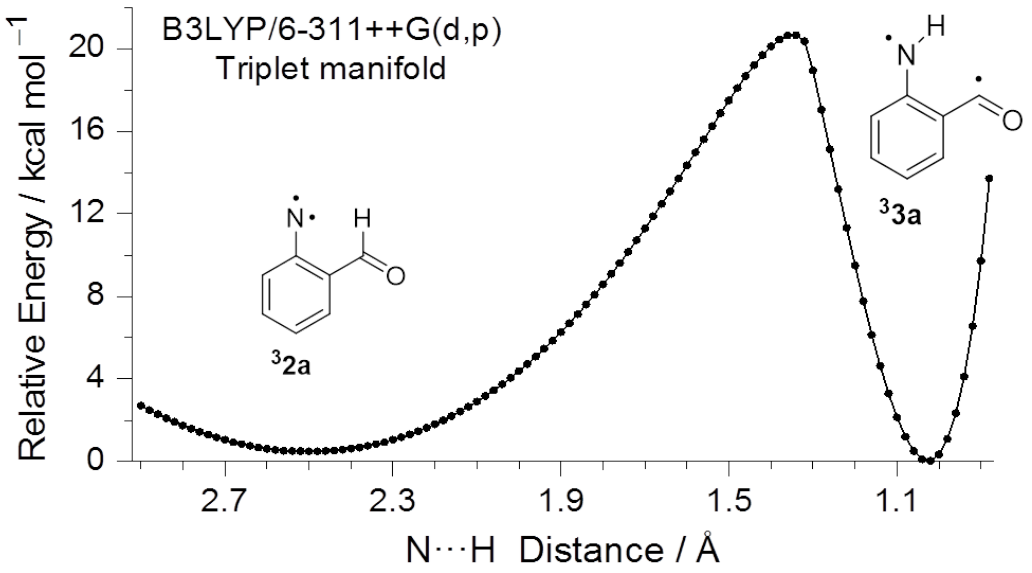

Figure 2.10. Relaxed PES scan, as a function of the NH distance, connecting phenylnitrene ^{3}**2a** (left) and the corresponding imine ^{3}**3a** (right), calculated at the B3LYP/6-311++G(d,p) level on the triplet manifold. All relative energies are with respect to the triplet ^{3}**3a**.

Another hypothesis involves the entire H-atom migration occurring on the triplet surface, from triplet ^{3}**2a** to triplet ^{3}**3a**, which then internally converts to the singlet ground state of **3a**. The feasibility of such mechanism was investigated by carrying out a PES scan connecting triplet ^{3}**2a** and triplet ^{3}**3a** as a function of the NH distance (Figure 2.10). Indeed, calculations indicate that triplet ^{3}**3a** (resembling a biradical formed by H-abstraction from triplet ^{3}**2a**) is more stable than ^{3}**2a** by ~0.15 kcal mol^{-1}. The reaction barrier for this transformation is estimated to be ~17 kcal mol^{-1} (ZPVE included), which clearly rules out the possibility of an over-the-barrier thermal reaction at 10 K. However, conditions for the occurrence of quantum tunneling seem to be satisfied because the width of the barrier is rather narrow, ca. ~1.7 Å, and the reaction coordinate is associated with the movement of the light hydrogen atom.[46] These data compare well, for instance, to the case of hydroxycarbenes that exhibit spontaneous [1,2] H-shift at 10 K *via*

tunneling through a barrier with 28 kcal mol^{-1} height and ~2.1 Å width.[47-52] Furthermore, this hypothesis can also explain why triplet 2-methyl phenylnitrene (^{3}**10)** does not rearrange to the corresponding imine **11** up to 80 K in Xe matrix (Scheme 2.2). The corresponding PES connecting ^{3}**10** to ^{3}**11** on the triplet manifold has a barrier of ~27 kcal mol^{-1} and, even more crucial, the putative rearrangement product triplet ^{3}**11** is by ~8 kcal mol^{-1} higher in energy than triplet ^{3}**10,** making the occurrence of tunneling virtually impossible (Figure S2.8).

Measurements of KIE through 2-Formyl Phenylazide-*d_1*

The current evidence indicates that the 2-formyl phenylnitrene system undergoes a tunneling reaction. Because the transformation occurs spontaneously at 10 K and appears to have little temperature dependence, tunneling is a strong contender for its mechanism. One way to build a stronger case for this hypothesis is to synthesize a deuterated analog of 2-formyl phenylnitrene and measure the kinetic isotope effect (KIE) of the system. The relationship between tunneling and KIE can be traced to two effects: 1. H has a longer de Broglie wavelength, giving it greater barrier penetration and 2. C—D bonds have a lower zero-point vibrational energies, sit lower in their energy wells, and experience broader barriers.[27] Using the deuterated analogue, the KIE can be measured, and a very large KIE would indicate a tunneling reaction. Because exact rate constants are difficult to determine in matrix isolation experiments, the comparison of reaction rate will need to be more qualitatively analyzed. However, if the hypothesized tunneling mechanism is at play, the rate decrease upon deuteration should be marked enough to be clear.

Scheme 2.5.

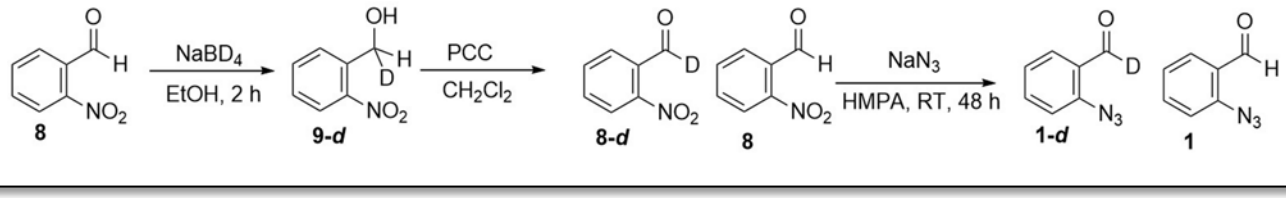

In order to study the kinetic isotope effect and probe the tunneling mechanism further, a deuterated analogue of 2-formyl phenylazide (**1-*d***) was synthesized. Starting from the same precursor, 2-nitrobenzaldehyde **8**, the deuterated benzyl alcohol **9-*d*** was synthesized by reduction with $NaBD_4$. The alcohol was then reoxidized using PCC to yield a mixture of 2-nitrobenzaldehyde-d_1 **8-*d*** and **8** and in a ratio of ~10:1 deuterated: protio (according to ^1H NMR). The azide was synthesized *via* S_NAr reaction in accordance with the initial azide to yield 2-formylphenylazide-d_1 **1-*d*** in 17% yield (Scheme 2.5).

While a mixture of protio and deutero aldehyde species was not the ideal outcome, the reaction proceeded quickly and easily and worked well to get initial results to probe tunneling. In preliminary experiments, the IR signals of the deutero and protio compounds were easily distinguishable by intensity and agreement with computed frequencies. IR experiments show formation of triplet nitrene from both the protio and deutero azide precursors. Following, the transformation to the imino ketene species is observed in the protio compound but not in the deutero. More extensive measurements are in progress, but the initial findings support the conclusion that the reaction occurs through tunneling.

Conclusions

The similarities and differences between carbene and nitrene reactivity have long been a topic of interest in the study of reactive intermediates. Indeed, the electronic structure differences between the two species can be invoked to explain differences in reactivity, but some variations remain unclear. Although tunneling reactions involving nitrenes have not yet been reported, spectroscopic observations of 2-formyl phenylnitrene ^{3}**2** strongly suggest that it undergoes a [1,4]-H migration by tunneling mechanism. IR spectroscopic studies agree well with computational predictions suggesting formation of triplet 2-formyl phenylnitrene ^{3}**2a** from 2-formyl phenylazide **1** and its subsequent transformation to imino ketene **3a**. EPR studies indicate that the intermediate formed is a triplet, and the signature is consistent with a triplet nitrene. The reaction appears to be temperature-independent and intitiates within 5 minutes at 10 K. Kinetic studies were done by our collaborators in Coimbra and the data were well-fit by dispersive kinetics, as expected for matrix-isolation systems of this type. The data can be found in the supporting information of this chapter. Further evidence for tunneling are underway by studying the deuterated analog and comparing the rates of the two systems. If the tunneling reaction occurs as predicted, this will be the first reported case of a tunneling reaction involving a nitrene as well as a tunneling reaction to an sp^2-hybridized carbon.

Experimental Section

WARNING. Azide compounds are highly explosive, and physical shocks can cause it to detonate. To minimize risk of injury, only work with very small quantities.[6,53]

General Information. Chemicals and solvents were purchased and used without purification, unless otherwise noted. ^{1}H NMR spectra (400 MHz) and ^{13}C NMR spectra (100.6

MHz) were obtained in $CDCl_3$ on a Bruker Avance III 400 spectrophotometer; chemical shifts (δ) are reported as ppm downfield from internal standard $SiMe_4$. Mass spectra were acquired using electrospray ionization on a Thermo Q-Exactive Plus™ mass spectrometer.

Synthetic Information

2-Formyl phenylazide (1).[34] To an oven-dried 25 mL round-bottom flask was added 2-nitrobenzaldehyde (**8**, 1.68 g, 11.1 mmol) and sodium azide (1.49 g, 22.9 mmol). To this was added HMPA (5 mL), and the resulting solution was stirred at ambient temperature in an atmosphere of N_2. After 48 h, the reaction ceased to change via TLC (eluent 20:1 hexane: ethyl acetate). At this point, the reaction mixture was diluted with ice water and allowed to warm to room temperature. The mixture was then extracted twice with diethyl ether. The combined organic layers were washed twice with water and once with brine. The organic layers were dried over $MgSO_4$ and concentrated to reveal a yellow solid. The solid was purified by column chromatography (SiO_2, 20:1 hexane: ethyl acetate) affording (**1**) (0.23 g, 1.6 mmol, 14%) as a white solid. ^{1}H NMR (400 MHz, $CDCl_3$): δ 10.4 (s, 1H), 7.89 (d, 8 Hz, 1H), 7.63 (t, 8 Hz, 1H). 7.28 (d, 8 Hz, 1H), 7.24 (t, 8 Hz, 1H) ppm. ^{13}C NMR ($CDCl_3$) δ 188.6 (C), 142.9 (C), 135.4 (CH), 129.0 (CH), 127.0 (C), 124.9 (CH), 119.1 (CH) ppm. HRMS (ESI-Q-IT) m/z: $[M+H]^+$ Calculated for $C_7H_7N_3O$ 148.0506; Found 148.0509. IR (Ar, 10 K) 2167 s, 1708 vs, 1608 vw, 1591 w, 1485 s, 1458 m, 1400 m, 1323 w, 1297 m, 1293 m, 1202 w, 1171 w, 1092 w, 840 w, 811 vw, 758 s, 704 vw, 624 w, 538 w, 464 w cm^{-1} (Figure 2.5); UV/vis (Ar, 10 K) λ_{max} 212, 233, 256, 310, 320 nm (Figure 2.7).

Triplet 2-Formyl phenylnitrene (2a). IR (Ar, 10 K) 2857/2853 br, 1703 s, 1558/1548 ov, 1421 w, 1411 vw, 1369/1366 w, 1301 m, 1283 m, 1246/1240 m, 1155 vw, 1134/1131 m,

1068/1065 w, 1008 vw, 956/954 vw, 851/850 w, 803 m, 751/749 s, 692 w, 622 w, 534 w cm^{-1} (Figure 2.5, 2.6); UV/vis (Ar, 10 K) λ_{max} 232, 237, 254, 322, 338, 355 nm (Figure 2.7); EPR (MCH frozen glass, 4K) measured resonances: 6721.7, 3334.5 G; microwave frequency 9.386 GHz (Figure 2.9).

2-(Nitrophenyl)methanol-*d*$_1$ (9-*d*)[54] To a 50 mL round bottom flask was added 2-nitrobenzaldehyde (**8**,1.51 g, 10 mmol) in 25 mL EtOH, and the solution was cooled to 0 °C. To the flask was added sodium borodeuteride (0.67 g, 16 mmol), and the solution was stirred at room temperature for 2 h. Upon completion, ethanol was removed, and a solution of saturated NH_4Cl was carefully added to the residue. The mixture was extracted three times with dichloromethane, and the combined organic layers were washed with brine solution, dried over $MgSO_4$, and concentrated by rotary evaporation to yield a tan solid (**9-*d***, 1.10 g, 7.0 mmol, 69% yield) that was sufficiently pure to proceed to the next step. ^{1}H NMR (400 MHz, $CDCl_3$): δ 8.11 (dd, 8.2, 1.0 Hz, 1H),7.74 (dd, 7.5, 1.0 Hz, 1H), 7.68 (td, 7.5, 1.0 Hz, 1H), 7.48 (td, 8.2, 1.0 Hz, 1H), 4.96 (s, 1H), 2.43 (br s, 1H) ppm. ^{13}C NMR ($CDCl_3$) δ 147.7, 136.69. 134.17, 130.07, 128.56, 125.04, 62.29 (m) ppm. HRMS (ASAP[55]-Q-IT) m/z: $[M-OH]^+$ Calculated for $C_7H_5DNO_2$ 137.0456; Found 137.0455.

2-Nitrobenzaldehyde-*d*$_1$ (8-*d*)[54,56] To benzyl alcohol **9-*d*** (1.10 g, 7.0 mmol) was added freshly-distilled dichloromethane (22 mL) and pyridinium chlorochromate (2.25 g, 10.4 mmol), and the mixture was stirred overnight (15 h) at room temperature under N_2. The solution was filtered over a pad of celite, and the celite was rinsed with an additional 50 mL of dichloromethane. Solvent was removed by rotary evaporation to reveal a dark oil. The crude product was purified by column chromatography (SiO_2, 20% EtOAc in hexane). Product was obtained as a yellow solid (0.8225 g ~78% yield) that was revealed to be a mixture of **8** and **8-d**

in a ratio of ~1:10. Signals in the aromatic region of the spectrum from **8** were overlapping **8-d**; however the aldehyde peak was clear (10.4 ppm), and the relative ratio was determined from its intensity. ^{1}H NMR (400 MHz, $CDCl_3$): δ 8.13 (dd, 7.5, 1.3 Hz, 1H),7.97 (dd, 7.5, 1.7 Hz, 1H), 7.82 (td, 7.5, 1.3 Hz, 1H), 7.78 (td, 7.5, 1.7 Hz, 1H) ppm.

2-Formyl phenylazide-*d*$_1$ (1-d)[57] Following the procedure for protio-compound **1**, 2-nitrobenzaldehyde-*d*$_1$ (**8-*d***) (0.8225 g, 5.4 mmol) was added to a 25 mL round-bottom flask, and to it was added sodium azide (0.723 g, 11.1 mmol). To this was added HMPA (3 mL), and the resulting solution was stirred at ambient temperature in an atmosphere of N_2. After 48 h, the reaction mixture was diluted with ice water and allowed to warm to room temperature. The mixture was then extracted twice with diethyl ether. The combined organic layers were washed twice with water and once with brine. The organic layers were dried over $MgSO_4$ and concentrated to reveal a yellow solid. The solid was purified by column chromatography (SiO_2, 20:1 hexane: ethyl acetate) affording (**1-d**) (0.136 g, 0.92 mmol, 17 % yield) as a white solid. ^{1}H NMR (400 MHz, $CDCl_3$): δ 7.89 (dd, 8, 2 Hz, 1H), 7.63 (td, 8, 2 Hz, 1H). 7.29 (d, 8 Hz, 1H), 7.24 (t, 8 Hz, 1H) ppm. ^{13}C NMR ($CDCl_3$) δ 142.9 (C), 135.4 (CH), 129.0 (CH), 124.9 (CH), 119.1 (CH) ppm. HRMS (ASAP^{55}-Q-IT) m/z: $[M+H]^+$ Calculated for $C_7H_5N_3OD$ 149.0568; Found 149.0567.

2,1-Benzisoxazole (**5**), was a commercial product purchased from Aldrich (purity 99%).

UV Irradiation Experiments

Samples were using an ILC Technology LX300UV 300 W high-pressure xenon arc lamp, and wavelength selection was achieved with a Spectral Energy GM 252 monochromator (bandpass of 20 nm centered at the specified wavelength) or using bandpass filters for broadband irradiation.

Matrix IR Spectroscopy

The matrix isolation apparatus and technique has been described previously.[58] In order to prepare the low-temperature matrices, the vapors over **1** or **5** were deposited, together with a large excess of the chosen matrix gas, onto a CsI window used as optical substrate and irradiated through a KBr window. Spectra were recorded on a Nicolet Nexus 870 FT-IR spectrometer with a DTGS detector.

Matrix Isolation UV Spectroscopy:

The matrix isolation apparatus and technique has been described previously.[58,59] In order to prepare the low-temperature matrices, the vapors over **1** or **5** were deposited, together with a large excess of the chosen matrix gas, onto a sapphire window used as optical substrate and irradiated through a quartz window. Irradiation was carried out with an ILC Technology LX300UV 300 W high-pressure xenon arc lamp, and wavelength selection was achieved with a Spectral Energy GM 252 monochromator (bandpass of 20 nm). UV-vis spectra were recorded with a Varian Cary 5000 UV/vis/NIR spectrophotometer utilizing a spectral bandwidth of 1.0 nm.

EPR Spectroscopy:

EPR measurements were carried out as previously described.[60] EPR spectra were obtained on a Bruker EleXsys E-500-A EPR spectrometer consisting of Bruker ER 049SX X-band microwave bridge (Gunn diode), ER 041-1161 microwave frequency meter, high-sensitivity resonator with optical port, and Oxford Instruments continuous-flow liquid helium cryostat (Model EPR 900).

A solution of 2-formyl phenylazide (**1**) was prepared by weighing the purified azide and dissolving in the appropriate amount of methylcyclohexane (MCH, spectroscopic grade) to give a solution of concentration ca. 5 mM. The solution was purged with N_2 and a small volume of this solution (ca. 0.4-0.5 mL) was transferred by cannula under an N_2 atmosphere into a 3 mm quartz EPR tube (Wilmad Glass Co., Inc.; model 727-SQ- 250M). To prevent crystallization and ensure formation of a glass, the EPR sample was first frozen by immersing in liquid nitrogen and rapidly transferring (ca. 1-2 s) the tube from the liquid nitrogen dewar to the pre-cooled liquid helium cryostat at 4.2 K.

Irradiation of azide **1** ($\lambda = 310 \pm 10$ nm, 40 min; MCH, 4.2 K) afforded the EPR spectrum of triplet 2-formyl phenylnitrene (**2**) (Figure 2.9). The spectrum of nitrene **2** is characteristic of many triplet aryl nitrenes in exhibiting only a single transition (XY_2) in the X-band EPR spectrum.[37,39] That the spectrum exhibits a single XY_2 transition, rather than features attributable to distinct X_2 and Y_2 transitions,[38] reveals that the local electronic environment at the nitrene center is axially symmetric and establishes that the magnitude of the zero-field splitting parameter E is very small ($|E/hc| < 0.002$ cm^{-1}). The zero-field splitting parameter D was evaluated in the standard way using equation (1) to afford a value of $|D/hc| = 0.979$ cm^{-1}.[37,39] This value is in good agreement with those of other triplet arylnitrenes, which typically fall in the range 0.9-1.2 cm^{-1}. In principle, triplet nitrene **2** exists as mixture of conformational isomers (**2a** and **2b**) that differ in the relative orientation of the formyl substituent relative to the nitrene center. The fact that a single XY_2 transition is observed suggests either that only a single conformer is observed, or, more likely, that the conformational perturbation is too subtle to be manifest in the X-band EPR spectrum.

$$(H_{ext})^2 = H_0(H_0 + D) \qquad (1)$$

Where H_{ext} is the resonance field of the XY_2 transition, H_0 is the resonance field of a free radical under the conditions, and the conversion factor between G and cm^{-1} is given by: 10,700 G = 1 cm^{-1}.[37]

Theoretical Calculations

All quantum-mechanical computations were carried out with the Gaussian 09,[61] using the standard 6-311++G(d,p) and CBS-QB3 basis sets defined in this program package. For the purpose of modeling IR spectra, the geometry optimization and the frequency calculations were done with the B3LYP/6-311++G(d,p) method.[62-64] After scaling the calculated frequencies by factors of 0.980 below 3000 cm^{-1} and by 0.950 above 3000 cm^{-1}, the resulting frequencies, together with the calculated intensities served to simulate the infrared spectra shown in the Figures by convoluting each peak with a Lorentzian function with a full width at half-maximum (FWHM) of 2 cm^{-1}, so that the integral band intensities correspond to the calculated infrared absolute intensity. Note that the peak intensities in the simulated spectra are several times less (in the arbitrary units of "Relative intensity") than the calculated intensity (in km mol^{-1}).

B3LYP/6-311++G(d,p) and CBS-QB3 methods were used to estimate relative energies of the 2-azidobenzadehyde **1** conformers.

Vertical excitation energies of the low-energy electronic excited states were calculated using the time-dependent density functional theory (TD-DFT). For the graphical representation, each calculated peak was convoluted with a Lorentzian function having FWHM of 0.12 eV (967.9 cm^{-1}). During this operation, the calculated excitation energies were not scaled. The resulting simulation is presented in Figure 2.8b.

Notes and References

1. Smith, P. A. S. *Nitrenes*; Wiley-Interscience: New York, 1970.

2. Breslow, D. S. *Azides and Nitrenes; Reactivity and Utility*; Academic Press: New York, 1984.

3. Meijer, E. W.; Nijhuis, S.; Van Vroonhoven, F. C. B. M. Poly-1,2-azepines by the photopolymerization of phenyl azides. Precursors for conducting polymer films. *J. Am. Chem. Soc.* **1988**, *110*, 7209-7210.

4. Schuster, G. B.; Platz, M. S. Photochemistry of phenyl azide. *Adv. Photochem.* **1992**, *17*, 69.

5. Huisgen, R. 1, 3-dipolar cycloadditions. Past and future. *Angew. Chem. Int. Ed. Engl.* **1963**, *2*, 565-598.

6. Bräse, S.; Banert, K. *Organic azides: syntheses and applications*; John Wiley: Chicester, West Sussex, U.K., 2010.

7. Bräse, S.; Gil, C.; Knepper, K.; Zimmermann, V. Organic Azides: An Exploding Diversity of a Unique Class of Compounds. *Angew. Chem. Int. Ed.* **2005**, *44*, 5188-5240.

8. Baron, W. J.; DeCamp, M. R.; Hendrick, M. E.; Jones, M. J.; Levin, R. H.; Sohn, M. B. *Carbenes*; Wiley: New York, 1973; Vol. I.

9. McMahon, R. J.; Chapman, O. L. Direct spectroscopic observation of intramolecular hydrogen shifts in carbenes. *J. Am. Chem. Soc.* **1987**, *109*, 683-692.

10. Morawietz, J.; Sander, W.; Traeubel, M. Intramolecular Hydrogen Transfer in (2-Aminophenyl)carbene and 2-Tolylnitrene. Matrix Isolation of 6-Methylene-2,4-cyclohexadien-1-imine. *J. Org. Chem.* **1995**, *60*, 6368-6378.

11. Platz, M. S. In *Reactive Intermediate Chemistry*; Moss, R. A., Platz, M. S., Jones, M. J., Eds.; John Wiley & Sons, Inc.: Hoboken, NJ, 2004.

12. Smolinsky, G.; Wasserman, E.; Yager, W. The EPR of Ground State Triplet Nitrenes. *J. Am. Chem. Soc.* **1962**, *84*, 3220-3221.

13. Karney, W. L.; Borden, W. T. Ab initio study of the ring expansion of phenylnitrene and comparison with the ring expansion of phenylcarbene. *J. Am. Chem. Soc.* **1997**, *119*, 1378-1387.

14. Travers, M. J.; Cowles, D. C.; Clifford, E. P.; Ellison, G. B. Photoelectron spectroscopy of the phenylnitrene anion. *J. Am. Chem. Soc.* **1992**, *114*, 8699-8701.

15. McDonald, R. N.; Davidson, S. J. Electron photodetachment of the phenylnitrene anion radical: EA, $\Delta H°_f$, and the singlet-triplet splitting for phenylnitrene. *J. Am. Chem. Soc.* **1993**, *115*, 10857-10862.

16. Dannenberg, J. J.; Vinson, L. K.; Moreno, M.; Bertran, J. A molecular orbital study of phenylcarbene and diphenylcarbene. *J. Org. Chem.* **1989**, *54*, 5487-5491.

17. Matzinger, S.; Bally, T.; Patterson, E. V.; McMahon, R. J. The C_7H_6 potential energy surface revisited: relative energies and IR assignment. *J. Am. Chem. Soc.* **1996**, *118*, 1535-1542.

18. Shavitt, I. Geometry and singlet-triplet energy gap in methylene: a critical review of experimental and theoretical determinations. *Tetrahedron* **1985**, *41*, 1531-1542.

19. Hrovat, D. A.; Waali, E. E.; Borden, W. T. Ab initio calculations of the singlet-triplet energy difference in phenylnitrene. *J. Am. Chem. Soc.* **1992**, *114*, 8698-8699.

20. Kim, S. J.; Hamilton, T. P.; Schaefer III, H. F. Phenylnitrene: energetics, vibrational frequencies, and molecular structures. *J. Am. Chem. Soc.* **1992**, *114*, 5349-5355.

21. Gritsan, N. P.; Zhu, Z.; Hadad, C. M.; Platz, M. S. Laser Flash Photolysis and Computational Study of Singlet Phenylnitrene. *J. Am. Chem. Soc.* **1999**, *121*, 1202-1207.

22. Tokunoh, R. *Synlett* **1995**, *491*.

23. Doyle, M. P.; Hu, W. Enantioselective carbon--hydrogen insertion is an effective and efficient methodology for the synthesis of (r)-(-)-baclofen. *Chirality* **2002**, *14*, 169-172.

24. Leyva, E.; Platz, M. S.; Persy, G.; Wirz, J. Photochemistry of phenyl azide: the role of singlet and triplet phenylnitrene as transient intermediates. *J. Am. Chem. Soc.* **1986**, *108*, 3783-3790.

25. Bell, R. P. *The Tunnel Effect in Chemistry*; Chapman and Hall: New York, 1980.

26. Bell, R. P. *The Proton in Chemistry*; Chapman and Hall: New York, 1973.

27. Sheridan, R. S. In *Reviews of Reactive Intermediate Chemistry*; Platz, M. S., Moss, R. A., Jones, M. J., Eds.; John Wiley & Sons, Inc.: Hoboken, N.J., 2007, p 415-463.

28. McMahon, R. J. Chemical Reactions Involving Quantum Tunneling. *Science* **2003**, *299*, 833-834.

29. Moss, R. A.; Sauers, R. R.; Sheridan, R. S.; Tian, J.; Zuev, P. S. Carbon tunneling in the ring expansion of noradamantylchlorocarbene. *J. Am. Chem. Soc.* **2004**, *126*, 10196-10197.

30. Sander, W.; Bucher, G.; Reichel, F.; Cremer, D. 1H-Bicyclo [3.1. 0] hexa-3, 5-dien-2-one. A strained 1, 3-bridged cyclopropene. *J. Am. Chem. Soc.* **1991**, *113*, 5311-5322.

31. Ley, D.; Gerbig, D.; Wagner, J. P.; Reisenauer, H. P.; Schreiner, P. R. Cyclopropylhydroxycarbene. *J. Am. Chem. Soc.* **2011**, *133*, 13614-13621.

32. Inui, H.; Sawada, K.; Oishi, S.; Ushida, K.; McMahon, R. J. Aryl Nitrene Rearrangements: Spectroscopic Observation of a Benzazirine and Its Ring Expansion to a Ketenimine by Heavy-Atom Tunneling. *J. Am. Chem. Soc.* **2013**, *135*, 10246-10249.

33. Murata, S.; Tsubone, Y.; Kawai, R.; Eguchi, D.; Tomioka, H. Mechanistic studies of intramolecular CH insertion reaction of arylnitrenes: isotope effect, configurational purity and radical clock studies. *J. Phys. Org. Chem.* **2005**, *18*, 9-20.

34. Capperucci, A.; Degl'Innocenti, A.; Funicello, M.; Mauriello, G.; Scafato, P.; Spagnolo, P. Hexamethyldisilathiane: its use in the conversion of aromatic and heteroaromatic azides to amines. *J. Org. Chem.* **1995**, *60*, 2254-2256.

35. Wasserman, E. Electron spin resonance of nitrenes. *Prog. Phys. Org. Chem* **1971**, *8*, 319-336.

36. Dunkin, I. R.; Lynch, M. A.; Withnall, R.; Boulton, A. J.; Henderson, N. The thermal decomposition of 1-methyl-1,2,3-benzotriazin-4-(1H)-one: matrix isolation of the reactive intermediates. *J. Chem. Soc., Chem. Commun.* **1989**, 1777-1778.

37. Platz, M. S. In *Azides and Nitrenes*; Scriven, E. F. V., Ed.; Academic Press: Orlando, FL, 1984.

38. Chapyshev, S. V. Zero-field splitting parameters of triplet nitreno-s-triazines: a new insight into the geometry of the nitrene centres of triplet and singlet nitrenes. *Mendeleev Commun.* **2002**, *12*, 227-229.

39. Wasserman, E. *Prog. Phys. Org. Chem.* **1971**, *8*, 319-336.

40. Wertz, J. E.; Bolton, J. R. *Electron Spin Resonance Spectroscopy*; Chapman and Hall: New York, 1986.

41. Pryor, W. A.; Hales, B. J.; Premoviv, P. I.; Church, D. F. *Science* **1983**, *220*, 425-427.

42. Senthilnathan, V. P.; Platz, M. S. Determination of the absolute rates of decay of arylcarbenes in various low temperature matrixes by electron spin resonance spectroscopy. *J. Am. Chem. Soc.* **1980**, *102*, 7637-7643.

43. Senthilnathan, V. P.; Platz, M. S. Conformational barriers in triplet 1- and 2-naphthylcarbene. 2. Absolute rate of decay of arylcarbenes by electron spin resonance spectroscopy. *J. Am. Chem. Soc.* **1981**, *103*, 5503-5511.

44. Zuev, P. S.; Sheridan, R. S. Low-Temperature Hydrogenation of Triplet Carbenes and Diradicaloid Biscarbenes Electronic State Selectivity. *J. Am. Chem. Soc.* **2001**, *123*, 12434-12435.

45. Fisher, J. J.; Michl, J. External and internal heavy-atom effects on the rate of spin-forbidden proton tunneling in the triplet ground state biradical 1,3-perinaphthadiyl. *J. Am. Chem. Soc.* **1987**, *109*, 583-584.

46. Ley, D.; Gerbig, D.; Schreiner, P. R. Tunnelling control of chemical reactions - the organic chemist's perspective. *Org. Biomol. Chem.* **2012**, *10*, 3781-3790.

47. Henkel, S.; Sander, W. Activation of Molecular Hydrogen by a Singlet Carbene through Quantum Mechanical Tunneling. *Angew. Chem. Int. Ed.* **2015**, *54*, 4603-4607.

48. Ley, D.; Gerbig, D.; Schreiner, P. R. Tunneling control of chemical reactions: C–H insertion versus H-tunneling in tert-butylhydroxycarbene. *Chem. Sci.* **2013**, *4*, 677-684.

49. Henkel, S.; Huynh, Y.-a.; Neuhaus, P.; Winkler, M.; Sander, W. Tunneling Rearrangement of 1-Azulenylcarbene. *J. Am. Chem. Soc.* **2012**, *134*, 13204-13207.

50. Schreiner, P. R.; Reisenauer, H. P.; Ley, D.; Gerbig, D.; Wu, C.-H.; Allen, W. D. Methylhydroxycarbene: Tunneling control of a chemical reaction. *Science* **2011**, *332*, 1300-1303.

51. Schreiner, P. R.; Reisenauer, H. P.; Pickard Iv, F. C.; Simmonett, A. C.; Allen, W. D.; Mátyus, E.; Császár, A. G. Capture of hydroxymethylene and its fast disappearance through tunnelling. *Nature* **2008**, *453*, 906-909.

52. Zuev, P. S.; Sheridan, R. S.; Albu, T. V.; Truhlar, D. G.; Hrovat, D. A.; Borden, W. T. Carbon tunneling from a single quantum state. *Science* **2003**, *299*, 867-870.

53. *Prudent Practices in the Laboratory, Updated Version*; National Academy Press: Washington, D.C., 2011.

54. Storz, M. P.; Maurer, C. K.; Zimmer, C.; Wagner, N.; Brengel, C.; de Jong, J. C.; Lucas, S.; Müsken, M.; Häussler, S.; Steinbach, A.; Hartmann, R. W. Validation of PqsD as an Anti-biofilm Target in Pseudomonas aeruginosa by Development of Small-Molecule Inhibitors. *J. Am. Chem. Soc.* **2012**, *134*, 16143-16146.

55. McEwen, C. N.; McKay, R. G.; Larsen, B. S. Analysis of solids, liquids, and biological tissues using solids probe introduction at atmospheric pressure on commercial LC/MS instruments. *Anal. Chem.* **2005**, *77*, 7826-7831.

56. Li, P.; Ji, Y.; Chen, W.; Zhang, X.; Wang, L. The facile synthesis of 2-bromoindoles via Cs_2CO_3-promoted intramolecular cyclization of 2-(gem-dibromovinyl)anilines under transition-metal-free conditions. *RSC Advances* **2013**, *3*, 73-78.

57. Stokes, B. J.; Liu, S.; Driver, T. G. Rh2(II)-Catalyzed Nitro-Group Migration Reactions: Selective Synthesis of 3-Nitroindoles from β-Nitro Styryl Azides. *J. Am. Chem. Soc.* **2011**, *133*, 4702-4705.

58. McMahon, R. J.; Chapman, O. L.; Hayes, R. A.; Hess, T. C.; Krimmer, H. P. Mechanistic studies on the Wolff rearrangement: the chemistry and spectroscopy of some .alpha.-keto carbenes. *J. Am. Chem. Soc.* **1985**, *107*, 7597-7606.

59. Seburg, R. A.; McMahon, R. J. Photochemistry of matrix-isolated diazoethane and methyldiazirine: ethylidene trapping? *J. Am. Chem. Soc.* **1992**, *114*, 7183-7189.

60. DePinto, J. T.; deProphetis, W. A.; Menke, J. L.; McMahon, R. J. Triplet 1,3-Diphenylpropynylidene (Ph−C−C−C−Ph). *J. Am. Chem. Soc.* **2007**, *129*, 2308-2315.

61. Frisch, M. J.; Trucks, G. W.; Schlegel, H. B.; Scuseria, G. E.; Robb, M. A.; Cheeseman, J. R.; Scalmani, G.; Barone, V.; Mennucci, B.; Petersson, G. A.; Nakatsuji, H.; Caricato, M.; Li, X.; Hratchian, H. P.; Izmaylov, A. F.; Bloino, J.; Zheng, G.; Sonnenberg, J. L.; Hada, M.; Ehara, M.; Toyota, K.; Fukuda, R.; Hasegawa, J.; Ishida, M.; Nakajima, T.; Honda, Y.; Kitao, O.; Nakai, H.; Vreven, T.; Montgomery, J. A., Jr.; Peralta, J. E.; Ogliaro, F.; Bearpark, M.; Heyd, J. J.; Brothers, E.; Kudin, K. N.; Staroverov, V. N.; Kobayashi, R.; Normand, J.; Raghavachari, K.; Rendell, A.; Burant, J. C.; Iyengar, S. S.; Tomasi, J.; Cossi, M.; Rega, N.; Millam, J. M.; Klene, M.; Knox, J. E. C., J. B.; Bakken, V.; Adamo, C.; Jaramillo, J.; Gomperts, R.; Stratmann, R. E.; Yazyev, O.; Austin, A. J.; Cammi, R.; Pomelli, C.; Ochterski, J. W.; Martin, R. L.; Morokuma, K.; Zakrzewski, V. G.; Voth, G. A.; Salvador, P.; Dannenberg, J. J.; Dapprich, S.; Daniels, A. D.; Farkas, Ö.; Foresman, J. B.; Ortiz, J. V.; Cioslowski, J.; Fox, D. J.; Gaussian, Inc.: Wallingford, CT, 2009.

62. Becke, A. D. Density-Functional Exchange-Energy Approximation with Correct Asymptotic Behavior. *Phys. Rev. A* **1988**, *38*, 3098-3100.

63. Lee, C. T.; Yang, W. T.; Parr, R. G. Development of the Colle-Salvetti Correlation-Energy Formula into a Functional of the Electron-Density. *Phys. Rev. B* **1988**, *37*, 785-789.

64. Vosko, S. H. W., L.; Nusair, M. Accurate Spin-Dependent Electron Liquid Correlation Energies for Local Spin Density Calculations: a Critical Analysis. *Can. J. Phys.* **1980**, *58*, 1200-1211.

Supporting Information for Chapter 2: Evidence of a Nitrene Tunneling Reaction

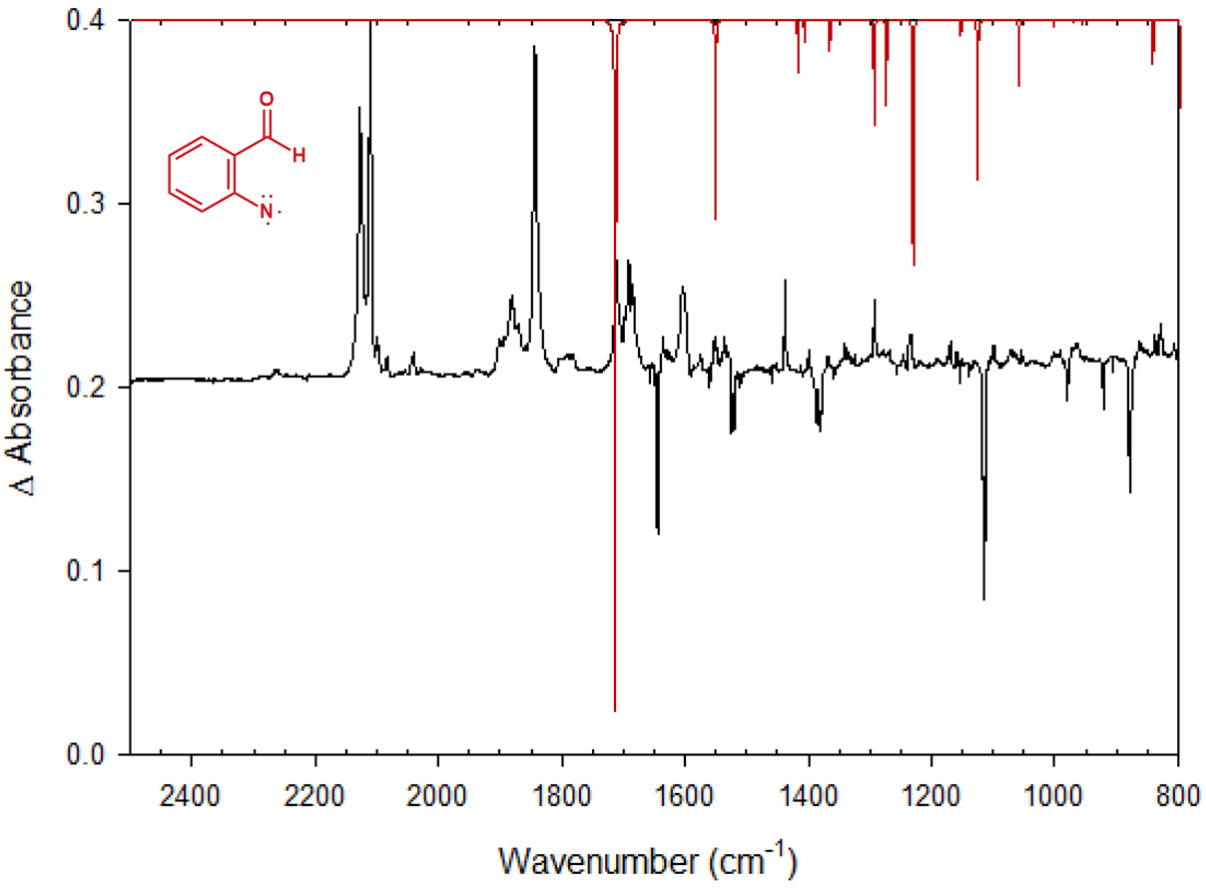

Figure S2.1. Infrared difference spectrum upon irradiation (λ = 260 ± 10 nm, 16h) of 2,1-benzisoxazole to form 2-formyl phenylnitrene. It was found that these irradiation conditions did not produce a high enough concentration of nitrene to detect changes in the spectrum upon waiting in the dark. Power of the lamp was too low, and other products dominated the spectrum. For the benzisoxazole system, broadband irradiation produced better results (Figure 2.1, 2.2).

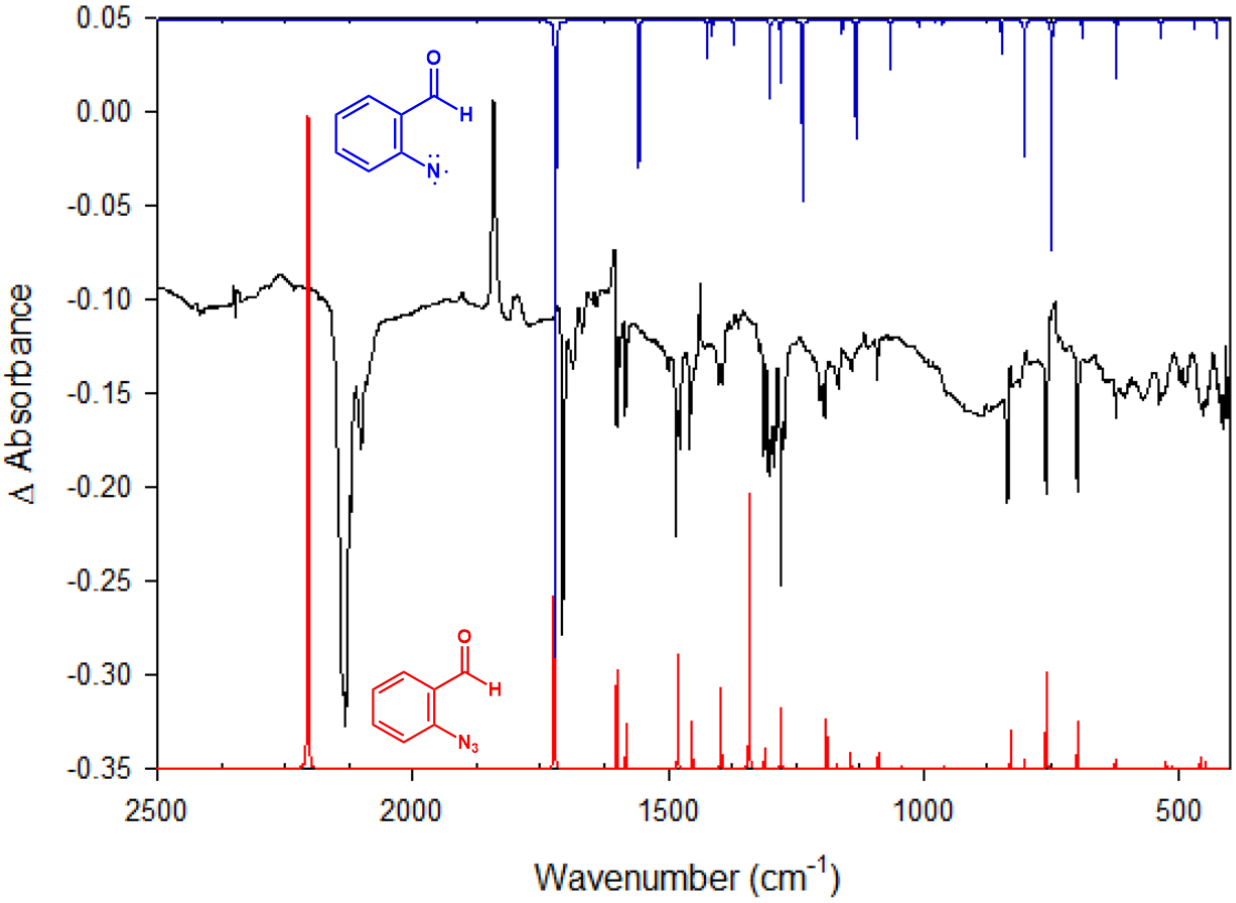

Figure S2.2. Infrared difference spectrum upon irradiation ($\lambda \geq 330$ nm, 60min) of 2-formyl phenylazide. It was found that these irradiation conditions did not produce a spectrum that agreed well with the computed nitrene spectrum. Additionally, no changes occurred in the spectrum upon waiting. It was concluded that these irradiation conditions produce the final photoproduct immediately, bypassing the nitrene intermediate. Better results were produced from monochromatic irradiation (Figure 2.4, 2.5).

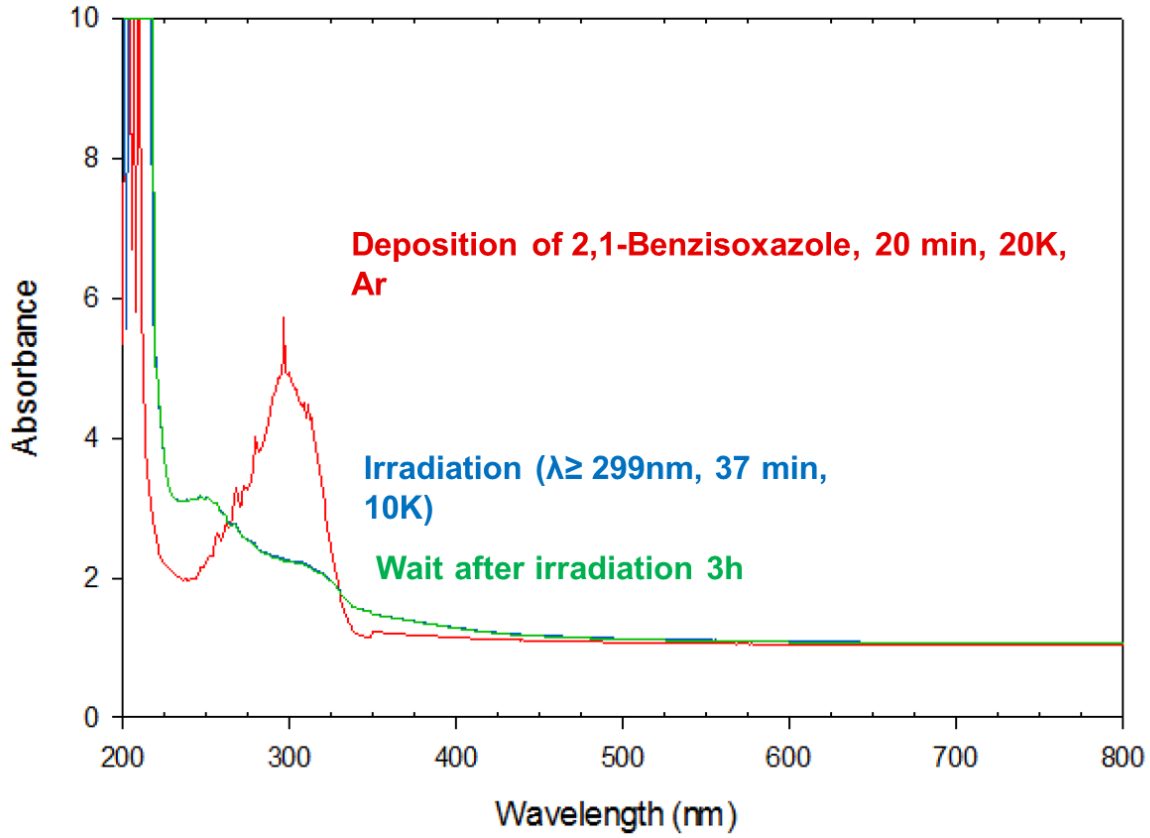

Figure S2.3. UV-visible spectrum of 2,1-benzisoxazole **5** upon deposition (20 min, 10 K, red trace), upon broadband irradiation ($\lambda \geq 299$ nm, 10 K, 37 min, blue trace), and after waiting in the dark 3h after irradiation (green trace). No changes were observed in the spectrum during this time.

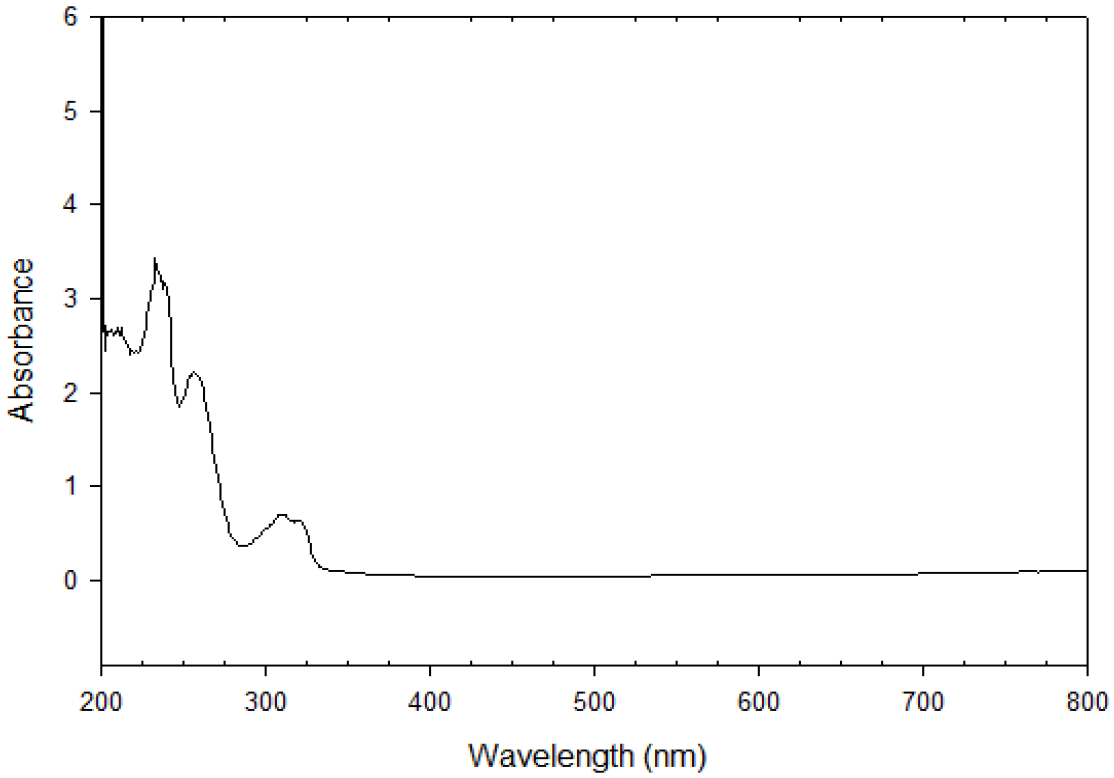

Figure S2.4. UV/visible absorption spectrum of 2-formyl phenylazide in hexanes.

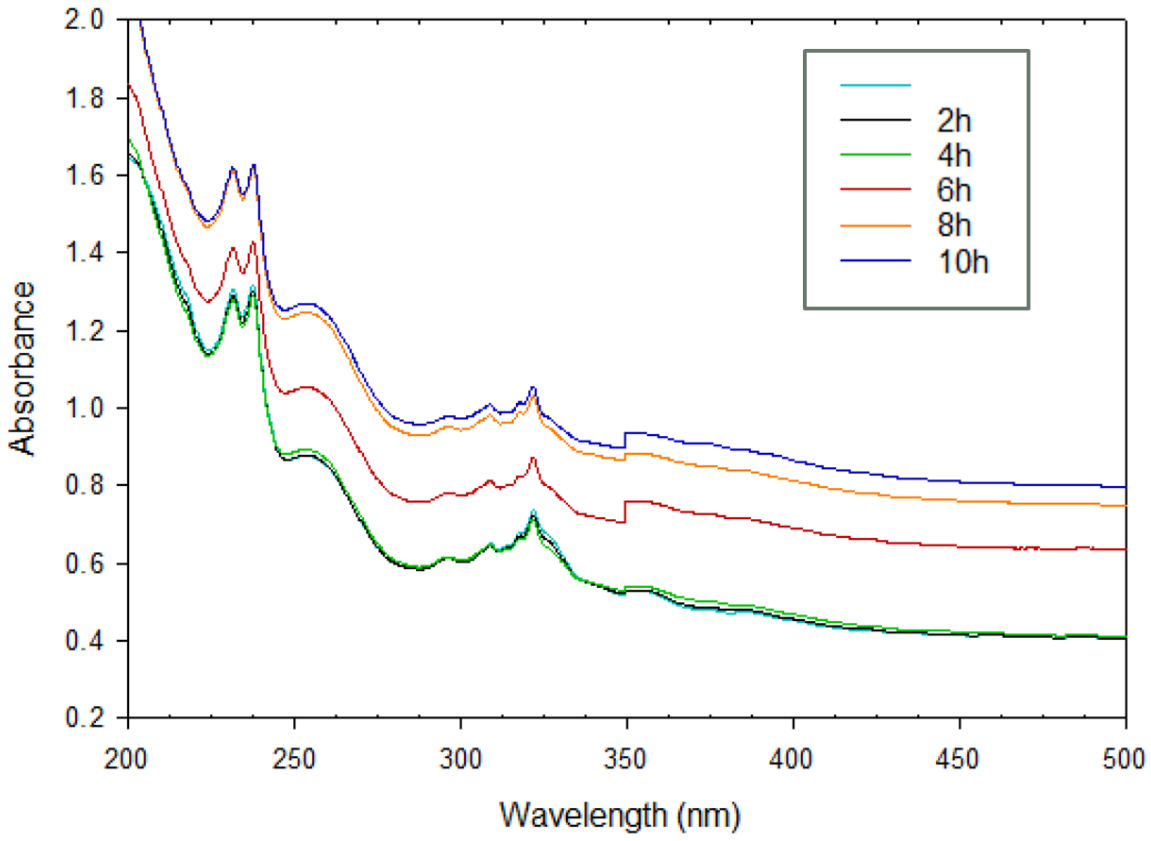

Figure S2.5. Subsequent UV/visible absorption spectra acquired upon waiting in the dark at 10 K after 2-formyl phenylazide at 10 K was irradiated ($\lambda = 320 \pm 10$ nm, 5min)

Kinetic studies were performed by Cláudio M. Nunes, Igor Reva, and Rui Fausto at the University of Coimbra in Coimbra, Portugal

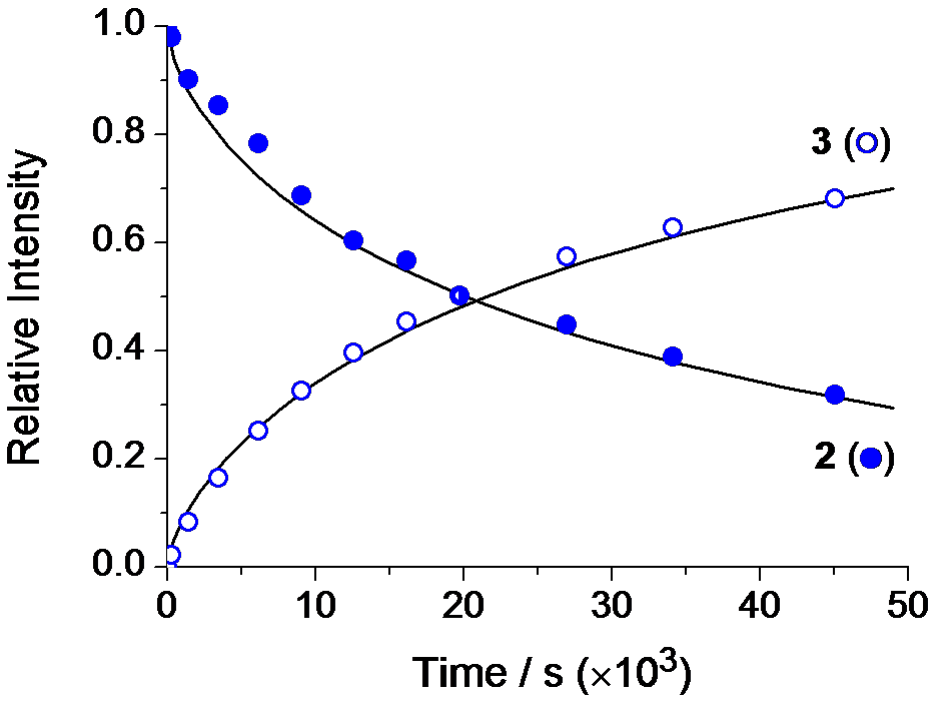

Figure S2.6. Kinetics of the spontaneous rearrangement of triplet nitrene **2** to imino ketene **3** in an argon matrix at 10 K. Solid (●) and open (○) circles represent the evolution of the amount of **2** (consumption) and **3** (production), respectively, with the time of keeping the sample in the dark (not exposed to the IR source of the spectrometer) and by collecting the IR spectra using a cutoff filter transmitting only up to 2200 cm^{-1}. Black lines represent the dispersive kinetics fits. The sample was exposed to the IR source of the spectrometer and no cutoff filter was used to collect the IR spectra.

The kinetics of the spontaneous rearrangement of **2** to **3** in argon matrix at 10 K was followed by monitoring the decrease and the increase of the IR bands due to **2** and **3**, respectively. Kinetics of the decay ofs **2** in Ar was followed by the **2** doublet band with maxima at 751.2 / 749.0 cm^{-1} and limited between 753.5 cm^{-1} and 745.5 cm^{-1}

(wavenumbers refer to an Ar matrix). Kinetics of **3** growth in Ar was followed by the **3** band centered at 2110.8 cm^{-1} and limited between 2116 cm^{-1} and 2106 cm^{-1} (wavenumbers refer to an Ar matrix).

Monitoring of the decay of **2** into **3** was carried out by successive registration of infrared spectra, as a function of time. Each of these spectra was collected using 64 scans. Under such a condition, the collection length of one spectrum equals to 261 seconds. Already during these initial minutes, a part of the photoproduced nitrene **2** undergoes decay into **3**. In the kinetic analysis, the moment of registration of the first spectrum was assumed to be the origin of time of decay, the intensity of the nitrene bands present in this first spectrum was assumed to be 100%, and the amount of ketene present in the same first spectrum (formed between the irradiation and the registration of the first spectrum) was assumed to be relative 0%. Decay of **2** in an argon matrix was monitored for 13.6 hours and, upon that time, 31% of nitrene remained in the sample. Decay of **2** in a krypton matrix was monitored for 14.3 hours and, upon that time, 20% of nitrene remained in the sample. The amount of ketene **3** generated in the process of tunneling was then normalized to be 69% in the argon matrix upon 13.6 hours, and 80% in the krypton matrix upon 14.3 hours. This normalization assumes a direct quantitative transformation of **2** into **3**, which was indeed confirmed spectroscopically. In a xenon matrix the spontaneous rearrangement was found to be much slower. Over a period of 7 days in the dark at 10 K only ~25% of **2** was transformed into **3**.

To verify that rearrangement of **2** to **3** is not stimulated by the IR radiation from the light source of the IR spectrometer, we performed independent measures with the matrix sample kept in complete dark (protected from the spectrometer IR source) and using, when collecting IR spectra, an IR cutoff filter transmitting only up to 2200 cm^{-1}. Similar kinetic data were obtained in both instances (Figure S2.6).

A solid matrix represents a reaction system in which the studied molecules (such as nitrene **2**) are embedded in a variety of different microenvironments (matrix sites), where the probability of rearrangement (i.e. the reaction barrier) slightly differs from one site to another. Moreover, one may assume that the internal structure of different matrix sites in a cryogenic matrix does not change over time, which means that the chemical reaction (such as decay of **2** to **3**) proceeds on a time scale shorter than rearrangement of the medium. Under such circumstances, the chemical reactions follow so-called dispersive kinetics,[1,2] rather than the classical first-order kinetics expected for unimolecular reactions in the gas phase. The dispersive kinetics is described by an empirical equation of the form

$$[R]_t=[R]_0 \exp[-(k\,\tau_{disp})^{\beta}], \quad 0 < \beta < 1 \qquad (1),$$

introduced by Siebrand and Wildman.[3] For dispersive kinetics, many time scales coexist and the rate coefficients for dispersive processes depend on time. Parameter β can be treated as a measure of inhomogeneity of the medium. Without environmental effects, β=1 should be observed. In matrices, β is reported to lie between 0.5 and 1, depending on the matrix, the temperature, and the time when the measurement of the kinetics is started.[4]

We used Equation (1) to fit the kinetic data of the **2** → **3** rearrangement. For an argon matrix at 10 K (Figure S2.6), the fit parameters for consumption of **2** are: β ~ 0.64, τ_{disp} ~ 4.9 h; for production of **3:** α ~ 0.67, τ_{disp} ~ 5.6 h. For a krypton matrix at 10 K (Figure S2.7), the fits gave for consumption of **2:** α ~ 0.76, τ_{disp} ~5.1 h; for production of **3:** α ~ 0.75, τ_{disp} ~ 4.9 h.

Though the matrix effects leading to dispersive kinetics make it difficult to extract physically meaningful rate constants from the kinetic data, it still can be noted

that the decays in argon and krypton result in similar fitted parameters. About 50% of **2** is converted to **3** within 5.8 h in argon and 4.5 h in krypton. [IR-B] The fitted parameter β is in accord with literature.[4,5]

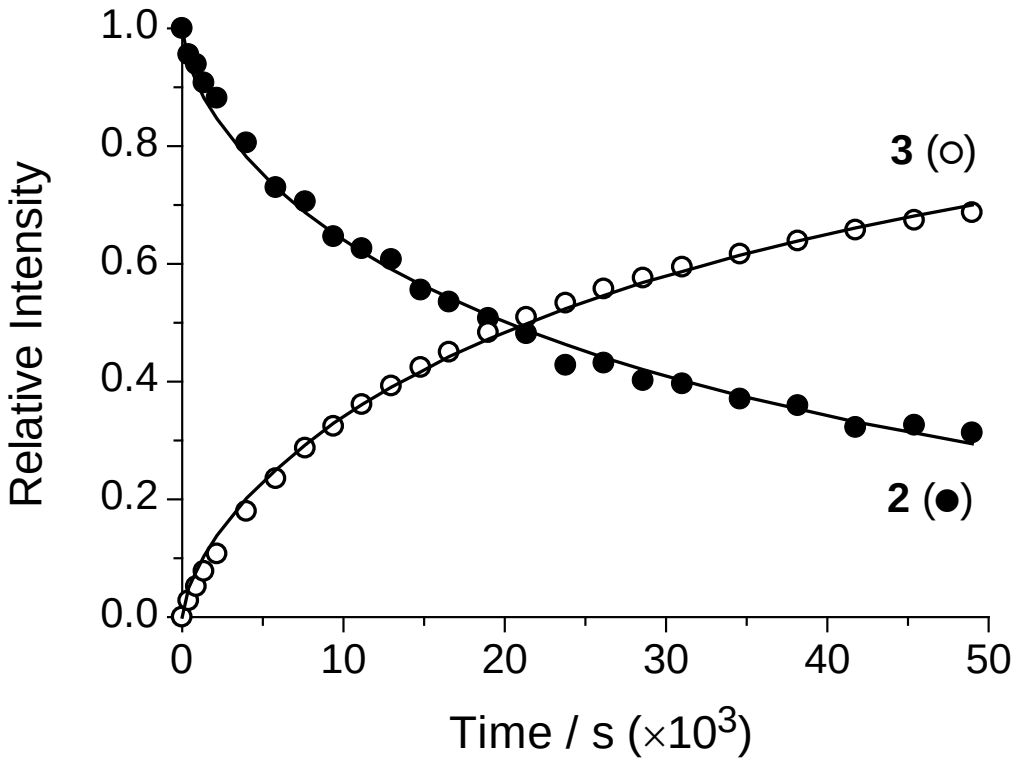

Figure S2.7. Kinetics of the spontaneous rearrangement of triplet nitrene ^{3}**2a** to imino ketene **3a** in an argon matrix at 10 K. Solid (●) and open (○) circles represent the evolution of the amount of **2** (consumption) and **3** (production), respectively, over the time the matrix was kept in the dark. Black lines represent fits using the equations of dispersive kinetics

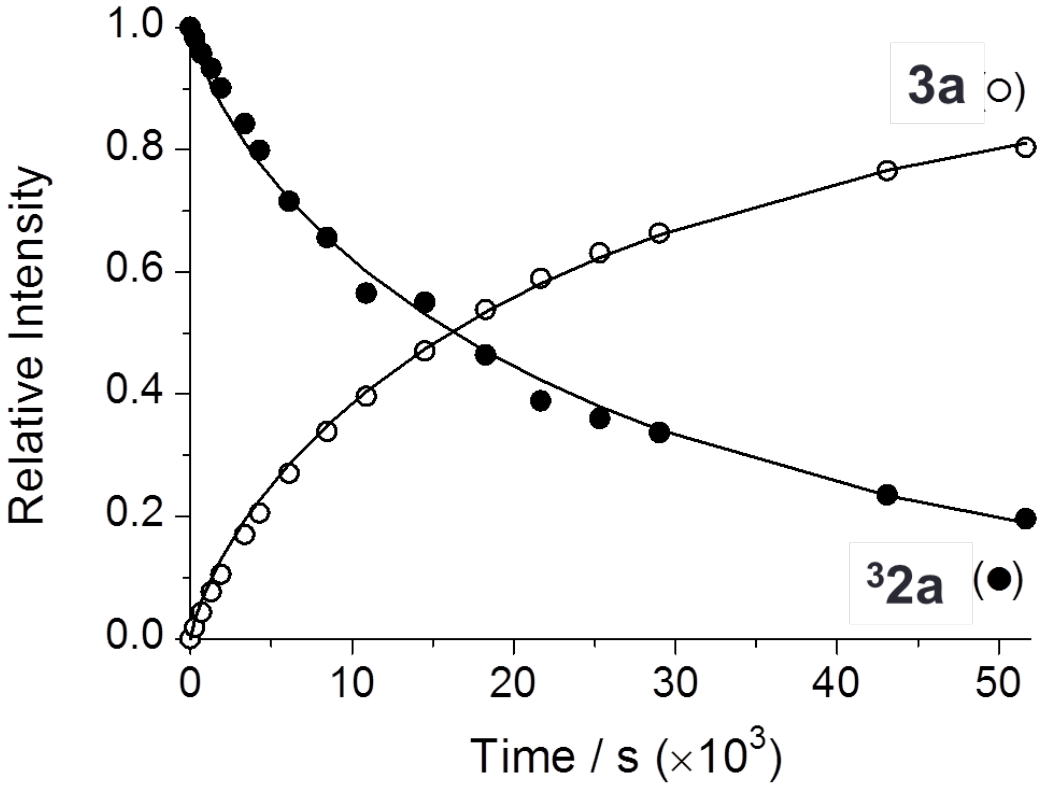

Figure S2.8. Kinetics of the spontaneous rearrangement of triplet nitrene ^{3}**2a** to imino ketene **3a** in a krypton matrix at 10 K. Solid (●) and open (○) circles represent the time evolution of the amounts of ^{2}**6a** (consumption) and **3a** (production), respectively (the sample was only exposed to the IR source of the spectrometer). Black lines represent fits using dispersive kinetics adjustments (see the "Kinetics" section for more information).

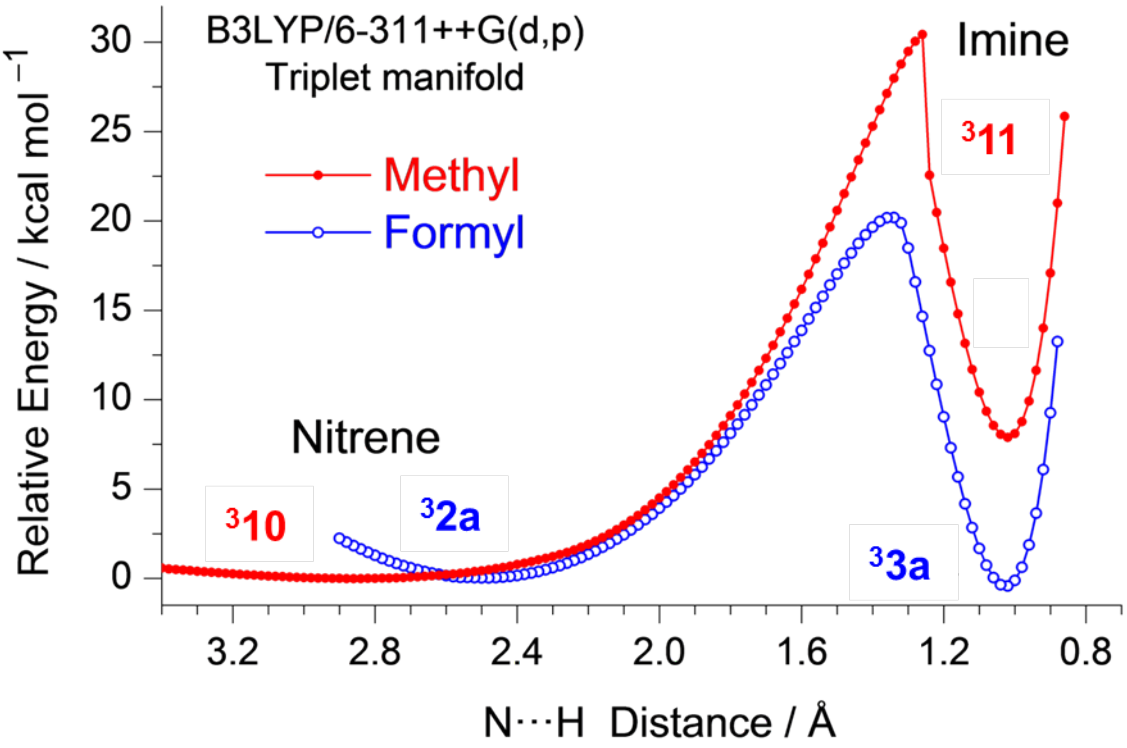

Figure S2.9. Relaxed potential energy scans, as functions of the NH distance, connecting phenylnitrenes (left) and the corresponding imines (right), with either formyl substituent (blue line) or methyl substituent (red line) at the *ortho*-position of the phenylnitrene species. Both scans were calculated at the B3LYP/6-311++G(d,p) level of theory on the triplet manifold. The electronic energies of the triplet nitrenes in each compound were assumed as the relative zeroes. See Scheme 2.1 for structures **3** and **4**, and Figure 2.9 for structures ^{3}**2a** and ^{3}**3a**.

Table S2.1. Experimental IR spectral data (argon matrix at 10 K), B3LYP/6-311++G(d,p) calculated vibrational frequencies (ν, cm^{-1}), absolute infrared intensities (A^{th}, km mol^{-1}), and vibrational assignment of triplet 2-formyl phenylnitrene ^{3}**2a**.[a]

Ar matrix[b]		Calculated[c]		Sym.	Approx. assignment[d]
ν	I	ν	A^{th}		
2857/2853	br	2885	45.7	A'	ν(OC−H)
1703	s	1718	263.5	A'	ν(C=O)
1558/1548	ov	1555	43.6	A'	ν(C=C) as
-	-	1513	0.1	A'	ν(CC) ring a
1421	w	1421	10.6	A'	δ(CH) a
1411	vw	1410	4.0	A'	δ(OC−H) + δ(CH) b
1369/1366	w	1369	6.2	A'	δ(OC−H) − δ(CH) b
1301	m	1298	20.2	A'	ν(C−N) + ν(CC) ring b
1283	m	1277	16.7	A'	ν(CC) ring b − ν(C−N)
1246/1240	m	1234	50.8	A'	ν(OC−C)
1155	vw	1156	3.1	A'	δ(CH) c
1134/1131	m	1130	30.2	A'	δ(CH) d
1068/1065	w	1062	12.9	A'	ν(CC) ring c
-	-	1017	0.06	A'	ν(CC) ring d
1008 (?)	vw	1006	1.4	A"	γ(OC−H)
-	-	976	0.4	A"	γ(CH) a
956/954	vw	960	1.1	A"	γ(CH) b
-	-	852	0.006	A"	γ(CH) c
851/850	w	845	8.2	A'	δ ring 1
803	m	799	33.9	A'	δ(OC−C)
751/749	s	747	63.5	A"	γ(CH) d
692	w	687	5.2	A"	τ ring 1
622	w	619	15.9	A'	δ ring 2
534	w	533	4.4	A'	δ ring 3
-	-	486	0.01	A"	τ ring 2
-	-	467	2.1	A'	δ(CN)

[a] Triplet 2-formyl phenylnitrene ^{3}**2a** was generated by irradiation of 2-formyl phenylazide **1** at λ = 308 nm in an argon matrix at 10 K. Only bands in the 3000–450 cm^{-1} region are included. [b] Experimental intensities are presented in qualitative terms: s = strong, m = medium, w = weak, vw = very weak, br = broad, and ov = overlapped. [c] B3LYP/6-311++G(d,p) calculated frequencies scaled by a factor of 0.98. [d] Assignments made by inspection of Chemcraft animation. Abbreviations: ν = stretching, δ = bending, γ = rocking, ω = wagging, τ = torsion, s = symmetric, and as = antisymmetric. Signs "+" and "–" designate combinations of vibrations occurring in "syn"-phase ("+") and in "anti"-phase ("–").

Table S2.2. TD-DFT calculated, at the B3LYP/6-311++G(d,p) level, transition wavelengths (λ/nm) and oscillator strengths (*f*) for the lowest twenty four excited states of triplet 2-formyl phenylnitrene ^{3}**2a** and imino ketene **3a**.

Nitrene ^{3}**2a**			Ketene **3a**		
Excitation[a]	λ_{calc}	*f*	Excitation[a]	λ_{calc}	*f*
1-(A″)	535.84	0	1-T(A′)	700.62	0
2-(A′)	449.09	0.0047	2-T(A″)	517.79	0
3-(A′)	364.70	0.0371	3-S(A″)	475.50	0.0000
4-(A″)	363.82	0.0001	4-S(A′)	**366.17**	**0.1050**
5-(A′)	355.81	0.0082	5-T(A′)	341.12	0
6-(A′)	**338.52**	**0.0471**	6-T(A″)	339.59	0
7-(A″)	319.11	0	7-T(A′)	310.25	0
8-(A′)	318.08	0.0361	8-S(A″)	304.89	0.0007
9-(A″)	317.14	0.0002	9-T(A′)	296.20	0
10-(A″)	301.18	0.0029	10-S(A′)	285.61	0.0143
11-(A″)	296.15	0.0001	11-T(A″)	268.98	0
12-(A′)	288.69	0.0001	12-T(A″)	265.21	0
13-(A″)	256.58	0.0002	13-S(A″)	262.58	0.0017
14-(A′)	245.14	0.0309	14-S(A″)	258.82	0.0000
15-(A′)	235.06	0.0387	15-T(A′)	241.96	0
16-(A′)	232.32	0.0372	16-S(A′)	**241.72**	**0.0411**
17-(A″)	228.59	0.0004	17-T(A″)	237.99	0
18-(A″)	225.18	0.0002	18-S(A″)	236.35	0.0000
19-(A′)	**222.77**	**0.1022**	19-S(A″)	**234.53**	**0.0448**
20-(A″)	222.42	0.0007	20-T(A′)	231.44	0
21-(A′)	215.23	0.0262	21-T(A″)	224.69	0
22-(A′)	**208.73**	**0.1994**	22-S(A″)	223.92	0.0020
23-(A″)	205.18	0.0011	23-S(A″)	214.53	0.0000
24-(A″)	202.10	0.0010	24-S(A′)	206.88	0.0009

[a] Symmetry is given in parentheses. Multitplicity; T = triplet and S = singlet. Transitions shown in bold are discussed in the text.

Table S2.3. Experimental IR spectral data (argon matrix at 10 K), B3LYP/6-311++G(d,p) calculated vibrational frequencies (ν, cm^{-1}), absolute infrared intensities (A^{th}, km mol^{-1}), and vibrational assignment of imino ketene **3a**.[a]

Ar matrix[b]		Calculated[c]		Sym.	Assignment[d]
ν	I	ν	A^{th}		
3266	br	3283	7.5	A'	ν(N−H)
2124/2111/2101	vs	2149	1180.1	A'	ν(C=C=O) as
1639/1637	m	1646	64.8	A'	ν(C=C) as
1553	m	1568	112.4	A'	ν(C=N)
1543/1540/1537	m	1541	123.2	A'	ν(C=C) sym
-	-	1431	1.7	A'	δ(CH) a
1400/1399	m	1390	32.2	A'	ν(CC) ring a + δ(CH) b
1328/1326	m	1306	47.3	A'	δ(NH) − δ(CH) b
1270/1269	w	1268	17.2	A'	ν(C=C=O) sym + δ(NH)
1232/1230	w	1224	6.3	A'	ν(CC) ring b
1175/1171	m	1171	36.2	A'	δ(CH) c
1152/1149	vw	1141	1.5	A'	δ(CH) d
1063/1058/	m/w/	1051	51.8	A'	ν(CC) ring c + δ(NH)
-	-	983	0.0	A"	γ(CH) a
975/972	w	972	14.6	A'	ν(CC) ring d
-	-	937	0.03	A"	γ(CH) b
853	w	849	6.9	A'	δ ring 1
-	-	829	0.7	A"	γ(CH) c − γ(NH)
808/806	w	789	24.1	A"	γ(NH) − γ(CH) d
726/722	m	716	82.6	A"	γ(CH) d + γ(NH)
689/686	m	683	15.9	A'	δ ring 2
668 (?)	w	674	20.5	A"	τ ring 1
-	-	627	1.8	A'	δ(C=C=O) (ip)
-	-	562	3.4	A'	δ ring 3
522	w	535	7.0	A"	δ(C=C=O) (oop)
468	w	470	15.5	A"	τ ring 2
-	-	455	3.6	A'	δ(CN)

[a] Imino ketene **3a** was generated by spontaneous rearrangement triplet 2-formyl phenylnitrene ^{3}**2a** in argon matrix at 10 K. Only bands in the 3000–450 cm^{-1} region are included, plus the ν(N−H), are included. [b] Experimental intensities are presented in qualitative terms: vs = very strong, m = medium, w = weak, vw = very weak, and br = broad. [c] B3LYP/6-311++G(d,p) calculated frequencies scaled by a factor of 0.98; except ν(N−H) that was scaled by 0.95. [d] Assignments made by inspection of Chemcraft animation. Abbreviations: ν = stretching, δ = bending, γ = rocking, ω = wagging, τ = torsion, s = symmetric, and as = antisymmetric. Signs "+" and "–" designate combinations of vibrations occurring in "syn"-phase ("+") and in "anti"-phase ("–").

Computational Data:

Table S2.4. Relative zero-point-corrected energies (kJ mol^{-1}) and Gibbs free energy at 298 K (kJ mol^{-1}), calculated at B3LYP/6311++G(d,p) and CBS-QB3 levels of theory for 2-formyl phenylazide **1** conformers.[a,b]

Structure	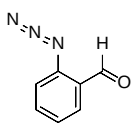	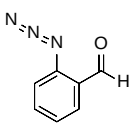	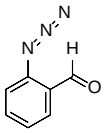	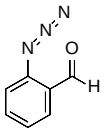
Name	**1**	**1b**	**1c**	**1d**
B3LYP	0.0 [0.0]	11.3 [11.1]	17.9 [17.6]	12.9 [14.2]
CBS-QB3	0.0 [0.0]	11.6 [11.4]	15.8 [15.2]	11.0 [12.0]

[a] The equilibrium populations of 2-azidobenzadehyde **1** conformers estimated from the CBS-QB3 relative Gibbs energies at 298 K are: **1** = 98.0 %, **1b** = 1.0 %, **1c** = 0.2 %, and **1d** = 0.8 %.

[b] Because of the dominating population of conformer **1** at room temperature in the gas phase (see the preceding footnote), it is only this particular conformer which is isolated in a detectable amount in the experiments presented in this work.

B3LYP/6-311++G(d,p) calculations

2-Formyl phenylazide **1**

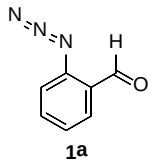

1a

Energy = -509.2978305 Ha, ZPE = 0.1122798 Ha

C	1.955382000	0.592911000	-0.000001000
C	0.931712000	-0.362925000	0.000001000
C	-0.408358000	0.072027000	0.000005000
C	-0.698886000	1.441689000	0.000004000
C	0.335903000	2.369262000	0.000001000
C	1.668855000	1.950075000	-0.000001000
H	2.977432000	0.232643000	-0.000004000
H	-1.728504000	1.781461000	0.000004000
H	0.098661000	3.427133000	0.000001000
H	2.469943000	2.679242000	-0.000002000
C	1.283634000	-1.805145000	0.000000000
O	2.424837000	-2.215871000	-0.000004000
H	0.431234000	-2.505832000	0.000002000
N	-1.412224000	-0.927092000	0.000002000
N	-2.595794000	-0.583668000	0.000002000
N	-3.714398000	-0.408532000	-0.000007000

$\tilde{\nu}$	A	$\tilde{\nu}$	A
3136	8.8	984	0.1
3126	2.3	958	1.4
3118	4.2	859	0.1
3107	1.9	827	28.9
2911	56.6	801	6.4
2203	893.4	758	69.7
1721	329.3	715	1.1
1599	75.3	696	34.2
1580	34.6	622	8.1
1479	91.6	523	5.3
1451	37.7	509	1.9
1394	60.1	497	1.0
1339	202.1	456	9.1
1309	15.1	444	5.5
1277	52.0	339	5.2
1188	45.4	258	2.1
1168	5.0	208	2.6
1140	14.7	160	7.9
1086	14.0	128	2.2
1041	2.1	112	5.3
1012	1.0	65	0.6

2-Formyl phenylazide **1b**

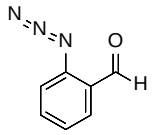

1b

Energy = -509.293291 Ha, ZPE = 0.1120503 Ha

C	-2.197474000	0.086981000	-0.000072000
C	-0.921187000	0.665032000	-0.000114000
C	0.20768s4000	-0.186272000	0.000015000
C	0.021893000	-1.574941000	0.000193000
C	-1.258001000	-2.117701000	0.000232000
C	-2.379982000	-1.289340000	0.000097000
H	-3.058662000	0.747810000	-0.000177000
H	0.883035000	-2.233801000	0.000301000
H	-1.376169000	-3.195366000	0.000368000
H	-3.376858000	-1.712490000	0.000126000
C	-0.861328000	2.147031000	-0.000289000
O	0.127886000	2.840425000	-0.000323000
H	-1.871870000	2.611717000	-0.000396000
N	1.483040000	0.405774000	-0.000021000
N	2.479112000	-0.319886000	0.000107000
N	3.481819000	-0.846748000	0.000198000

$\tilde{\nu}$	A	$\tilde{\nu}$	A
3134	9.6	975	0.0
3120	5.6	943	1.7
3108	1.9	855	0.6
3098	4.9	854	35.6
2809	135.0	782	3.9
2196	902.8	755	70.4
1741	295.2	722	3.6
1602	48.9	654	28.7
1573	81.1	641	24.0
1481	127.8	533	2.6
1449	22.6	520	4.3
1403	28.3	515	3.7
1351	241.5	438	2.7
1318	6.1	411	3.0
1269	4.8	370	3.6
1182	72.3	265	3.4
1169	7.2	209	4.7
1150	9.5	184	5.3
1104	17.1	123	1.5
1046	2.8	79	2.7
1003	0.4	69	1.2

2-Formyl phenylazide **1c**

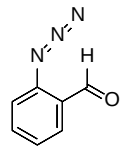

1c

Energy = -509.2909377 Ha, ZPE = 0.1121905 Ha

C	-1.602548000	1.038997000	0.192096000
C	-0.289946000	0.619579000	-0.077517000
C	-0.037075000	-0.761029000	-0.221347000
C	-1.094459000	-1.673371000	-0.162319000
C	-2.387317000	-1.230486000	0.085639000
C	-2.644714000	0.129792000	0.277857000
H	-1.774270000	2.102912000	0.305065000
H	-0.878171000	-2.726141000	-0.294239000
H	-3.196216000	-1.950342000	0.137132000
H	-3.652795000	0.472360000	0.478038000
C	0.745562000	1.659930000	-0.295357000
O	0.579313000	2.836790000	-0.058979000
H	1.699876000	1.319927000	-0.737544000
N	1.242568000	-1.332950000	-0.475526000
N	2.239395000	-0.926746000	0.125999000
N	3.236615000	-0.685091000	0.605108000

$\tilde{\nu}$	A	$\tilde{\nu}$	A
3138	6.6	986	0.3
3133	4.4	964	2.3
3124	4.0	875	1.9
3111	2.3	831	10.9
2886	70.4	789	29.6
2200	694.9	762	65.0
1721	266.9	724	3.9
1602	105.1	651	4.6
1571	7.6	629	11.9
1472	64.8	524	10.4
1448	63.1	511	0.5
1410	37.3	502	2.4
1351	117.3	456	4.1
1296	48.3	444	3.9
1266	39.5	329	1.2
1188	33.4	272	4.5
1160	5.3	225	6.4
1129	18.6	197	6.9
1083	11.4	117	1.9
1036	3.9	90	2.7
1006	0.8	55	0.9

2-Formyl phenylazide **1d**

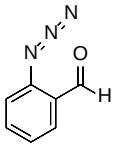

1d

Energy = -509.2929335 Ha, ZPE = 0.1122956 Ha

C	-1.663707000	1.225537000	0.269550000
C	-0.359609000	0.754897000	0.038757000
C	-0.168450000	-0.633697000	-0.173305000
C	-1.287925000	-1.473784000	-0.226776000
C	-2.566755000	-0.974700000	-0.019598000
C	-2.763009000	0.381916000	0.247454000
H	-1.799868000	2.288302000	0.443807000
H	-1.125088000	-2.527973000	-0.413597000
H	-3.413536000	-1.650649000	-0.055498000
H	-3.758354000	0.771238000	0.422772000
C	0.689342000	1.785230000	-0.090954000
O	1.820901000	1.612076000	-0.489751000
H	0.339691000	2.804319000	0.174905000
N	1.059902000	-1.291486000	-0.385336000
N	2.097842000	-0.931071000	0.181336000
N	3.115204000	-0.773764000	0.643265000

$\tilde{\nu}$	A	$\tilde{\nu}$	A				
3137	5.1	980	0.2	1399	22.8	502	3.0
3130	9.3	948	2.2	1369	136.2	441	3.5
3113	4.3	868	6.8	1308	82.2	405	4.6
3098	3.6	862	8.8	1258	9.9	381	2.1
2839	102.9	760	68.2	1186	47.9	279	4.2
2220	689.2	741	30.9	1161	7.9	218	3.7
1724	249.3	718	4.2	1139	14.7	200	5.3
1606	84.8	665	8.4	1101	11.5	167	0.4
1562	36.2	643	17.6	1040	5.7	86	2.9
1471	78.9	536	2.0	1001	0.6	76	0.9
1448	49.4	520	7.3				

Triplet 2-Formyl phenylnitrene ^{3}**2a**

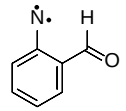

2a

Energy = -399.7375001 Ha, ZPE = 0.0999678 Ha

C	-1.783368000	0.791600000	-0.000066000
C	-0.373313000	1.075195000	-0.000087000
C	0.547911000	-0.041091000	0.000003000
C	0.052036000	-1.339356000	0.000109000
C	-1.320661000	-1.584394000	0.000131000
C	-2.230365000	-0.511885000	0.000042000
H	-2.472472000	1.626692000	-0.000135000
H	0.763970000	-2.156650000	0.000177000
H	-1.688236000	-2.603555000	0.000215000
H	-3.296069000	-0.711210000	0.000060000
C	2.007217000	0.212559000	-0.000018000
N	0.038007000	2.326835000	-0.000195000
O	2.841097000	-0.667196000	0.000058000
H	2.301234000	1.278684000	-0.000106000

$\tilde{\nu}$	A
3139	4.9
3133	4.2
3123	1.9
3111	2.3
2885	45.7
1718	263.5
1555	43.6
1513	0.1
1421	10.6
1410	4.0
1369	6.2
1298	20.2
1277	16.7
1234	50.8
1156	3.1
1130	30.2
1062	12.9
1017	0.1
1006	1.4
976	0.4
960	1.1
853	0.0
845	8.2
799	33.9
747	63.5
687	5.2
619	15.9
533	4.4
486	0.0
467	2.1
424	4.5
338	0.5
242	1.1
200	7.3
160	14.8
109	2.0

Triplet 2-Formyl phenylnitrene **2b**

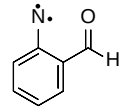

2b

Energy = -399.7344308 Ha, ZPE = 0.099838 Ha

C	0.150930000	-1.832738000	0.000000000
C	-0.669111000	-0.651521000	0.000000000
C	0.000000000	0.633697000	0.000000000
C	1.388708000	0.679584000	0.000000000
C	2.159051000	-0.485869000	0.000000000
C	1.527893000	-1.738845000	0.000000000
H	-0.347526000	-2.794084000	0.000000000
H	1.878814000	1.648301000	0.000000000
H	3.240374000	-0.421471000	0.000000000
H	2.126106000	-2.643008000	0.000000000
C	-0.759279000	1.897764000	0.000000000
N	-1.978321000	-0.792227000	0.000000000
O	-1.965029000	1.992290000	0.000000000
H	-0.118441000	2.805087000	0.000000000

$\tilde{\nu}$	A		
3138	4.3	993	1.3
3130	6.7	967	0.1
3112	4.0	940	1.5
3099	3.4	876	13.3
2829	113.5	847	0.0
1722	230.4	743	66.5
1558	18.6	731	13.1
1512	13.2	687	5.5
1426	6.8	646	12.3
1409	3.7	552	0.5
1377	5.7	496	0.2
1295	21.6	415	1.9
1290	11.4	408	3.1
1227	29.7	398	9.1
1159	11.1	264	2.8
1131	45.4	189	5.4
1093	12.5	177	8.2
1020	0.4	92	0.7

2-imino ketene **3a**

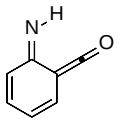

3a

Energy = -399.7773394 Ha, ZPE = 0.1021899 Ha

C	-0.029202000	-1.869850000	0.000000000
C	-0.829349000	-0.648088000	0.000000000
C	0.000000000	0.601984000	0.000000000
C	1.455606000	0.554923000	0.000000000
C	2.086876000	-0.638547000	0.000000000
C	1.322829000	-1.865328000	0.000000000
H	-0.596459000	-2.792699000	0.000000000
H	2.008749000	1.486283000	0.000000000
H	3.168906000	-0.681018000	0.000000000
H	1.859052000	-2.808137000	0.000000000
C	-0.615320000	1.783457000	0.000000000
N	-2.114940000	-0.745614000	0.000000000
O	-1.174507000	2.793089000	0.000000000
H	-2.588249000	0.158853000	0.000000000

$\tilde{\nu}$	A		
3283	7.5	972	14.6
3137	7.6	937	0.0
3132	5.9	849	6.9
3117	1.2	829	0.7
3105	8.9	789	24.1
2149	1180.1	716	82.6
1646	64.8	683	15.9
1568	112.4	674	20.5
1541	123.2	627	1.8
1431	1.7	562	3.4
1390	32.2	535	7.0
1306	47.3	470	15.5
1268	17.2	455	3.6
1224	6.3	374	9.5
1171	36.2	365	0.9
1141	1.5	186	0.5
1051	51.8	133	2.1
983	0.0	56	0.1

2-imino ketene **3b**

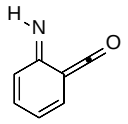

3b

Energy = -399.7824878 Ha, ZPE = 0.1024504 Ha

C	-0.010908000	-1.864025000	0.000000000
C	-0.811412000	-0.643057000	0.000000000
C	0.000000000	0.600563000	0.000000000
C	1.446767000	0.577092000	0.000000000
C	2.095761000	-0.611353000	0.000000000
C	1.344187000	-1.842775000	0.000000000
H	-0.550894000	-2.805427000	0.000000000
H	1.989479000	1.514710000	0.000000000
H	3.177789000	-0.643972000	0.000000000
H	1.890469000	-2.780295000	0.000000000
C	-0.662348000	1.764506000	0.000000000
N	-2.099175000	-0.554885000	0.000000000
O	-1.211955000	2.774055000	0.000000000
H	-2.529272000	-1.478964000	0.000000000

$\tilde{\nu}$	A
3308	3.3
3138	8.2
3118	3.7
3112	12.9
3095	3.7
2164	1211.4
1638	103.2
1563	150.4
1533	130.7
1439	6.0
1396	15.5
1338	10.9
1263	37.2
1234	74.0
1173	6.6
1147	16.5
1064	28.0
978	1.2
971	0.0
936	0.1
848	5.6
832	54.3
778	56.8
719	4.5
699	14.2
696	13.3
624	1.5
555	2.7
553	16.6
472	11.1
447	16.1
374	3.2
360	1.8
183	0.2
144	0.1
78	2.4

CBS-QB3 calculations

2-Formyl phenylazide **1a**

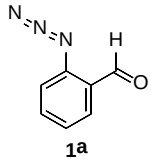

1a

CBS-QB3 (0 K) = -508.364452 Ha

C	1.952314000	0.593367000	-0.000001000
C	0.929730000	-0.362457000	0.000000000
C	-0.410154000	0.070050000	0.000001000
C	-0.700844000	1.439436000	0.000001000
C	0.332598000	2.367534000	0.000001000
C	1.665581000	1.949737000	-0.000001000
H	2.972936000	0.229367000	-0.000002000
H	-1.731072000	1.777112000	0.000003000
H	0.094193000	3.425092000	0.000001000
H	2.466196000	2.679375000	-0.000001000
C	1.290352000	-1.803178000	-0.000001000
O	2.433003000	-2.204856000	-0.000001000
H	0.439515000	-2.507146000	0.000001000
N	-1.412391000	-0.930556000	0.000001000
N	-2.596276000	-0.586572000	0.000003000
N	-3.714653000	-0.410284000	-0.000002000

2-Formyl phenylazide **1b**

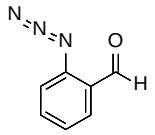

1b

CBS-QB3 (0 K) = -508.360047 Ha

C	-2.197842000	0.090024000	-0.000072000
C	-0.921800000	0.666414000	-0.000109000
C	0.206456000	-0.184714000	0.000028000
C	0.019039000	-1.572790000	0.000198000
C	-1.260474000	-2.114540000	0.000232000
C	-2.381442000	-1.285534000	0.000097000
H	-3.058125000	0.752091000	-0.000178000
H	0.880422000	-2.231222000	0.000304000
H	-1.379274000	-3.192078000	0.000363000
H	-3.378514000	-1.708196000	0.000122000
C	-0.854958000	2.148859000	-0.000293000
O	0.137082000	2.834965000	-0.000341000
H	-1.865778000	2.615854000	-0.000379000
N	1.482874000	0.406812000	-0.000013000
N	2.476343000	-0.323622000	0.000107000
N	3.476601000	-0.854973000	0.000194000

2-Formyl phenylazide **1c**

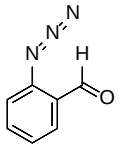

1c

CBS-QB3 (0 K) = -508.358453 Ha

C	-1.608082000	1.026957000	0.184546000
C	-0.291141000	0.613331000	-0.069403000
C	-0.029920000	-0.766675000	-0.205274000
C	-1.086730000	-1.681106000	-0.153949000
C	-2.383296000	-1.243429000	0.078168000
C	-2.648001000	0.116008000	0.263033000
H	-1.780046000	2.091145000	0.292887000
H	-0.863335000	-2.732920000	-0.280363000
H	-3.189307000	-1.966838000	0.123696000
H	-3.659075000	0.455894000	0.452098000
C	0.734949000	1.668464000	-0.266179000
O	0.531298000	2.845857000	-0.072561000
H	1.718882000	1.336383000	-0.645205000
N	1.248076000	-1.343333000	-0.444420000
N	2.256789000	-0.912269000	0.118506000
N	3.265967000	-0.651802000	0.561874000

2-Formyl phenylazide **1d**

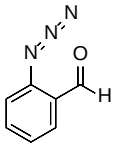

1d

CBS-QB3 (0 K) = -508.360278 Ha

C	-1.670554000	1.225663000	0.255163000
C	-0.365128000	0.756090000	0.035297000
C	-0.169401000	-0.633218000	-0.166995000
C	-1.288205000	-1.474949000	-0.214501000
C	-2.568179000	-0.977587000	-0.015834000
C	-2.767931000	0.380530000	0.238028000
H	-1.808857000	2.289688000	0.419787000
H	-1.120715000	-2.529857000	-0.392113000
H	-3.413109000	-1.655963000	-0.047769000
H	-3.764693000	0.769400000	0.405970000
C	0.685619000	1.785579000	-0.091960000
O	1.824770000	1.607601000	-0.460718000
H	0.324876000	2.808360000	0.148753000
N	1.056741000	-1.295366000	-0.369928000
N	2.104596000	-0.926432000	0.173187000
N	3.131094000	-0.766072000	0.613302000

Notes and References.

1. Plonka, A. Progress in Reaction Kinetics and Mechanism. **2000**, *25*, 109-218.

2. Sponsler, M. B.; Jain, R.; Coms, F. D.; Dougherty, D. A. *J. Am. Chem. Soc.* **1989**, *111*, 2240-2245.

3. Siebrand, W.; Wildman, T. A. *Acc. Chem. Res.* **1986**, *1*, 238-243.

4. Ertelt, M.; Hrovat, D. A.; Borden, W. T.; Sander, W. *Chem. Eur. J.* **2014**, *20*, 4713-4720.

5. Reva, I.; Nowak, M. J.; Lapinski, L.; Fausto, R. *J. Chem. Phys.* **2012**, *136*, 064511.

Chapter 3: Progress toward *in situ* Kinetic Studies of Enetetraynes and their Derivatives

Contributions have been made by Katherine Windsor

Introduction

The thesis work of Katherine Windsor details thorough investigation of the kinetics of Bergman cyclization reactions of tetraethynylethene (**1**) and its derivatives.[1] The reactions are of interest in the fields of organic chemistry, combustion chemistry, and astrochemistry, and the study aimed to provide insight into the mechanistic details of processes involving these scaffolds. While a great deal of insight resulted from a number of studies, the use of GC-MS and NMR as the primary means for analyzing product outcomes limited the scope of mechanistic information that could be obtained. This chapter describes efforts to adapt Windsor's work to analysis on the ReactIR apparatus in order to obtain kinetic information from *in situ* measurements rather than backing it out of product mixtures.

Background

Tetraethynylethene (TEE; **1**) is known as a fundamental unit of many acetylenic scaffolds that have found application as molecular switches and nonlinear optical materials.[2] As in any system suitable for application, the thermal reactivity of this compound is of interest for better manipulation. Tetraethynylethene contains two enediyne moieties that share a common alkene core, making it a natural candidate for Bergman cycloaromatization under the right conditions (Figure 3.1).[3] This reactivity is interesting because it is relevant to several realms. First, it

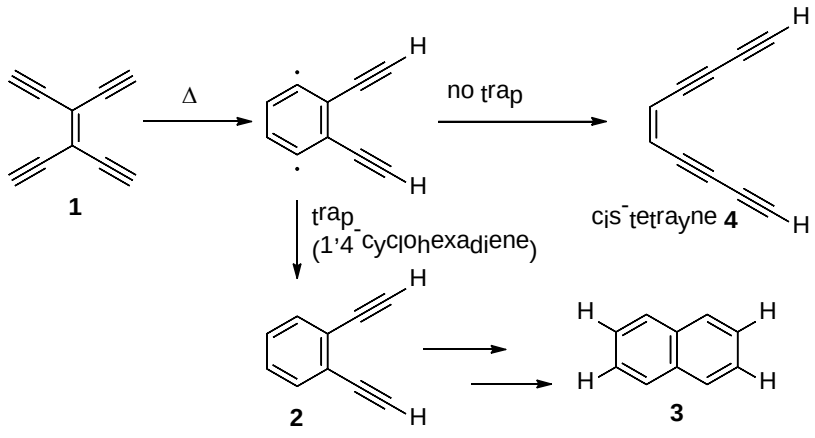

Figure 3.1 Bergman cyclization of tetraethynylethene (**1**) in the presence and absence of a radical trap

can provide a description of carbon-rich compounds under high temperature and/or pressure—conditions common in the production of fullerenes and carbon nanotubes.[4] Additionally, the chemistry of unsaturated carbon compounds can pertain to the formation of polycyclic aromatic compounds that have been detected in the interstellar medium.

Tetraethynylethene was identified as an interesting target molecule as the result of previous work in the McMahon lab on the synthesis and characterization of the HC_5H carbene.[5] The UV/vis spectrum of this matrix-isolated compound showed a number of absorptions not attributable to the parent carbene, leading to the investigation of carbene dimers and their isomers (Figure 3.2)[6].

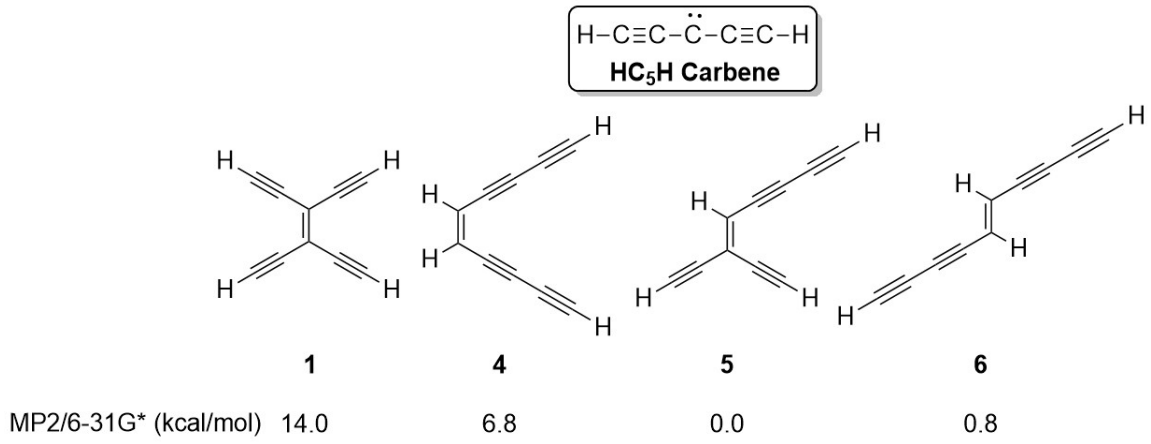

Figure 3.2 HC_5H carbene , its dimer (**1**) and other possible isomers (**4**-**6**). Relative energies in kcal/mol.

These molecules were synthesized and characterized for comparison with the HC_5H spectrum.[6] Interestingly, tetraethynylethene (**1**) is the only of the four compounds studied whose spectroscopic signatures were absent. This is even more surprising because our studies indicate that electron density of HC_5H resides primarily on the central carbon (C3), and isomer **1** is the expected product of dimerization at the central carbon. Calculations (B3LYP/6-31G* and MP2/6-31G*) indicate that this species is significantly higher in energy than the others—

rationalizing the limited presence of enyne **1** if carbene dimerization is controlled by thermodynamic stabilities of the products. Furthermore, since carbene dimerization is substantially exothermic, enyne **1**, if formed, could possess sufficient energy to rearrange to the lower energy isomer (**4**).[6] A mechanism consistent for this reactivity is the thermal Bergman cyclization followed by ring opening *via* diradical 1,2-diethynylbenzene as seen in Figure 3.1.

Katherine Windsor studied this system at length using ^{1}H NMR spectroscopy to establish the reactivity followed by GC-MS to determine activation parameters and potential side products of the reaction. She investigated the pathway of tetraethynylethene to naphthalene in the presence of a trapping agent as well as the pathway from TEE to *cis*-tetrayne **4** (Figure 3.1).[1] The experimental setup involved preparing small sealed sample tubes from Pasteur pipets containing the reaction mixture, thermolyzing them in an oil bath, and removing them individually at predetermined times to monitor the disappearance of the starting material. As a test, the disappearance of 1,2-diethynylbenzene was fitted to a first-order curve affording a pseudo-first order rate constant of $k = 2.7\times10^{4}$ s^{-1} ($t_{1/2}$ = 42.7 min), agreeing well with the literature value.[7] With confirmation that the experimental setup was valid, Windsor began work on acquiring activation parameters for the complete double cyclization of tetraethynylethene.

There were several issues encountered during these studies, mostly due to the thermal instability of tetraethynylethene and its tendency to polymerize or undergo other side reactions. This was particularly problematic under cyclization conditions and upon injection into a GC-MS apparatus.[1,8] Because of this, the rate of the Bergman cyclization was not reflected by the rate of enediyne disappearance. Additionally, the GC detectors can often vary and require internal standards to obtain accurate kinetic data. A number of additional studies have been suggested to

improve the accuracy of the kinetic data, but the limitations of the experimental setup need to be addressed first to help ensure the integrity of the data obtained.

A proposed solution to many of these problems involves the use of the ReactIR apparatus that had been acquired by the department around 2011. In principle, the system could be used to monitor disappearance of tetraethynylethene, formation of 1,2-diethynylbenzene, and formation of naphthalene. Coupled with a Parr pressure reactor, this apparatus was expected to eliminate two limitations encountered in Windsor's work: (1) Windsor's original setup facilitates cycloaromatization of only the most reactive tetraynes, leading to the issue of side products and polymerization, especially upon injection into the GC-MS.[8] (2) The use of GC-MS limits the weight of the compounds possible to study. Many interesting systems cannot be studied using GC-MS but have no limitation with ReactIR.

Results and Discussion

Synthesis of Substrates

In order to establish a working experimental setup with the ReactIR instrument, I first sought to replicate the well-studied cycloaromatization of 1,2-diethynylbenzene using the ReactIR setup.

Scheme 3.1.

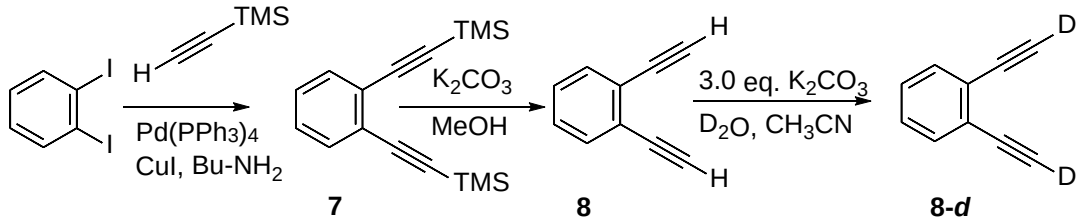

Synthesis of 1,2-diethynylbenzene

1,2-Diethynylbenzene was synthesized by Sonagashira coupling to 1,2-diiodobenzene, a method by Popik *et al.*[9] Preliminary IR data indicates that the signal associated with the C-H acetylenic

proton stretch occurs at ~3300 cm^{-1} (Figure 3.3). This would be the strongest signal to track the disappearance of the alkyne moieties in the cycloaromatization reaction. Unfortunately, the ReactIR instrument only measures absorptions as high as 2900 cm^{-1}.

Synthesis of 1,2-diethynylbenzene-d_2

Because of restrictions in the ReactIR wavelength range, the deuterated version of 1,2-diethynylbenzene was synthesized. 1,2-Diethynylbenzene-d_2 was synthesized according to Scheme 3.1. The acetylenic C-H positions were deuterated according to a method by Bew *et al.*[10] The resulting C-D IR stretch occurs at ~2600 cm^{-1}, within the window of the ReactIR spectrometer. This stretch can be used to track the disappearance of the starting material, as confirmed by a trial run of the reaction in the original conditions (tube furnace for 10 h), which results in an IR spectrum devoid of the 2600 cm^{-1} IR stretch (Figure 3.3).

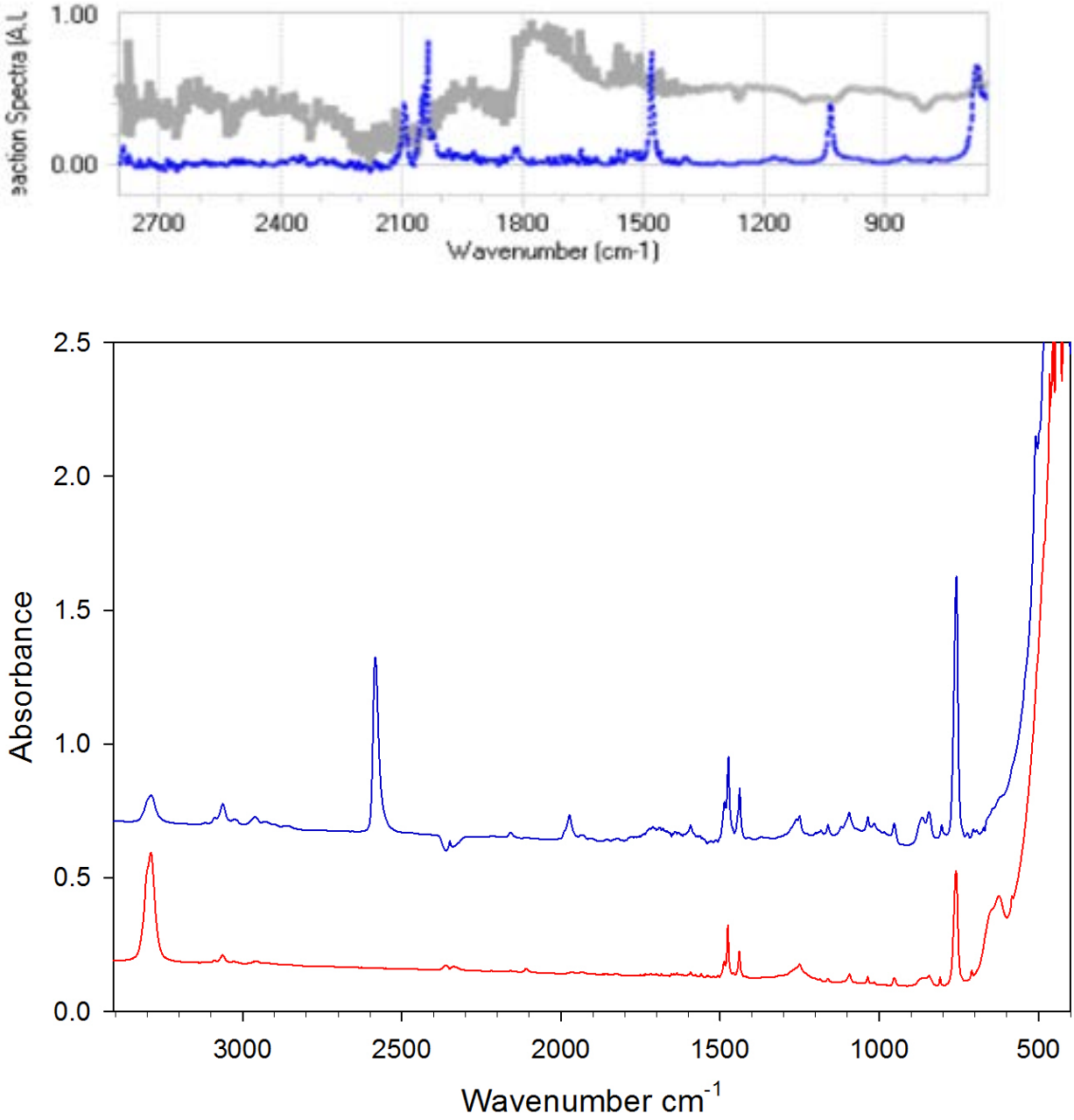

Figure 3.3. Top panel: IR spectrum of 1,2-diethynylbenzene in benzene (with solvent subtracted) in ReactIR, showing the window does not allow for tracking of the characteristic acetylenic C-H stretech at 3300 cm^{-1}

Bottom panel: IR spectra of 1,2-diethynylbenzene (below in red) and 1,2-diethynylbenzene-d_2 (above in blue). Sampling *via* ATR between two NaCl windows.

Optimization of ReactIR Conditions

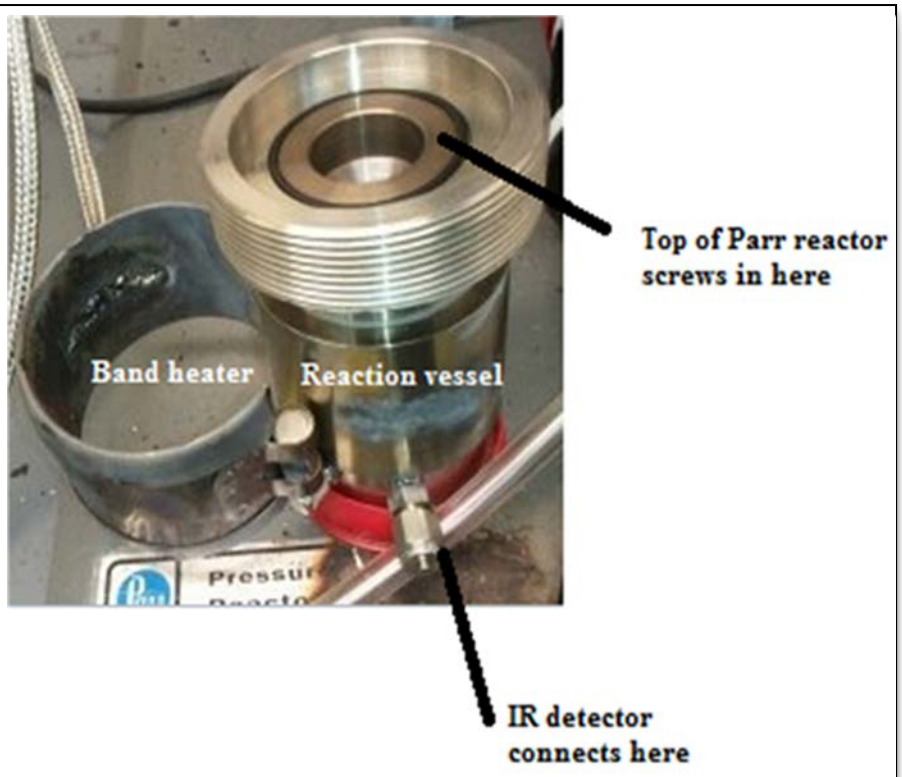

Figure 3.4. Parr reactor vessel and band heater.

General ReactIR Setup

With the starting material in hand, I began to familiarize myself with the React-IR apparatus. I began by running solvent scans on benzene both at room temperature and at temperatures elevated to the established reaction temperature (170°-180°C).[1,3] I found several issues with alignment and spectral quality, but the largest issue that had a hand in all the others was the issue of temperature control and apparatus design.

Alignment

The alignment of the instrument is particularly sensitive. During setup before an experiment, both the “peak height” and “contrast” parameters need to be optimized above a particular level. If these two parameters are not sufficiently optimized, the experiment will end with a message “unsuitable interferogram peak”. A number of instrumental setup problems have been found to cause this error. In one case, the instrument itself needs to have the signal strength increased by adjusting the preamp gain. This can often be necessary when switching between probe types. A dirty lens on the probe has also been the cause of these problems. This can be complicated because the probe itself is quite delicate, but generally a heated ultrasonic solvent bath will sufficiently clean the lens. Occasionally these two measures were not enough, and it is difficult to tell whether in this case the alignment issues are dependent upon some issue with the seal of the reactor.

Spectral Quality

The last significant issue encountered with the apparatus is the quality of the spectra. I have been able to get a clear spectrum of 1,2-diethynylbenzene-d_2 at room temperature but not

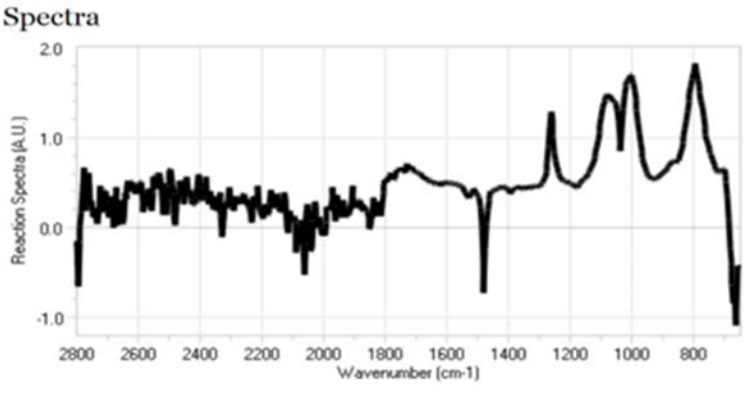

Figure 3.5. Example reaction spectrum of 1,2-diethynylbenzene-d_2 at 180 °C.

consistently. The region above 1800 cm^{-1} appears to have a lower signal to noise ratio (Figure 3.5), and it has remained unclear why this is. The ReactIR software holds great promise for analyzing kinetic data. The organization and workup of the data it acquires is user-friendly, and easy to transport into various other programs; however, apparatus limitations prevented our ability to utilize these features.

Temperature Control and Apparatus Design

It quickly became clear that many of the issues stemmed from the design of the apparatus. The following observations led to this conclusion: (1) During the course of an experiement, the spectra (set to be scanned anywhere from every minute to every 10 minutes) exhibit poorer and poorer resolution. By the end, there is generally only noise and no defined peaks at all. This is likely due to the fact that (2) all solvent escapes from the vessel by the end of the trial. When the vessel is opened and taken apart, it is clear that the o-ring that was meant to seal the reaction vessel and the probe had suffered substantial thermal degradation. This same process has occurred on a number of different o-rings that are rated to much higher temperatures than 200° C. (3) Additionally, the controller box would frequently burn out the band heater (see Figure 3.4) and occasionally failed to maintain the temperature at which it was set. The source of this problem is likely related to the burning out of the o-rings as well. All of these factors coupled together causes the reactor to leak, and every attempt to track a reaction failed.

The core of the problem seems to be at the interface between the thermocouple, controller box, and band heater *vis a vis* the thick-walled reaction vessel. Upon consulting with the representatives from Parr, it seems that the issue arises from the power of the band heater in relation to how thick the walls of the vessel are (Figure 3.6). It seems that the particular model at hand was designed for high pressure reactions but not really high pressure and high temperature.

Specifically, the band heater addition for high temperature reactions does not seem to be a commonly-used feature.

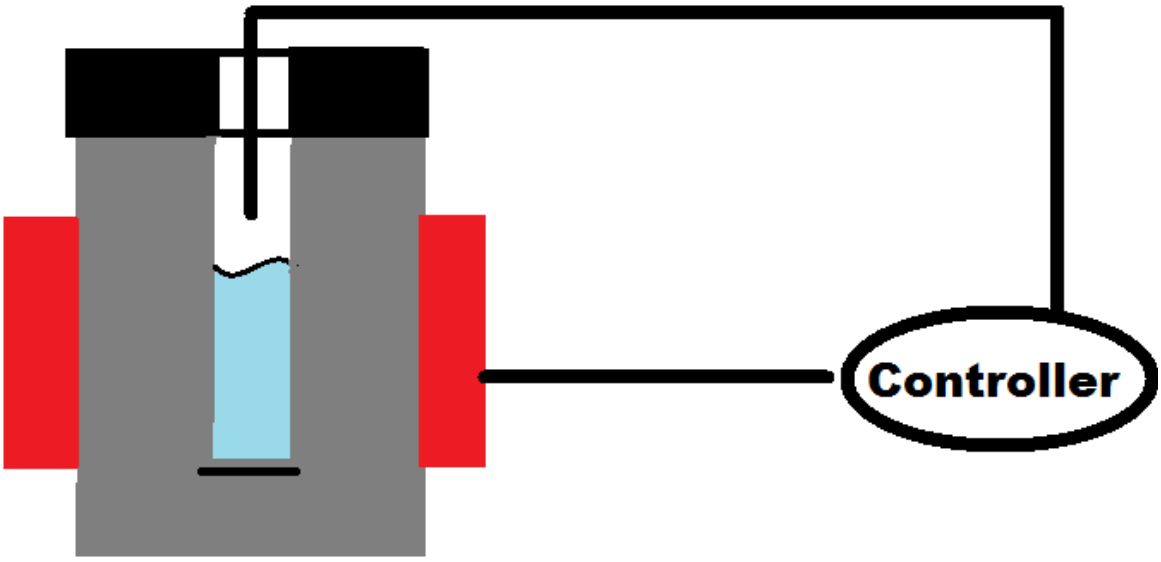

Figure 3.6. Diagram of Parr reactor. The thick walls of the reactor require extensive power from the band heater to heat the reaction mixture. The walls of the reactor become much hotter than the thermocouple can detect, causing degredation of o-rings and loss of solvent.

Future Directions

ReactIR

The model of ReactIR that was used in this study was intended primarily for reactions at high pressure, with high temperature reactions as a bit of an afterthought. I believe that the issues with the reactor may be remedied by acquiring a different model of Parr reactor and controller box. The newer models of controller box allow for programmed temperature increases over a long period of time. If the thermocouple is able to detect an accurate temperature with regard to the outside of the reaction vessel, perhaps the hardware will be less compromised in the process. If we are able to maintain the proper reaction temperature without losing any solvent, any other issues with spectrum acquisition will be clearer.

Kinetic experiments

Provided the appropriate apparatus is acquired, the next step will be to replicate data acquired by Windsor and others[1,7] for the Bergman cyclization of 1,2-diethynylbenzene-d_2. The best way to carry this out would be to track the reaction *via* disappearance of the acetylenic C-D stretch and compare the acquired reaction parameters to those established.

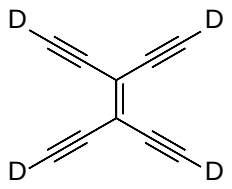

Figure 3.7

Tetraethynylethene-*4d*

If the reaction parameters are accurately acquired, the project could progress by looking at the deuterated tetraethynylethene system. By synthesizing tetraethynylethene-d_4 we can ensure that the stretches of interest are within the React-IR window (Figure 3.7).

Before acquiring activation parameters, supplemental studies should be carried out to understand the reactivity observed for tetraethynylethene's double cycloaromatization.[1] One suggested study involves determining the dependence of the activation parameters on the concentration of the trapping agent (1,4-cyclohexadiene). The reactions in Windsor's prior work used 1,4-cyclohexadiene concentrations well above the pseudo-first-order thresholds for known cyclizations.[11] Pseudo-first-order parameters were achieved using this excess, but in order to validate the assumptions made, quantitative fundamental studies such as obtaining a linear plot of ln[1,4-CHD] versus time or verifying that *k* remains constant over a range of [1,4-CHD] will be necessary. A dependence on 1,4-CHD can alter the activation energy (E_a) dramatically,[11] and in the case the tetraethynylethene study, E_a does not agree with what would be expected based on related enediyne cyclizations. Once the dependence of the system on the trapping agent is clear, confident measures of activation parameters for tetraethynylethene-d_4 can be made and compared to those acquired by Windsor.

Conclusions

Analysis of reaction kinetics using ReactIR holds great potential for reactions under harsh conditions. The current study revealed the limitations of the apparatus at hand for reactions at high temperatures, but a great deal of development has been done on the apparatus, and it is quite possible that present or future models hold more promise. If the right model was identified, the implementation of the kinetic studies outlined in this chapter should be quite straightforward. The substantial groundwork laid by Windsor through her NMR and GC-MS kinetic studies provides clear expectations for ReactIR experiments. Once the physical limitations of the apparatus have been addressed, the power of the ReactIR analysis software has great potential for confirming the validity of the activation parameters previously obtained.

Experimental Section

General Information. Chemicals and solvents were purchased and used without purification, unless otherwise noted. . ^{1}H NMR spectra (300 MHz) and ^{13}C NMR spectra (75.4 MHz) were obtained in $CDCl_3$ on a Bruker AC+ 300; chemical shifts (δ) are reported as ppm downfield from internal standard $SiMe_4$.

Synthetic Information

1,2-Bis[(trimethylsilyl)ethynyl]benzene (7).[9] To a solution of 0.5 mL (3.9 mmol) of 1,2-diiodobenzene in THF were added 1.3 mL (13.2 mmol) of *n*-$BuNH_2$, 0.66 g (0.38 mmol) of CuI, 0.204 g (0.18 mmol) of $Pd(PPh_3)_4$ and 1.3 mL (9.2 mmol) of trimethylsilylacetylene. The mixture was stirred at room temperature for 18 h. The black reaction mixture was transferred to a separatory funnel with 50 mL hexane and washed three times (once with 50 mL aq. NH_4Cl, once with 50 mL water, and once with 50 mL sat. aq. $NaHCO_3$ solution). The organic phase was dried

with $MgSO_4$, filtered and concentrated under reduced pressure to afford an amber oil. The oil was purified by flash column chromatography (silica gel/ hexane) to afford 1.065 g (99% yield) of the 1,2-bis[(trimethylsilyl)ethynyl]benzene as a pale yellow oil. ^{1}H NMR δ 7.46 (dd, 2H), 7.24 (dd, 2H), 0.5 (s, 9H) ppm.

1,2-Diethynylbenzene (8).[9] To a solution of 1,2-bis[(trimethylsilyl)ethynyl]benzene (1.05g, 3.77 moles) in 5 mL MeOH was added K_2CO_3 (0.80 g, 5.8 mmol). The reaction was stirred at room temperature for 1 h. The mixture was transferred to a separatory funnel with 15 mL pentane and washed twice with 20 mL water. The organic phase was dried with $MgSO_4$, filtered and concentrated under reduced pressure to yield 0.472 g (99% yield) of 1,2-diethynylbenzene as a pale yellow oil. ^{1}H NMR δ 7.52 (dd, 2H), 7.31 (dd, 2H), 3.34 (s, 2H) ppm. ^{13}C-NMR δ 132.9, 128.7, 128.4, 82.0, 81.4 ppm.

1,2-Diethynylbenzene-*d_2* (8-*d*).[10] A 10 mL round-bottom flask was charged with 1,2-diethynylbenzene (0.2466 g, 1.954 mmol) and potassium carbonate (0.810 g, 5.864 mmol) in 8 mL acetonitrile. This mixture was allowed to stir under and atmosphere of N_2 for 30 minutes. To this, D_2O (3.5 mL, 20.0 mmol) was added and stirred at room temperature for 1 hour. The resulting mixture was diluted with 10 mL of dichloromethane and transferred to a separatory funnel. The organic layer was separated and dried with $MgSO_4$, filtered, and solvent was removed under reduced pressure to yield 1,2-diethynylbenzene-*d_2* (0.177 g, 71% yield). ^{1}H NMR δ 7.52 (dd, 2H), 7.31 (dd, 2H) ppm.

Notes and References

1. Windsor, K. M., R.J. Doctoral Thesis. **2010**.

2. Nielsen, M. B.; Diederich, F. The Art of Acetylenic Scaffolding: Rings, Rods, and Switches. *Chem. Rec.* **2002**, *2*, 189-198.

3. Bergman, R. G. Reactive 1,4-dehydroaromatics. *Acc. Chem. Res.* **1973**, *6*, 25-31.

4. Goroff, N. S. Mechanism of Fullerene Formation. *Acc. Chem. Res.* **1996**, *29*, 77-83.

5. Bowling, N. P.; Halter, R. J.; Hodges, J. A.; Seburg, R. A.; Thomas, P. S.; Simmons, C. S.; Stanton, J. F.; McMahon, R. J. Reactive Carbon-Chain Molecules: Synthesis of 1-Diazo-2,4-pentadiyne and Spectroscopic Characterization of Triplet Pentadiynylidene (H−C∶C−C̈−C∶C−H). *J. Am. Chem. Soc.* **2006**, *128*, 3291-3302.

6. Bowling, N. P.; McMahon, R. J. Enediyne isomers of tetraethynylethene. *J. Org. Chem.* **2006**, *71*, 5841-5847.

7. Alabugin, I. V.; Manoharan, M.; Kovalenko, S. V. Tuning Rate of the Bergman Cyclization of Benzannelated Enediynes with Ortho Substituents. *Org. Lett.* **2002**, *4*, 1119-1122.

8. Grob, K. *Split and Slitless Injection for Quantitative Gas Chromatography: Concepts, Processes, Practical Guidelines, Sources of Error*; 4 ed., 2000.

9. Poloukhtine, A.; Popik, V. V. Photoswitchable enediynes: use of cyclopropenone as photocleavable masking group for the enediyne triple bond. *Chem. Commun.* **2005**, 617-619.

10. Bew, S. P.; Hiatt-Gipson, G. D.; Lovell, J. A.; Poullain, C. Mild Reaction Conditions for the Terminal Deuteration of Alkynes. *Org. Lett.* **2012**, *14*, 456-459.

11. Zeidan, T. A.; Kovalenko, S. V.; Manoharan, M.; Alabugin, I. V. Ortho Effect in the Bergman Cyclization: Comparison of Experimental Approaches and Dissection of Cycloaromatization Kinetics. *J. Org. Chem.* **2006**, *71*, 962-975.

Chapter 4: Synthesis of Unsaturated Nitriles to Model Titan's Photochemistry

Contributions have been made by Joseph Korn, Deepali Mehta-Hurt, and Khadija Jawad at Purdue University

Introduction

The shared interests of the McMahon and the Zwier research groups in astrochemical spectroscopic investigations have led to fruitful collaborations. The Zwier group's expertise in probing the photo sinduced and discharge-driven chemistry of molecules relevant to planetary atmospheres has led to a number of comprehensive studies. The techniques and methods used by the Zwier group differ from those that we utilize; however, our skills in the area of organic chemistry are a good complement to allow their studies to range over a wider breadth of potential compounds.

Background

The atmosphere of Saturn's moon, Titan, has been of great interest since the Cassini-Huygens spacecraft provided quantitative data regarding its composition in 2005.[1] Between the Voyager missions (beginning 1977) and Cassini-Huygens (beginning 1997), a diverse array of hydrocarbons has been identified within the atmosphere of Titan, and its mechanistic origin is the subject of great study. The solar flux on Titan's atmosphere is high enough to induce photochemical activity,[3] and it is speculated that these processes underlie the formation of many detected hydrocarbons.[4] A visible light-absorbing haze in the atmosphere of Titan masks its surface in the visible domain, and the contents of the haze have been predicted. It is believed that large polyaromatic hydrocarbons (PAHs) contribute considerably, especially in light of the presence of benzene, as confirmed by Ion and Neutral Mass Spectrometry (INMS) on Cassini.[5,6] Many of the components of the atmosphere are known, but theoretical modeling and laboratory simulations are crucial to elucidate formation and loss mechanisms of the detected molecules.[3] Experimental simulations aim to mimic the chemical processes active in Titan's atmosphere by

modeling a representative gas mixture and energy source in line with those known on Titan. The Zwier group has already undergone a series of studies relevant to this type of analysis.[4,7-9]

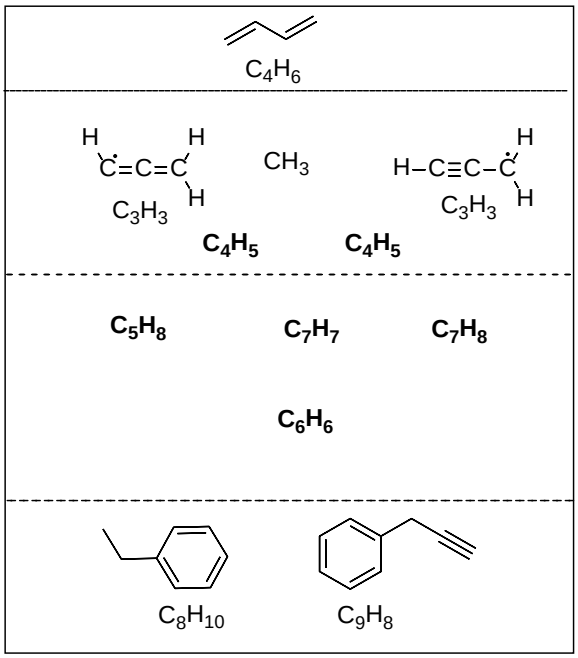

Figure 4.1. Summary of the primary (top panel), secondary (middle panel), and higher order (bottom panel) products formed in 218 nm photochemistry of a 6% butadiene in helium mixture. Bold formulas indicate no structural determination was possible.

The reaction of small hydrocarbons to produce benzene, the prototypical aromatic, is an important process to understand. The photochemical pathway from species such as the propargyl radical is especially relevant, as this reaction has been used to rationalize the observation of benzene in Titan's atmosphere.[10] The propargyl radical can be formed from photolysis of 1,3-butadiene, as confirmed by the Zwier group, and the results of subsequent product formation can be summarized in Figure 4.1.[4] Although the dominant secondary product of photodissociation was found to have the formula C_6H_6, (middle panel, Figure 4.1) further investigations proved no correspondence to benzene. Small amounts of aromatic species ethylbenzene and 3-phenylpropyne were confirmed as higher order products (bottom panel, Figure 4.1) and their pathways of formation hypothesized.[4] While benzene is typically the target aromatic in studies such as these, identification of any aromatic species can elucidate formation of larger aromatic frameworks.

In addition to the study of 1,3-butadiene photodissociation products, the Zwier group looked into the discharge-driven chemistry of 1,3-butadiene under similar pressure and temperature conditions.[4] The precedent for this type of study has been established in the discharge-driven chemistry leading to "thiolins", a group of compounds believed to analogize the physical properties of the aerosol haze in Titan's atmosphere.[11,12] There are a few immediately notable comparisons and contrasts that are present between the products formed in electric discharge (Figure 4.2) and UV light source excitation mechanisms (Figure 4.1). Most notably, however, the electric discharge pathway yielded a much larger variety of aromatic products than the photochemical pathway as seen in Figure 4.2.[4] It is clear that the discharge provides greater chemical processing. As before, the presence of benzene was of particular interest, and the mechanism of formation is believed to be either propargyl recombination or complete scrambling. These studies have begun the mechanistic investigation of 1,3-butadiene to aromatic products, shedding light on the potential formation of aromatics in the atmosphere of Titan. The study of similar systems will complement these findings by providing more insight to these types of mechanisms.

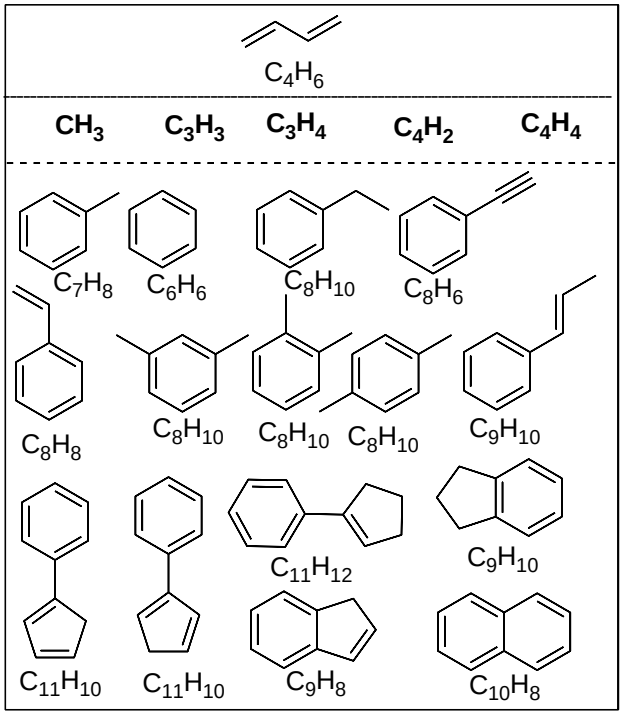

Figure 4.2 Summary of molecules identified as products of electric discharge of 6% butadiene in Ar. Bold formulas indicate no structural determination was possible.

Another study done by the Zwier group involves conformational isomerization of *o*-, *m*-, and *p*-ethynylstyrenes.[9] Substituted benzenes are known to play a role in pathways to larger

polycyclic hydrocarbons during processes such as combustion and soot formation and might have a role in the chemistry at play in the haze over Titan's surface. It is intuitive that structural isomers vary in reactivity and would vary in their ability to form larger PAH molecules. The same is true for conformational isomers, where conformational isomerization may be necessary to precede structural isomerization by bringing ring-forming segments into close proximity to one another.[9] In this study, a variety of methods were used to gain information about the isomerization processes of these species, including resonance-enhanced two-photon ionization (R2PI), UV-UV hole-burning spectroscopy (UVHB), resonant ion-dip infrared spectroscopy (RIDIRS), rotationally resolved fluorescence excitation spectroscopy, and a newly developed method of stimulated emission pumping-population transfer spectroscopy (SEP-PTS).[9] With these many methods, a thorough picture of the isomerization process was gained and is described below.

The first objectives pursued were isomer-specific infrared and ultraviolet spectra of the four structural isomers of ethynylstyrene. Additionally, it was found through UVHB experiments that both the *cis*- and the *trans*- isomers exist for *m*-ES, but only the *trans*- was found for *o*-ES (Figure 4.3). This also provided some insight into the potential isomerization of *o*-ES to naphthalene. Further work elucidated the roles of the ethynyl and vinyl substituents in the perturbation of the electronically excited state. It was found that each substituent had an independent effect, and the extent of the effect depended on what aspect of spectroscopy was being probed.[9]

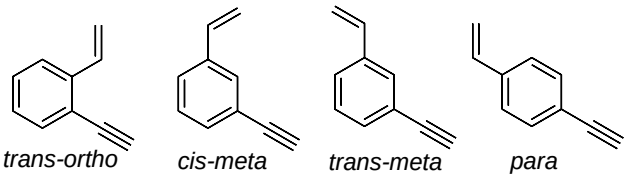

Figure 4.3 Planar conformations of the isomeric ethynylstyrene

The vibronic structure of these molecules was also investigated and compared to molecules such as phenylacetylene[13,14] and diethynylbenzene.[15,16] It was found that the *ortho*-isomer shares much in common with these species due to its strong vibronic coupling to the S_2 state, indicating that the ethynyl group plays a more active role in the spectroscopy of this isomer. Additionally, all the Franck-Condon activity displayed in this isomer was found to be caused by the vinyl group.[9]

Finally, SEP-PT spectroscopy was used to directly measure the energy barriers for *cis* → *trans* and the reverse isomerization in *m*-ES. This method was coupled with DFT to provide a clear picture of the energetics of the transformation. The result was remarkably close to the previous results on styrene,[17] indicating that the ethynyl group does little to affect this isomerization.

It is clear that these types of studies can provide a wealth of information, and the Zwier group does excellent work pairing many types of spectroscopy together to truly understand conformational isomerization energetics. The two aforementioned hydrocarbon studies have provided a thorough picture of potential photochemical pathways on Titan; however, a major player is absent: nitrogen. N_2 accounts for the majority of Titan's atmosphere, with several percent of CH_4. The predicted similarities between Titan's atmosphere and that which hosted the prebiotic chemistry of early Earth enhance interest in its study.[3,18] Current photochemical models hypothesize most of the complex products found on Titan originate from photocatalytic dissociation of CH_4 in the stratosphere[19-23] coupled with dissociative ionization of N_2 in the upper atmosphere by energetic electrons and solar extreme-ultraviolet radiation (Scheme 4.1).[24-26] It follows that nitrogen-containing hydrocarbons would account for a large fraction of organic molecules found on Titan, and indeed, this is the case. Many of these models were developed

Scheme 4.1.

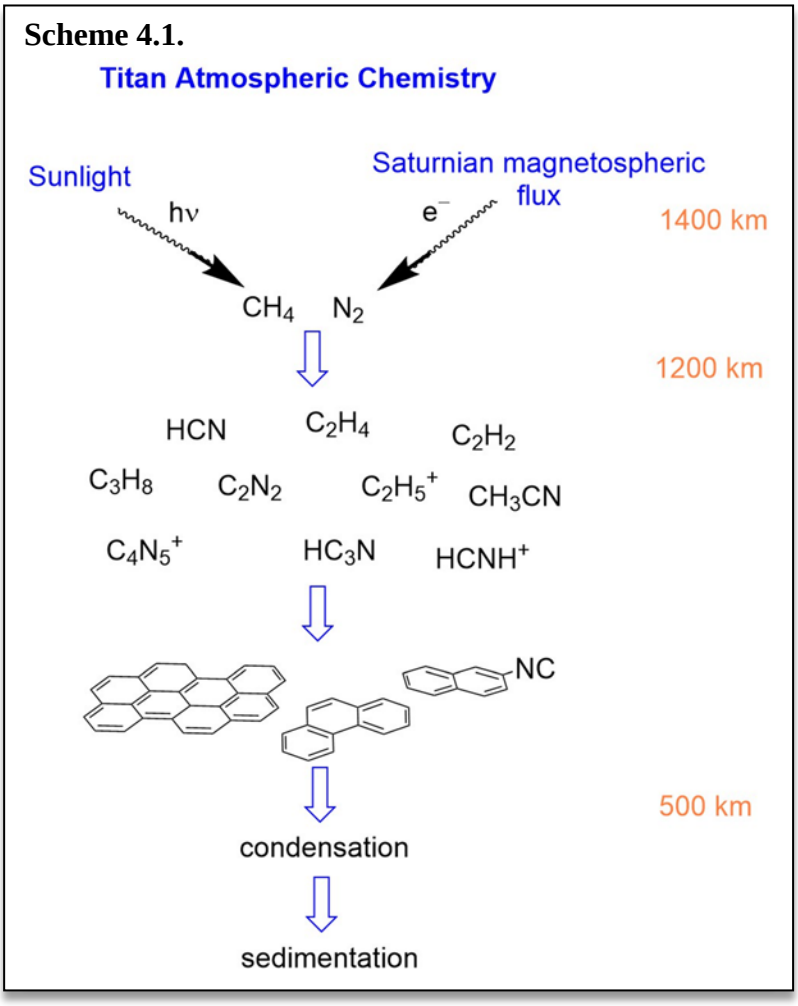

before the Cassini mission, and since then, nitrogen has been found to be even more involved in the organic chemistry of Titan than originally imagined.[27]

Nitrile compounds are major components of Titan's atmosphere. Hydrogen cyanide (HCN) is one of the most abundant compounds found on Titan, and cyanoacetylene (HC_3N), acetonitrile (CH_3CN), and cyanogen (C_2N_2) have also been detected.[28] Studying reactions of 1-cyano-1,3-butadiene will provide an effective complement to the study of butadiene and reflects chemistry likely relevant to Titan. Additionally, a very similar species (CH_2=CH—CN) has already been detected *via* INMS on Cassini.[3] In the same vein, *o*-, *m*-, and *p*- cyanostyrenes can be synthesized and subjected to similar studies to those performed on ethynylstyrene to

determine the feasibility of nitrogen-containing PAH formation from small aromatic nitriles. The cyanostyrenes are of particular interest, in part because they have the same molecular formula (C_9H_7N) as quinoline, a prototypical heteroaromatic, and therefore could engage in photochemical isomerization to form this molecule of significant prebiotic relevance. By coupling the foundational studies the Zwier group has already undertaken with nitrile compounds universal to the chemistry expected on Titan, the photochemistry of the planetary atmosphere can be more fully realized.

Results and Discussion

Synthesis of 1-Cyano-1,3-butadiene

Scheme 4.2

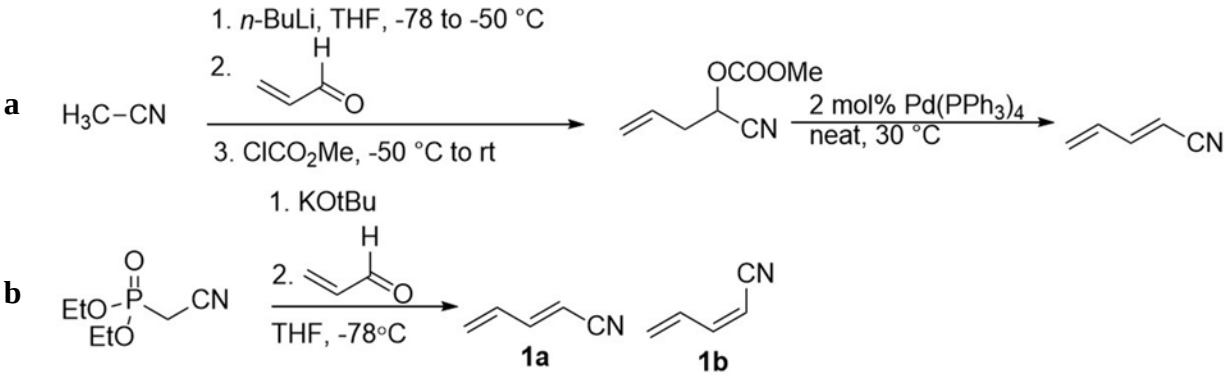

To date, only two published synthetic routes to 1-cyano-1,3-butadiene (**1**) have been reported.[2,29] The procedure described by Braun *et al.* can be seen in Scheme 4.2a. Attempts to replicate this reaction were unsuccessful, and all subsequent attempts were performed using the procedure reported by Clary *et al.*[2] (Scheme 4.2b). The procedure involves the formation of a phosphonate ylide followed by reaction with acrolein in a Horner-Wadsworth-Emmons type olefination. As can be seen in Scheme 4.2b, this reaction appears to be straightforward; however,

the resulting ^{1}H NMR spectrum does not agree with what was published. Upon closer investigation, the previously reported ^{1}H NMR data do not account for all the hydrogens in the molecule. Although each isomer (**1a** and **1b**) should have five signals in the spectrum, the *trans*-isomer (**1a**) has four reported signals and the *cis*- (**1b**) has only three.[2] Additionally, the reaction inherently undergoes a side reaction, and not all signals in the crude spectrum are attributable to **1**. The combination of the two issues combined with challenges encountered in purification created confusion in characterization and complicated the optimization and troubleshooting process. Some of the older literature concerning cyanobutadiene describes the dimerization by Diels-Alder reaction[30,31] as well as polymerization.[32] However, these processes generally need to be facilitated by more extreme conditions than those present in the reaction. Polymerization may be possible, as the anionic polymerization of this species has been described with strong bases. This observation led to our attempts to synthesize the product with alternative base systems.[33,34] During the course of the reaction in KO^{t}Bu, a thick, jelly-like substance appears that is not soluble in any typical extraction solvent. It would make sense that the substance was some kind of polymerized product, and its presence not only negatively impacts the yield of reaction but also the facility of workup.

In order to test the reaction conditions, I performed a sample reaction with an analogous system. In the HWE reaction of benzaldehyde to yield cinnamonitrile (**2**) (Scheme 4.3), it was clear that much of the starting material was unreacted. The aldehyde peak was still prevalent in the ^{1}H NMR spectrum; although there were also peaks that

Scheme 4.3

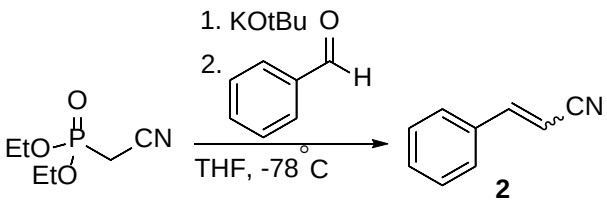

were not clearly attributable to starting material or either isomer of the predicted product. This leads us to expect potential side reactions as well as incomplete reaction of the starting material in our system.

Purification and Isolation

The situation was complicated by the issue of purification. The reaction inherently proceeds with a few side products, and attempted purification with silica gel chromatography changes the NMR spectrum entirely (Figure 4.4). Until GC-MS characterization was optimized (see below), it was difficult to determine which NMR signals were attributable to **1**. With further analysis, it became clear that the product is sensitive to silica gel, and an alternative purification method was necessary. The volatility of the compound created issues with initial workup, as most extraction solvents have similar or higher boiling points than the compound. Paying careful attention to keeping the solution on the rotovap for as short a time as possible allowed for minimal loss of product, but the crude mixture was still not entirely pure. Because the product

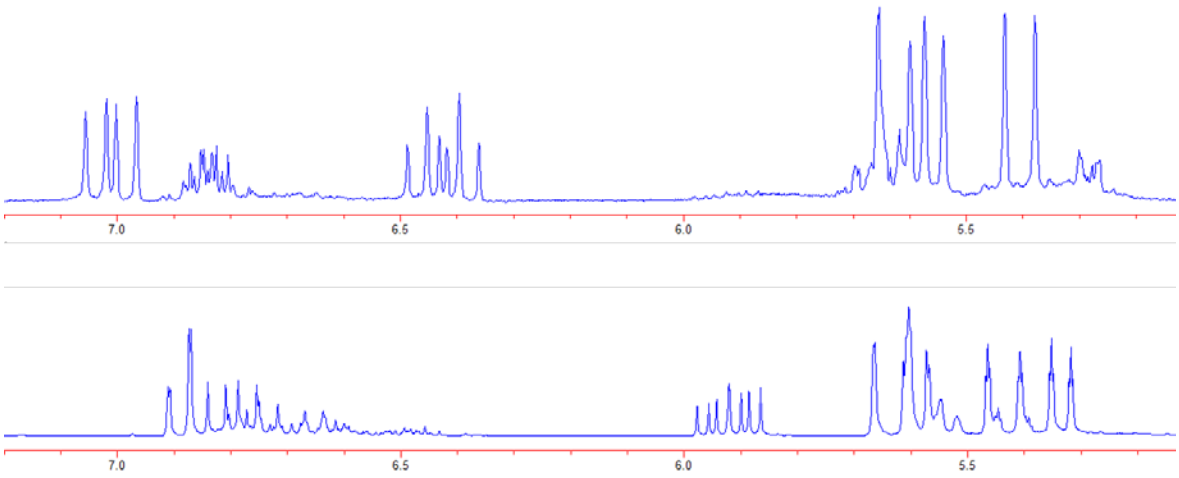

Figure 4.4. ^{1}H NMR spectrum of cyanobutadiene before silica gel chromatography (above) and after (below).

was sensitive to silica, we tried purification on a low activity alumina column. While the alumina column did not degrade the same entirely (some fractions containing **1** were recovered), the compound was not effectively separated from side products. Furthermore, additional signals appeared in the aliphatic region of the ^{1}H NMR spectrum after chromatography, indicating the possibility of polymerization on alumina as well. In addition, chromatographic purification exacerbates the issue of isolation of cyanobutadiene from similarly volatile solvents. Because the compound is known to evaporate off in the rotovap, any method of purification requiring dilution in a large amount of solvent will impact the yield of the reaction.

Various methods of distillation were also attempted. Immediately following workup, most of the solvent is removed *via* rotary evaporation. What is left of the solution is subjected to vacuum distillation, in which the distillation flask is cooled to 0 °C, and the receiving flask is cooled to -78 °C. This process separates **1** and the remaining solvent (THF) from some impurities, such as leftover starting material (diethyl cyanomethylphosphonate). In an attempt to separate **1** from the THF, a heated distillation was attempted. However, when the temperature approached the boiling point of THF, the solution started to turn from colorless to yellow. The distillation was stopped at this point, especially in light of reported temperature sensitivity reported in studies of cyanobutadiene polymerization.[32] Efforts are currently underway to develop the best method for isolation of cyanobutadiene; however, the issue is currently unresolved.

Base Modifications

In order to assess the effect of the base on the reaction, the reaction of interest was performed using two additional bases often used in Horner-Wadsworth-Emmons reactions: NaH and *n*-BuLi (Figure 4.5).

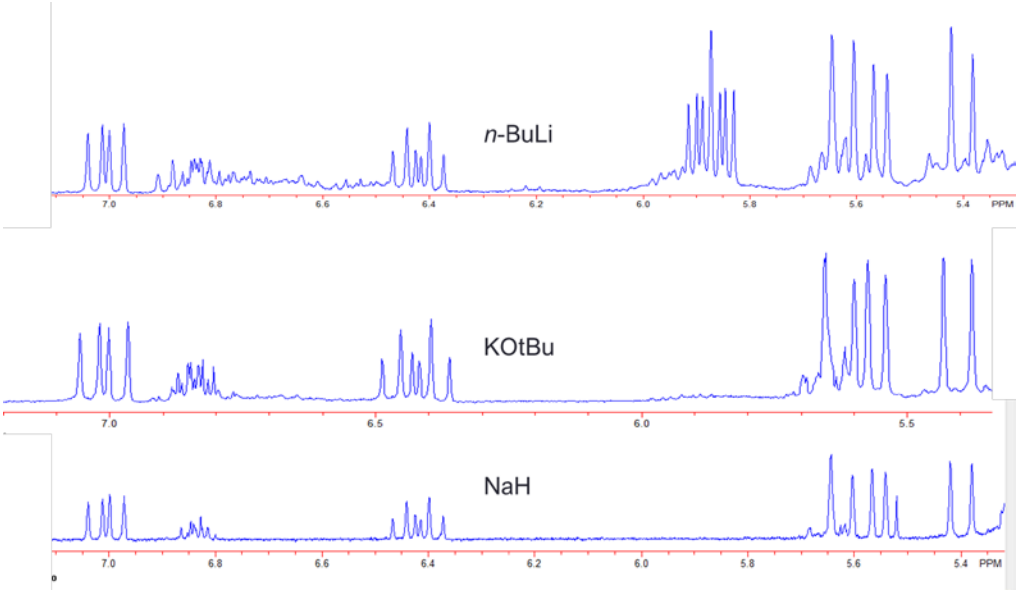

Figure 4.5. Comparison of ^{1}H NMR spectra in the vinyl region of product using *n*-BuLi (above), KO^{t}Bu (middle), and NaH (below).

Reaction with Butyllithium: Upon reaction with *n*-butyllithium, the spectrum shows formation of the product. However, in addition, there are signals that do not correspond to **1a** or **1b**. Interestingly, the characteristic multiplet at 5.9 ppm appears in the NMR spectrum that results from the degradation of the product after exposure to silica gel (Figure 4.4). The origin of this multiplet and others that are not attributed to the product have not yet been identified. The presence of polymeric product seen upon reaction with KO^{t}Bu was reduced but still present.

Reaction with Sodium Hydride: The reaction with sodium hydride produced the cleanest reaction mixture (free of polymeric growth) and the cleanest NMR spectrum (Figure 4.5). It appears that the reaction proceeds with a mixture of **1a** and **1b** in a ratio of ~2:1 *trans:cis*. At this point, the identity of the side product present in other base systems is unknown but is believed to be some kind of polymer or a mixture of polymers.

Characterization

Mass Spectrometry: Characterization of the diene was complicated in the initial stages. Because the ^{1}H NMR does not agree with the published values and there were unidentified side products upon initial reaction, the mass spectrometry data were crucial. Because of the size and volatility of the compound, GC-MS was the initial approach. GC-MS analysis is often complicated with products as small and volatile as cyanobutadiene because of potential interactions with the column. In addition, it is often difficult to find a solvent to dilute the sample that does not elute with the compound of interest (a similar issue encountered in the workup). Indeed, most elution solvents had elution times that overlapped with cyanobutadiene (**1**). In acetonitrile, however, a method was developed where the *cis* and *trans* cyanobutadiene peaks were visible and resolved. Solvent mass spectral features were subtracted out to reveal an EI mass spectrum that agrees well with the NIST library spectrum for cyanobutadiene (**1**) (Figure 4.6).

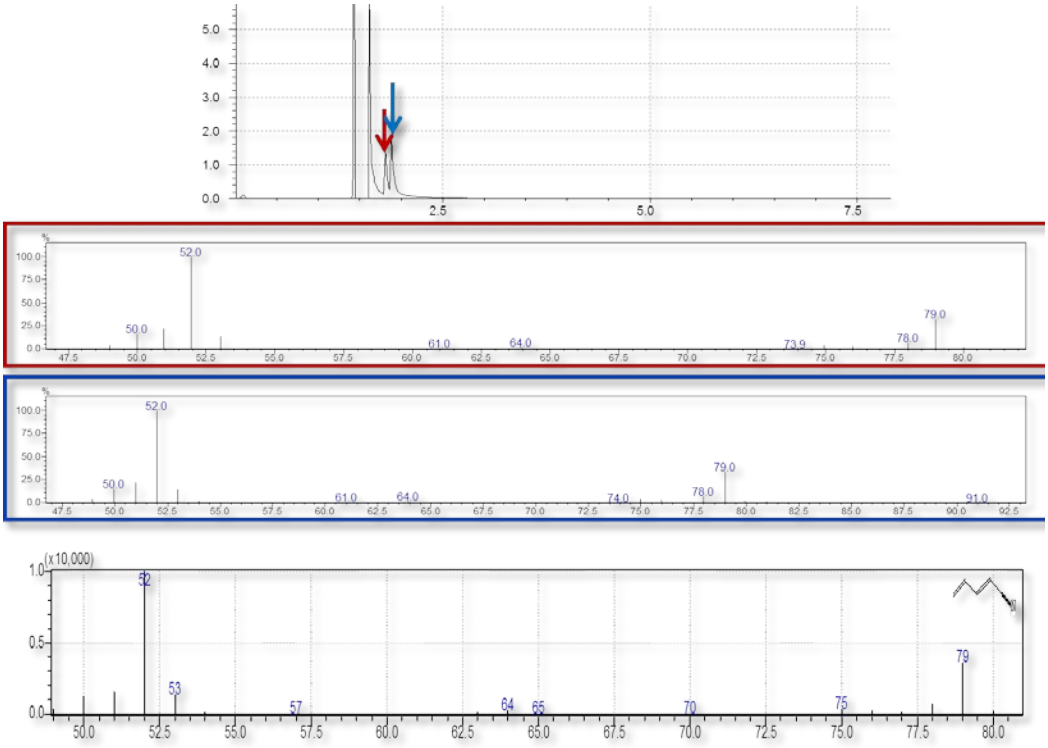

Figure 4.6. GC-MS analysis of *trans* and *cis* cyanobutadiene (**1a** and **1b**) crude reaction mixture in acetonitrile. Top: GC trace with *cis* (red arrow) and *trans* (blue arrow) cyanobutadiene. Middle: Mass spectra of the indicated GC peaks with solvent subtraction. Bottom: NIST library spectrum for cyanobutadiene **1a**.

It was with this information that the degradation of cyanobutadiene on the silica column was confirmed. By establishing the presence of cyanobutadiene in the crude product and its absence in purified product, it became obvious which ^{1}H NMR signals corresponded to cyanobutadiene, and the aforementioned modifications led to progress toward purification. In order to obtain a high-resolution exact mass for the structure, I turned to a fairly new method of ionization commonly referred to as ASAP-MS (Atmospheric Solids Analysis Probe Mass Spectrometry).[35] Most high resolution exact mass measurements are acquired by electrospray ionization. Unfortunately, many compounds, such as small hydrocarbons and alcohols, cannot be

easily ionized by electrospray. This type of analysis works quite well for these compounds. Using the same instrument as the ESI, the ASAP works by simply exposing the sample at the closed end of a glass capillary tube to a corona discharge. Using this method, the mass was identified within 2.5 ppm (calculated $[M+H]^+$ 80.0495, found 80.0493). In addition to providing an exact mass to four decimal places, ASAP on the Q-Exactive also provides MS/MS data. The MS/MS of **1** shows loss of CN as the major fragment (calculated 53.0386, found 53.0388), providing compelling evidence that the compound has been correctly identified (Figure 4.7).

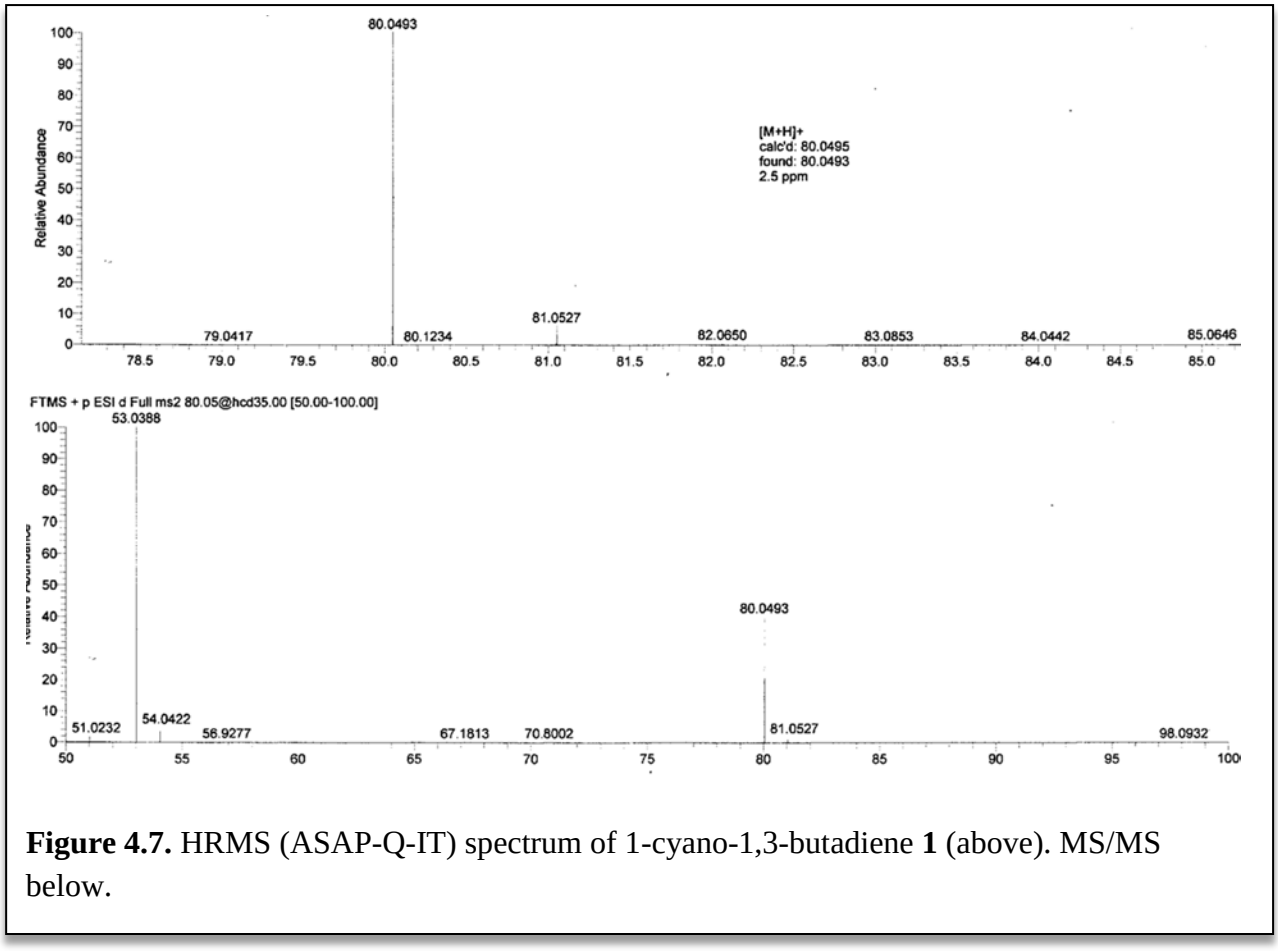

Figure 4.7. HRMS (ASAP-Q-IT) spectrum of 1-cyano-1,3-butadiene **1** (above). MS/MS below.

^{1}H NMR: One of the most challenging aspects of the characterization of **1** was the assignment of its ^{1}H NMR spectrum. In addition to the incomplete assignment from the literature, the coupling patterns present are clearly second order and require a more sophisticated treatment for assignment. Each isomer displays the ABX characteristic of vinyl protons with the addition of coupling from the protons on the second alkene moiety. The initial spectrum in $CDCl_3$ is shown in the bottom panel of Figure 4.8. One way to get around complicated second order effects is to use NMR solvents that cause significant upfield shifts, such as benzene-d_6.[36] It is often the case with alkenes in $CDCl_3$ that two or more of the protons are nearly superimposed, and the remaining protons that are coupled to them become quite complicated. By spreading out the signals in the spectrum, the degeneracy of the overlapping signals is lifted, and the spectrum can be interpreted as first order. The upfield shift in C_6D_6 aids in the elucidation of the downfield signals but the signals further upfield remained somewhat overlapping (Figure 4.8, top panel). As the figure shows, in order to get a clear picture of all signals in the spectrum, multiple NMR solvents (C_6D_6—above, CD_3CN—middle, $CDCl_3$—below) are required.

Using the C_6D_6 spectrum, the protons of *trans* **1a** and *cis* **1b** 1-cyano-1,3-butadiene were assigned (Figure 4.9). Signals in the downfield region (top panel of Figure 4.9) are more spread out and allow for identification of coupling constants in each isomer. Realtive intensities reveal which signals belong to which isomer, and from there protons in similar environments can be identified by their coupling patterns. Using the coupling constants identified in the downfield region, the overlapping signals in the upfield region can be teased apart and assigned. Some coupling in these signals is still unclear, but the assignment given is logical and consistent with expectations for a compound of this type.

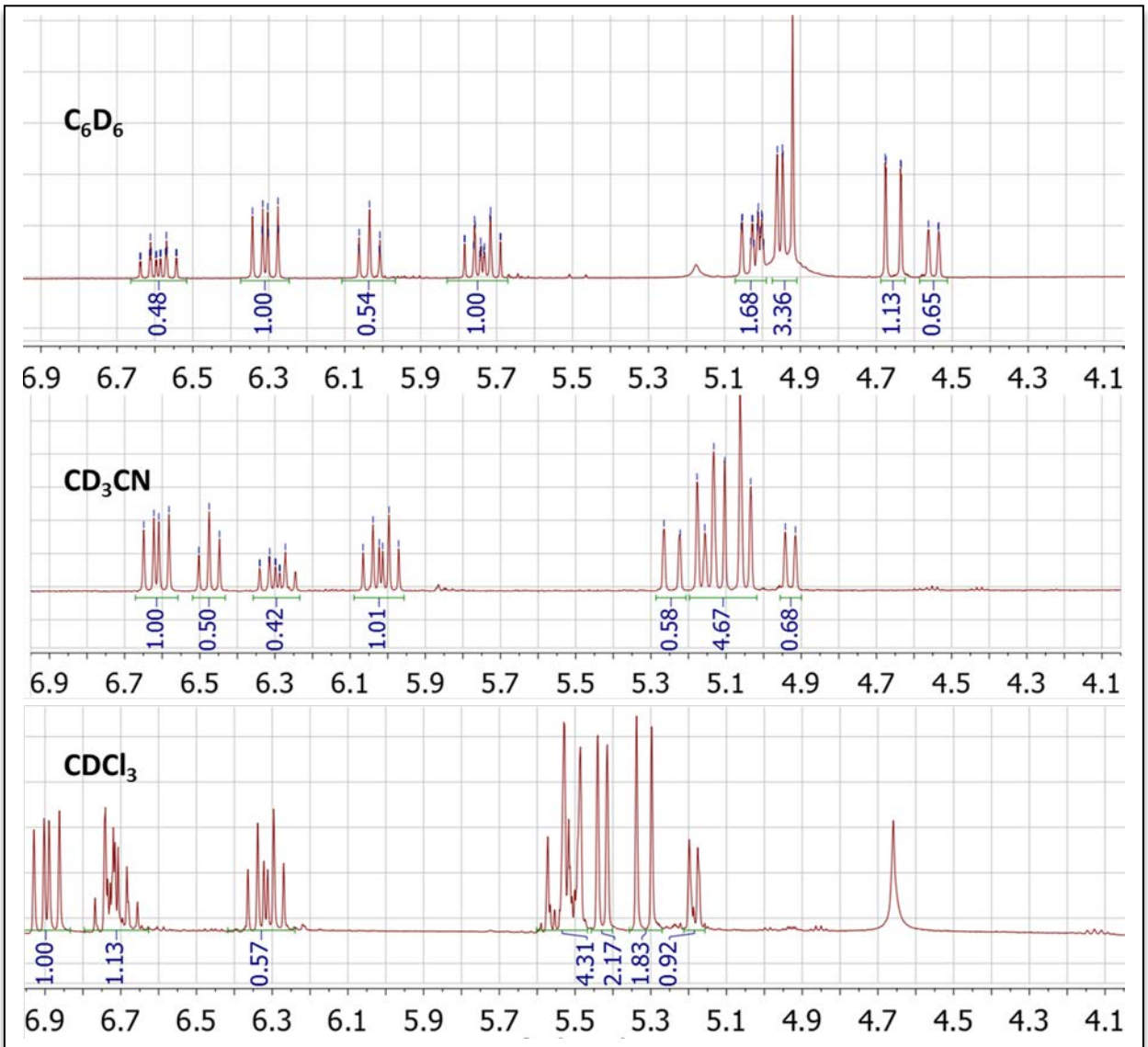

Figure 4.8. Vinyl region of 1-cyano-1,3-butadiene (**1**)^{1}H NMR spectrum (400 MHz) in C_6D_6 (above) CD_3CN (middle) and $CDCl_3$ (bottom).

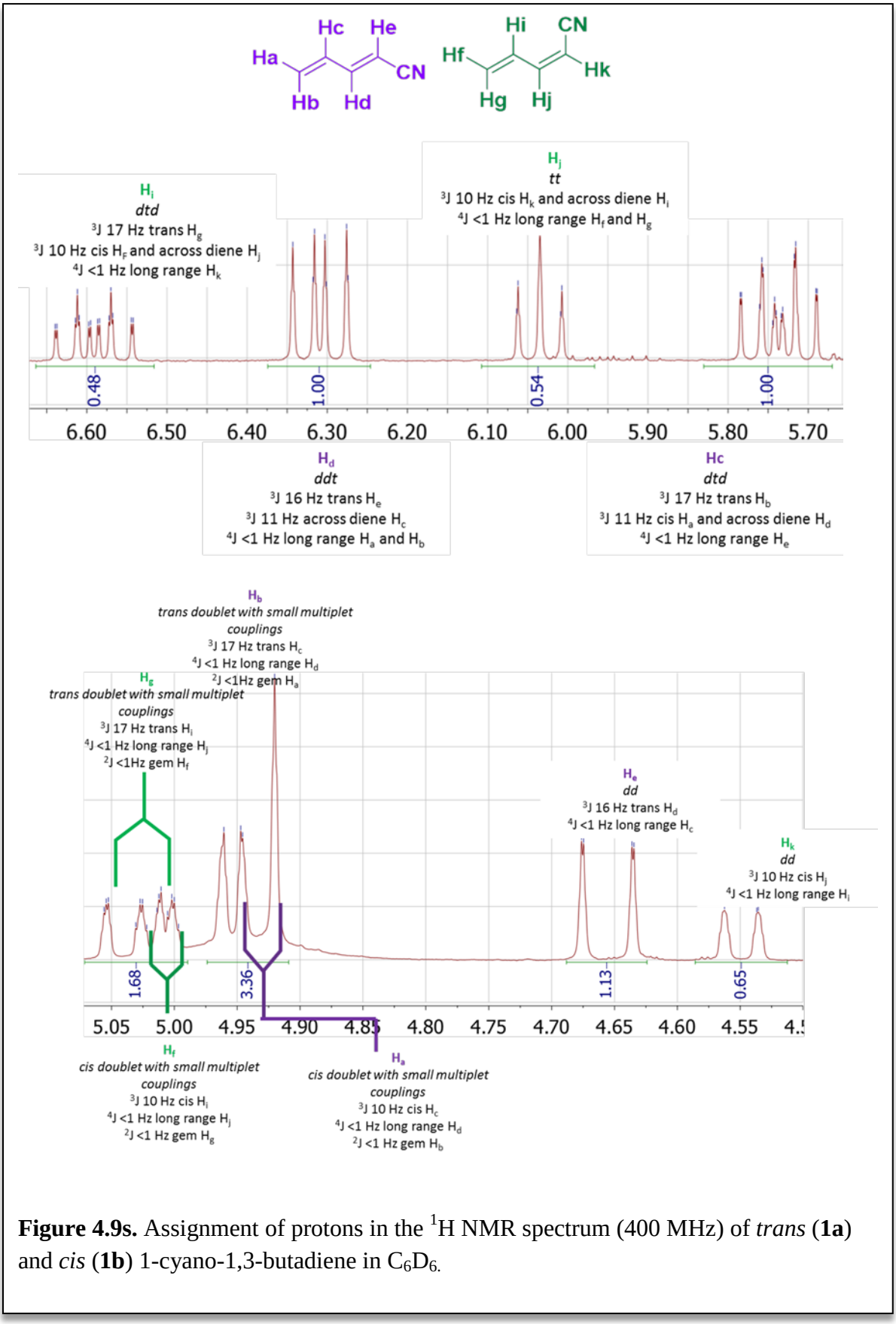

Figure 4.9s. Assignment of protons in the ^{1}H NMR spectrum (400 MHz) of *trans* (**1a**) and *cis* (**1b**) 1-cyano-1,3-butadiene in C_6D_6.

Table 4.1 shows a comparison of the previously reported ^{1}H NMR spectrum with the current interpretation of the spectrum. The analysis was done on the spectrum in $CDCl_3$ to maintain consistency between the two, even though some of the couplings are subject to second order effects. By understanding the spectrum in C_6D_6, the spectrum in $CDCl_3$ is much more navigable, and the overlapping signals can be more easily distinguished. It is clear that the agreements between the two reports differ, but because the ^{1}H NMR spectrum from the previous report are not available, it is difficult to determine the source of the discrepancy.

Table 4.1. ^{1}H NMR signal assignments of **1a** and **1b** in $CDCl_3$ previously reported[2] and found in this work. Estimated coupling constants affected by second order effects. For more accurate coupling constants, see data from spectrum in C_6D_6 (Figure 4.7).

***trans* 1a Clary**	***trans* 1a this work**	***cis* 1b Clary**	***cis* 1b this work**
7.00 dd, *J* = 15.9, 10.8 Hz	6.90 dd, *J* = 16.1, 10.8 Hz	7.24 d, *J* = 6.7 Hz	6.73 dt, *J* = 13.3, 10.2
6.42 dt, *J* = 16.9, 10.8 Hz	6.32 dt, *J* = 16.9, 10.6 Hz	7.17 d, *J* = 7.2 Hz	6.68 t, *J* = 10.6
5.61 d, *J* = 16.9 Hz	5.51 d, *J* = 16.9 Hz	6.83 dt, *J* = 10.3, 5.1 Hz	5.55 d, *J* = 17.6
5.55 d, *J* = 10.2 Hz	5.43 d, *J* = 10.1 Hz		5.51 d, *J* = 9.6
	5.32 *J* = 16.1 Hz		5.19 d, *J* = 9.0

Synthesis of *o*-, *p*- and *m*- Cyanostyrene

The synthesis of *o*- , *p*- and *m*- cyanostyrene was completed and the product was sent to the Zwier group to do excitation studies. The studies are complete and in preparation for publication. All isomers were synthesized using the Molander modification of the Suzuki-Miyaura cross coupling reaction[37] according to Figure 4.4. This synthesis was quite facile, and the *o*- (**3a**), *p*- (**3b**) and *m*- (**3c**) cyanostyrene were isolated with few problems, with data in good agreement with those reported by Molander.[37]

Scheme 4.4

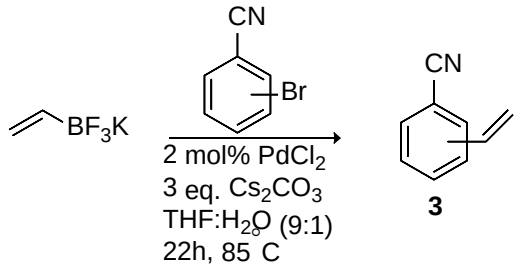

As a first step in understanding the potential pathways leading to heteroaromatics, the Zwier group has studied the isotope-selective spectroscopy of these compounds under jet-cooled conditions relevant to Titan's atmosphere. The excitation and emission spectra for the three isomers have been acquired and are under analysis. Using a combination of resonant two-photon ionization, LIF excitation, and dispersed fluorescence spectroscopies, the vibronic spectroscopy of the three isomers were recorded and compared. The *meta* isomer has two conformational isomers, which have been distinguished and studied using hole-burning methods. A publication is in preparation[38] detailing the comparisons and contrasts in the UV spectral signatures of the set of structural and conformational isomers of the cyanostyrenes, using the ethynylstyrene counterparts as points of comparison.[9]

Procedures toward the Synthesis of Propargyl Cyanide

In studies analogous to those intended for cyanobutadiene (**1**) the Zwier group was interested in the photochemical and discharge-driven chemistry of propargyl cyanide (**7**). Scheme 4.5 describes the intended synthesis of the compound by the cobalt-mediated synthesis procedure described by Nicholas.[39] The preparation of **5** proceeded as expected, but the conversion of **5** to **6** was problematic. It was challenging at first to detect that the reaction hadn't

Scheme 4.5.

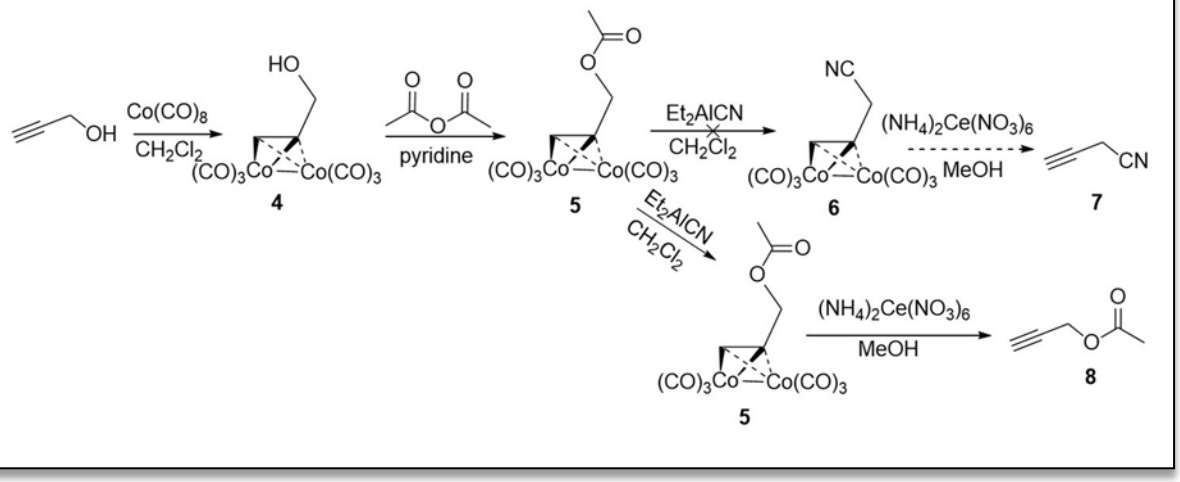

worked because the procedure, as written, describes direct reaction from **5** to **7** without characterization of **6** in between; however, the paper only describes the NMR and MS spectra of **6**, and no data were provided regarding the NMR characterization of **7**. Upon GC-MS analysis of the final product, however, it was clear that **7** was not formed. Instead, a mass that corresponded to **8** was consistently detected, and the presence of the methyl group of **8** in the final NMR spectrum confirms that the conversion of **5** to **6** never occurs. The decomplexation of unreacted **5** leads to **8** as the final product.

Scheme 4.6.

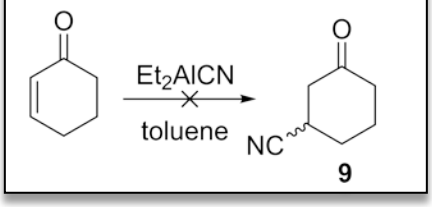

When it became clear that the transformation of **5** to **6** was the issue, the quality of the reagent, diethylaluminum cyanide (Et_2AlCN), was called into question. Since the reaction was very straightforward, only involving adding the two components together and stirring at room temperature, few other factors could be the cause of the issue. In order to test the reagent effectiveness, two diagnostic reactions were performed. Looking through the Encyclopedia of Reagents for Organic Synthesis (EROS),[40] I found the first and most prevalent use of Et_2AlCN, initially reported by Nagata.[41] The first reaction took the form of this classic reaction (Scheme 4.6). As shown, the reaction did not proceed to the expected product. In order to be certain, another reaction using the same cobalt complexation mechanism also reported by Nicholas (Scheme 4.7) was also attempted to no avail. From these

Scheme 4.7

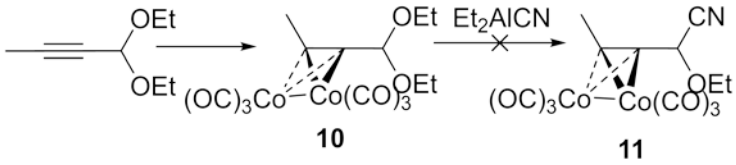

tests, it can be concluded that reactions performed using the Et_2AlCN reagent are consistently failing to provide the expected product. The issue is likely related to the purity or identity of the reagent itself. Attempts to resolve the issue with the supplier have so far been unsuccessful, as the reagent is not in very high demand. The synthesis of the molecule will have to proceed *via* a different pathway in order to procure the desired product **7**.

Conclusions

Laboratory simulations are a key component of astrochemical investigations. In order to predict specific reactivity present in planetary atmospheres like Titan, it is crucial to have laboratory models that utilize astronomically observed conditions. The Zwier group's interest in sophisticated spectroscopic investigations of the photochemistry and discharge-driven chemistry of astrochemically relevant systems are well in line with our research. When interest in expanding their spectroscopic search to nitrile functionality necessitated the synthesis of a small family of unsaturated nitriles, we were pleased to facilitate the collaboration. The synthesis of these compounds, especially that of 1-cyano-1,3-butadiene, proved to be a fascinating story in itself. By stumbling upon a sparsely studied compound, we were able to push beyond a simple synthesis for collaboration and contribute to the synthetic procedure, mass spectrometric, and NMR characterization of this unexpectedly complex molecule.

Experimental Section

General Information. Chemicals and solvents were purchased and used without purification, unless otherwise noted. ^{1}H NMR spectra (300 or 400 MHz) and ^{13}C NMR spectra (75.4 or 100.6 MHz) were obtained in $CDCl_3$ on a Bruker Avance III 400 spectrophotometer or a Bruker AC+ 300; chemical shifts (δ) are reported as ppm downfield from internal standard $SiMe_4$. Mass spectra were acquired using electrospray ionization or ASAP on a Thermo Q-Exactive Plus™ mass spectrometer. GC/MS analysis was performed on a Shimadzu GCMS-2010S.

Synthetic Information

1-Cyano-1,3-butadiene (1).[2,42] To a suspension of sodium hydride (2.88 g, 120 mmol) in freshly-distilled THF (500 mL) was added diethyl cyanomethylphosphonate (8.1 mL, 50.1 mmol

dropwise *via* syringe at 0 °C. After stirring for 1 h freshly distilled acrolein (3.6 mL, 53.9 mmol) was added dropwise. The reaction was stirred for 5 h at 0 °C and then warmed to room temperature and quenched with sat. aq. NH_4Cl solution. The solution was extracted with diethyl ether, washed with brine and water, and dried over $MgSO_4$. The ether was removed under reduced pressure at room temperature, and the resulting mixture was fractionally distilled (collection flask cooled to -78 °C, and distillation flask cooled to 0 °C. The distillate consists of a mixture *trans* and *cis* isomers in a ratio of 2:1 in THF. ^{1}H-NMR (400 MHz, $CDCl_3$) *trans*-isomer δ 6.31 (ddt, *J* = 16, 11, <1 Hz, 1H), 5.74 (tt, *J* = 10, <1 Hz, 1H), 4.94 (dm, *J* = 17, <1, <1 Hz, 1H), 4.93 (dm, *J* = 10, <1, <1 Hz, 1 H), 4.65 (dd, *J* = 16, <1 Hz, 1H) ppm *cis*-isomer δ 6.59 (dtd, *J* = 17, 10, <1 Hz, 1H), 6.03 (tt, *J* = 10, <1 Hz, 1H), 5.03 (dm, *J* = 17, <1, <1 Hz, 1H), 5.02 (dm, *J* = 10, <1, <1 Hz, 1 H), 4.55 (dd, *J* = 10, <1 Hz, 1H). HRMS (ASAP^{35}-Q-IT) *m/z*: $[M+H]^+$ Calc'd for C_5H_6N 80.0495; Found 80.0493

Cyanostyrenes.[37] Following the procedure by Molander, a solution of potassium vinyltrifluoroborate (142 mg, 1.06 mmol), bromobenzonitrile (184 mg, 1.01 mmol), triphenylphosphine (23.6 mg, 0.09 mmol), cesium carbonate (1.05 g, 3.22 mmol), and palladium(II) chloride (3.6 mg, 0.02 mmol) in THF/H_2O (9:1) was prepared in a sealed tube reactor. Nitrogen gas was bubbled through the solution for 30 minutes, and a Teflon screw cap was screwed on tightly by hand. The solution was heated to 85°C in an oil bath for 22 h, then cooled to room temperature and diluted with H_2O (3 mL) followed by extraction with dichloromethane (3x 10 mL). The organic layers were combined and washed with H_2O (10 mL), dried over $MgSO_4$, and solvent was removed via rotary evaporation. The resulting crude product was purified by silica gel column chromatography (eluting with 20:1 pentane: diethyl ether) to yield the cyanostyrene product (Rf =0.2).

***o*-Cyanostyrene:** 32 % yield ^{1}H NMR (300 MHz, $CDCl_3$) δ 5.54 (d, 1H, *J* = 11 Hz), 5.95 (d, 1H, *J* = 17 Hz), 7.09 (dd, 1H, *J* = 17, 11), 7.35 (td, 1H, *J* = 7,3 Hz), 7.56 (td, 1H, *J*=8, 3 Hz), 7.64 (dd, 1H, *J* = 8, 1 Hz), 7.68 (dd, 1H, *J* = 8,1 Hz).

***m*-Cyanostyrene:** 52% yield ^{1}H NMR (300 MHz, $CDCl_3$) δ 5.40 (d, 1H, *J* = 11 Hz), 5.83 (d, 1H, *J* = 18 Hz), 6.70 (dd, 1H, *J* = 18, 11 Hz), 7.44 (t, 1H, *J* = 8 Hz), 7.54 (dt, 1H, *J* = 8, 1.5 Hz), 7.63 (dt,1H, *J* = 8, 1.5 Hz), 7.68 (s, 1H).

***p*-Cyanostyrene:** 48% yield ^{1}H NMR (300 MHz, $CDCl_3$) δ 5.45 (d, 1H, *J* = 11 Hz), 5.88 (d, 1H, *J* = 18 Hz), 6.73 (dd, 1H, *J* = 18, 11 Hz), 7.50 (d, 2H, *J* = 8.5), 7.62 (d, 2H, *J* = 8.4 Hz).

Cobalt-complexed Propargyl Alcohol (4). To an oven-dried 250 mL round-bottom flask was added propargyl alcohol (0.80 mL, 13.7 mmol) in freshly-distilled CH_2Cl_2 (36 mL). To this was added cobalt carbonyl (4.8 g, 14.0 mmol) and was stirred under N_2 at room temperature for 4 h.

Cobalt-complexed Propargyl Acetate (5). Pyridine (3 mL) and acetic anhydride (36 mL) was then added to the solution containing **4** and stirred for an additional 5 h. At this time, cold $NaHCO_3$ solution (110 mL) was added to the solution. The layers were separated, and the aqueous layer was extracted three times with 50 mL CH_2Cl_2 . The organic extract was dried over $MgSO_4$, filtered and concentrated under reduced pressure to ~25 mL. ^{1}H NMR (400 MHz, $CDCl_3$)) δ 6.06 (s, 1H), 5.28 (s, 2H), 2.13 (s, 3H).

Atttempt to synthesize Cobalt-complexed Propargyl Cyanide (6). The extract of **5** was added dropwise to a stirring solution of diethylaluminum cyanide (1.0 M solution in toluene, 18 mL) in CH_2Cl_2 (18 mL) at 0 °C and stirred for 50 min. s(This step was unsuccessful and resulted in no change to **5**). To the solution was added ice water (100 mL) and the mixture was

extracted twice with diethyl ether. The combined ether extract was dried over $MgSO_4$. No changes in the spectrum were observed between **5** and **6**.

Propargyl Acetate (Decomplexation) (8). The solution was filtered and added to a mixture of silica gel (7.8 g) and $(NH_4)_2Ce(NO_3)_6$ (15.4 g) at -78 °C in MeOH (125 mL). The dropwise addition was complete after ~35 min, and the mixture remained at -78 °C until CO evolution ceased. The mixture was then warmed to 20 °C and stirred for 3h. Water (~70 mL) was added to the flask and the mixture was extracted twice with CH_2Cl_2, dried over $MgSO_4$, filtered, and concentrated under reduced pressure. The crude product was purified using flash column chromatography (SiO_2, 3:1 hexanes: diethyl either). ^{1}H NMR (400 MHz, CD_3CN)) δ 4.63 (d, 2.5 Hz, 2 H), 2. 74 (t, 2.5 Hz, 1 H), 2.02 (s, 3 H).

Reactions to test reagent quality:

3-Cyanocyclohexanone (9).[41] To a 100 mL oven-dried round bottom flask under N_2 was added 0.3 mL cyclohex-2-en-1-one in 60 mL toluene. To this mixture was added Et_2AlCN (6.0 mL, 1.0 M solution in toluene), and the mixture was stirred under N_2 for 15 min. The mixture was added to 100 mL 2N NaOH cooled to 0 °C and stirred for 2 h. The mixture was extracted with 100 mL CH_2Cl_2, dried over $MgSO_4$, and concentrated under reduced pressure.

NMR and GC/MS results indicate no reaction.

Cobalt-complexed Diethylacetal (10) To an oven-dried round bottom flask under N_2 was added cobalt carbonyl (0.708, 2.1 mmol) in freshly distilled CH_2Cl_2 (6.5 mL). To this was added 0.320 mL 2-butyn-1-al diethyl acetal (0.320 mL, 2.0 mmol) dropwise. After CO emission (~10 min) the mixture was stirred at room temperature for 3 h. ^{1}H NMR (400 MHz, $CDCl_3$)) δ

Attempt to synthesize (11) To a stirred solution of diethylaluminum cyanide (3.0 mmol)was added the cobalt-complexed cobalt-complexed diethylacetal (**10**) dropwise at 0 °C. The reaction was checked at 40 min, 2 h, and 12 h with no change in the spectrum.

Notes and References

1. Flasar, F. M.; Achterberg, R. K.; Conrath, B. J.; Gierasch, P. J.; Kunde, V. G.; Nixon, C. A.; Bjoraker, G. L.; Jennings, D. E.; Romani, P. N.; Simon-Miller, A. A.; Bézard, B.; Coustenis, A.; Irwin, P. G. J.; Teanby, N. A.; Brasunas, J.; Pearl, J. C.; Segura, M. E.; Carlson, R. C.; Mamoutkine, A.; Schinder, P. J.; Barucci, A.; Courtin, R.; Fouchet, T.; Gautier, D.; Lellouch, E.; Marten, A.; Prangé, R.; Vinatier, S.; Strobel, D. F.; Calcutt, S. B.; Read, P. L.; Taylor, F. W.; Bowles, N.; Samuelson, R. E.; Orton, G. S.; Spilker, L. J.; Owen, T. C.; Spencer, J. R.; Showalter, M. R.; Ferrari, C.; Abbas, M. M.; Raulin, F.; Edgington, S.; Ade, P.; Wishnow, E. H. Titan's Atmospheric Temperatures, Winds, and Composition. *Science* **2005**, *308*, 975-978.

2. Clary, K. N.; Back, T. G. Preparation of Unsaturated Aminonitriles from the Aza-Morita-Baylis-Hillman Reactions of Aldimines with Penta-2,4-dienenitrile. *Synlett* **2007**, *2007*, 2995-2998.

3. Raulin, F.; Brasse, C.; Poch, O.; Coll, P. Prebiotic-like chemistry on Titan. *Chem. Soc. Rev.* **2012**, *41*, 5380-5393.

4. Newby, J. J.; Stearns, J. A.; Liu, C.-P.; Zwier, T. S. Photochemical and Discharge-Driven Pathways to Aromatic Products from 1,3-Butadiene. *J. Phys. Chem. A* **2007**, *111*, 10914-10927.

5. Niemann, H. B.; Atreya, S. K.; Bauer, S. J.; Carignan, G. R.; Demick, J. E.; Frost, R. L.; Gautier, D.; Haberman, J. A.; Harpold, D. N.; Hunten, D. M.; Israel, G.; Lunine, J. I.; Kasprzak, W. T.; Owen, T. C.; Paulkovich, M.; Raulin, F.; Raaen, E.; Way, S. H. The abundances of constituents of Titan's atmosphere from the GCMS instrument on the Huygens probe. *Nature* **2005**, *438*, 779-784.

6. Waite, J. H.; Young, D. T.; Cravens, T. E.; Coates, A. J.; Crary, F. J.; Magee, B.; Westlake, J. The Process of Tholin Formation in Titan's Upper Atmosphere. *Science* **2007**, *316*, 870-875.

7. Arrington, C. A.; Ramos, C.; Robinson, A. D.; Zwier, T. S. Aromatic Ring-Forming Reactions of Metastable Diacetylene with 1,3-Butadiene. *J. Phys. Chem. A* **1998**, *102*, 3315-3322.

8. Bandy, R. E.; Lakshminarayan, C.; Frost, R. K.; Zwier, T. S. Direct Detection of C$_4$H$_2$ Photochemical Products: Possible Routes to Complex Hydrocarbons in Planetary Atmospheres. *Science* **1992**, *258*, 1630-1633.

9. Selby, T. M.; Clarkson, J. R.; Mitchell, D.; Fitzpatrick, J. A. J.; Lee, H. D.; Pratt, D. W.; Zwier, T. S. Isomer-Specific Spectroscopy and Conformational Isomerization Energetics of o-, m-, and p-Ethynylstyrenes. *J. Phys. Chem. A* **2005**, *109*, 4484-4496.

10. Wilson, E. H.; Atreya, S. K. Current state of modeling the photochemistry of Titan's mutually dependent atmosphere and ionosphere. *J. Geophys. Res.* **2004**, *109*, E06002.

11. Sagan, C.; Khare, B. N. Tholins: organic chemistry of interstellar grains and gas. *Nature* **1979**, *277*, 102-107.

12. Tran, B. N.; Joseph, J. C.; Ferris, J. P.; Persans, P. D.; Chera, J. J. Simulation of Titan haze formation using a photochemical flow reactor: The optical constants of the polymer. *Icarus* **2003**, *165*, 379-390.

13. Ribblett, J. W.; Borst, D. R.; Pratt, D. W. Styrene and phenylacetylene: Electronic effects of conjugating substituents“off” and“on” the axis of a benzene ring. *J. Chem. Phys.* **1999**, *111*.

14. King, G.; So, S. Ethynylbenzene analysis of the 2790 Å absorption system. *J. Mol. Spectrosc.* **1971**, *37*, 543-570.

15. Stearns, J. A.; Zwier, T. S. Infrared and Ultraviolet Spectroscopy of Jet-Cooled o rtho-, m eta-, and p ara-Diethynylbenzene. *J. Phys. Chem. A* **2003**, *107*, 10717-10724.

16. Laposa, J. Fluorescence of para-diethynylbenzene in polycrystalline methylcyclohexane at 77 K. *J. Lumin.* **1979**, *20*, 67-72.

17. Hollas, J. M.; Musa, H.; Ridley, T.; Turner, P. H.; Weisenberger, K. H.; Fawcett, V. The $\tilde{A}1A'$-$\tilde{X}1A'$ single vibronic level fluorescence and Raman spectra of styrene-β-D2 vapor and their use in determining the C(1)-C(α) torsional potential function in the $\tilde{X}$ state. *J. Mol. Spectrosc.* **1982**, *94*, 437-455.

18. Raulin, F.; Bruston, P.; Coll, P.; Coscia, D.; Gazeau, M.-C.; Guez, L.; de Vanssay, E. Exobiology on Titan. *J. Biol. Phys.* **1995**, *20*, 39-53.

19. Yung, Y. L. An update of nitrile photochemistry on Titan. *Icarus* **1987**, *72*, 468-472.

20. Yung, Y. L.; Allen, M.; Pinto, J. P. Photochemistry of the atmosphere of Titan - Comparison between model and observations. *Astrophys. J., Suppl. Ser.* **1984**, *55*, 465-506.

21. Lara, L. M.; Lellouch, E.; López-Moreno, J.; Rodrigo, R. Vertical distribution of Titan's atmospheric neutral constituents. *J. Geophys. Res.* **1996**, *101*, 23261-23283.

22. Toublanc, D.; Parisot, J.; Brillet, J.; Gautier, D.; Raulin, F.; McKay, C. Photochemical modeling of Titan's atmosphere. *Icarus* **1995**, *113*, 2-26.

23. Lebonnois, S.; Toublanc, D.; Hourdin, F.; Rannou, P. Seasonal variations of Titan's atmospheric composition. *Icarus* **2001**, *152*, 384-406.

24. Fox, J. L.; Yelle, R. V. Hydrocarbon ions in the ionosphere of Titan. *Geophys. Res. Lett.* **1997**, *24*, 2179-2182.

25. Keller, C.; Anicich, V.; Cravens, T. Model of Titans ionosphere with detailed hydrocarbon ion chemistry. *Planet. Space Sci.* **1998**, *46*, 1157-1174.

26. Banaszkiewicz, M.; Lara, L.; Rodrigo, R.; Lopez-Moreno, J.; Molina-Cuberos, G. A coupled model of Titan's atmosphere and ionosphere. *Icarus* **2000**, *147*, 386-404.

27. Vuitton, V.; Yelle, R. V.; Anicich, V. G. The Nitrogen Chemistry of Titan's Upper Atmosphere Revealed. *Astrophys. J. Lett.* **2006**, *647*, L175.

28. Coustenis, A.; Bézard, B.; Gautier, D. Titan's atmosphere from voyager infrared observations. *Icarus* **1989**, *80*, 54-76.

29. Braun, M.; Mroß, S.; Schwarz, I. Mild and Stereoconvergent Palladium-Catalyzed Carbonyl Alkenation Reaction of α,β-Unsaturated Aldehydes. *Synthesis* **1998**, *1998*, 83-88.

30. Snyder, H. R.; Stewart, J. M.; Myers, R. L. 1-Cyano-1,3-butadienes: cis, trans-Isomers of 1-Cyano-1,3-butadiene. *J. Am. Chem. Soc.* **1949**, *71*, 1055-1056.

31. Snyder, H. R.; Poos, G. I. 1-Cyano-1,3-butadienes. II. Carbon Structure of the Adduct Formed by the Diels--Alder Condensation of 1-Cyano-1,3-butadiene with 1,3-Butadiene. *J. Am. Chem. Soc.* **1949**, *71*, 1057-1058.

32. Worley, R.; Young, R. N. Anionic polymerization and copolymerization of 1-cyanobutadiene. *Eur. Polym. J.* **1972**, *8*, 1355-1359.

33. Paterson, I.; Yeung, K.-S.; Smaill, J. B. The Horner-Wadsworth-Emmons Reaction in Natural Products Synthesis: Expedient Construction of Complex (E)-Enones Using Barium Hydroxide. *Synlett* **1993**, *1993*, 774-776.

34. Rathke, M. W.; Nowak, M. The Horner-Wadsworth-Emmons modification of the Wittig reaction using triethylamine and lithium or magnesium salts. *J. Org. Chem.* **1985**, *50*, 2624-2626.

35. McEwen, C. N.; McKay, R. G.; Larsen, B. S. Analysis of solids, liquids, and biological tissues using solids probe introduction at atmospheric pressure on commercial LC/MS instruments. *Anal. Chem.* **2005**, *77*, 7826-7831.

36. Reich, H. J. *Chem 605 Structure Determination Using Spectroscopid Methods Handouts*, 2012.

37. Molander, G. A.; Brown, A. R. Suzuki−Miyaura Cross-Coupling Reactions of Potassium Vinyltrifluoroborate with Aryl and Heteroaryl Electrophiles. *J. Org. Chem.* **2006**, *71*, 9681-9686.

38. Korn, J. A.; Knezz, S. N.; McMahon, R. J.; Zwier, T. S. Jet-Cooled Vibronic Spectroscopy of o-,m-, and p-Cyanostyrene. **2016**.*In preparation*

39. Stuart, J. G.; Nicholas, K. M. Cobalt-Mediated Synthesis of Propargyl Nitriles and α-Alkoxy Propargyl Nitriles. *Synthesis* **1989**, *1989*, 454-455.

40. Nakai, T.; Tomooka, K. In *Encyclopedia of Reagents for Organic Synthesis*; John Wiley & Sons, Ltd: 2001.

41. Nagata, W.; Yoshioka, M.; Hirai, S. Hydrocyanation. IV. New hydrocyanation methods using hydrogen cyanide and an alkylaluminum, and an alkylaluminum cyanide. *J. Am. Chem. Soc.* **1972**, *94*, 4635-4643.

42. Noguchi, M.; Yamada, H.; Takamura, S.; Uchida, T.; Hironaka, M.; Kakehi, A.; Yamamoto, H. Stereoselective Azepine-Ring Formation Through Ene Reactions of 3-(Alk-2-enyl)amino-2-cyanoacrolein Derivatives. *Eur. J. Org. Chem.* **2000**, *2000*, 1489-1496.

Chapter 5: Assessment of Cognitive Skills in the Flipped Chemistry Classroom

Introduction

For generations, information has been passed in the form of lectures by an expert in a particular field. In the context of formal education, this method has persisted as the dominant means by which students acquire knowledge from instructors. In 1993, a seminal paper by Alison King describes the instructor in this context as the "sage on the stage", the transmitter of knowledge.[1] In more recent years, through work and insight by education researchers like King, mounting evidence suggests that the role of the instructor is actually more effective when he or she acts as more of a "guide on the side."

My time as a graduate student at UW-Madison has involved its fair share of teaching responsibilities. Most of the classes with which I've been involved in our chemistry department have showcased remarkably engaging lectures, and students have generally positive things to say about the courses and the instructors. Although my experience has been largely positive, there is no escaping the fact that UW-Madison is an RO1 institution, and as such, organic chemistry lectures are large. Large courses come with their own set of rewards and challenges for instructors and students alike. In most of my teaching experiences, I have only witnessed the traditional classroom, where a professor delivers a lecture to a large room of students. There are few complaints about this framework, largely because most students do not realize there is any alternative. Unfortunately, in chemistry, one of the largest issues is that students try to learn material by rote memorization rather than deep conceptual learning. If information is only disseminated through continuous exposition by an instructor, students receive the message that this information needs to be memorized, and that is where the learning ends.

By participating in the Delta internship, I hoped to employ innovative teaching techniques in a small classroom environment. To achieve this, I connected with a faculty partner at Madison College. Dr. Christen Smith teaches several general chemistry courses and was willing to hand a unit of one of these courses over to me to do with what I wished. For the two-day unit on acids and bases, I decided to flip her class. "Flipping" a class refers to the process of offloading lecture content to some other formats so that students can access it before class time. The in-class time is then spent doing more engaged work (in this intervention, students worked on group problem sets together). The instructor is then able to be present while students actively work through course material and can observe and address student confusion in real time.

Educational Context

The concept of the flipped classroom draws primarily from two major educational constructs. Fundamentally, the constructivist theories of learning view knowledge as a state of understanding in the mind of the subject, rather than something that can be transmitted from person to person.[1] Further, knowledge must be constructed or reconstructed within the framework of the subject's existing knowledge. A classroom then should be an environment for the construction of knowledge, and the instructor should be the facilitator of the construction. In addition, cognitive load theory asserts that the learning process imposes a load on the working memory which has limited processing power at any given time. It follows that providing information prior to class time offers students the opportunity to process the information ahead of time, reducing the cognitive load.[2] For clarity, the definition of the flipped classroom, as defined by the Flipped Learning Network is as follows:

"Flipped Learning is a pedagogical approach in which direct instruction moves from the group learning space to the individual learning space, and the resulting group space is

transformed into a dynamic, interactive learning environment where the educator guides students as they apply concepts and engage creatively in the subject matter."

While the flipped classroom model draws heavily from educational theory, the idea actually arose from observing positive effects after implementing a variety of different approaches,[3] not from within theory itself. Flipped learning can also be viewed as the logical extension of efforts to integrate active learning into the classroom with the necessity that students be exposed to the material before engaging with it actively.

The implementation of the flipped classroom structure came about in the early 2000s[4-6] and has since taken off in many educational settings. There is particular interest in applying the model to courses in STEM fields, where there is a large divide between high- and low-achieving students[7] and where the large lecture course is a prevalent model. Introducing active learning into the classroom has shown to increase student success in a variety of arenas.[7-10] This model remains somewhat controversial, however, as quantitative and peer-reviewed studies in the physical sciences remain somewhat scarce.[11-13] It is possible with a new generation of well-informed science educators to change the norm, but first there must be enough compelling evidence that the model is an improvement.

It was, in fact, two chemistry teachers who wrote one of the first major texts describing the flipped classroom at a high school level.[3] In the context of college-level chemistry, there has been a boom of recent reports following a 2015 conference[14] on the topic including a review on emerging trends.[15] The trends that were consistent among reported implementations generally had four major considerations: student engagement prior to class, incentives for completing pre-class work, time used during class, and evaluation of effectiveness.

Although advocates of the flipped classroom assert that the out-of-class initial exposure to content can be accessed in many ways, in the field of higher education chemistry, almost all examples rely on some kind of video that can be accessed on the computer. Most often these videos take on the form of a narrated PowerPoint presentation, referred to as screencasts. Screencast run times ranged from 5-20 minutes, with the average length around 10 minutes. Notable also is the time required to prepare the screencasts. One study proposed a 1:10 ratio of produced material: preparation time.[16] It is generally accepted that this method requires a considerable amount of time compared to the traditional lecture, but the benefits outweigh the initial time investment.[15] Additionally it was found that providing a schedule assists students in organizing the new structure.[16]

An obvious concern with placing the responsibility on the students to access the material prior to class is the students' motivation to actually do so. To this end, many different methods for incentivizing the screencast were implemented. In many cases, this was done by having a quiz to complete after the screencast to be collected at the beginning of class. Alternatively, some have found that grading an in-class activity was sufficient, as students needed to be familiar with the material in order to perform well. This also ensures that students attend and engage in the in-class portion, the main reason to flip the class in the first place.

The in-class portion of the flipped framework is intended to be an active learning activity that will facilitate the construction of knowledge with the guidance of the instructor. In most implementations within chemistry, this portion consists of problem-solving sessions of some variety. Often, students would work through problems in groups, and groups periodically report progress on the whiteboard.[17] Bridging the pre-class and in-class proved to be useful for getting students ready to engage fully in the active learning portions. In some instances, students were

asked on their pre-class quiz what topics were most troubling, and those topics were covered in a mini-review lecture.[17] The review serves to jog students' memories about what they had learned in the screencasts while also exposing them to a more comfortable form of class-time to ease them into the more unfamiliar format.

Assessment of the success of lecture-flipping generally fell into two arenas: student satisfaction and learning gains.[15] In general, students had positive reactions to the model. With few exceptions, greater than 70% of the students preferred the flipped model to the traditional classroom. It should be noted, however, that most students also stated that the model took time to get used to.[17] There were several recurring comments among student evaluations. First, students appreciated the ability to access the material in their own time.[18] Pacing in the traditional classroom is set entirely by the instructor and does not consider the diversity of student learning styles. In a similar way, students appreciated the ability to engage with the lecture material multiple times if necessary. In terms of learning gains, there were no obvious and consistent improvements or declines in exams scores across the studies. There are several possible explanations for this. One notable consistency that may be related is the reduction of withdrawal rates in the flipped classroom.[16] Students who may have withdrawn before are staying in the class, perhaps not performing extremely well and masking the improvement of more "middle of the pack" students.

In general, the flipped classroom seems to have great potential for undergraduate chemistry students. The discipline has been slow to adopt new pedagogies, and the diversity in the field has likely suffered as a result. By appealing to a more diverse student population, chemistry can be communicated to a wider breadth of students. By reaching and engaging a wider range of students, the field can begin to develop and flourish.

Goals of Intervention

The flipped classroom has been implemented and evaluated extensively since its initial conception. The goals of this particular intervention are more specific than evaluating the effectiveness of the classroom format itself. In one respect, the study was intended to illustrate how the flipped classroom would work in the context of general chemistry at a technical college. While the specificity of this context might not be generalizable, the results will be helpful for the instructor of the course as well as other instructors in a similar context. The main goal of the intervention is to improve learning in the classroom in which it was carried out. In addition, I hoped to gain some insight about the cognitive skills obtained from each portion of the flipped classroom. This insight would be used to design both offloaded lecture content and in-class activities in order to optimize higher level cognitive development in future classes.

In addition to assessing and improving the learning process, I wanted to assess student response to the intervention. One reason for this was simply to gauge whether students enjoyed the intervention, gaining general attitudinal response. In addition, I was also interested to find the sense that students had of their cognitive development and compare this to what my assessments indicated. Since self-efficacy is arguably as strong a predictor about student success as academic performance, students' assessments of how they developed is an integral aspect of the intervention.

Summary of Experience

Upon entering the internship, my intention was to finish with a clear idea of how cognitive skills developed over the course of the flipped classroom. I hypothesized that students would improve their higher level cognitive skills after engaging in the in-class problem solving session and that the assessment scores would reflect this quantitatively. However, in an attempt to be flexible and implement the intervention so that the students could receive the greatest benefit, the assessments were all completed on the students' own time. As a result, students performed quite well on both assessments, and quantitative comparisons were inconclusive. As a result, I relied heavily on qualitative analysis of student approach to problems. Further description and analysis will be discussed within.

While my internship might not have addressed the research goals initially imagined, my experience exceeded expectations in terms of my development as an educator. Part of this development arises from the fact that the research aspect did not reveal the expected results. One of my personal goals for this internship was to learn how to develop, implement, and assess a classroom intervention in the context of a small, undergraduate chemistry classroom. Through this lens, I learned a tremendous amount by simple trial and error. One of the most important things that I learned is how context-specific an intervention is and how the purpose of the intervention should drive the type of data that is collected through assessment.

In addition to my personal development as a reflective practitioner, I had an incredibly positive experience just witnessing a student-centered classroom. During the two days of my implementation at Madison College I was able to observe the atmosphere of a flipped chemistry course. It was so refreshing to watch students come together and learn concepts from each other.

I watched diverse groups of students at different ages and from different backgrounds discuss principles from the videos I had made. I watched them work through the questions I had designed and encounter the snags that were intended to make them think. Seeing students instruct each other was even more exciting than I could have anticipated. Also, being available to help when students needed it felt quite comforting. In my previous teaching experience, I have only been able to address student questions long after they have initially encountered them, either by e-mail or at class meetings a day or more later. Being able to face the student confusion as it was happening made me feel even more connected to their learning. There was no sense of losing control over the material; my response was completely the opposite.

Assessment

The goal of the assessments involved in this intervention was to determine the proficiency of students' cognitive skills at different junctures of the flipped classroom. In order to achieve this, assessments related to the material taught on each day were developed with one question at each of five levels of Bloom's taxonomy,[19] increasing from lower order cognitive skills to higher order (knowledge, comprehension, application, analysis, and synthesis, see Supporting Information). The assessment on day one of the intervention was administered after

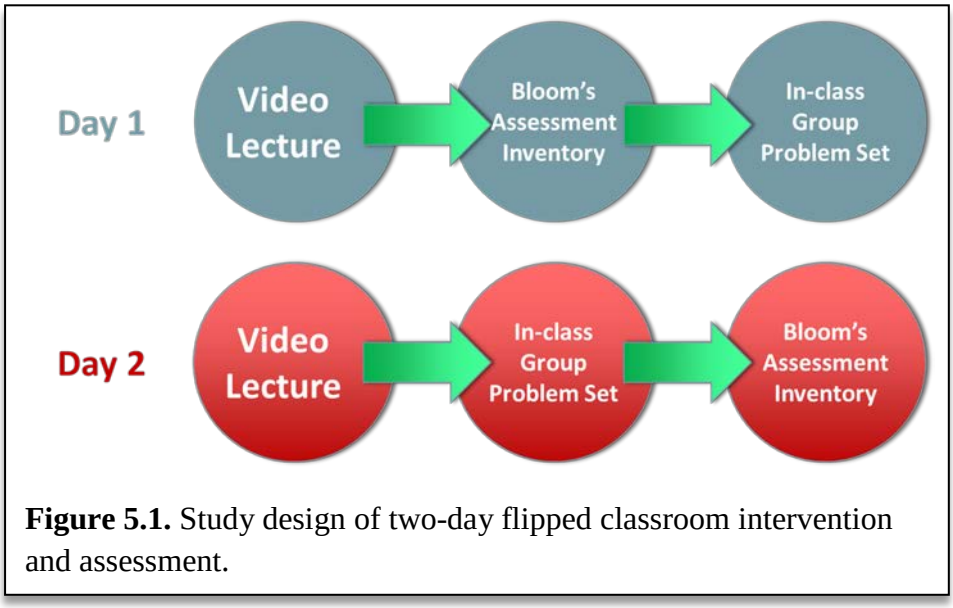

Figure 5.1. Study design of two-day flipped classroom intervention and assessment.

the video lecture but before the in-class group problem set. On the second day, the assessment was given after the in-class group work (Figure 5.1). The material on these days was on the same general topic but was not the same material. As such, the assessments were not intended to be directly compared. Rather, they were intended to be an inventory of what cognitive skills were at play during each component of the flipped classroom, respectively.

The rubrics for grading the assessments were emergent from student response, and within each Bloom's category, four levels of efficacy were established as achievable. It was initially

imagined that the four levels could be used as a crude quantitative tool to evaluate student performance at each Bloom's level. This rubric had scores from 1-4, where 4 is a completely correct answer, correctly solved through a reasonable process and 1 was a completely incorrect or incomplete answer, with no reasoning on the path to the correct answer provided. As it turned out, student response did not differ much with respect to the "correctness" of answers. Rather, the variance seemed to emerge between student approaches to problems. The rubric, as a result, was less useful as a tool for quantitative analysis than it was as a guide toward qualitative analysis.

Results

Generally, when assessing the success of flipped classrooms, two criteria are considered: learning gains and student satisfaction.[15] The aforementioned assessments were a measure of the learning gains. In addition, upon completion of the intervention, I administered a survey to the students designed on the Student Assessment of Learning Gains (SALG) website. The results of both will be described.

Learning Gains

My initial vision for the assessment results was based on a rubric emergent from student response described in the above section. In an attempt to be flexible and implement the intervention so that the students could receive the greatest benefit, the assessments were all completed on the students' own time. While one was still collected after the initial video-watching and the other after the in-class group activity, students were given a few days to complete the assessments and turn them in later.[20] What resulted was the most common score on all questions for both assessments being a 4. There was some movement within the middle-range scores between post-video and post-activity, but the change overall was fairly minimal. The assessments were never intended to be directly compared, as they addressed different material, but even as an inventory for what cognitive skills the students mastered, the quantitative analysis yielded little information (Figure 5.2, more detailed breakdowns can be found in Supporting Information).

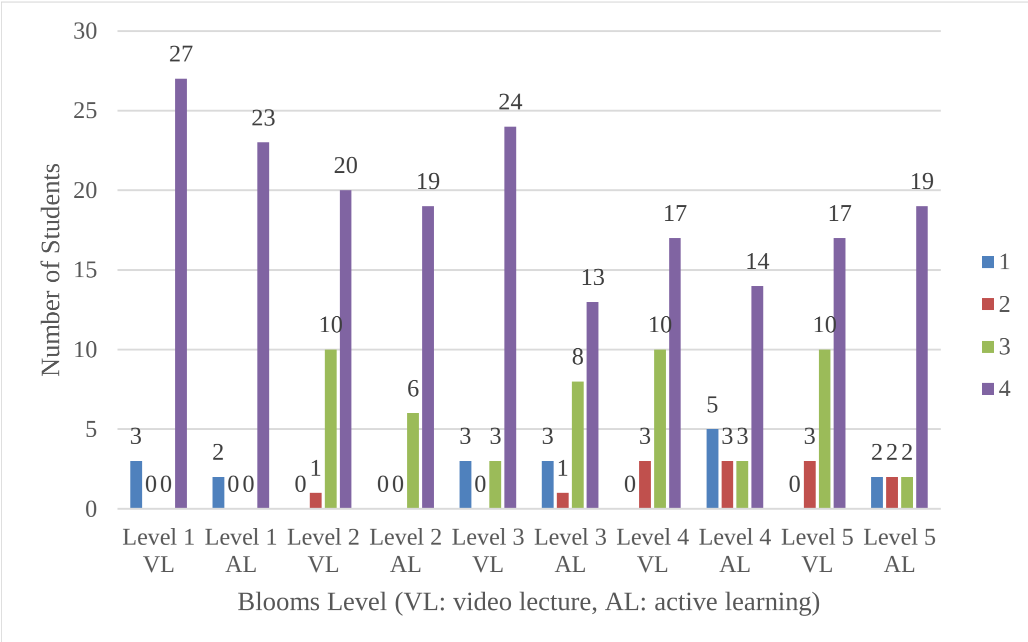

Figure 5.2. Quantitative analysis of assessments. Level 1-5 refers to Bloom's taxonomy level (retention-synthesis, respectively). VL refers to the assessment after the video lecture. AL refers to the assessment after the active learning segment.

As I was analyzing the assessments, I felt as if there was a dimension of analysis that wasn't being addressed by the emergent rubric. Since the rubric didn't yield coherent results, I returned to the notes I had taken on the assessments. It seemed from the notes I had made that while students were performing well and getting correct answers on the assessments, there were developments in student approach to problems that were occurring. Additionally, the *types* of errors that were being made went unaddressed. I was interested in taking a deeper look at this metric of analysis. Since the students who are usually most impacted by the flipped classroom are those who are lower-performing students to begin with,[20] it is worthwhile to qualitatively assess the types of errors that are being made at each Bloom's level and track any changes that may have occurred between the first and second assessments.

It became clear that the types of errors made fell into four distinct categories: conceptual, terminology/notation, calculation, and following directions (Figure 5.3). An additional category was made for problems which the students did not attempt or essentially did not attempt. Conceptual errors embodied the largest number of total mistakes and generally referred to the student missing a problem because there was some misconception about the underlying concept of the question. Interestingly, at lower levels of Bloom's taxonomy, the number of conceptual errors decreased across the course of the intervention, but at higher levels of Bloom's taxonomy they increased. Keeping in mind that the assessments were on different material, it is possible that the synthesis- and analysis- level questions on the second assessment were conceptually harder. The category of terminology/notation refers to mistakes that were made as a result of misunderstanding standard chemistry terms or standard chemical representations. These errors remained about the same on both assessments. Calculation errors decreased fairly markedly on the second assessment, especially at the higher Bloom's levels. Student engagement with peers during problem-solving may be at play for students who misunderstand simple calculation procedures. Even within my time circulating during the in-class problem-solving session, I was able to observe students clearing up other students' misconceptions about how to approach basic calculations regarding stoichiometry and log functions. There were no direction-following errors on the second assessment. Again, this can be attributed to students having experience answering similar problems on the in-class activity and figuring out what the directions mean from their peers. One metric that was very promising was the number of "no attempts" which decreased markedly from the first to the second assessment. It would be encouraging to believe that this reflects an increase in student self-efficacy after performing in-class problem solving, but further study would need to be done to determine this.

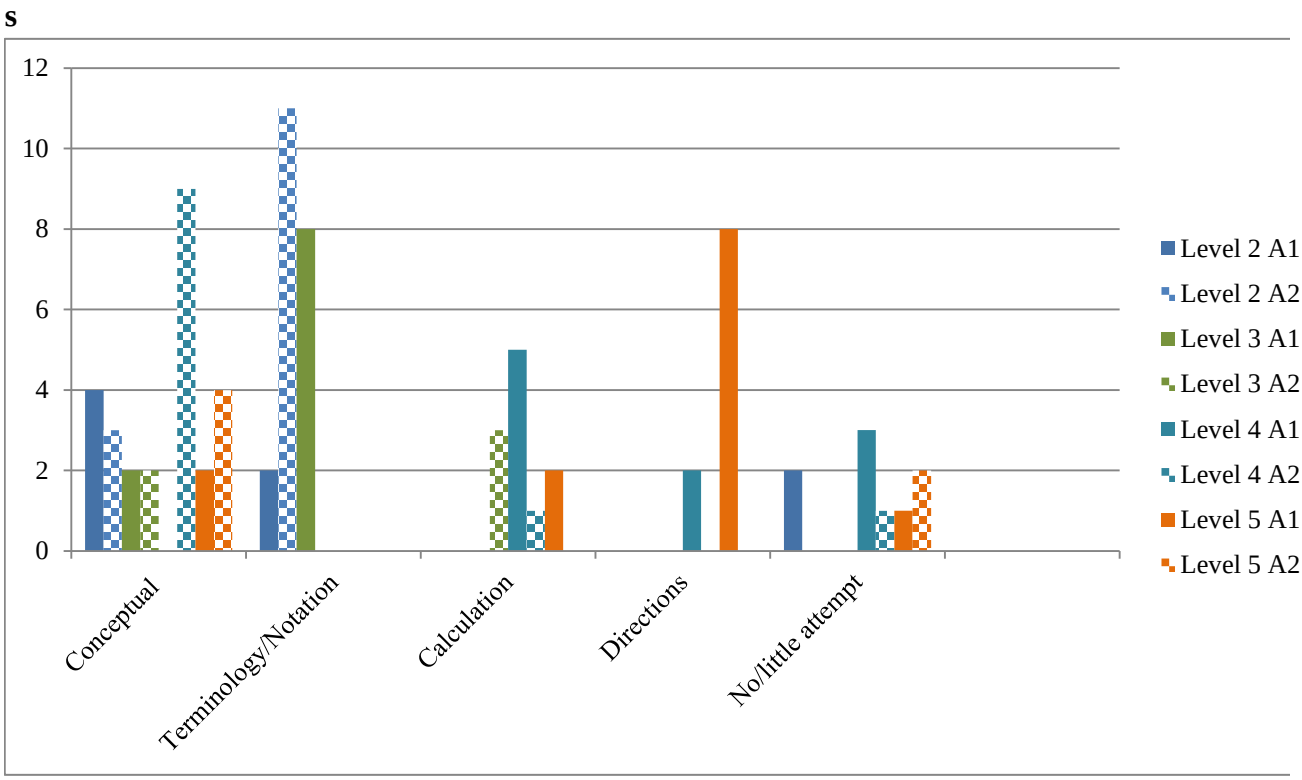

Figure 5.3. Qualitative analysis of assessments. Using a more qualitative approach to analyzing the Bloom's assessment inventories, the number of errors in various categories was totaled. Solid bars represent the number of errors on assessment from day 1 (after video) and the hatched bars represent the number of errors on the assessment from day 2 (after in-class activity).

Student Attitudes

The student response to the intervention was admittedly quite mixed. From a class of thirty students, there was not a clear positive or negative response overall. From the multiple choice section of the survey, most of the results skewed toward the middle or were even across the board (See Supporting Information). However, there were a few trends in the comments students provided that gave some insight about their initial feelings on the flipped lecture framework. The attitudes were divided into three categories: screencasts, in-class group problem solving, and the model as a whole.

Screencasts:

Since students are accustomed to receiving information through lecture, their response to the effectiveness of the video lecture screencast was important. In general, students seemed to appreciate many aspects of the video format. For example, many responses indicated that the ability to stop the video to take notes, review the parts they didn't understand, and generally work through the lecture at their own pace was the best aspect. Students also seemed to appreciate seeing visual representations and examples through the video. The most consistent criticism of the videos was that it was difficult to retain information. I believe if students were more explicitly encouraged to take notes as they would in class, this issue may resolve in large part. Some students suggested that they'd prefer a longer video with more real life examples. The videos were both just under 15 minutes, which is generally a good cutoff. Students often struggle to continue paying attention after this amount of time. This is relevant to other student suggestions such as "more worked out examples" and "too cramped". Going forward, it will be

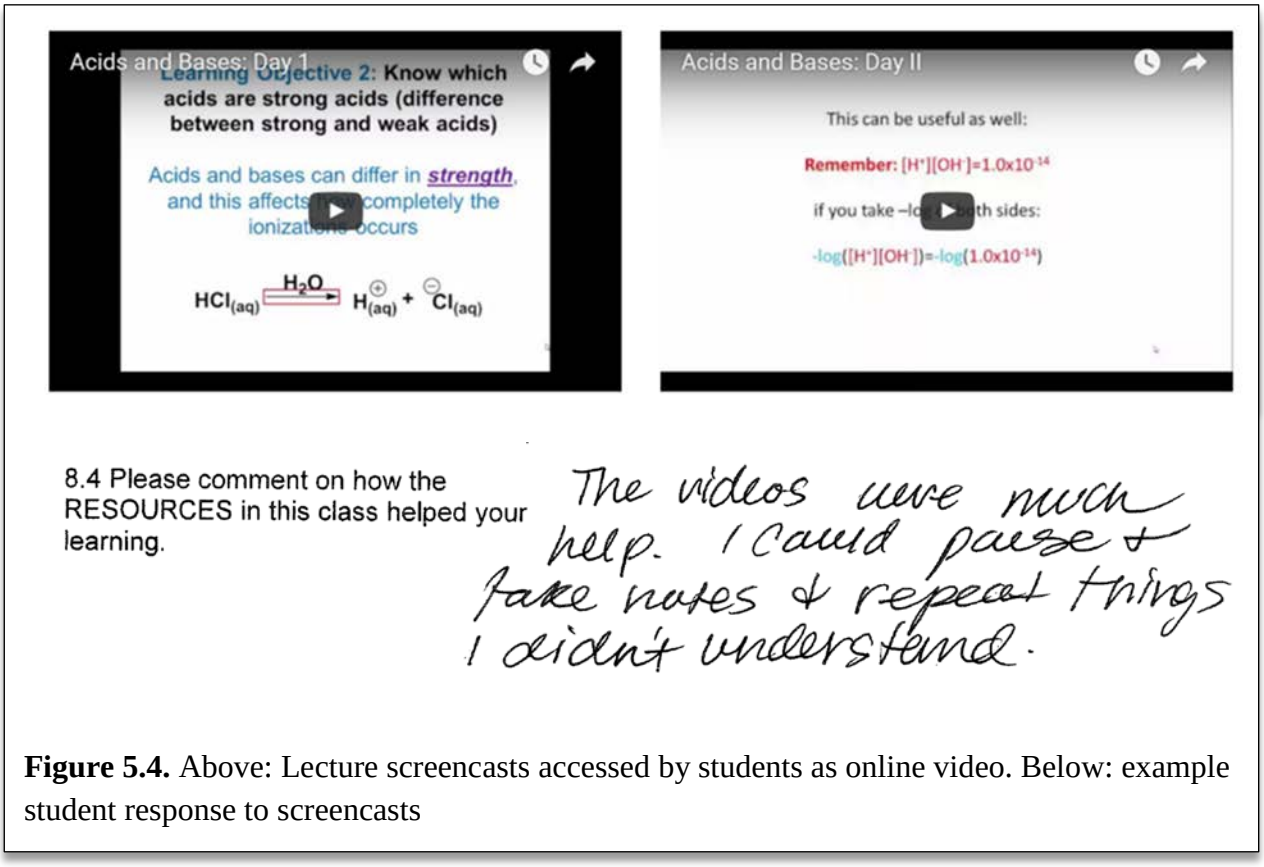

Figure 5.4. Above: Lecture screencasts accessed by students as online video. Below: example student response to screencasts

of interest to find the right balance between making content less concentrated and keeping the length of the videos manageable.

In-class Groupwork:

As is usually the case, students were also quite divided on their affinity for group work. The responses ranged from overwhelmingly positive to overwhelmingly negative. The most consistent positive comment was related to the instructor's presence during class. Students felt that having the instructor present while they worked through the snags of problem-solving was vital to their learning progress. Many students asserted this even if they also claimed to dislike group work in general. Other students voiced that learning from peers allowed them to get a new

perspective on the material or the approach they were taking to problems and that bouncing ideas off of other students helped to develop understanding. One very promising comment referred to a support network that was developed during the exercise that continued to meet outside of class to study. Developments like this indicate that the flipped model aided in the formation of a learning community, one of the major goals. For the most part, the criticisms tended to relate to discouraging situations when the group as a whole was lost. Students expressed that when the different members of the group had different levels of understanding, it was often difficult to reach a level field on which to solve the problems. I believe these issues can be addressed by instructing students about how to form and operate in a constructive group.

Finally, students were asked to reflect on the flipped classroom as a whole, compared to their experiences in a traditional classroom. Some students felt as if they missed information or that they required more practice than the model provided. Similarly, it also seemed that the transition from the video lecture to solving complex problems seemed difficult. Others felt that the noise in the room distracted from mental processes and made it difficult to get the instructor's attention. It seemed that in particular, students who were naturally quite motivated did not find

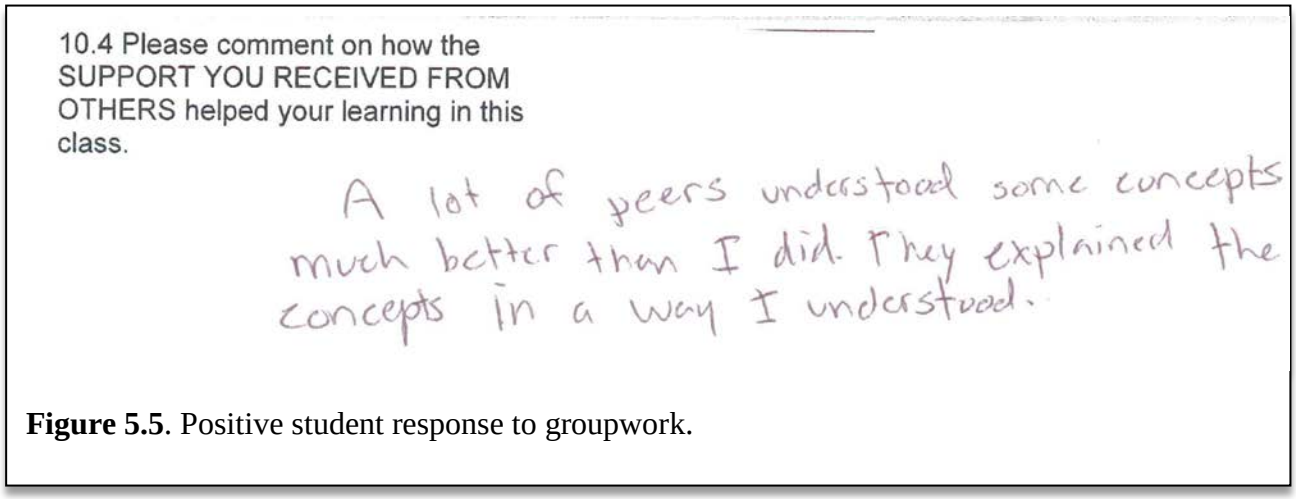

Figure 5.5. Positive student response to groupwork.

the flipped classroom particularly appealing. This makes sense, as they presumably excel within the current system, and previous implementations have shown that high-performing students don't receive much added benefit from the flipped classroom.[20] The positive responses often centered on the flipped lecture being a "good, refreshing change of pace" or "a lively and excited atmosphere", indicating that students might prefer a hybrid classroom with a bit of traditional lecture and a bit of flipped lecture. Students voiced that they felt more comfortable asking others for help after engaging with fellow students during class. Additionally, the appreciation of having the instructor present for problem-solving surfaced again, further emphasizing how impactful this aspect was for the students.

Discussion

The intention of this study was to explore the effect of the flipped classroom on the cognitive development of students in a technical college context. Specifically, I hoped to inventory the cognitive skills imparted by specific components of the flipped classroom model. As a student of a hard science STEM field, I began this internship with little appreciation for the value of qualitative data. It became clear through the course of my analysis of this intervention, however, just how valuable qualitative data would be in addressing my objective. In particular, if the purpose of the intervention is simply to evaluate the success of a new teaching technique, qualitative analysis can often be much more informative than trying to quantify feedback. Given the size of the class, I feel that I got much richer results by paying careful attention to how students were answering questions and actual comments provided by students in surveys.

The assessments indicate that most student learning gains were made in the students' approach to problem solving. Students' ability to do calculations and follow directions improved dramatically between the first and second assessment. It was somewhat discouraging that there was no marked improvement in the conceptual performance across the two, but it is possible that this is because the material was inherently more difficult on the second day. Nevertheless, it might be a sign that the in-class activities should focus more on deeply conceptual questions rather than all problem-solving. The synthesis-level questions on both assessments were in the format of designing an experiment, which was conceptually challenging, but also fairly systematic in terms of how the solution could be set up. One way to get at conceptual development would be to integrate more free writing response questions into the in-class activity. This process would get students thinking about concepts and require them to face and work through misconceptions in the presence of their peers and instructor and would hopefully

stimulate the conceptual progress of the students' learning to match their increased ability to solve practical problems. Another promising result from this intervention was the decrease of students who did not attempt problems at all. This phenomenon may be an indication of an increase in student confidence in their ability to answer questions correctly, or self-efficacy. I would like to explore this metric in future implementations of this type of framework. While there was not an obvious pattern of cognitive skills that prevailed after each component of the flipped classroom in terms of Blooms' taxonomy, the in-class component proved to provide a toolbox for problem solving. Additionally, students' confidence in their ability to solve problems appears to have increased after solving problems with peers. Upon supplementing the in-class activities with more work that explicitly exercises conceptual engagement, this feature of the flipped classroom will prove to be an asset to student development.

As far as student feedback, the most discouraging result was the number of students who voiced that overall they preferred a traditional classroom to the flipped model. Regardless of other positive feedback, if students feel dissatisfied with how the classroom is run, it will be difficult to get the greatest benefit out of their learning. It is possible, however, that students may have had a negative response because they only had one flipped unit and didn't have a chance to settle into the framework. In studies that measured student attitudes about the flipped classroom, students who shared positive opinions very often also asserted that the model took a good deal of time to get used to.[15] As a result, it is reasonable to predict that some of the negative responses to this study might have changed if the students were allowed time to become more comfortable with the model. Additionally, it was clear from some comments that many of the students who were dissatisfied with the model were also high-performing students to begin with. They would often preface complaints with statements such as, "I already study hard and do well in school…"

This is not surprising and is particularly interesting in light of the result that many studies find that students getting As and Bs in their chemistry courses rarely see much improvement with the flipped classroom model. Most of the improvement in learning gains is seen within the C, D and F students.[15,20]

Another student concern was the inability to retain and recall the information from the video lectures for use in problem solving. One approach that has proven effective at addressing information retention, established by Fautch,[17] was to give quick review mini-lectures at the beginning of class to refresh before diving into problem-solving. While this does spend some class time "delivering" information, it would serve to refresh students' memories as well as ease them into the flipped format by giving them a little bit of more comfortable lecture. In addition, recommending that students take notes on the videos the same way they would a normal lecture can help mentally solidify material. Another way to ensure student engagement with the video is to change the way the assessments are administered. The first assessment was given to the students prior to their watching the video. Some student comments indicated that having an assessment during the video helped with following along and making sure they understood the material (in addition to incentivizing the watching of the screencast). This method of assessment has seen success in other implementations of the flipped classroom as well.[15]

One concern that did not come up in this implementation, but was raised by my faculty partner, is the potential for exclusivity in the flipped classroom format. The necessity of the students to access the videos out of class with a computer connected to the internet assumes a lot about the time and resources they have available. Computer access at campuses is fairly universal now, but it is important to make sure students have the time to access it. Particularly at a technical college, students are often spread very thin in terms of available time. Many students

work at least one other job, have families, or are involved in other time-consuming activities in addition to going to school. With that in mind, it is important to be sensitive to student feedback when implementing a classroom framework that necessitates time outside of class to access content. The best way to ensure that students are not feeling excluded is to survey the class long before the end of the semester. If a survey was administered after a few implementations of flipping, the instructor could clearly ascertain whether all the students felt comfortable with the model and accommodate those who needed it.

Conclusions

In the current state of educational awareness, it is becoming difficult to justify the universality of the "sage on the stage" lecture. Even in courses where this has been the preferred classroom framework for years, it is time to re-evaluate how we are engaging students and impacting their learning. The flipped lecture format is one window into the potential of improved active classrooms where students engage in constructive learning. The field of chemistry is finally starting to gain momentum in its willingness to change the way its classes are run, and students will benefit from these changes. It is my hope that by making a classroom where students' voices can be heard, the field of chemistry will be diversified from its current state, and a rich new perspective will result. My small implementation of a flipped lecture is a simple example of ways in which I will experiment and figure out what practices work best in my classroom in the future. By learning how to write questions to assess different levels of cognitive skills, I will be able to evaluate any number of classroom models and their impact on student cognitive development. As an educator, I want to be constantly experimenting and evaluating to make sure that students are getting the highest benefit from the class time available.

I also hope that in my future as an instructor of organic chemistry, I am able to draw on the educational literature for inspiration about how to integrate active learning strategies and flipped classroom into my course. While exploring the research on this method in general chemistry, I encountered several examples that are specific to organic[16,17] that I am excited to try. Since it seems that the effectiveness of classroom approaches such as these are very context-specific, it will be an asset to be familiar with approaches that are specific to teaching organic chemistry. From this intervention, it is clear that becoming a reflective and experimental practitioner in the classroom requires a great deal of work. However, the resulting classroom is one that I can feel ownership of, rather than an artifact that has been passed down from chemistry educators of the past. I look forward to using this experience as a springboard to develop my own dynamic, active classroom.

Notes and References:

1. King, A. From Sage on the Stage to Guide on the Side. *College Teaching* **1993**, *41*, 30-35.

2. Mayer, R. E. In *Cambridge Handbook of Multimedia Learning*; Mayer, R. E., Ed.; Cambridge Univesity Press: Cambridge, 2005.

3. Bergmann, J.; Sams, A. *Flip Your Classroom: Reach Every Student in Every Class Every Day*; International Society for Technology in Education: Washington, DC, 2012.

4. Baker, J. W. Selected Conference Papers. In *Conference Selected Conference Papers*. **2000**.

5. Lage, M. J.; Platt, G. J.; Treglia, M. Inverting the Classroom: A Gateway to Creating an Inclusive Learning Environment. *J. Econ. Educ.* **2000**, *31*, 30-43.

6. Lage, M. J.; Platt, G. The Internet and the Inverted Classroom. *J. Econ. Educ.* **2000**, *31*, 11-11.

7. Haak, D. C.; HilleRisLambers, J.; Pitre, E.; Freeman, S. Increased Structure and Active Learning Reduce the Achievement Gap in Introductory Biology. *Science* **2011**, *332*, 1213-1216.

8. Deslauriers, L.; Schelew, E.; Wieman, C. Improved Learning in a Large-Enrollment Physics Class. *Science* **2011**, *332*, 862-864.

9. Freeman, S.; Eddy, S. L.; McDonough, M.; Smith, M. K.; Okoroafor, N.; Jordt, H.; Wenderoth, M. P. Active learning increases student performance in science, engineering, and mathematics. *Proc. Natl. Acad. Sci. U.S.A.* **2014**, *111*, 8410-8415.

10. Michael, J. Where's the evidence that active learning works? *Adv. Physiol. Educ.* **2006**, *30*, 159-167.

11. Schultz, D.; Duffield, S.; Rasmussen, S. C.; Wageman, J. Effects of the Flipped Classroom Model on Student Performance for Advanced Placement High School Chemistry Students. *J. Chem. Educ.* **2014**, *91*, 1334-1339.

12. Goodwin, B.; Miller, K. Evidence on Flipped Classrooms Is Still Coming In. *Educ. Leadership* **2013**, *70*, 78-80.

13. Abeysekera, L.; Dawson, P. Motivation and cognitive load in the flipped classroom: definition, rationale and a call for research. *High Educ. Res. Dev.* **2015**, *34*, 1-14.

14. 2014 Spring ConfChem: Flipped Classroom. In *Conference 2014 Spring ConfChem: Flipped Classroom*. **2015**.

15. Seery, M. K. Flipped learning in higher education chemistry: emerging trends and potential directions. *Chem. Educ. Res. Pract.* **2015**, *16*, 758-768.

16. Flynn, A. B. Structure and evaluation of flipped chemistry courses: organic & spectroscopy, large and small, first to third year, English and French. *Chem. Educ. Res. Pract.* **2015**, *16*, 198-211.

17. Fautch, J. M. The flipped classroom for teaching organic chemistry in small classes: is it effective? *Chem. Educ. Res. Pract.* **2015**, *16*, 179-186.

18. Christiansen, M. A. Inverted Teaching: Applying a New Pedagogy to a University Organic Chemistry Class. *J. Chem. Educ.* **2014**, *91*, 1845-1850.

19. Bloom, B. S. E., M.D.; Furst, E.J.; Hill, W.H.; Krathwohl, D.R. *Taxonomy of educational objectives: The classification of educational goals*; David McKay Company: New York, 1956.

20. Ryan, M. D.; Reid, S. A. Impact of the Flipped Classroom on Student Performance and Retention: A Parallel Controlled Study in General Chemistry. *J. Chem. Educ.* **2016**, *93*, 13-23.

Supporting information for Chapter 5: Assessment of Cognitive Skills in the Flipped Chemistry Classroom

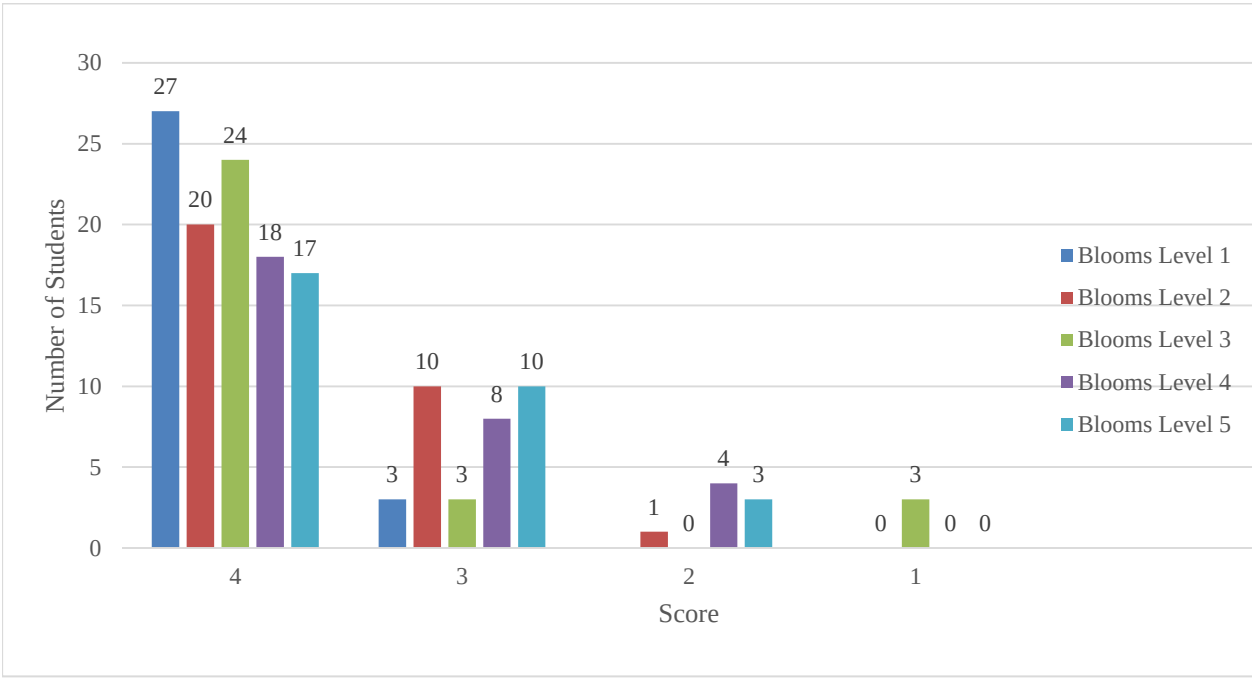

Figure S5.1. Assessment 1: number of students who received each score (4= highest score, 1=lowest score) broken down by Bloom's level.

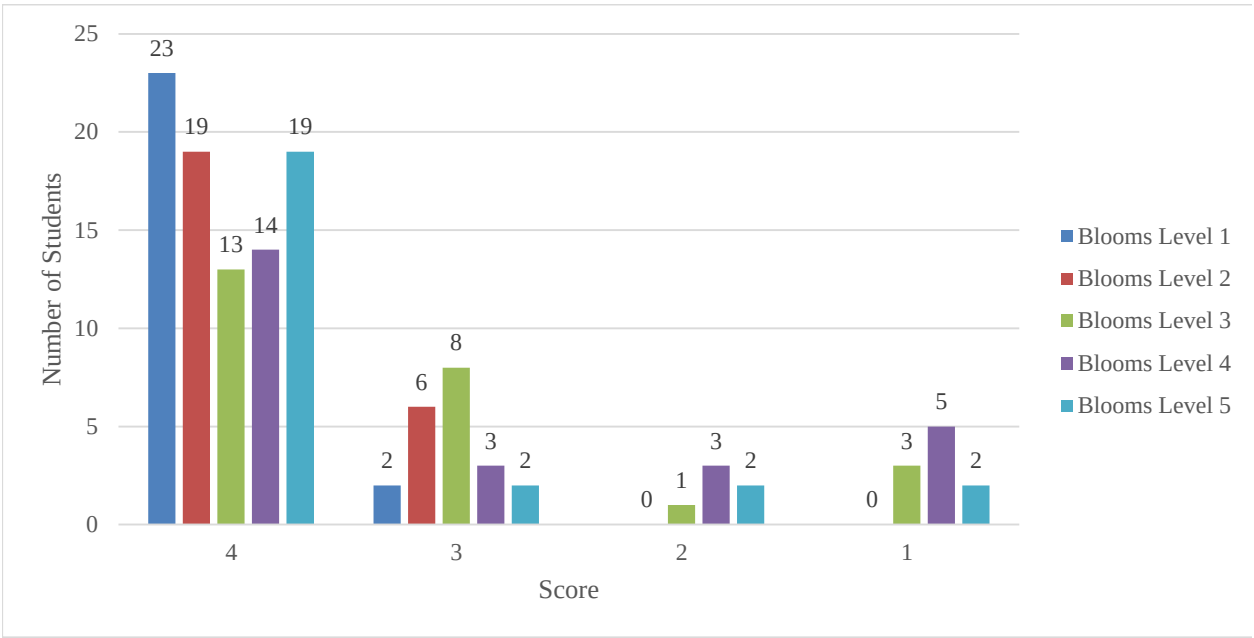

Figure S5.2. Assessment 2: number of students who received each score (4= highest score, 1=lowest score) broken down by Bloom's level.

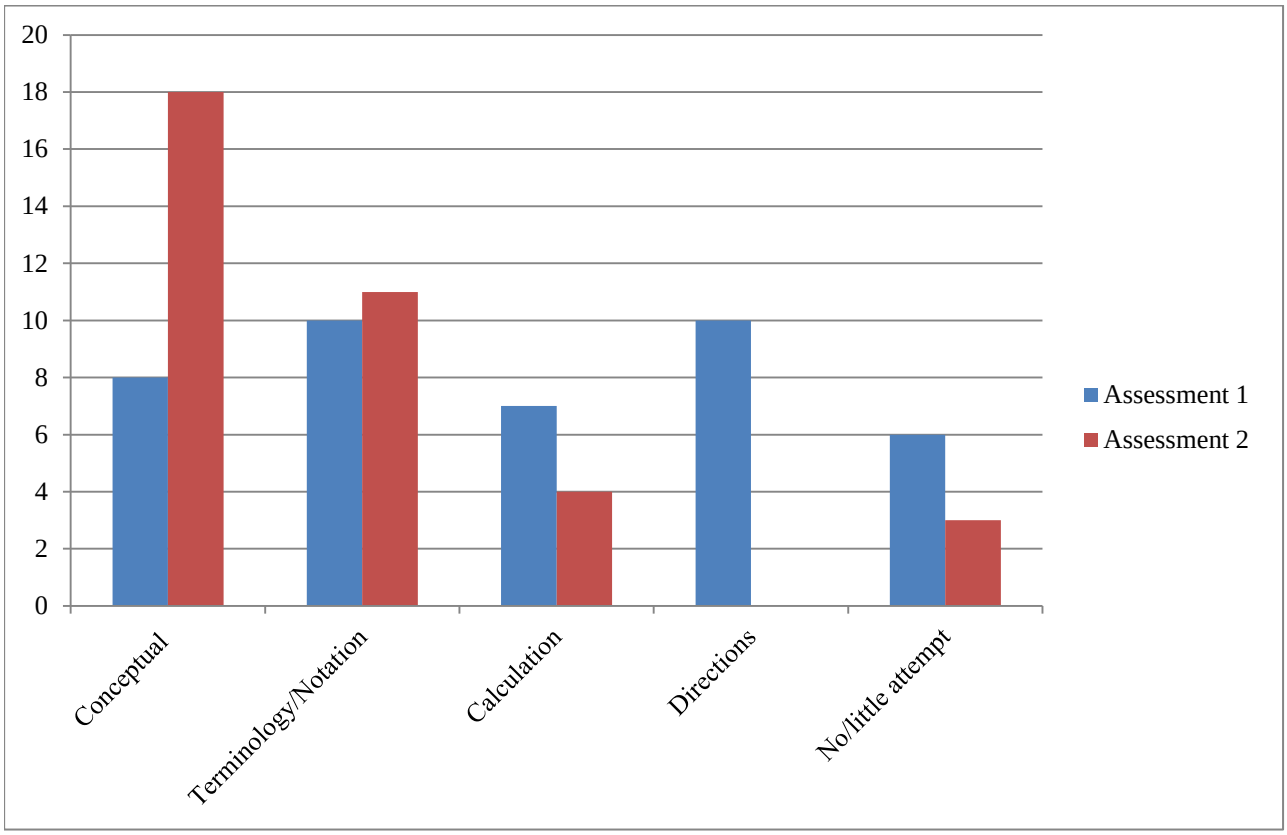

Figure S5.3. Qualitative analysis of assessments. Using a more qualitative approach to analyzing the Bloom's assessment inventories, the number of errors in various categories was totaled. Blue bars represent number of occurrences on assessment 1 (after video lecture). Red bars represent number of occurrences on assessment 2 (after in-class activity).

Survey Results:

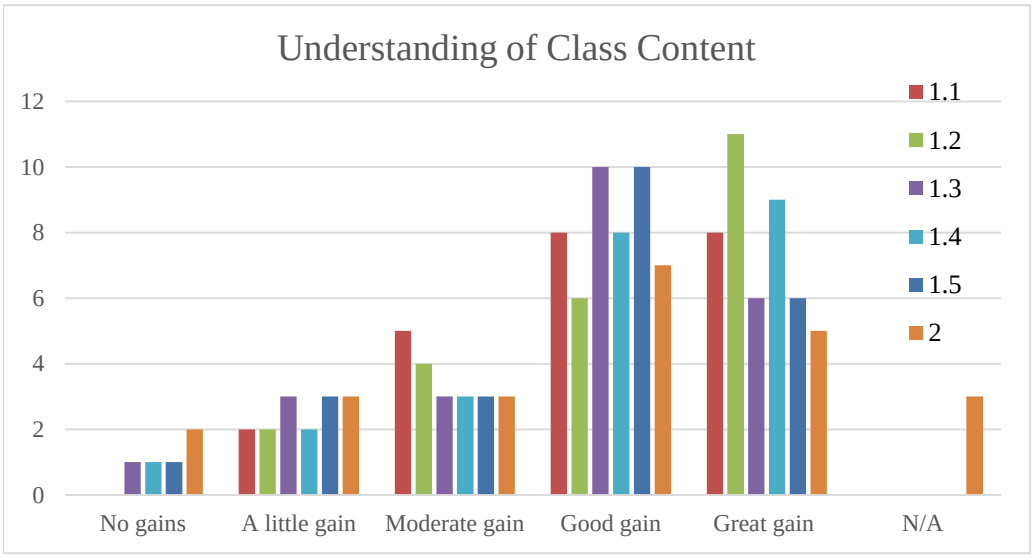

Figure S5.4. Survey results for questions related to students' understanding of class content. Each bar corresponds to a different question (copy of survey questions can be found on page 204).

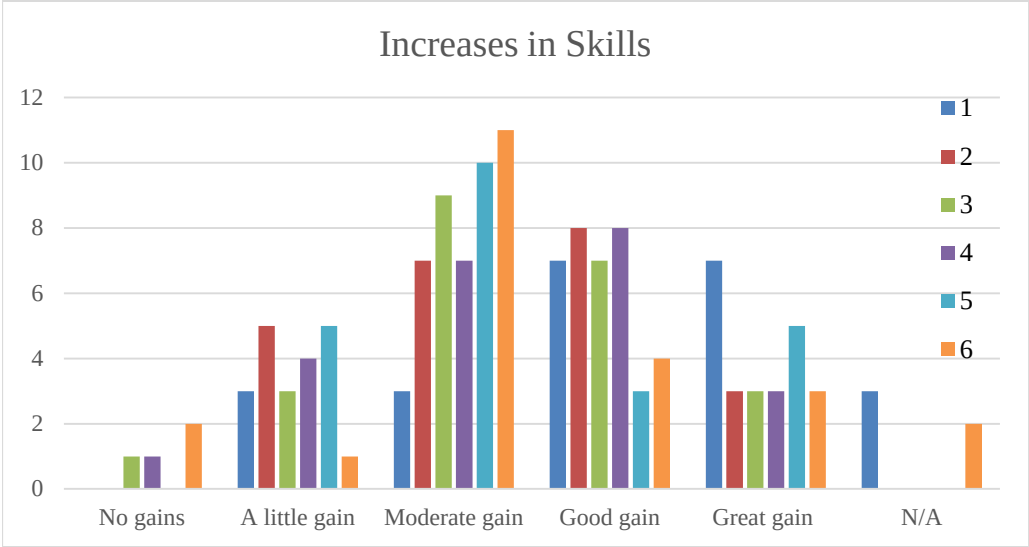

Figure S5.5. Survey results for questions related to students' sense of their skill development. Each bar corresponds to a different question (copy of survey questions can be found on page 204.

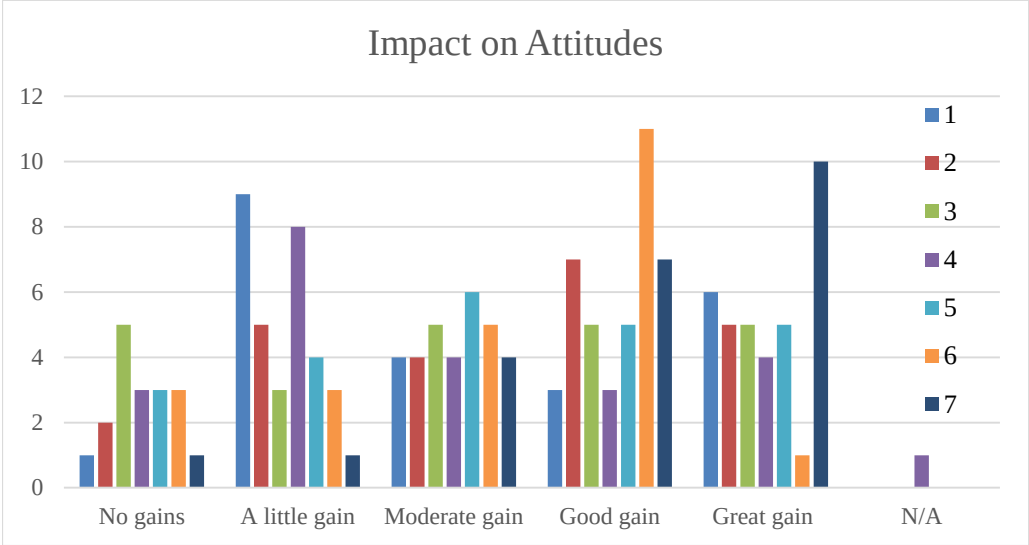

Figure S5.6. Survey results for questions related to students' sense of their positive attitude development toward the course and the topic. Each bar corresponds to a different question (copy of survey questions can be found on page 204.

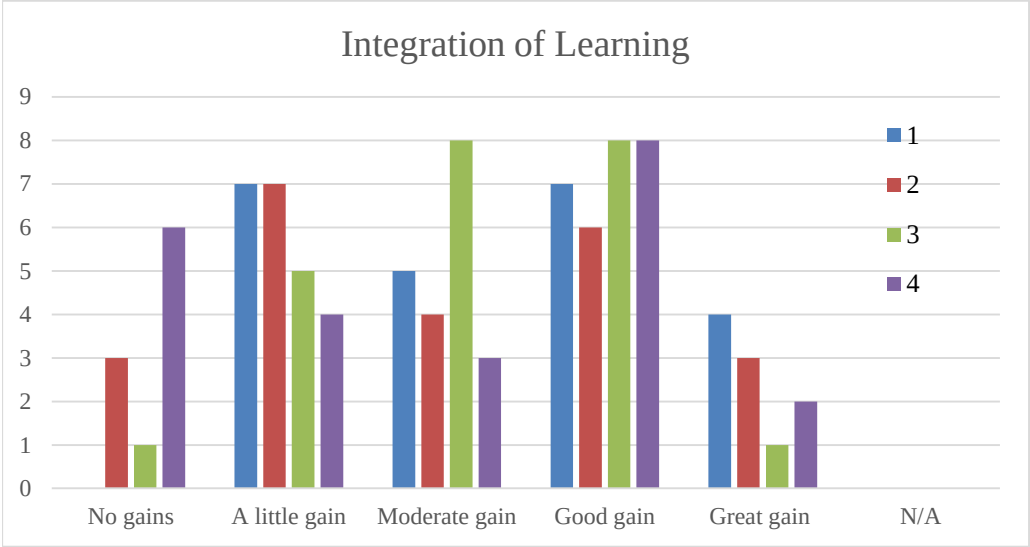

Figure S5.7. Survey results for questions related to students' sense of the integration of their learning. Each bar corresponds to a different question (copy of survey questions can be found on page 204.

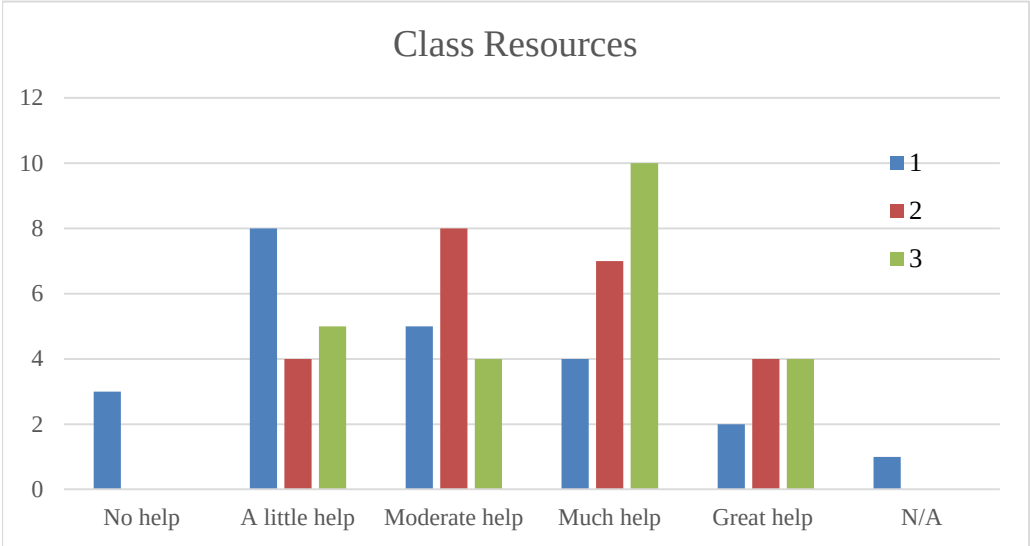

Figure S5.8. Survey results for questions related to students' value of various class resources. Each bar corresponds to a different question (copy of survey questions can be found on page 204.

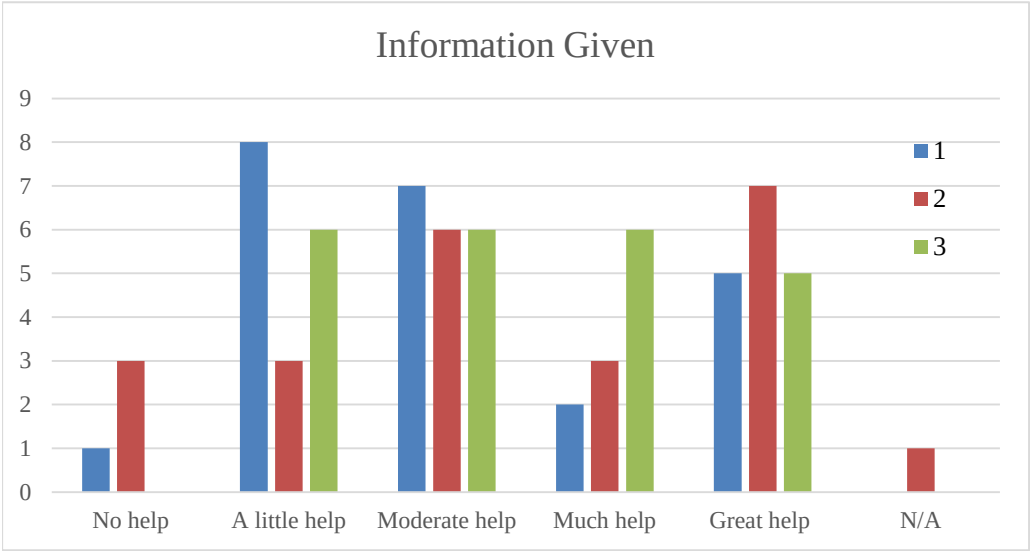

Figure S5.9. Survey results for questions related to students' value of various information given. Each bar corresponds to a different question (copy of survey questions can be found on page 204.

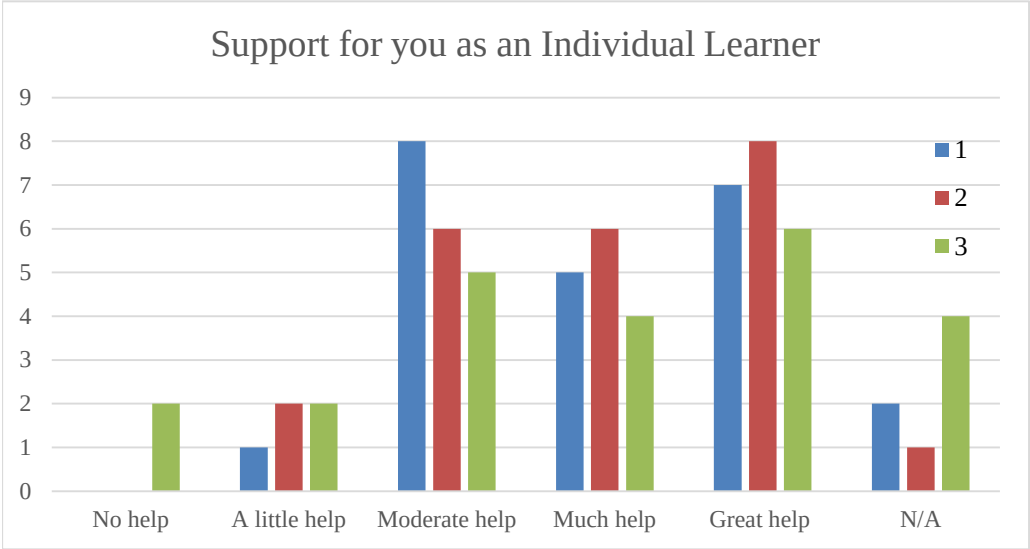

Figure S5.10. Survey results for questions related to students' sense of support for them as individual learners. Each bar corresponds to a different question (copy of survey questions can be found on page 204.

In-class activities.

Acids and Bases: Part 1, In-Class Activity **Name:**

Level 1: Knowledge *Recall or recognize information, ideas and principles*

1. An acid is an Arrhenius acid if it
   _____.
   An acid is a Brønsted acid if it
   _____.

   A base is an Arrhenius base if it
   _____.
   A base is a Brønsted base if it
   _____.

2. A weak acid: a.) donates H^+ completely
   b.) is in equilibrium with its conjugate base
   c.) None of these

3. An acid that has multiple acidic protons (H^+) is called _____.

4. What are the products when you mix a strong acid and a strong base?

Level 2: Comprehension *Translate, comprehend, or interpret information based on prior learning*

5. Describe the difference between **(a)** a monoprotic and a diprotic acid **(b)** a weak acid and a strong acid **(c)** an acid and a base.

6. Ammonia (NH_3) is a weak base. Write the equation for its reaction with water. Label the acid, base, conjugate acid, and conjugate base.

7. Write the balanced equation for the following neutralization reactions:
   (a) Aqueous acetic acid (CH_3COOH) is neutralized by aqueous potassium hydroxide (KOH)

   (b) Solid chromium(III) hydroxide ($Cr(OH)_3$) reacts with nitric acid (HNO_3).

(c) Aqueous hypochlorus acid (HClO) and aqueous calcium hydroxide ($Ca(OH)_2$) react.

8. Complete the table which outlines 6 strong acids:

Name	**Formula**	**Ions in aqueous solution**
	HI	
Hydrobromic acid		
		$H^+_{(aq)} + Cl^-_{(aq)}$
		$H^+_{(aq)} + HSO_4^-{}_{(aq)}$
Nitric acid		
	$HClO_4$	

Level 3: Application *Select, transfer, and use data and principles to complete a problem or task*

9. a. The following picture represents a molecular view of an acid, HA, in water. Is the acid strong or weak? Explain your choice.

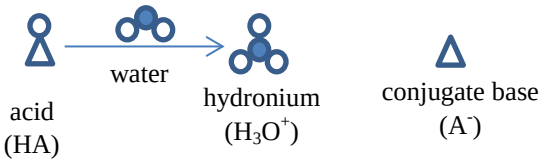

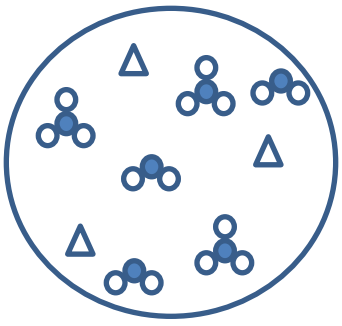

b. What would the molecular view look like if it were the opposite choice from the question above?

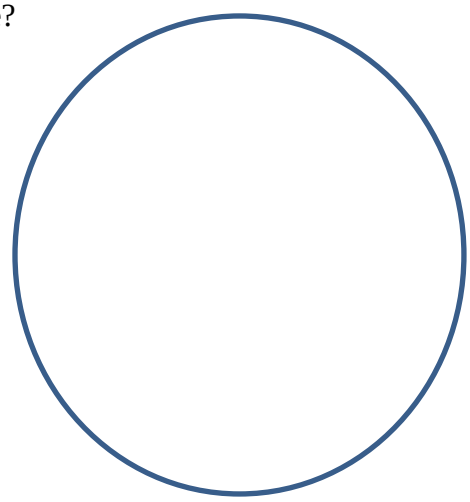

Level 4: Analysis *Distinguish, classify, and relate the assumptions, hypotheses, evidence, or structure of a statement or question*

10. How much 0.8 M HCl (in mL) would be necessary to neutralize the following solutions:
    a. 1.0 g NaOH dissolved in 10 mL water

    b. 20 mL of 3M LiOH

    c. 60 mL of 1.5 M $Sr(OH)_2$

Level 5: Synthesis *Originate, integrate, and combine ideas into a product, plan, or proposal that is new to you*

11. ***A solution that has a high proportion of ions will conduct electricity better than one with fewer ions.***
    You are given a light bulb that can be connected via appropriate circuit (that you don't need to worry about) through a solution. The solution is either hydrobromic acid or hydrofluoric acid. Explain how you would identify the acid.

Acids and Bases: Part 2, In-Class Activity **Name:**

Level 1: Knowledge *Recall or recognize information, ideas and principles*

1. Fill in the blanks in the following chemical equilibria:

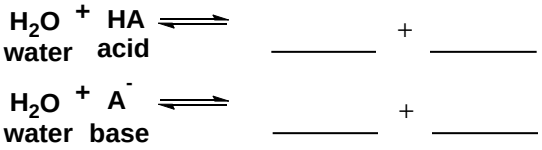

What characteristic of water does this display?

2. Fill in the blanks to complete the following equations:

a. pH = _____$[H^+]$

a. $K_w=[H^+][OH^-]$ = _____

b. pH + pOH = _____

c. In a neutral pure water sample, what is $[H^+]$? $[OH^-]$?

d. If a sample is considered acidic, what is the relationship of $[H^+]$ to $[OH^-]$? What do you know about the pH of the sample?

3. Fill in the chart with the appropriate description:

Solution character	**$[H^+]$**	**pH**
Acidic		
	1.0x10-7	
		>7

Level 2: Comprehension *Translate, comprehend, or interpret information based on prior learning*

4. a. What is meant by the term autoionization?

b. Explain why pure water is a poor conductor of electricity.

5. Label each of the following as a strong acid or weak acid and write the formula of its conjugate base.

a. H_2SO_4

b. HPO_4^{2-}

c. HNO_2

5. a. If the pH of Lake Mendota is 8.3, what is the $[H^+]$?

b. What is the $[OH^-]$?

Level 3: Application *Select, transfer, and use data and principles to complete a problem or task*

6. What is the pH of a 0.034 M HNO_3 solution? (Start by writing out the ionization of HNO_3)

7. What is the pH of a $4.3x10^{-4}$ M NaOH solution?

8. Which solution has a lower pH, 0.5 M H_2SO_4 or 0.5 M H_2CO_3? Explain.

9. If NaOH is added to water, how does the $[H^+]$ change? How does the pH change?

10. The average pH of normal arterial blood is 7.40. Calculate $[H^+]$ and $[OH^-]$.

EXTRA BONUS CHALLENGE: At normal body temperature (37°C), $K_w=2.4x10^{-14}$, solve for $[H^+]$ and $[OH^-]$, at this temperature.

Level 4: Analysis *Distinguish, classify, and relate the assumptions, hypotheses, evidence, or structure of a statement or question*

11. Calculate the pH of the following strong acid solutions:

    a. 1.52 g of HNO_3 in 575 mL of solution

b. a solution formed by mixing 10.0 mL of 0.100 M HBr with 20.0 mL of 0.200 M HCl

Level 5: Synthesis *Originate, integrate, and combine ideas into a product, plan, or proposal that is new to you*

12. You are given a solution of pH = 12.0 and a 5 M solution of HCl. Explain (with equations and words) how you would neutralize the solution.

Assessments and Survey.

Attitudinal Survey:

Your understanding of class content

1. As a result of your work in this class, what GAINS DID YOU MAKE in your UNDERSTANDING of each of the following?						
1.1 The following concepts that have been explored in this class	no gains	a little gain	moderate gain	good gain	great gain	not applicable
1.1.1 Identifying an acid/base reaction	○	○	○	○	○	○
1.1.2 Predicting how strong and weak acids and bases ionize in aqueous solution.	○	○	○	○	○	○
1.1.3 Predicting what happens when acids and bases are mixed.	○	○	○	○	○	○
1.1.4 Understanding the acid/base nature of water.	○	○	○	○	○	○
1.1.5 Using the pH scale to gauge acidity and manipulate problems.	○	○	○	○	○	○
1.2 How ideas from this class relate to ideas encountered in other classes within this subject area	○	○	○	○	○	○
1.3 Please comment on HOW YOUR UNDERSTANDING OF THE SUBJECT HAS CHANGED as a result of this class.						

Increases in your skills

2. As a result of your work in this class, what GAINS DID YOU MAKE in the following SKILLS?	no gains	a little gain	moderate gain	good gain	great gain	not applicable

2.1 Working effectively with others						
2.2 Recalling specific information from lecture or reading						
2.3 Comprehending concepts enough to put them in your own words						
2.4 Applying concepts from the lesson to new problems or situations						
2.5 Analyzing a system in order to break it down into the important features to solve a problem						
2.6 Designing your own experiment to test related concepts						
2.7 Please comment on what SKILLS you have gained as a result of this class.						

Class impact on your attitudes

3. As a result of your work in this class, what GAINS DID YOU MAKE in the following?	no gains	a little gain	moderate gain	good gain	great gain	not applicable

3.1 Enthusiasm for the flipped classroom compared to a traditional classroom						
3.2 Enthusiasm for the subject of chemistry						
3.3 Interest in discussing chemistry with friends or family						
3.4 Interest in taking or planning to take additional classes in chemistry						
3.5 Confidence that you understand the material						
3.6 Your comfort level in working with complex ideas						
3.7 Willingness to seek help from others (teacher, peers, TA) when working on academic problems						
3.8 Please comment on your attitude toward the flipped classroom compared to your traditional classroom experience.						

Integration of your learning

4. As a result of your work in this class, what GAINS DID YOU MAKE in INTEGRATING the following?	no gains	a little gain	moderate gain	good gain	great gain	not applicable
4.1 Connecting key class ideas with other knowledge						
4.2 Applying what I learned in this class in other situations						
4.3 Using systematic reasoning in my approach to problems						
4.4 Using a critical approach to analyzing						

data and arguments in my daily life

4.5 What will you CARRY WITH YOU into other classes or other aspects of your life?	

The Class Overall

5. HOW MUCH did the following aspects of the class HELP YOUR LEARNING?	no help	a little help	moderate help	much help	great help	not applicable
5.1 The instructional approach taken in this class						

Class Activities

6. HOW MUCH did each of the following aspects of the class HELP YOUR LEARNING?	no help	a little help	moderate help	much help	great help	not applicable
6.1 Out of class video lectures						
6.2 In-class group activities.						

Assignments, graded activities and tests

7. HOW MUCH did each of the following aspects of the class HELP YOUR LEARNING?	no help	a little help	moderate help	much help	great help	not applicable
7.1 The assessment on each day						

Class Resources

8. HOW MUCH did each of the following aspects of the class HELP YOUR LEARNING?	no help	a little help	moderate help	much help	great help	not applicable
8.1 The primary textbook						
8.2 Online materials (other than teacher-provided online notes or presentations)						

8.3 Online notes or presentations posted by instructor						
8.4 Please comment on how the RESOURCES in this class helped your learning.						

The information you were given

9. HOW MUCH did each of the following aspects of the class HELP YOUR LEARNING?	no help	a little help	moderate help	much help	great help	not applicable
9.1 Explanation of how the class activities, reading and assignments related to each other						
9.2 Explanation given by instructor of how to learn or study the materials						
9.3 Explanation of why the class focused on the topics presented						
9.4 Please comment on HOW the INFORMATION YOU RECEIVED about the class helped your learning.						

Support for you as an individual learner

10. HOW MUCH did each of the following aspects of the class HELP YOUR LEARNING?	no help	a little help	moderate help	much help	great help	not applicable
10.1 Interacting with the instructor during class						
10.2 Working with peers during class						
10.3 Working with peers outside of class						
10.4 Please comment on how the SUPPORT YOU RECEIVED FROM OTHERS helped your learning in this class.						

Acids and Bases: Part 1 Assessment Rubric

1. Which of the following does not fit the definition of a Brønsted acid

   a. H_3PO_4
   b. H_2O
   c. CO_2
   d. NH_4^+
   e. HCO_3^-

Blooms score: 1

Scoring:
1: wrong
4: right

2. The following diagrams represent aqueous solutions of two monoprotic acids, HX and HY (water molecules not shown but implied).
   a. Identify each acid (HX and HY) as a strong or weak acid. **HY is a strong acid. HX is a weak acid.**
   b. Write one sentence to explain your answer.
   HY is completely ionized. HX is not completely ionized.

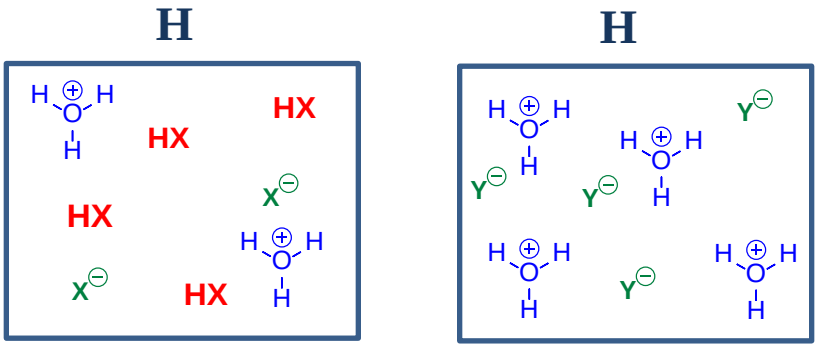

Blooms score: 3

Scoring:
1: Doesn't answer or nothing correct.
Example of incorrect answer: misassign both HX and HY and explain by saying the strong acid has "less charges" and weak has "more charges"
2: One correct identification only.
3: Both correct identification, but incorrect or absent explanation.
Example of explanation with misconception: more H^+ means that it is a strong acid
4: Correct identification and explanation.

3. Label each member of the following weak acid ionization as acid, base, conjugate acid, and conjugate base. Draw lines connecting the conjugate acid/base pairs.

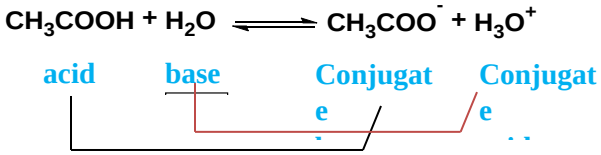

Blooms score: 2

Scoring:
1: No part correct
2: Some correct designations
Example: correct acid/base but not conjugate acid/conjugate base
3: All correct designations but not CAB pairs OR correct CAB pairs but not designations
Most common example: designations correct but the lines connect the acid to the conjugate acid and base to conjugate base
4: All correct

4. If a teaspoon of milk of magnesia contains 12.0 mg of $Mg(OH)_2$, what volume of 0.01M HCl (stomach acid) can be neutralized? (Hint: start by writing a balanced chemical equation).

$2\ HCl_{(aq)} + Mg(OH)_{2(s)} \rightarrow 2H_2O^{(l)} + MgCl_{2(aq)}$

mg $Mg(OH)_2$ → g $Mg(OH)_2$ → mol $Mg(OH)_2$ → mol HCl → liters 0.01M HCl

MW$Mg(OH)_2$ = 58.33 g/mol

12.0 mg (1g/1000 mg) (1mol/58.33 g) (2mol HCl/ 1mol $Mg(OH)_2$) (1L/0.01 mol HCl) = 0.041 L HCl= 41. mL HCl

Blooms score: 4

Scoring:
1: No part correct
2: Balanced equation correct only or very few correct conversions
3: Balanced equation correct, conversions thought out correctly, incorrect math, final calculation error
4: All correct

5. In the lab, you need to dispose of 500 mL of a 6.0 M solution of hydrochloric acid. You have a solution of 1.0 M sodium hydroxide. Explain (with a calculation and in words)

how to neutralize the acid so it can be safely poured down the drain.

1. **Figure out the neutralization reaction of HCl and NaOH.**
2. **Determine the number of moles that need to be neutralized. (0.500 L * 6.0 mol/L)**
3. **Recognize that the 1:1 mol ration means that you need the same # moles NaOH**
4. **Determine the number of mL NaOH corresponds with those moles (moles / 1.0 mol/L)**
5. **Add sodium hydroxide to HCl solution**

Blooms score: 5

Scoring:
1: No part correct
2: Recognize the neturalization reaction
Example: Recognize neutralization but use molar mass of NaCl (don't understand proper stoichiometry)
3: Recognize you need to use amount of ^{-}OH needed to neutralize and this is the H+ present but execute incorrectly (poorly calculated)
Example: calculate grams of NaOH instead of mL
4: All correct
Another acceptable answer: use $C_1V_1=C_2V_2$ (works because we have a 1:1 ratio)

Acids and Bases: Part II Assessment Rubric

1. Water has the special characteristic of being able to act like an acid or base. What is this called?

a.) ampicillin
b.) amphobulous
c.) amphoteric

Blooms score: 1

Scoring:
1: wrong
4: right

2. Write a chemical equation that illustrates the autoionization of water.

$H2O_{(l)} \rightleftharpoons H^+_{(aq)} + OH^-_{(aq)}$

Blooms score: 2
Scoring:
1: Not correct
Example of misconception: Thinking autoionization is amphoteric, showing water being protonated or deprotonated
2: Multiple mistakes
Example: both not using reversible arrow AND don't show ion charges
3: Don't use reversible arrow or don't show ion charges
4: All correct

3. Complete the chart below using the following relationships:
   $pH=-\log[H^+]$
   $[H^+]=10^{-pH}$
   $1.0x10^{-14}= [H^+][OH^-]$
   $pOH=-\log[OH^-]$

$[H^+]$	$[OH^-]$	pH	pOH	Acidic or basic
$7.5x10^{-3}$	**$1.33x10^{-12}$**	**2.12**	**11.88**	**Acidic**
$2.78x10^{-5}$	$3.6x10^{-10}$	**4.56**	**9.44**	**Acidic**
$5.62x10^{-9}$	**$1.78x10^{-6}$**	8.25	**5.75**	**Basic**
$5.01x10^{-9}$	**$2.0x10^{-6}$**	**8.3**	5.70	**Basic**

Blooms score: 3
Scoring:

1: None correct
2: Randomly sometimes correct
3: Able to do one correctly consistently but not the other (ie. Can go from $[H^+]$ to $[OH^-]$ but not $[H^+]$ to pH etc)

4. If a solution is made by adding water to $4.6x10^{-5}$ moles of KOH and $2.7x10^{-3}$ moles HCl until the final volume is 1 L, what is the pH of the solution?

KOH + HCl → H_2O + KCl
$4.6x10^{-5}$ mol $2.7x10^{-3}$ mol
(limiting reagent)

$4.6x10^{-5}$ mol KOH x (1 mol HCl)/(1 mol KOH) = $4.5 x 10^{-5}$ mol HCl neutralized

Mol Hcl remaining: $2.7x10^{-3}$ mol HCl- $4.6x10^{-5}$ mol HCl = $2.7x10^{-3}$ mol
(negligible)

$[HCl] = [H^+] = 2.7 x 10^{-3}$ mol/ 1L = $2.7x10^{-3}$ M

pH = $-\log(2.7x10^{-3})$ = 2.6

Blooms score: 4

Scoring:

1: Nothing right
2: Just take pH with HCl and ignore neutralization (still get right answer)
3: Recognize KOH neutralizes HCl but don't execute correctly
Example: Calculation error or do 2, but they have the proper neutralization reaction
4: All right

5. You are asked to make a 100 mL solution with a pH of 4.2. You are given water, a beaker, a graduated cylinder, and any strong acids you want. Explain how you would make the solution step by step. Include the amounts of everything you would use (MANY correct answers).

Molarities of concentrated strong acids:
HCl: 12.1 M
HBr: 8.9 M
H2SO4: 18.0 M
HNO3: 15.9 M (source: SigmaAldrich.com)

1. **Determine $[H^+]$ by taking $[H^+]= 10^{-4.2} = 6.3x10^{-5}$**
   (1 and 2 can be reversed)

2. **Determine the number of moles you need for your volume**
   $[H^+]$ = ($6.3x10^{-5}$ moles H^+)/0.1 L
3. **Determine how many mL of strong acid you need to get the correct # moles based on the starting concentration**
   ex: moles x (1L HCl)/12.1mol HCl = L HCl = mL HCl
4. **Determine how much water will be needed to make the volume**
   (100 mL total – mL strong acid)→ add acid to water!
   Blooms score: 5

Scoring:
1: Nothing toward the answer
2: Calculate correct # of moles but don't get past that
Example: Many of the pieces are present, but answer is not cohesive
3: Calculate correct # of moles of acid and volume of acid but don't dilute properly
4: Correctly accomplish goal

Spectral Files

Raw data can be found in SigmaPlot files on the fs3 server under McMahon Group\sknezz\Thesis\Raw Data from Figures*filename*

Chapter 1 all files in the folder \MeC3Me

Figure 1.1	Figure 2-IR diazo-472nm irradiation
Figure 1.2	Figure 3- IR dirad-330nm irradiation
Figure 1.3	Figure 5- thick matrix UVvis diazo-472nm
	Figure 5- thick matrix UVvis dirad- 330nm irradiation
Figure S1.3	Figure S5- annealing expt
Figure S1.4	Figure S6- solution spectrum
Figure S1.5	Figure 4- thin matrix- UVVis diazo- 472 nm irradiation
Figure S1.6	Figure 5- thick matrix UVVis diazo-472nm
	Figure 5- thick matrix UVVis diazo-330nm irradiation
Figure S1.7	Figure S3- IR diazo dirad alt calc
Figure S1.8	Figure S4- IR dirad enyne authentic + calc

Chapter 2 all files in the folder \Nitrene Tunneling

Figure 2.2	Anthranil IR
Figure 2.3	Anthranil IR
Figure 2.4	Anthranil UV-vis
Figure 2.5	2-Azidobenzaldehyde IR
Figure 2.6	2-Azidobenzaldehyde IR
Figure 2.7	2-Azidobenzaldehyde UV-vis (calculated spectrum from Clásudio)
Figure 2.9	2-Azidobenzaldehyde EPR

Figure S2.1 Anthranil IR

Figure S2.2 2-Azidobenzaldehyde IR

Figure S2.3 Anthranil UV-vis

Figre S2.4 2-Azidobenzaldehyde UV-vis

Figure S2.5 2-Azidobenzaldehyde UV-vis

Chapter 3 all files in the folder \Bergman

Figure 3.3 1,3-diethynylbenzene vs deuterated

Chapter 4: all files in the folder \Zwier

Figure 4.4 SNK1144.001 and SNK1144.004

Figure 4.5 SNK2037.001 (BuLi)

SNK2154.002 (NaH)

SNK2156.001 (KO^tBu)

Figure 4.6 ASAP+GCMS_1327_001

Figure 4.7 ASAPMS_1327_001

Figure 4.8 SNK2196.001 ($CDCl_3$)

SNK2196.002 (CD_3CN)

SNK2196.003 (C_6D_6)

Figure 4.9 SNK2196.003

Chapter 5 all files in the folder \Flipped Classroom

All Figures from *Assessment Stats* Excel spreadsheet